On the Adaptation of Building Controls to the Envelope and the Occupants

EPFL

ÉCOLE POLYTECHNIQUE
FÉDÉRALE DE LAUSANNE

Suisse
2011

Abstract

The sun is the biggest known source of energy in our solar system. We feel its strength when it gets hot during the the day and we notice its absence during the night when we feel cold. So as to be less dependent on the sun as an energy source, we implemented additional heating and cooling sources to maintain the temperature within a comfortable range. The downside to this is that the majority of energy consumed within the housing sector is used up on the heating and cooling alone.

To profit from the vast energy source of the sun we propose a user-adaptive and building-adaptive blind control for residential buildings, that is implemented in prefabricated modules for facade renovation. User-adaptive means that it is the occupant who is responsible for the temperature control within the home. Building-adaptive, in this context, means that the temperature control is established automatically without any user input.

Through the evaluation of occupant queries we have shown that a general measure for thermal comfort is not possible for all occupants. Consequently, there is a need for a personalized measure of thermal comfort. In order to create this the occupant enters votes via the interface; from this we deduced statistically the probability of comfort relative to the indoor temperature. According to the profile the control sets its target temperature. The profile steadily adapts the user's preferences and through this we can also capture seasonal changes in comfort temperature. This guarantees that at each point in time the control system knows the desired temperature and is taking action to achieve it.

The adaption to the building is achieved with the fitting of a simple thermal building model with data collected by the sensors of the control system. We showed that the monitored data sufficiently fits the model. With the help of the simple model we evaluated different control strategies and optimized them according to the thermal profile.

For our performance tests we conducted computer simulations as well as a 6-month field study. For the simulations, a specific test bed was suggested that would assess the saving potential, which can then be compared to the performance of the tested control. Results showed that the suggested control system is capitalizing on most of the achievable energy savings and thermal comfort.

A 6-month field study in the LESO-PB building was carried out to test the impact on energy demand as well as comfort under real conditions. It appeared that the automatically controlled office needed only approximately 50% of the average heating energy that was used in the manually controlled offices.

Furthermore, the probability of thermal comfort was, on average, 10% higher in the automatically controlled offices when compared to those that were controlled manually.

Zusammenfassung

Die Sonne ist die größte Energiequelle unseres Planeten. Während des Tages spüren wir ihre Wärme, bei Nacht Kälte durch ihre Abwesenheit. Um weniger von der Sonne abhängig zu sein, statten wir Gebäude mit Heizung und Klimaanlagen aus, um die Temperatur in einem schmalen Bereich zu halten, den wir als komfortabel empfinden. Der Nachteil ist, dass dies den Großteil des Energieverbrauchs eines Gebäudes ausmacht.

Um mehr von der unerschöpflichen Energie der Sonne zu nutzen, entwickelten wir eine Steuerung für die Jalousien, die sich an den Bewohner und an das Gebäude - in dem sie installiert ist - anpasst, um die Strahlungsenergie der Sonne effizient zu nutzen. Die Anpassung an den Bewohner wird erreicht, indem aus seinen Handlungen statistisch die Wohlfühltemperatur berechnet wird. Die Adaption an das Gebäude wird sichergestellt durch ein thermisches Model, welches sich automatisch an die Gegebenheiten des Gebäudes anpasst.

Durch eine Feldstudie hat sich gezeigt, dass ein allgemeines Maß für thermischen Komfort nicht alle Nutzer zufrieden stellt. Folglich kann dies nur bei einem individuellen Maß der Fall sein. Um solch ein Maß zu erstellen, gibt der Nutzer sein momentanes thermisches Empfinden ein; statistisch wird aus diesen Eingaben die Wahrscheinlichkeit von Komfort relativ zur Temperatur errechnet. Das erhaltenen Profil passt sich durchgehend anhand der Eingaben an, also auch an die saisonalen Änderungen der Komforttemperatur. Anhand dieses Profils kann die Steuerung die nötigen Schritte berechnen. Um verschiedene Steuerungsstrategien evaluieren zu können, passen wir ein thermisches Model über seine Parameter an das Gebäude an. Dies erfolgt automatisch durch vorher von Sensoren aufgezeichnete Daten.

Um die Leistungsfähigkeit zu testen, führten wir verschiedene Computersimulationen sowie eine sechsmonatige Feldstudie durch. Für die Computersimulationen implementierten wir eine spezielle Testumgebung, um das Potenzial bezüglich Energieeinsparungen und Komfort zu berechnen. Die Resultate zeigen, dass unsere Steuerung das theoretische Potenzial bezüglich Energieeinsparungen und Komfort zu einem hohem Anteil ausnutzt.

Der sechsmonatige Test wurde im LESO Gebäude ausgeführt, um die Steuerung unter reellen Bedingungen und mit realen Menschen zu testen. Büros mit automatischer Steuerung benötigten etwa 50% weniger Energie als manuell gesteuerte Räume. Desweiteren lag die Wahrscheinlichkeit von thermischem Komfort 10% über dem Durchschnitt der manuellen Räume.

Schlagwörter: Gebäudesimulation, Adaptive Gebäudesteuerung, Adaptive Fuzzy logic, Genetische Algorithmen, Pareto-front, Feldstudie, Thermische Komfort

Acknowledgements

First of all, I want to thank Prof. Jean-Louis Scartezzini, my thesis director, for giving me the opportunity to complete this thesis at the Solar Energy and Building Physics Laboratory at the Federal Institute of Technology in Lausanne, for his valuable criticism and for providing his broad knowledge.

Dr. Nicolas Morel my thesis supervisor who provided we with enough freedom to pursue this work, but where I also found a sympathetic ear for discussing all questions.

Dr. Michael Wetter for giving me the opportunity to work with him and his team at the Lawrence Berkeley National Laboratory. The insights I gained during that time into building simulation have been extremely valuable for the further development of this thesis.

Laurent Deschamps for his persistent work on the EIB interface, that made the experiments possible.

Dr. Frédèric Haldi, with whom I shared my office during my time at the LESO, for the good atmosphere that made daily routine more enjoyable. I also thank him for many fruitful discussions about various topics but especially his support in regard to statistical modeling. He also advised me of R, the statistical program all calculations and figures are made with.

I would also like to thank all my colleagues who contributed to make the LESO a more than pleasant place to work. Especially my fellows PHD candidates Apiparn Borisuit, Chantal Basurto, Diane Perez, Urs Wilke, Friedrich Linhart, Nikos Zarkadis, André Kostro, Martin Joly, Stefan Mertin, Raquel Peres Gagliano and Antonio Paone.

Special thanks are due to Susanne, Sylvette and Barbara , without whom the daily bureaucracy would look much more opaque.

The work would not have been possible without the financial support of the projects *Advanced Energy-Efficient Renovation of Buildings* and *Innovative Building Technologies for the 2000-Watt Society* by the Competence Center Energy and Mobility, ETH Domain, Switzerland, which is gratefully acknowledged.

Finally, I want to thank my family whose constant support have led me here, for their encouragement and interest that helped me to achieve this work. And of course, thanks to Corinna, who strongly supported and encouraged me throughout my doctorate.

Contents

CONTENTS

List of Figures

LIST OF FIGURES

List of Tables

GLOSSARY

Glossary

ANF   Adaptive Neuro-Fuzzy

ANFIS   Adaptive Neuro-Fuzzy Inference System

ANN   Artificial Neural Network

ASHRAE American Society of Heating, Refrigerating, and Air-Conditioning Engineers

BEMS   Building Energy Management Systems

BLX   Blend Crossover

CCEM   Competence Center Energy and Mobility

CGI   CIE Glare Index

CHASE   Context-Aware Heterogenous Adaptive Smart Environment

CIE   Commission International de l' Eclairage

CoP   Coefficient of Performance

CRT   Cathode Ray Tube

DAE   Differential Algebraic systems of Equations

DALI   Digital Addressable Lighting Interface

DGI$_n$ new Daylight Glare Index

DGI   Daylight Glare Index

DGP   Daylight Glare Probability

DLL   Dynamic Link Library

DNA   DeoxyriboNucleic Acid

EA   Evolutionary Algorithms

GLOSSARY

EIB   European Installation Bus

FL   Fuzzy Logic

FLC   Fuzzy Logic Control

GA   genetic algorithm

GGR   Large Room Glare Rating

GHGs   Green House Gases

HFL   Hierarchical Fuzzy Logic

HFS   Hierarchical Fuzzy System

HVAC   Heating, Ventilating, and Air Conditioning

ICE   Indoor Climate and Energy

IDA   Implicit Differential Algebraic Solver

IEA   International Energy Agency

IES   Illuminating Engineering Society

IESNA   Illuminating Engineering Society of North America

IP   Internet Protocol

IPCC   International Panel on Climate Change

ISO   International Organization for Standardization

KB   Knowledge Base

LESO-PB   Laboratoire d'énergie solaire et physique du bâtiment

MF   Membership Function

MIT   Massachusetts Institute of Technology

MOEA   Multi-Objective Evolutionary Algorithms

MPC   Model Predictive Control

MSE   Modular Simulation Environments

Mtoe   Million tonne of oil equivalent

NMF   Neutral Model Format

NSGA   Non-dominated Sorting Genetic Algorithm

ODE   Ordinary Differential Equation

PC   Personal Computer

PDE   Partial Differential Equation

PID   Proportional Integral Derivative

PLR   Part Load Ratio

PMV   Predicted Mean Vote

ppb   Part per Billion

PPD   predicted percent of dissatisfied

ppm   Part per Million

SBX   Simulated Binary Crossover

SHGC   Solar Heat Gain Coefficient

SRES   Special Report on Emission Scenarios

TSK   Takagi-Sugeno-Kang

UGR   Unified Glare Rating

UNFCCC   United Nations Framework Convention on Climate Change

VCP   Visual Comfort Probability

1

Introduction

In the last decade the sentiment for energy demand and supply was changing fundamentally. The rapidly growing demand for energy raised concerns over supply, consumption of fossil energy sources and environmental impacts. Policy makers understood that the energy supply has to get sustainable, such that it meets the needs of the present without compromising the ability of future generations. Based on the projected growth in population also energy demand will rise. Basically, there are two ways for saving fossil energy; first we simply use the energy more efficient second we produce *renewable energy*, for example via solar collectors. In this work we strike the first path.

1.1   General Context

Today climate change[1] is unequivocal as the rise of air and ocean temperatures and widespread melting of snow and ice is evident from observations (see Figure 1.1). The drivers of climate change can be identified as natural and anthropogenic sources. Changes in the atmospheric concentrations of GHGs (Green House Gases) and aerosols, land cover and solar radiation alter the energy balance of the climate system and drive the climate change. They affect the absorption, scattering and emission of radiation within the atmosphere and at the Earths' surface. The resulting positive or negative modifications in energy balance due to these factors are expressed as radiative forcing, which is used to compare warming or cooling influences on a global scale. Human activities result in emissions of four long-lived GHGs: CO_2, methane CH_4, nitrous

---

[1]Climate Change according to the IPCC (129) (International Panel on Climate Change) refers to a change in the state of the climate that can be identified (e.g. using statistical tests) by changes in the mean and/or the variability of its properties, and that persists for an extended period, typically decades or longer. It refers to any change in climate over time, whether due to natural variability or as a result of human activity. This usage differs from that in the United Nations Framework Convention on Climate Change (UNFCCC), where climate change refers to a change of climate that is attributed directly or indirectly to human activity that alters the composition of the global atmosphere and that is in addition to natural climate variability observed over comparable time periods.

oxide[1] N_2O and halocarbons (a group of gases containing fluorine, chlorine or bromine). The global atmospheric concentrations of CO_2, CH_4 and N_2O have increased markedly as a result of human activities since 1750 and now far exceed pre-industrial values determined from ice cores spanning many thousands of years. For example, CO_2 increased from 280ppm[2] to 379ppm in 2005. The global atmospheric concentration of CH_4 has increased even more from a pre-industrial value of about 715ppb to 1732ppb[3] in the early 1990s, and to 1774ppb in 2005 (129).

The main sources of CO_2 due to human activity are the burning of fossil fuels and deforestation, which accounts for up to one third of the antropogenic CO_2 emissions (154). N_2O is emitted mainly through the use of fertilizer during agricultural activities and halocarbons are released in connection with refrigeration systems, fire suppression systems and manufacturing processes. A source of CH_4 are enteric fermentation[4] and manure management (156).

With all these scientific facts it cannot be longer denied that climate change is also based on our behaviour regarding fossil energy and its use. Since it is utopian that society will change over night it is important to identify sources of CO_2 emissions where economic cost of mitigation are low or even negative, which means that saving CO_2 also saves money.

1.1.1 Mitigation of CO_2 in the housing sector

In 2004 the building sector was responsible for 3 Gt CO_2 in direct emissions and 5.6 Gt CO_2 in indirect emissions caused via usage of electricity, which adds to total emissions of 8.6 Gt CO_2 (136). In Europe, the building sector accounts, depending on the countries, for around 40% of the total energy consumption (see Figure 1.2) and consumes by far more energy as the industrial sector. During the years from 1970 and 2004 the carbon dioxide emissions grew at a rate of 2.5% a year for commercial buildings and 1.7% for residential buildings.

The largest increase in CO_2 emissions (including electricity) in this sector was coming from Asia (30%), North America (29%) and OECD Pacific (18%). Figure 1.3 shows the result of two scenarios developed for the IPCC Special Report on Emission Scenarios (SRES) (118). The dark red coloured curve stands for the historic emissions 1971-2000, based on Prices (136) modifications of IEA data. The light red curve are the projections for 2001-2030, based on Prices (136) disaggregation of SRES data.

According to the IPCC, mitigation in the building sector can reduce the GHG in the most efficient way. In other words, investments in the housing sector can mitigate the most GHG per invested unit of capital (129) compared to the other sectors as transportation and industry.

---

[1]Commonly known as laughing gas.

[2]Part per Million

[3]Part per Billion

[4]Enteric fermentation occurs when methane (CH_4) is produced in the rumen as microbial fermentation takes place. Most of the CH_4 byproduct is belched by the animal, however, a small percentage of CH_4 is also produced in the large intestine and passed out as gas. (Source: Wikipedia: Enteric fermentation)
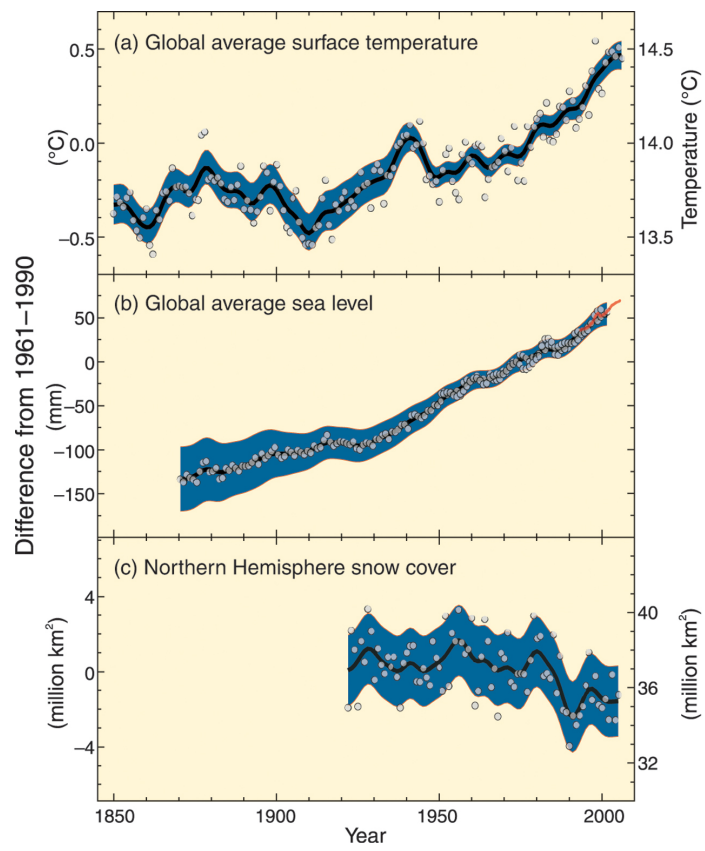
Figure 1.1: Process of the global surface temperature, the sea level and snow coverage according to IPCC.
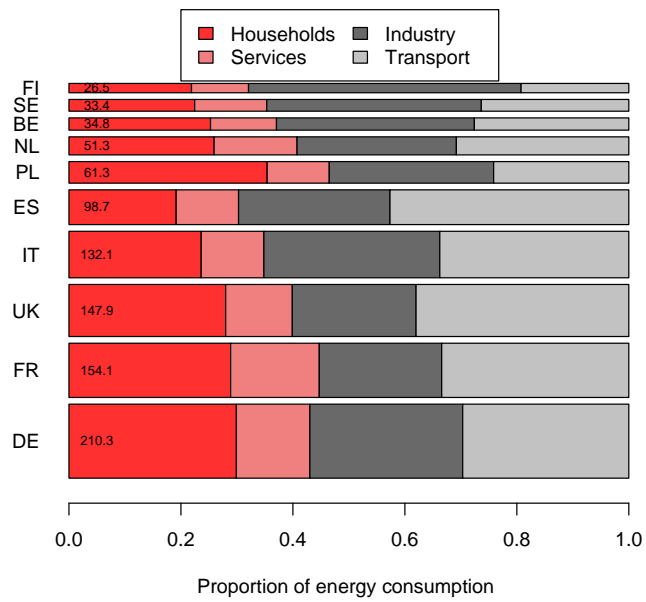
Figure 1.2: Proportion of energy consumption according to sectors for the 10 biggest consumers in Europe. The width of the bars reflect the absolute value, indicated on each bar in [Mtoe] (Million tonne of oil equivalent) (34).
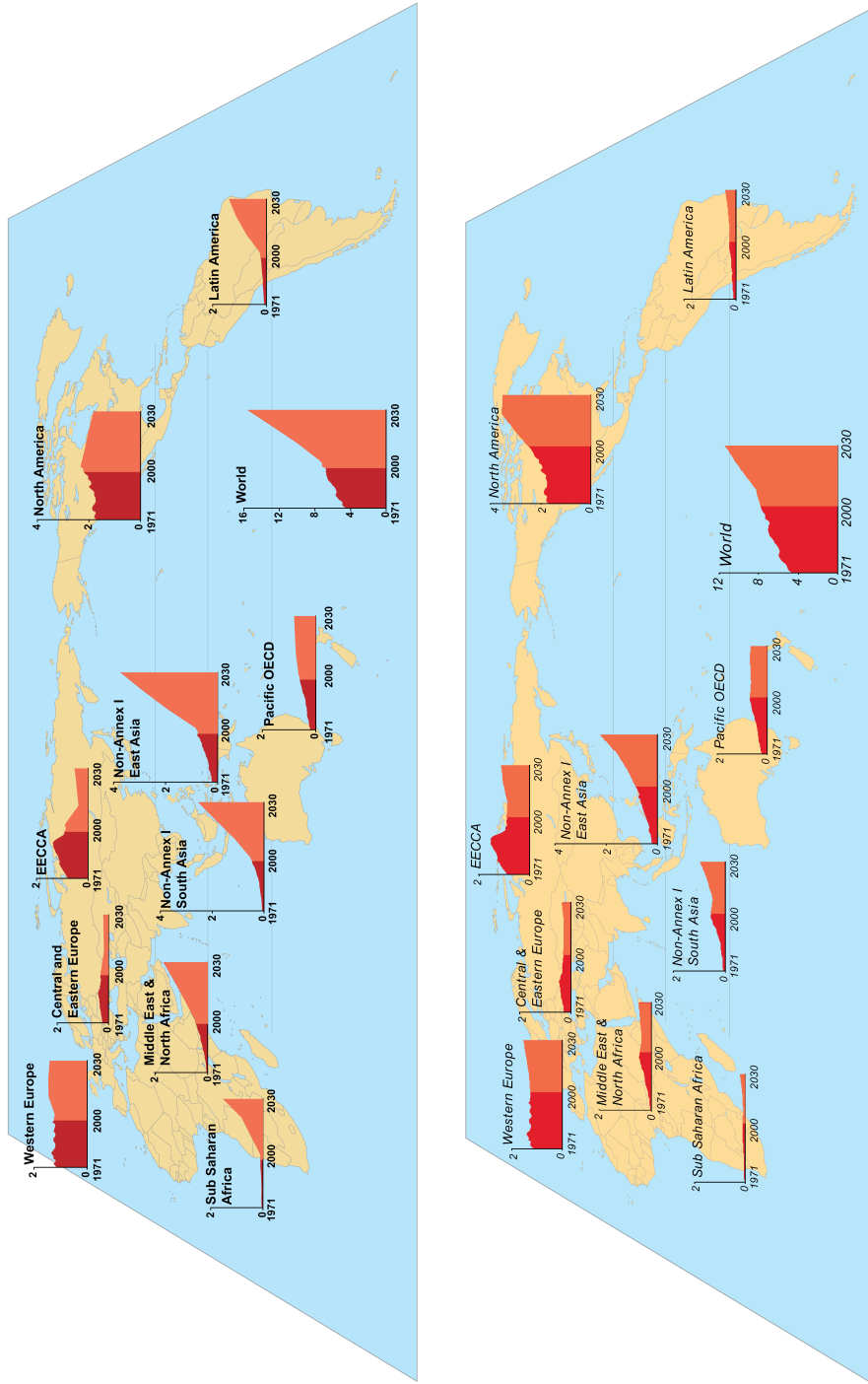
Figure 1.3: CO2 emissions including through the use of electricity: A1B (top) and B2 (bottom) IPCC (SRES) (118) scenarios.

Prior to discussing the possibilities of reducing the CO_2 emission we have taken a glance at the consumption: Figure 1.4 shows a breakdown of energy used in residential and commercial buildings. The single largest consumer of energy is space heating and cooling, which is included in energy for HVAC's. In the US the amount allocated to space cooling is nearly the same in residential and in commercial buildings, reflecting the high standard of living where cooling is affordable for the mass-market. In China cooling did not reach the mass-market yet and is reserved to commercial buildings. If the standard of living is increasing in China it is very probable that also for residential buildings cooling will become an option and the fraction may also reach the same level as in the commercial sector. Unfortunately, on the European level, the energy consumption for the single users in the housing sector is unknown (133). But data for the United Kingdom (133), Spain (133) and Germany (59) for the residential sector (shown also in Figure 1.4) shows similar ratios.

The setting of the shading devices is important to reduce the two major fractions of energy use for buildings, the space heating and the space cooling.

The optimal use of solar radiation refers to passive solar heating which includes south-facing glazing, double facade wall constructions and also an optimal use of the shading devices. Real world case studies are given for example in Hastings (72; 73) and Hestnes (74).

1.2 Problem statement

In western Europe about 55% of the building stock was constructed between 1950 and 1990. During that time the regulations concerning the insulation of buildings have been much weaker than in the last 20 years. Consequently, in these buildings doze a great potential for energy savings. To exploit that potential Competence Center Energy and Mobility (CCEM) started a project to develop prefabricated facades which can be mounted on the original facade and include the insulation, new windows, new blinds and also novel blind controls. One of the main goals was to keep the renovation costs for the landlord to a minimum that also economically a benefit can be achieved.

The main goal of this doctorate is to develop a blind control strategy that can be incorporated into prefabricated modules, is capable of improving thermal comfort, is easy to install with no configuration and can be realized with manageable costs.

The main differences to this work compared to the reviewed research in this area are as follows:

- The control should only need very few sensors and has a plug and play character.

- The automatic adaptation will include also the building and not only the occupants.

- The energy savings will be larger than existing controls thanks to the adaptation to the building.
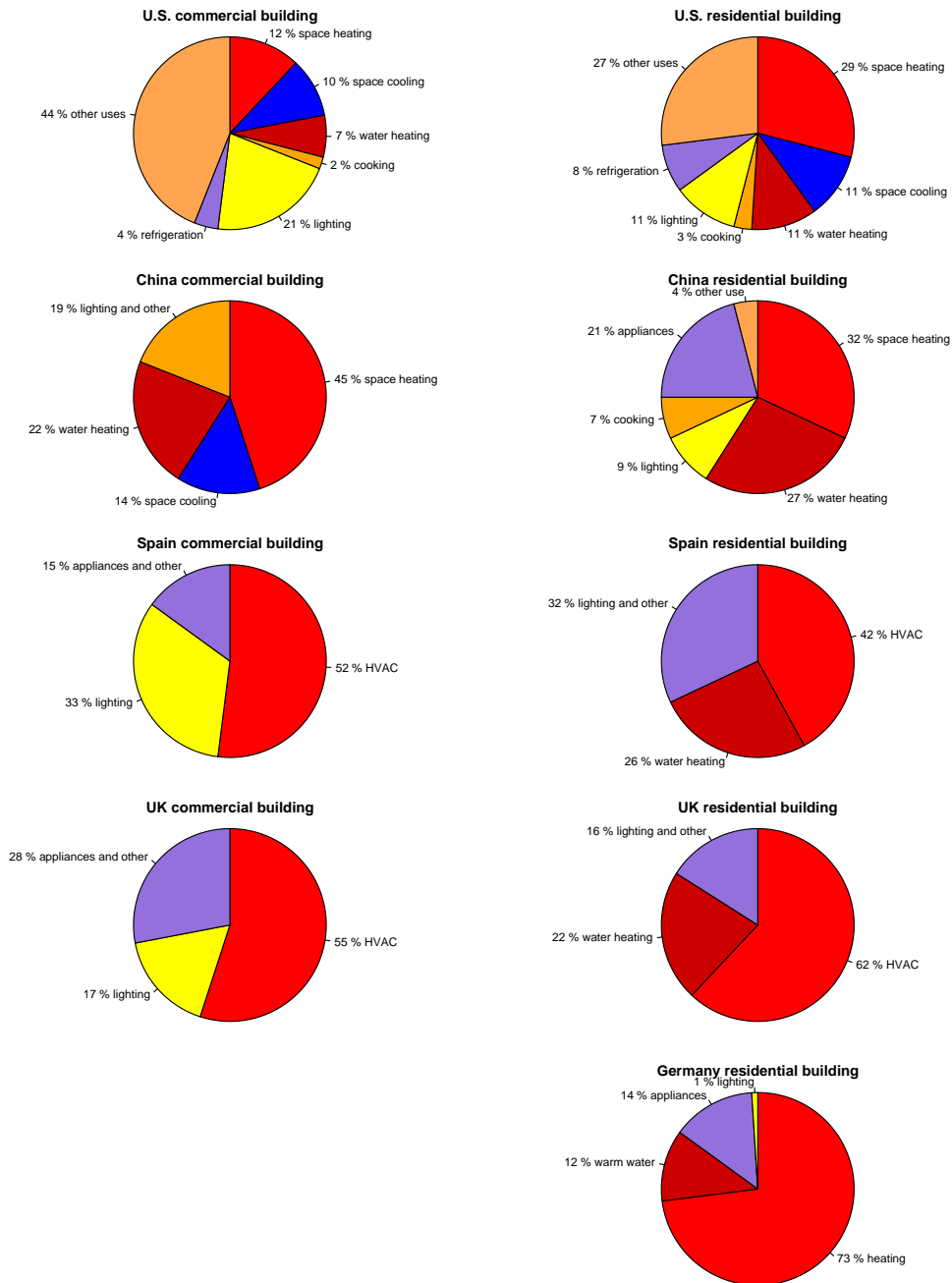
Figure 1.4: Breakdown of residential and commercial sector energy use in United States (2005) (82), China (2000) (178), Spain (2003) (133), United Kingdom (2003) (133) and Germany(2005) (59).
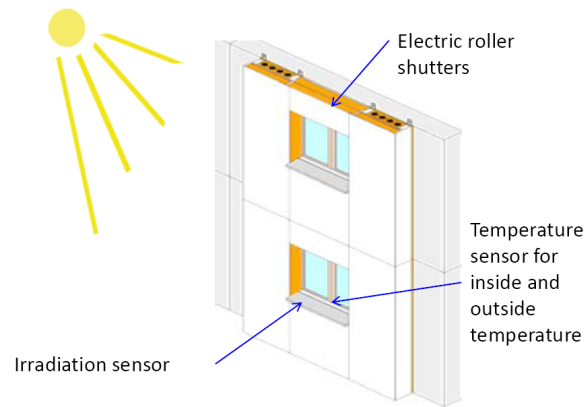
Figure 1.5: The developed module for advanced facade renovation includes automatic blinds, which can be controlled with our proposed algorithm without any adaptation form the user.

Even with growing interest in building automation, advanced controls cannot be easily found in standard residential buildings. On the other hand it was proven that they save energy and do even payoff. In our eyes this mismatch is due to their costs and inefficient installation of such systems.

With including an adaptation not only to the occupant, which has been already done, but also the environment, the process of installation and customization can be cut short. Today, the cost of labor is too high to provide technical support for most electronic products and the same applies to controls. A device that is able to be delivered with the prefabricated modules could solve these problems. A schematic layout is shown in Figure 1.5:

We try to reach this goal with the following steps:

1. Through the coupling of a building simulation program and stochastic modeling for the behavior of occupants a simulation test bed will be created which allows realistic and extensive testing and developing of a novel control strategy.

2. Via multi-objective optimization and the simulation test bed an *optimal* control will be established. The advantage is that the complete saving potential can be assessed and different control strategies can be compared to the optimal case rather than worst case. Therefore the performance can be stated as: Control A is 10% worse than the *optimal* control.

3. The question, which variables are needed for fulfilling the needs of a control has not yet been addressed enough in research. We try to find out the important state variables that are needed for the adaptation to the building and for energy efficiency.

4. For the adaptation to the occupant we collect the user wishes to calculate a probability of thermal comfort, enabling us to optimize the control to the wishes of each occupant (personalized thermal profile).

5. Finally we combine the collected information and create a control strategy, which is as simple as possible in terms of usage and sensors needed but still supplies energy reduction and creates an agreeable building environment. In the final control all actuators will be still accessible for the occupant, enabling him to immediately overwrite the system.

Also the question has to be addressed why our only concern is the control of the shading devices. MIT announced recently the SMART house project which even takes care for switching on the coffee machine. In literature already a lot of nuances of control systems for all kind of subject have been proposed but in reality not very much has happened. This means not that these approaches do not work, they work perfectly in a lab and it is important to investigate further. However, regarding the saving potential which can be already achieved with a simple thorough control of the shading devices this also needs attention. In simulations, explained in Chapter 5, we found that saving potentials by the ideal control of the shading devices are up to 84% of the combined heating, cooling and lighting energy: of course this is not applicable to every building. They also showed that additional intelligent control of heating and cooling improves further the efficiency but not of the same magnitude.

If the shading devices can reduce the energy bill and we try to adapt our control to the occupants, why not let the occupants themselves manage their shading devices? There are many answers to this question, lets start with the obvious ones. Humans are intrinsically lazy, they do accept small levels of discomfort and can also adapt to it. For example, Sutter et al. (157) found that most of the time shading devices are either fully retracted or fully closed. Furthermore in residential buildings, which are our target, the occupant will be absent during daytime and has no influence on the setting. When he comes home in the evening during summer time the apartment is too hot without a control of the shading devices. During winter the shading will stay closed during the whole day an solar gains can not help heating up the apartment.

That means a simple shading control, which can be easily installed, may have better chances to be effectively used and by that contributes to save energy in real life.

1. INTRODUCTION

2

Status of advanced control systems

For an overview, we split the existing research in four groups: in Chapter 2.1 systems for HVAC are explained, Chapter 2.2 introduces electric lighting control strategy, Chapter 2.3 is concerned with shading device controls, in Chapter 2.4 the combination of the prior mentioned are covered, Chapter 2.5 handles controls that include also HVAC. Chapter 2.6 shortly covers the work going on in complete integrated home environments ranging from switching on the coffee machine to automatic groceries orders.

2.1 Control systems for HVAC

Energy management of heating, ventilating and air-conditioning (HVAC) systems is a primary concern in building projects, since HVAC systems have the largest allotment of electric energy consumption among all building service installations and electric appliances. Behind the abbreviation HVAC all systems are summarized whose objective is the optimization of thermal and ventilation conditions in a building.

2.1.1 Control systems using fuzzy logic

One important artificial intelligence tool for building automation is fuzzy logic which is based on linguistic rules comprising expert knowledge (174). For interested reader we refer to (91; 158) and Section 4.4, which gives an introduction and further applications.

Dounis et al. (49) presented a living space thermal-comfort control based on fuzzy logic. The thermal comfort is expressed in terms of the PMV (Predicted Mean Vote)[1] (53) comfort index, which is together with the outdoor temperature the only input to the system. The system has three actuators: heater, cooler and natural ventilation (window). The fuzzy system was

---

[1]The Predicted Mean Vote (PMV) index is a quantitative measure of the thermal comfort of a group of people at a particular thermal environment. It depends on the metabolic rate [met], the cloth index [clo], air velocity [m/s], mean radiant temperature $[^\circ C]$, ambient air temperature $[^\circ C]$, and vapour pressure of water in ambient air [Pa].

tested on a model for two different climate conditions, one day in summer and one in winter. The results show that the system is capable of keeping the PMV level within the predefined range but no statement is made about the energy efficiency or expected energy savings of the system. Additionally they proposed general guidelines for the design of fuzzy logic thermal controllers.

A similar system was proposed by Calvino et al. (22) which tries to maintain the PMV (53) at a certain level by controlling the speed of the heating fan. It is tested in a real room but only during winter time, where it performed well: no information is given about energy savings.

In Rahmati et al. (137) a hybrid of fuzzy logic and PID [1] controller is proposed for optimizing a standard HVAC system. By way of simulations they showed a better control performance than a standard PID system.

Previous related research of fuzzy logic systems for controlling HVAC systems was also carried out by the following authors: Fraisse (57) and Arima (10).

2.1.1.1 Genetic rule selection

As previously stated, fuzzy logic is based on linguistic rules established by an expert. However in complex, real world problems often an expert fails to define rules with optimal performance as it is difficult for human beings to guarantee good interaction among rules. To remove this drawback and to enhance the performance of the control various techniques have been applied. One of the most frequently used approaches, known as tuning, consists of refining the connection between the rules once the rule base has been obtained to create an optimal cooperation among them (5).

For the tuning often a genetic algorithm (GA) (64; 76; 141) is used, which is a global search algorithm that tries to imitate the natural evolutionary principles according to Darwin while searching for an optimum. A population of solutions is maintained that is run through the three steps: Evaluation, Selection and Alteration. Good solutions are selected for reproduction and replace the bad ones which are sorted out. By the process of competition over time solutions with a better *fitness* evolve, increasing the average quality of the population. Since we used this approach for our control a more detailed introduction is given in Section 4.1.

In Alcala et al. (7), the main criteria is explicitly the energy efficiency, while maintaining the required levels of thermal comfort (PMV is maintained in a range), indoor air quality (concentration of CO_2 is below 800ppm) and system stability (minimizing the changes in the system). The HVAC system controlled by the algorithm was a fan coil unit supplied by a reverse-cycle heat pump with variable fan speed. The algorithm was tested within the frame-

---

[1]A proportional-integral-derivative controller (PID controller) is a generic linear control loop feedback mechanism widely used in industrial control systems. A PID controller attempts to correct the error between a measured process variable and a desired set-point by calculating and then outputting a corrective action that can adjust the process accordingly (108).

work of the GENESYS [1] project which includes a real test building consisting out of seven test chambers. Around the wall an artificial climate regarding temperature and humidity can be created at any time. The control system is compared against an ON-OFF control regarding energy consumption. The fuzzy system was tested in three different configurations (energy saving compared to the ON-OFF system are in brackets): without improvement (9.5%), considering rule weights (13.21%), considering rule weights and rule selection (14.05%). All the proposed techniques show much better performance than the classical ON-OFF controller; better results can be obtained with optimization of the fuzzy control. Additional publications of the same author regarding similar topics are (5; 6).

2.1.2 Control systems using artificial neural networks

An artificial neural network (ANN) is a mathematical model or computational model mimiking biological neural networks. It consists of an interconnected group of artificial neurons and processes information using a connectionist approach for computation. In most cases an ANN is an adaptive system that changes its structure based on external or internal information that flows through the network during the learning phase. It can be used to model complex relationships between inputs and outputs or to find patterns in data. A review of artificial neural networks is given in Zhang et al. (177)

Yang et al. (172) developed an ANN for predicting the start time of the heating system in a non-residential building. For training of the neural network a simulation program based on the finite difference method was used to collect training data for various conditions. The following input variables were used: indoor temperature, varying rate of indoor temperature, outdoor temperature, varying rate of outdoor temperature. From these factors the start time of the heating system was predicted, which is accurately done by the ANN. The algorithm does not consider the inertia of the building, which could further reduce the start time of the heating as well as its energy consumption.

2.1.3 Control systems using hybrids of GA, ANN and fuzzy logic

Jian et al. (87) used an Adaptive Neuro-Fuzzy (ANF) method to control a standard HVAC system for which the only output is the speed of the fan. The authors compared this system to a PID controller and found it superior because of its robustness.

Huang (78) presented an adaptive learning algorithm based on genetic algorithms (GA) for automatic tuning of proportional, integral and derivative (PID) controllers in HVAC systems. The simulation results show that the genetic algorithm-based optimization procedures are useful for automatic tuning of PID controls for HVAC systems, yielding minimum overshoot and minimum settling time.

---

[1]GENESYS Project: Fuzzy controllers and smart tuning techniques for energy efficiency and overall performance of HVAC systems in buildings, European Commission, Directorate-General XII for Energy (contract JOE-CT98-0090)

Bauer (12) proposed a predictive and adaptive heating controller, using artificial neural networks to allow the adaptation of the control model to the real conditions (climate, building characteristics, user's behavior. It consists of three self-learning artificial neural networks, one for the building model and two for the climate model, that allow a prediction of the variables involved in the heating controller (outside temperature, solar radiation, inside temperature) over a 6-hours time horizon. Simulations gave a 11% heating energy saving over a whole year, when comparing the NEUROBAT controller with an advanced conventional heating controller (using start-stop optimisation, heating curve correction with the inside air temperature, and control parameter adaptation). The experimental tests gave a 13% heating energy saving over the whole year 1997.

2.2 Control systems for electric lighting

Lighting controls should not only provide the occupants with a comfortable lighting environment; they must also aim at the reduction of energy consumption. A crucial point for the practicability is the satisfaction of the user. The question is also how much energy can be saved with smart lighting strategies and how much of the complete energy consumption of a building is allotted to light. According the IESNA *Lighting Handbook* (139) 20-25% of the energy consumption in a building is used for lighting. Additioanlly, the heat produced by electric lighting counts for 15-20% of the air condition's energy. Corresponding to studies (139) it is possible to achieve 40% of savings with predictable scheduling (timers) and up to 60% with unpredictable scheduling (sensors), regarding the lighting energy.

Roisina et al. (146) gave a short overview of reported saving potentials and tried to predict the energy performance of three different control systems. In their study they included also the energy consumed by controlling devices. The results show that the savings are larger especially for south oriented locations. They found that with an occupancy rate higher than 44% dimming of electric lighting is preferrable and if it is less than 27% an occupancy sensor is preferrable. By using both approaches together an even higher level of efficiency should be reached.

Bourgeois et al. (18) tried to quantify the energy impact between manual and automated lighting controls in two offices, one in Rome and one in Quebec, and found savings of about 5%. In this study the inhabitants are modelled in an active way (switching out the lighting most of the time when they leave the office, reducing heat in the evening, etc.), with more passive users the energy gains would be much higher compared to automated systems. Assuming no interaction of the user (light stays on the whole day, constant temperature) the automated system reduces the energy consumption by 78%.

Additional to the energy savings it was shown that sun light has positive influence on the human body and can raise the productivity, which is very important for office buildings (14). An overview of current research regarding the influence of daylight on people is given by Galasiu and Veitch (61).

2.3 Control systems for shading devices

Shading device controls have either been time dependent, or have been based on a threshold value, for example solar radiation. Over the years more variables have been added and the outcome was no longer linearly dependent upon variables. In recent years adaptation to the occupant and acceptance by the occupant have attracted the attention of researchers and developers in this field.

In the early approaches, shading devices were adjusted based on one variable, as in Inoue et al. (84) or Leslie et al. (104). In Newsham's (123) model the shading devices were lowered, if the solar irradiance, which fell on the occupants work plane, exceeded 233 W/m^2. With this rather simple rule it was already possible to lower the average predicted percentage of occupants dissatisfied with the thermal environment (PPD)[1] from 22% to 13%.

More sophisticated controls include more than one variable and follow closed-loop algorithms, for example Lawrence et al. (101). Lah et al. (99) built a fuzzy logic system to manage a roller blind in respect to lighting levels in the building. The inputs for the system are: internal illuminance, global and reflected solar radiation as well as the current position of the roller blind. The system was applied to a test chamber where it showed good performance in controlling the inside illuminance in correlation with the available solar radiation. Thermal comfort is not adjusted by the system.

In general the development of shading device controls was focused on providing a comfortable environment and saving energy. However the adaptation to and the acceptance of the occupant is increasingly the center of interest. Another trend is that more sensors are included into controls. This may not be a problem in a laboratory setting, but in real world, additional sensors increase the cost of the control device, make its installation more complex and hence unattractive for users.

In most of the publications it has been shown that the proposed controller in terms of energy consumption is superior to an on-off controlled counterpart (60; 93; 95).

2.3.1 Control systems using fuzzy logic

Lah et al. (99) built a fuzzy logic system for managing a roller blind in respect to the lighting environment in the building. The input informations of the system are: internal illuminance, global and diffuse solar radiation and the current position of the roller blind. The system was applied to a test chamber where it showed good performance in controlling the indoor illuminance in correlation with the available solar radiation. The thermal comfort is not considered by the system.

---

[1]PPD is the predicted percent of dissatisfied people at each PMV. As PMV changes away from zero in either the positive or negative direction, PPD increases.

2.4   Control systems for electric lighting and shading devices

If daylight is sufficient and there is such a potential for energy savings why not let the occupants manage the lighting themselves? Sutter et al. (157) observed the shading device movements in eight offices over a period of 30 weeks by measuring the shading device setting every 15 minutes. They found that most of the time the shading devices are either fully retracted or fully closed. In one office the electric light was always on even if sun light would have been sufficient. Nevertheless the use of the shading devices was consistent during that period which suggests that an automated system can fulfill the requirements of the user. This shows that the occupants behavior towards a comfortable lighting and especially energy efficient lighting is far from optimal and gives enough room for improvement.

Reinhart (142) suggested a simulation algorithm that estimates the energy savings of manually and automatically controlled electric lighting and shading devices in a two person office. The study compares four different user types which differ in the way they use the artificial lighting and the shading devices (Daylight dependent lighting use; Daylight independent lighting use; Blinds static; Blinds dynamic). The most energy efficient user is the one who combines a dynamic shading device with a daylight respective use of electric lighting. With the switch-off occupancy sensor the savings are about 20%, whereas in the best case with the daylight-linked photocell control 60% savings are possible. One handicap of the proposed method is that the results are based on a specific setting and need to be adapted to other kinds of controls and offices. It would be interesting to see if automated shading devices can reduce the energy consumption any further: therefore also the thermal influences need to be included in the model.

In Lee et al.(102) a nine month field study of two commercially available daylighting control systems is discussed. The systems are tested in a unoccupied and furnished mockup, which mimicked the southwest complex of a commercial building in New York. The first system has dimmable ballasts with an open-loop proportional control system and automated shading devices to reduce window glare and increase the daylight flux, the second has digital addressable lighting interface (DALI) ballasts with a closed-loop integral reset control system and an automated shading control in order to block direct sun. Daylighting control system performance and lighting energy use were monitored. The results show savings from 30-60% at a distances of 3.35 m from the window and 5-40% at a distance between 4.57-9.14 m from the window. Including the higher installation costs the economic calculation leads to a positive return on investment.

2.4.1   Control systems using fuzzy logic

Kolokotsa (94) presented a fuzzy logic controller for indoor thermal, visual comfort and air quality based on the EIB (European Installation Bus) and Matlab. The system is tested and implemented in an experimental chamber (size: 1m x 1m x 2m) which is equipped with sensors for outdoor-, and indoor-temperature, humidity, illuminance, air flow and CO_2 concentration. The fuzzy controller is fed with the following informations: Predicted Mean Vote (PMV) (53), outdoor temperature, heating or cooling requirements, window opening, indoor illuminance,

status of electric lighting and shading and generates the following outputs: status of electric lighting and shading position. The system was tested for a period of three days, which is rather short; it showed a good performance in terms of keeping the target values temperature, PMV index and illuminance in the defined range. No information is given about energy savings resulting from the system. Their goal was also to create a plug and play test environment for controllers in real time.

Kurian *et al.* (96) developed a combined system for controlling shading devices and lighting. The system consisted of three fuzzy logic controls (glare, visual comfort, energy effectiveness (user absent)) for setting the shading devices and an adaptive neuro-fuzzy inference system (ANFIS) (97) for prediction and lighting control. The control system has been compared to a simple on/off scheme, which yielded in energy savings between 5% and 60%.

2.5 Control systems for electric lighting, shading devices and HVAC

The role of these systems, also called BEMS (Building Energy Management Systems), is of increasing importance especially in large office buildings.

2.5.1 Control systems using fuzzy logic

In a study carried out by Kolokotsa et al. (93) five different fuzzy controls are compared regarding the response performance and energy savings. In addition to a previous study, the fuzzy controls drive the heating/cooling and the window openings. All fuzzy controls try to keep the values for PMV index, CO_2 concentration and illuminance at a constant level while reducing the energy consumption of the system. For the exact specifications of the controls we refer to Kolokotsa et al. (92; 93; 95). The controls are installed in a laboratory of the Technical University of Crete and compared against historical data, were lighting and heating were manually controlled. The results show that all five controls satisfy the requirements of keeping a stable environment and can reduce the heating/cooling energy by 20% and the lighting energy by 77%, which is an combined enegy saving of 37%. The data was collected during a 10 days period in winter with measurements every 15 s.

2.5.2 Control systems using hybrids of GA, ANN and fuzzy logic

Guillemin and Morel (67; 68; 69) proposed an integrated self adaptive control system for heating, shading and lighting. The driving variables for the controller are: current time, indoor-outdoor temperatures, solar radiation, presence or absence of occupant in the room and additionally set-points (concerning illuminance and temperature) expressed by the user. The control consists of two ANN's for prediction of room temperature and weather, a fuzzy logic for heat control and a fuzzy logic for lighting control that also drives the shading devices. In order to continuously optimize the system a self adaptation process using genetic algorithms looks each night for the most efficient set of control parameters. The controller was compared in terms of

global energy consumption (heating, artificial lighting, electrical appliances) and user comfort with a conventional controller (no automatic shading device control, no artificial lighting control, proportional heating controller with saturation). The experiments have been carried out in two identical rooms of the LESO-PB[1] experimental building at the EPFL for winter, summer and mid-season period. It is shown over the whole period that the suggested control system outperformed a conventional one by 24% in terms of energy savings, most benefits appeared during winter time (40%). The comfort levels were expressed using the PMV (53) for thermal comfort and a novel index PIECLE[2] for visual comfort. It shows nearly equal thermal comfort for both controls but better visual comfort for the proposed system resulting out of the automated shading devices that are not existend in the convential approach.

2.6 Smart Homes

The intelligent room project (32; 33) at MIT focuses on computer-human interaction to support what is traditionally non-computer work. It is equipped with numerous computer vision, speech and gesture recognition systems that connect to what its inhabitants are doing and saying.

In (35) such an architecture is called MavHome (**M**anaging **A**n intelligent **V**ersataile **Home**). The goal is to create a home that acts like an intelligent agent, maximizing the comfort and productivity of its inhabitants while minimizing operational costs. While perceiving the status of inhabitants and the home through sensors the house must be able to predict, reason about, and adapt to its inhabitants. The architecture is divided in four layers, the Decision layer (selects actions to be executed), the Information layer (gathers, stores, and generates knowledge for decisions), the Communication layer (communicates the information) and the Physical layer (contains all the hardware). The most interesting aspect is located in the Information layer, which is responsible for predicting the next actions of the inhabitants. For this the authors suggest three algorithms: Prediction using sequence matching, compression-based prediction and prediction using a task-based Markov-Model. For the final prediction a meta-predictor is used that is based on a neural network to learn a confidence value for each prediction algorithm based on the gathered data. The goal is to predict the actions taken by the inhabitant, removing the need for manual control of the devices. However a wrong prediction can be annoying if the habitant must reverse the action executed by the house.

In CHASE (**C**ontext-Aware **H**eterogenous **A**daptive **S**mart **E**nvironment) (150) an universal framework is developed for tracking residents in smart homes. The idea is that the sensors operate independent from each other without a given topology. The sensors gather data and predict with a Bayesian algorithm the most likely paths of the inhabitants. The main focus of this work lies in the accurate prediction of the routes for inhabitants, stating that this is the crucial point for smart environment controls. For performance evaluation they used a straight forward

---

[1]Laboratoire d'énergie solaire et physique du bâtiment (LESO-PB)

[2]The idea is to use only two sensors: one that measures horizontal illuminance on desk and one that measures vertical illuminance near the eyes of the user. The method gives an estimation of the visual quality at the work place through the percentage of unsatisfied people. (58).

simulation framework, where only lighting and heating needs are considered and switched on or off based on the prediction of the algorithm. These results are compared with an optimal (inhabitant switches off the lighting and heating system whenever he leaves the house) and worst case scenario (lights are on, heating remains at the same set-point the hole time). The results show that the reached energy savings are close to the optimal case. However it is not clear if the savings are due to the tracking inside the house or mainly because the heating is switched of during periods the occupants are absent. It would also be interesting to compare the performance with other tracking algorithms and with a simple off-the-shelf heating control.

2.7   Chapter Summary

In this chapter we divided the existing research on advanced building control systems according to the *depth of control*. In each section we gave an overview of the current status and which techniques are used. Regarding the performance assessment in many cases the proposed controls are compared against a worst case (ON/OFF) or against fixed schedules. The real performance of the control is left uncovered. The comparison was carried out via simulation and real measurements. Most of the time for the simulation a simple room model was used; we found no case where stochastic models for simulation of the occupants were included in the simulation. In The real measurements vary from one year to one day. Summing up, it can be said that with the used performance monitoring it is not easy to compare single controls with each other. In this thesis we want to compare the performance against a *best* case to uncover the real saving potential. Furthermore we include stochastic models to increase the accuracy of the simulations. In the reviewed literature the design of the fuzzy logic did not always follow a coherent structure. We will discuss each step in the design of the fuzzy logic and try to discuss the outcome. The adaptation to the occupant will be a central point in our thesis. To prove our procedure a field study will be carried out under real conditions.

2. STATUS OF ADVANCED CONTROL SYSTEMS

3

The simulation test bed

Part of the work described in this chapter has already been published in (39):

D. DAUM AND N. MOREL. **Assessing the saving potential of blind controller via multi-objective optimization**. *Building Simualtion*, 2 (3):175-185, 2009.

For developing a blind control you need the possibility of excessive testing. It was clear at an early stage of work that this could only be handled by a good simulation test bed that provides a lot of freedom for customization. We found this in the IDA (Implicit Differential Algebraic Solver) ICE (Indoor Climate and Energy) 4.0 building simulation software package.

In this chapter we present the simulation software we used and additional modules we implemented in IDA ICE.

3.1 The IDA ICE Building Simulation Software

The IDA ICE 4.0 Software(3; 147) is a modular and dynamic whole-building simulator allowing simultaneous performance assessments of all issues fundamental to a successful building energy design: form, fabric, glazing, HVAC systems, controls, light, indoor air quality, comfort, energy consumption etc. The accuracy of IDA ICE has been assessed by the IEA solar heating and cooling program, Task 22, subtask C (111). It was shown that after correcting software errors using HVAC BESTEST diagnostics, the mean results of COP and total energy consumption for the simulation programs are on average smaller than 1% of the analytical solution results, with average variations of up to 2% for the low part load ratio (PLR) dry-coil cases (E130 and E140).

The IDA Simulation Environment (IDA SE), for which IDA ICE is a specific add on, is a general purpose modeling and simulation tool for modular systems where components are

described with equations. Each component contains between a single and a few hundred differential and/or algebraic equations. Ready-made components are interconnected by the user in arbitrary combinations. Problems that are suitable for IDA SE occur in virtually all engineering disciplines and industrial sectors.

The program can be split in three parts: The solver, the Neutral Model Format (NMF) translator, and the modeler:

IDA Solver

IDA SE is based on a general purpose DAE (Differential-Algebraic Equations) solver called IDA Solver. The solver relies on precompiled models of physical components. Component models are packaged as Windows DLLs (Dynamic Link Library); their interconnection into systems is described in a system description file. Component DLLs are normally generated automatically from NMF (Neutral Model Format) source code.

NMF Translator

IDA Solver itself is also contained in a DLL that may be called from any front-end program. If the solver is operated directly with a hand-coded system description file, a small front-end program is used. This is the most basic IDA environment, consisting of an NMF Translator, a Fortran, C or C++ compiler, and IDA Solver.

IDA Modeler

The native IDA front-end is IDA Modeler, which is used to interactively connect component models into system models. Large models are hierarchically structured into multiple levels of subsystems. IDA Modeler is also used as a development and runtime environment for special purpose applications.

In the following subsections Modular Simulation Environments and the Neutral Model Format are explained in more detail.

3.1.1 The Modular Simulation Environments

Physical systems that are simulated in Modular Simulation Environments (MSEs) are modular in nature, i.e. they naturally decompose into subsystems. Frequently, identical subsystems are repeated a number of times in a model, a fact that is taken advantage of in many tools. Furthermore, the systems should have a basically continuous behavior, meaning that equations used to describe them, as well as forcing functions, will have a limited number of discontinuities. Purely event driven systems are excluded. If characterized by equations, the physical systems under consideration will require both algebraic and differential equations. Differential equations can be either ordinary (ODE) or partial (PDE), although current tools, and the present NMF, require that PDEs are explicitly discretized in space and thus turned into ODEs.

They allow a free mixture of algebraic and ordinary differential equations generally referred to as differential algebraic systems of equations (DAE). In addition, the simulation tools under discussion are rarely used for applications where a strict formalism for generating governing equations exists.

In contrast to mainstream design tools in, e.g., building simulation, MSEs separate strictly between the modelling and subsequent system solution activities. A modelling tool is often used for model formulation. It generates a system model, generally expressed in a modelling language. The model is then treated by a solver. An important benefit of a separate solver is that it may be altered or even exchanged with minimal interference with the modelling environment. Some MSEs rely on regular programming languages as part of their system model description. For these, component models are typically described as subroutines with prescribed structure, while interconnection of pre-programmed component models into system models is described with a dedicated language. Other environments have complete modelling languages, which describe component as well as system behavior.

3.1.2   The Neutral Model Format

Without a comprehensive, validated library of ready made component models for a relevant application area most simulation environments are rather useless. To develop all necessary models from scratch is, in many projects, quite unrealistic. And since the cost of developing a substantial library easily exceeds the development cost of the simulation tool itself, it is important to be able to reuse what other people already have done. This was the reason Sahlin and Sowell proposed a text based neutral model format to the building simulation community in 1989. Since then the proposal has attracted a great deal of interest from environment developers and users in several application fields. Additional to IDA, translators have been developed for SPARK (119), ESACAP, TRNSYS (2), HVACSIM+ (2), and MS1. In the present version of NMF, component models (primitive models) are automatically translated from NMF to the proprietary format of the target simulation environment. For example, an NMF model of an axial fan is used to generate an axial fan class in, e.g. IDA, or a corresponding type subroutine in TRNSYS or HVACSIM+. The class is then instantiated in the target environment. The instances are furnished with suitable parameters, and incorporated into a system model.

Pending formal standardization, ASHRAE (American Society of Heating, Refrigerating, and Air-Conditioning Engineers) has formed an ad hoc committee that approves changes to the present format.

NMF has two main objectives: (1) models can be automatically translated into the local representation of several simulation environments, i.e. the format is program neutral and machine readable; and (2) models are easy to understand and express for non-experts. The first objective enables development of common model libraries, which can be accessed from a number of simulation environments. For visualization we show the source code for the Light3[1] model in Appendix A.

---

[1]Light3 is a self written model that controls the light according to the radiation of the sun.

In the last years researchers putting effort into creating a Modelica[1] based library for building simulation (e.g. Wetter (165), Felgner et al. (54), Sahlin et al. (148)). On that account, IDA ICE 4.0 is able to compile also Modelica models and integrate them into the simulation.

3.2 The Occupant Simulation

To make our simulation test bed more realistic we programmed modules for different stochastic processes which are able to simulate the interaction of the inhabitants with the building. The influence of the occupants on the building can be classified through several means of interaction (144):

- Productions of internal metabolic heat gains and pollutants

- Use of appliances (additional free gains)

- Use of artificial lighting (additional free gains)

- Modification of HVAC set points

- Position of blinds

while the first is directly connected to the attendance of a person; the others occur as a consequence of the attendance. As each human being emits heat and pollutants her/his presence directly modifies the indoor environment. In addition to that the interaction with electrical appliances as well as the use of artificial lighting increases the internal heat gains and the consumption of electricity. In office buildings this will mostly be the computer and the coffee machine while in residential buildings the focus will be on the dish cleaner and dryer as consumer. Additionally occupants also interact with the building to enhance their thermal and visual comfort by using the windows, doors and blinds. These interactions will in turn affect the energy consumption for the buildings HVAC unit.

We use the stochastic models originally developed at LESO-PB by Jessen Page (131), they include the latest development in this field of study and are adaptable to our requirements.

3.2.1 Stochastic Model of Occupancy

The stochastic occupancy model can be seen as a centerpiece for the simulation of the occupants behavior since it acts as input to the other stochastic models. The used model predicts the occupancy level using Markov chains. The probability p_t of finding someone in the room only depends on the effective occupancy at the previous time-step p_{t-1} (time appears in discrete time-steps) and on time itself. We must know the occupancy probabilities at different times of

---

[1]Modelica is an object-oriented, declarative, multi-domain modeling language for component-oriented modeling of complex systems, e.g., systems containing mechanical, electrical, electronic, hydraulic, thermal, control, electric power or process-oriented subcomponents

the day, for different days of the week and will most likely consider three different categories: week-days, Saturdays and Sundays, eventually for different months of the year. These probability distributions have a big influence on the model and differ substantially in residential settings compared to offices.

At each time-step, the value of p_t, the occupancy probability of the room, is supposed to be known. Another parameter will have to be entered in order to entirely determine the transition probabilities. So far it has been decided to use a parameter we called the "shuffling" parameter, which is proportional to the intensity of mobility of the occupants. Time is subdivided into discrete time-steps of a duration ranging from 10 minutes (less would go beyond the typical buffer-time of presence detectors) to 60 minutes. In the IDA ICE simulation environment normally variable time steps are used. For that reason the shuffling parameter is modified accordingly to the time steps.

Once the parameters are entered, an algorithm provides a simulation of the occupation of a room over any time span. Theoretically also for more than a single person but the IDA software allows only binary choices for the occupants. This means that the number N of occupants can be chosen before the simulation but not during the simulation, resulting in a binary choice (N or 0).

The algorithm is based on the inverse function method, which is used to draw the values of a random variable given it's distribution law. Once we have an hourly profile of the occupancy probability p_t and a value for the shuffling parameter (which can be time-dependent or constant), we are able to calculate the transition probabilities at each time-step and use the inverse function method to simulate the occupancy.

Let T_{ij} be the transition probability from state i at time t to state j at time $t + 1$. We know that $T_{00} + T_{01} = 1$ as well as $T_{10} + T_{11} = 1$; we therefore only need to calculate T_{01} and T_{11} from our occupancy probabilities. One of the two can be derived from the fact that the probability of having occupancy at time $t + 1$ is given by the case where we had occupancy at time t followed by the transition "occupied to occupied" characterized by T_{11} and the case where we had no occupancy at time t followed by the transition "unoccupied to occupied" characterized by T_{01}. The total probability of having occupancy at time $t + 1$ is therefore given by :

$$p_{t+1} = p_t * T_{11} + (1 - p_t) * T_{01} \tag{3.1}$$

We can then write T_{11} as a function of p_t, p_{t+1} and T_{01} :

$$T_{11} = \frac{1}{p_t} \left(p_{t+1} - (1 - p_t) * T_{01} \right) \tag{3.2}$$

Nevertheless we still have one variable left undefined which in this case is T_{01}. It is therefore necessary to define a new parameter that can easily be understood and quantified by the user. Our proposal is what we called the "shuffling parameter" and that is defined as follows:

$$\beta = \frac{T_{01} + T_{10}}{T_{00} + T_{11}} \tag{3.3}$$

The elements in the numerator represent the possibility of changing states of occupancy whereas those in the denominator represent that of staying in the same state. For example: it is possible to transit from an occupancy probability of $p_t = 0.8$ at time t to $p_{t+1} = 0.8$ at time $t + 1$ with minimal shuffling $\beta = 0$, in which case no one present leaves and no one absent arrives, or maximal shuffling $\beta = \frac{1 + \frac{1}{4}}{0 + \frac{3}{4}} = 1.66$, in which case 60% of the total amount of people stay and 20% leave to be replaced by the 20% that were absent (or also $\frac{3}{4}$ of the people that were present stay while $\frac{1}{4}$ of people that were present are replaced by the people that were absent). Besides, even though the concept behind the shuffling parameter is intuitively understandable, it is still rather difficult to quantify it for the user. For intrested readers we refer to Page (131).

3.2.2 Stochastic model of appliances

The principles below are used for the model suggested by Jessen Page(131), which we implemented in IDA ICE:

- There are two kinds of appliances: the ones which operate independently of the user presence (for instance a refrigerator), and those which are directly driven by the occupancy (for instance, a computer or a TV set). In the latter category, some appliances are only driven by the occupancy (for instance a computer in an office room), and some are additionally following a profile of use (for instance a TV set, which is biased towards the evening, or a cooker, which is biased towards the one or two hours time intervals before the meals).

- A given appliance can be either on or in standby, each of these two states being characterized by a nominal power [W]. Appliances having no standby state are simply characterized by a standby power consumption, equal to nul.

- The stochastic behavior is based on switch-on and switch-off probabilities.

- Finally, each appliance category is characterized by an ownership, i.e. a number of appliances attributed to one person, or to one household (or one unit for an office building). For instance, saying that a fridge has an ownership of 90 % means that the average number of fridge per household is 0.9 (the fridge ownership is given by household); or saying that a computer has a 100 % ownership in office buildings means that everybody has a computer (the computer ownership is specified by person).

3.2.3 Models for artificial lighting

How the artificial lighting is used depends mostly on the occupant and whether there are automated schedules already installed in the building. In Chapter 2.2 we already mentioned the importance of electric lighting regarding the energy consumption. To get a sound comparison

between the different lighting systems we implemented some strategies which mimic the behavior of the occupants. They can be used "out of the box" and easily inserted into an IDA model:

Light1

Light is switched on at a starting time (e.g. 8 am) and switched of at an end time (e.g. 6 pm) during the weekdays. This reflects a worst-case scenario, however it can be observed in many office spaces, especially in open-plan offices.

Light2

Light is switched on if an occupant enters the zone and switched off if the zone is deserted again. This schedule applies to a diligent occupant not taking into account daylighting or an occupancy sensor.

Light3

In addition to the *Light2* control model, the light flux is dimmable and reduced linearly according to the illuminance of daylight:

$$P_{rel} = \begin{cases} (E_{max} - E_{daylight})/E_{max} & \text{if } E_{daylight} < E_{max} \\ 0 & \text{if } E_{daylight} \geq E_{max} \end{cases} \tag{3.4}$$

P_{rel} = relative power of the artificial light [%]
E_{max} = maximum illuminance of the artificial light [lx]
$E_{daylight}$ = illuminance of the daylight [lx]

If there is no occupant it is switched off. This requires an occupancy sensor and an illuminance sensor. Compared with *Light2*, more savings are expected, as during summer time less artificial light will be used. The simulated behavior is shown in Figure 3.2(a).

Light4

This controller realistically mimics the individual control decisions of a human occupant. It is based on the Lightswitch 2002 algorithm of Reinhart (142). As driving parameters for the occupancy and the daylight radiation on the work plane we use the data from our occupancy model and the calculated radiance from IDA. Since the setting of artificial lighting and blinds is often codependent, this is an important input factor for this model.

The original structure of the algorithm slightly changed in order to adapt it to the different time steps that occur in IDA ICE. The Lightswitch 2002 algorithm was originally implemented based on a 5-min time step. For the use in IDA ICE, which is using variable time steps, the stochastic processes must be adapted since the switch on probability depends on the frequency of checking. The controller includes three stochastic processes:
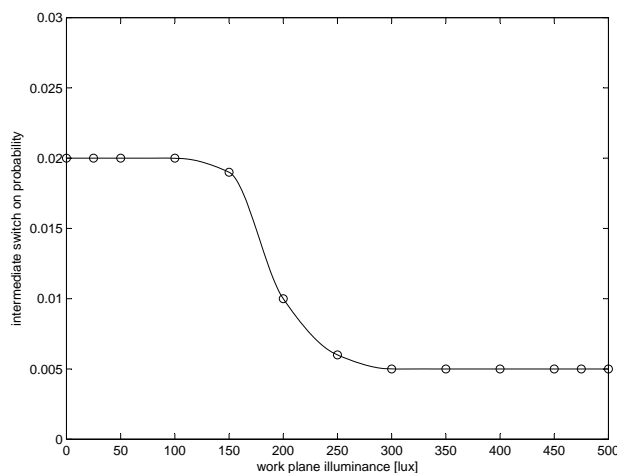
Figure 3.1: Intermediate switch on probability during the next 5 minutes.

- Switch on probability if an occupant arrives or if he just changed the setting of the blinds.

- Intermediate switch on probability. See Figure 3.1.

- Switch off probability if an occupant leaves the zone dependent on the duration of the absence.

The first process does not depend on the length of the time step and therefore can be used directly with variable time steps; it resembles Hunts' (81) function. Also the third process, which determines if the light is switched off before leaving the room, does not depend on the time step of the simulation. In the original model the switch-off probability increases with the absence of the occupant, which sounds comprehensible. Unfortunately, we cannot determine the length of the absence beforehand from the stochastic process. For this reason we use a probability distribution where the switch-off probability is larger in the evening and lower during the daytime.

The second process (Figure 3.1) is more difficult to model because the probability suits a time step of five minutes. In our case we will have different time steps, so we will adjust the probability in the following way:

$$P_{Inter,T} = \begin{cases} 1 - (1 - P_{Inter,300})^{\frac{T}{300}} & \text{if } E_{daylight} \neq 0 \\ 1 & \text{if } E_{daylight} = 0 \end{cases} \tag{3.5}$$

$P_{Inter,T}$ = adapted intermediate switch-on probability during the next time step T [-]
$P_{Inter,300}$ = intermediate switch-on probability during the next 300 seconds [-]
$E_{daylight}$ = illuminance of the daylight [lx]
T = time step [s]

28

For example, if the workplane illuminance is equal to 100 lux the probability that the user will switch on the light is $P_{Inter} = 0.02$ each five minutes. But if it is checked only every ten minutes the probability has to be higher to reflect the original process, therefore the adapted probability is $P_{Inter\,Adapt} = 1 - (1 - P_{Inter})^{\frac{600}{300}} = 0.0396$.

The simulated behavior is shown in Figure 3.2(b).

3.2.4   Models for blinds

Additional to the artificial lighting the blinds are important instruments for controlling the room environment. On one hand they affect the lighting situation; on the other hand they have a large influence on the solar gains through the window. Therefore we implemented three different module (Blind1, Blind2, Blind3) which simulate the behavior of an occupant regarding the use of blinds.

Blind1

The blinds are never used and stay open for the entire day. This situation reflects buildings without blinds, which is the best case for minimizing the heating cost by maximizing solar gains. However it is the worst case regarding the cooling energy consumption during summer time and mid-season.

Blind2

The blinds are lowered (in this case at 8am) and opened (at 6pm) at the same time every week-day. On weekends they stay open. In offices where occupants' work in front of computer screens all day, even the slightest sun can induce glare. Therefore, sometimes open-plan offices are lit completely by artificial lighting while the blinds stay closed during daytime. A consequence of this is that most of the solar gains are blocked and more heating energy is required; it diminishes however cooling during summer.

Blind3

With this controller we try to mimic the behavior of an occupant regarding the use of blinds. We assume that textile blinds are used and therefore do not consider slat angles in this controller. The flow chart of the algorithm is shown in Figure 3.3. The model resembles the branch of Reinhart's (142) blind model where manual control is assumed with two major changes:

1. The blinds are lowered directly if solar irradiance is larger than 100 W/m^2 and its incident angle is lower than 55° since the risk of glare increases with low incident angle.

2. A stochastic process is included to determine when the occupants check the above-mentioned conditions. If they still apply the blinds stay closed, if not they are opened.
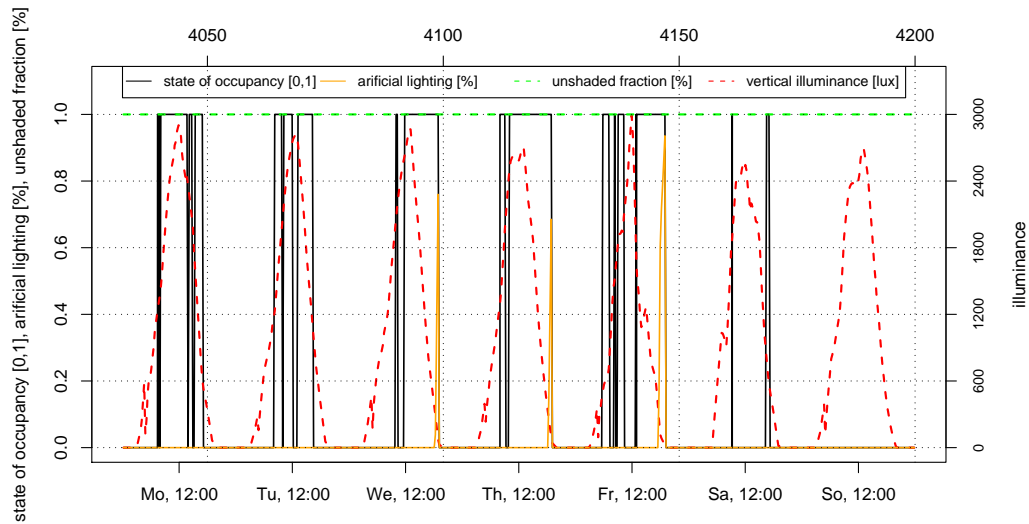
(a) Simulated switch-on profile for Light3 control model in combination with Blind1.
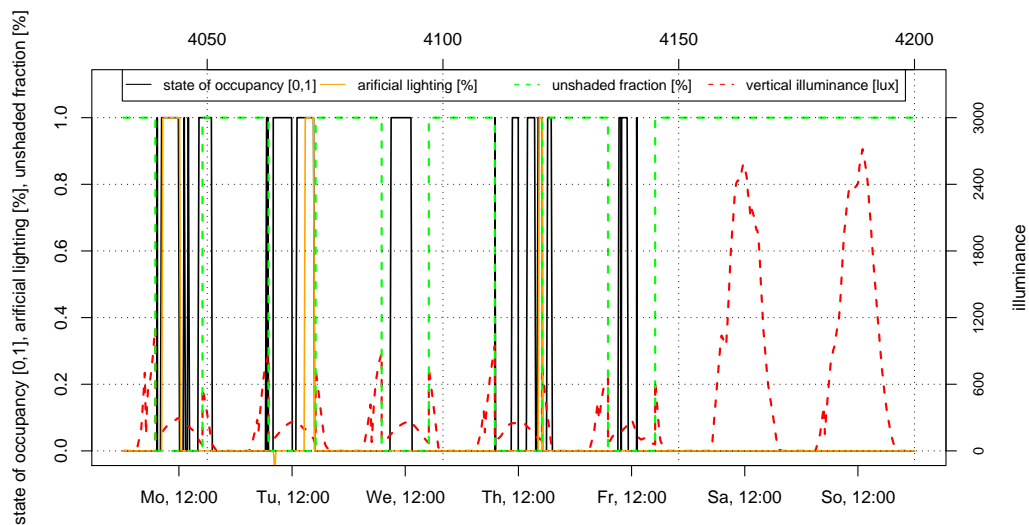
(b) Simulated switch-on profile for Light4 control model in combination with Blind2.

Figure 3.2: The state of occupancy is shown with a black line, the unshaded fraction of the window is shown with a green dashed line, the relative power of artificial lighting with a orange line, and the horizontal illuminance is shown with a dashed red line. On the upper x-axis the time in total hours of the year is shown; it corresponds to the third week of June.
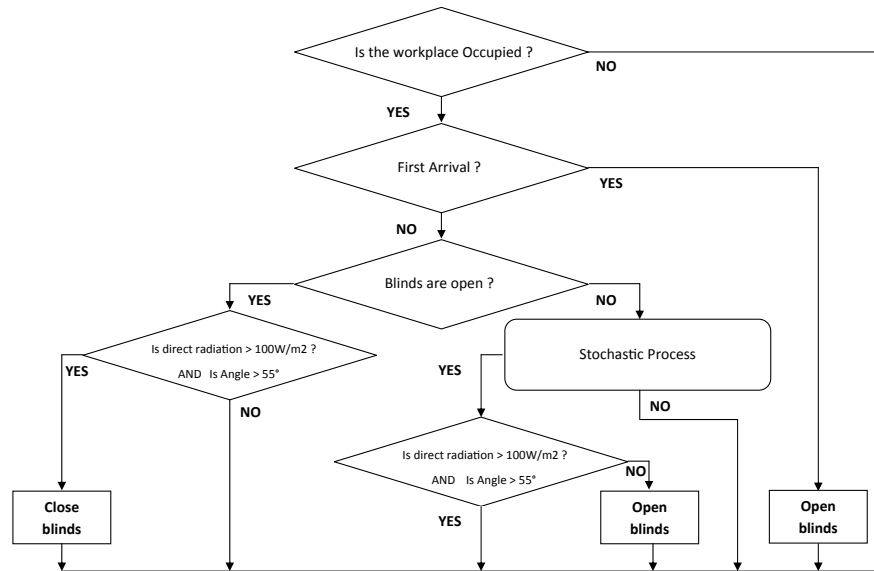
Figure 3.3: Flow Chart for the Blind3 algorithm. In the case of *Close blinds* the blinds are completely lowered and in the case of *Open blinds* they are completely opened. The stochastic process checks the condition of openings with a 5% probability during the next 300 seconds.

In the original Ligthswitch algorithm blinds are only opened once a day, and closed according to a fixed threshold for visual comfort. This is based on former studies that report predominant passive action on blinds. Foster and Oreszcyn (56) reported that blinds are left untouched in single offices for weeks while Inoue et al. (84) found that some occupants tend to open their blinds once a day. In recent studies Nicol and Humphreys (125) and Haldi and Robinson (71) mentioned an increase of blinds lowered as indoor and outdoor temperature increases. Mahdavi et al. (112) surveyed three different buildings and found strong distinctions in the frequency of blind use (opening and closing) for the different buildings, according to the different occupants. However, this study also found a relationship between global vertical irradiance and *closing of the blinds*. No clear relationship is found for the *opening of the shades*. In all the mentioned studies they reported major differences between single occupants.

It is fair to say that the use of blinds strongly depends on the occupant. In this case we want to model a diligent and active occupant, which is the reason why we add a stochastic process that is triggering the blind opening action. In the original model there is no opportunity for the blinds to be opened once they have been closed. To incorporate this, a 5% chance (based on a 5-min time step) of opening the blinds if the meterological conditions have changed, is included in our control model. This change is not based on a field study but makes a *best-case* estimation for a diligent occupant.

Blind4

This is an optimized blind control that is explained in Chapter 5.7. It is used as reference for the best case.

3.3 Chapter summary

In this chapter we introduced the building simulation software we use for evaluating the blind control system and showed that it can be coupled and extended with stochastic processes (occupancy and appliances) for occupants simulation. They can be easily inserted into any building simulation carried out with IDA ICE. Since the occupancy is used as driving variable for many controls it is important for the accuracy of our simulation. With the implementation and adaptation of the Lightswitch 2002 algorithm we can also simulate the behavior of an occupant in regard to the use of artificial lighting and blinds. We also introduced more basic control models for blinds and artificial lighting that are often found in office space or resemble simple controls; those can be used for benchmarking our control.

4

The optimization environment

In this chapter we want to establish an environment where it is possible to optimize different properties of a building. For our research this framework is mostly used for optimizing the behavior of shading devices, however it can also be used for any other control, but also for design of windows, layers of insulation or any other characteristic. The framework stays the same, only the objectives of the optimization and the search space have to be customized to the problem.

The object of our optimization is not directly the movement of the blind or any actuator; it is the control. For that reason the control has to meet some specifications, for example that it can emulate all kind of nonlinear function with its parameters. For that, the concept of fuzzy logic control fits best the requirements.

First we present the basic concepts of genetic algorithms (GA) which we use for optimization, and explain the concept of fuzzy logic and fuzzy logic controls, afterwards the connection to the simulation environment (Chapter 3) is shown.

4.1   Optimization process

Optimization is something all of us do constantly in our everyday lives, even if we are not aware of it. We try to find the fastest way to get to the office or try to cook our eggs to exactly the degree of done-ness we like. We do these things to find a better solution to our problems. In fields such as industry, economics or engineering, the goal is similar but the problems are much more sophisticated. For example, an optimized design of a gas-turbine in a power plant can save a lot of money. Generally, optimization refers to a problem in which one is trying to maximize or minimize a system performance with some systematic procedure, also called optimization algorithm. The large variety of different optimization problems requires different strategies for solving them. Corne and Knowles (38) gave a good definition of an optimization algorithm:

An optimization algorithm is a process which generates a sequence of points from the search space, i.e. it visits points in the search space one by one in a given order. Which point is visited next depends only on the points visited previously.

In the following section, we present an introduction to optimization and the evolutionary approach which can help to solve some optimization problems.

4.1.1   Single Objective Optimization

In general a single optimization problem can be written as:

$$
\begin{aligned}
&\underset{\mathbf{x}}{\text{Minimize}} && f(\mathbf{x}), \\
&\text{Subject to} && g_i(\mathbf{x}) \geq 0, && i = 1, 2, ..., I, \\
& && h_k(\mathbf{x}) = 0, && k = 1, 2, ..., K, \\
& && \mathbf{x}^{(L)} \leq \mathbf{x} \leq \mathbf{x}^{(U)}
\end{aligned}
$$

$$(4.1)$$

where $\mathbf{x}$ is the solution vector, $g_i(\mathbf{x})$ is the constraint function and the last set of constraints are the variable bounds which restrict each variable to a lower $\mathbf{x}^{(L)}$ and an upper bound $\mathbf{x}^{(U)}$. Furthermore we define that $f : \mathbb{R}^n \to \mathbb{R}$, $g : \mathbb{R}^I \to \mathbb{R}$, and $h : \mathbb{R}^K \to \mathbb{R}$ for some $n, I, K \in \mathbb{N}$, and that $\mathbf{x}^{(L)}, \mathbf{x}^{(U)} \in \mathbb{R} \cup \{\pm\infty\}$, with $\mathbf{x}_i^{(L)} < \mathbf{x}_i^{(U)}$, for all $i \in \{i = 1, 2, ..., n\}$. The inequality constraints are $g_i(\mathbf{x})$ and $h_k(\mathbf{x})$ are the equality constraints. All constraints can be expressed as inequality constraints. Thus, a solution that satisfies all constraints is called a feasible solution. On the other hand, if a solution violates at least one constraint it is called an infeasible solution. Throughout this work we always define the optimization as a minimization problem.

Definition 4.1.1 (Feasible Set)

The Feasible Set $\Omega_S \subset \mathbb{R}^n$ of the search space for problem (4.1) is the set of feasible solutions. These are all $x \in \mathbb{R}^n$ that satisfy

$$
\begin{aligned}
&g_i(\mathbf{x}) \geq 0, && i = 1, 2, ..., I, \\
&h_k(\mathbf{x}) = 0, && k = 1, 2, ..., K, && \text{and} \\
&\mathbf{x}^{(L)} \leq \mathbf{x} \leq \mathbf{x}^{(U)}.
\end{aligned}
$$

$$(4.2)$$

Definition 4.1.2 (Infeasible Set)

The Infeasible Set $\Omega_F \subset \mathbb{R}^n$ of the search space for problem (4.1) is the set of infeasible

solutions. These are all $x \in \mathbb{R}^n$ that satisfy at least one of the equations

$$
\begin{aligned}
g_i(\mathbf{x}) &< 0, & i &= 1, 2, ..., I, \\
h_k(\mathbf{x}) &\neq 0, & k &= 1, 2, ..., K, \\
\mathbf{x}^{(L)} &> \mathbf{x}, & &\text{or} \\
\mathbf{x} &> \mathbf{x}^{(U)}.
\end{aligned}
$$

(4.3)

Optimization algorithms try always to find a global optimum, which is the best value of the objective function in the search space. During the search they may identify many local optima, that is only the best choice for a defined neighborhood of the solution, hoping also to find the global optimum.

Definition 4.1.3 (Neighborhood)

In the neighborhood of point x are all points y with

$$
N_t(x) = \{ y \in S | d(x, y) \leq t \}
$$

Definition 4.1.4 (Local Optimum)

A point x is a local optimum of the objective function f if

$$
f(x) \leq f(y), \quad \forall y \in N_t(x) \cap \Omega_S
$$

Definition 4.1.5 (Global Optimum)

A point x is a global optimum of the objective function f if

$$
f(x) \leq f(y), \quad \forall y \in \Omega_S
$$

4.1.2 Multi-Objective Optimization

In the real world, it is rare that any problem can be represented adequately through the consideration of only a single objective. That means, in general we have to deal with a multi-objective optimization problem (MOOP) where we can find a vector of objective functions

$$
\mathbf{f}(x) = \{ (f_1(x), f_1(x), \ldots, f_m(x) \}
$$

(4.4)

that must be traded off in some way. The relative importance of these objectives cannot normally be foreseen and can only be determined when the capabilities of the solutions are

known and the problem is fully understood. As the number of objectives increases, the trade-off also gets more complex and cannot be quantified directly. We may also have to handle redundant objectives which are not identified as redundant yet (19; 44). However, there are different approaches to face these problems. In this section, we give an introduction to multi-objective-optimization and introduce both some classical methods, as well as the use of genetic algorithms to handle these kinds of problems.

4.1.2.1 Multi-Objective Optimization Problem

The general form of a multi-objective optimization problem is:

$$
\begin{aligned}
\underset{(\mathbf{x})}{\text{Minimize}} \quad & f_m(\mathbf{x}), & m &= 1, 2, ..., M, \\
\text{Subject to} \quad & g_i(\mathbf{x}) \geq 0, & i &= 1, 2, ..., I, \\
& h_k(\mathbf{x}) = 0, & k &= 1, 2, ..., K, \\
& \mathbf{x}^{(L)} \leq \mathbf{x} \leq \mathbf{x}^{(U)}
\end{aligned}
\tag{4.5}
$$

where f_m is the fitness of the objective m, which is the only difference between this case and the single-objective optimization problem in equation 4.1. The most evident difference from single objective optimization is that there is not necessarily one *best* solution to the problem because all the components of $\mathbf{f}(x)$ are competing. The constraint functions are the same in the single- and multi-objective cases. The only difference are the multiple objectives.

4.1.2.2 Classical Methods

Most classical approaches just convert the multi-objective problem into a single-objective problem, for which classical optimization algorithms work well. The drawback with those approaches is that with a preselection of parameters, which is needed for the different methods, the search space is influenced and *good* solutions may be excluded.

Weighted Sum Method

The weighted sum method converts the multi-objective problem of minimizing the vector $f(\mathbf{x})$ into a single-objective by constructing a weighted sum of all objectives.

$$
\text{Minimize} \qquad f_{sum}(\mathbf{x}) = \sum_{m=1}^{M} w_m f_m(\mathbf{x})
\tag{4.6}
$$

Here M is the number of objectives, f_m is the fitness function of the objective m, and w_m is the corresponding weight of that objective. The weighted coefficients do not necessarily correspond directly to the relative importance of the objectives and the tradeoff has to be specified
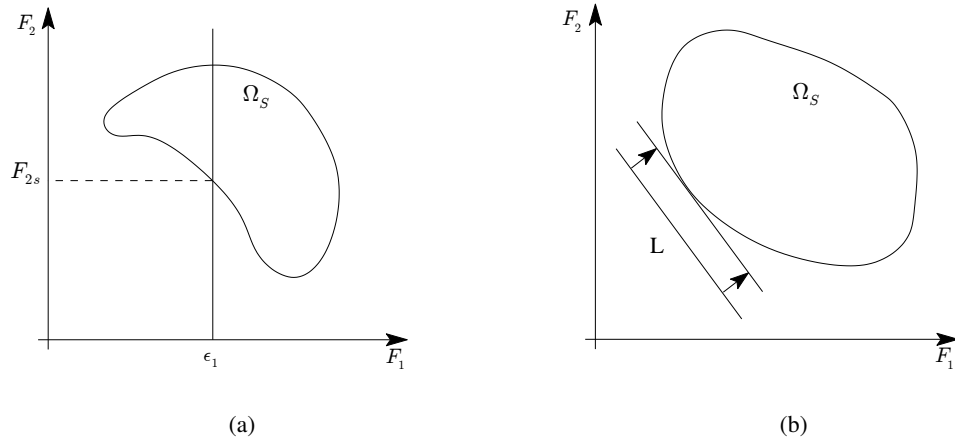
Figure 4.1: (a) The ϵ-Constraint Method (b) The Weighted Sum Method

by the decision-maker before anything is known about the solutions. Figure 4.1(b) illustrates the procedure, in which we consider a two-objective case. The slope of the line L which is drawn is defined by the weights w_1 and w_2; the minimization can be interpreted as finding a value so that L just touches the feasible area on one point as it proceeds outward from the origin.

epsilon-Constraint Method

Another popular approach is the ϵ-constraint method. Here one of the objectives is chosen and the others are treated as constraints by limiting each of them to a pre-defined range which can be expressed as follows:

$$\begin{aligned} & \text{Minimize} && f_p(\mathbf{x}) \\ & \text{Subject to} && f_i(\mathbf{x}) \geq \epsilon, && i = 1, 2, ..., I, && i \notin p \end{aligned}$$

(4.7)

This procedure overcomes some of the convexity problems and is able to identify a number of non-inferior solutions on a non-convex boundary that are not obtainable using the weighted sum approach. A problem with this method is, however, a suitable selection of ϵ (shown in Figure 4.1(a)) to ensure a feasible solution and to express the true design objectives of the decision maker. It is often difficult to generate this information at an early stage of the optimization process. A further disadvantage of this approach is that the use of hard constraints is rarely adequate for expressing true design objectives.

4.1.2.3 Pareto Dominance

The concept of Pareto[1] dominance is used in most of the multi-objective optimization algorithms. Assuming the above mentioned optimization problem 4.5 with m objectives and the solution vectors x_1 and x_2 we can define:

Definition 4.1.6 (Pareto dominance)

A solution x_1 is said to dominate the solution x_2, if both conditions 1 and 2 are true:

1. The solution x_1 is not less than x_2 in all objectives.

2. The solution x_1 is strictly greater than x_2 in at least one objective.

Then $x_1 \succ x_2$ (x_1 Pareto-dominates x_2).

With the help of Pareto dominance we cannot rate all solutions against each other but at the end we can identify a set of solutions which are non-dominated in respect to the solutions outside that set. That means that all the solutions outside this set are dominated by at least one solution inside the set. Now it is possible to identify a set of solutions which is better than all the other solutions without simplifying the problem. We can define a non-dominated set as follows:

Definition 4.1.7 (Non-dominated set)

Among a set of solutions P, the non-dominated set of solutions P' are those that are not dominated by any member of the set P.

To illustrate the concept of Pareto dominance see Figure 4.2.

4.2   Evolutionary Optimization

Evolutionary computation is a steadily increasing research discipline covering computer algorithms that are inspired by principles of natural evolution. Basically, it is a mimiking of three main mechanisms which drive evolution forward - reproduction, mutation and natural selection. Nature was capable of finding lots of solutions to environmental problems such as the self-cleaning surface of the lotus or the aerodynamic shape of a shark. So why not simulate these well-established events to find solutions in optimization problems? This chapter will give the reader the essential knowledge about evolutionary computation and its core theory based on the theories of Darwin.

---

[1] The term is named after Vilfredo Pareto, an Italian economist who used the concept in his studies of economic efficiency and income distribution. Informally, Pareto efficient situations are those in which it is impossible to make one person better off without necessarily making someone else worse off.
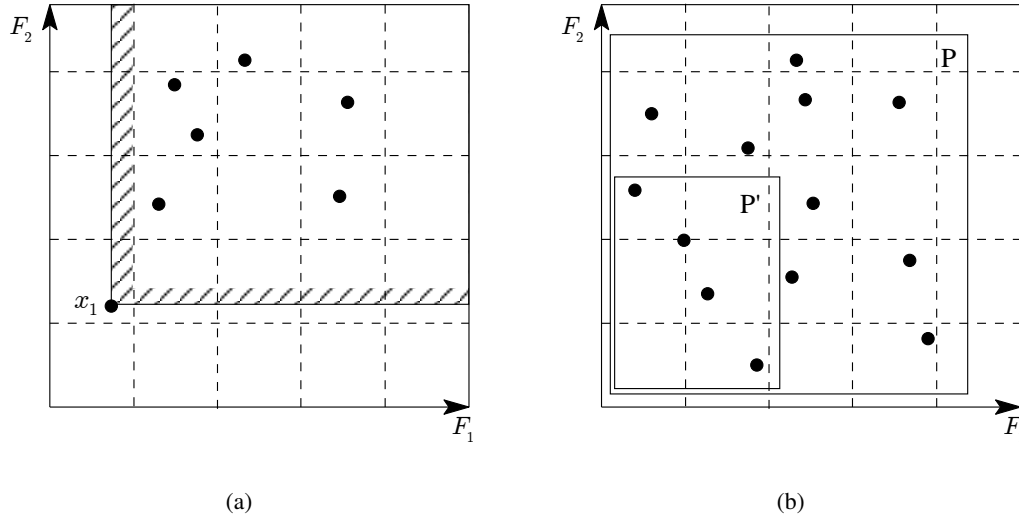
Figure 4.2: (a) x_1 dominates the rest of the solutions (b) P' is the non-dominated set and P the set of solutions

4.2.1 Biological Evolution

Biological evolution was and still is capable of creating all kinds of creatures during the last millions of years, all of which were specially adapted to their environment. This adaptation to the environment did not happen in a sudden shift between parents and offspring. It is a slow process involving minor changes in every generation, called evolution. If the changes that occur during one generation are helpful to the individual in some way, it increases the probability of surviving and reproducing. Over the generations, the change will accumulate and lead to better adaptation of the species. Darwin described the principles of evolution for the first time in his work 'The Origin of the Species':

> *Owing to this struggle, variations, however slight and from whatever cause proceeding, if they be in any degree profitable to the individuals of a species, in their infinitely complex relations to other organic beings and to their physical conditions of life, will tend to the preservation of such individuals, and will generally be inherited by the offspring. The offspring, also, will thus have a better chance of surviving, for, of the many individuals of any species which are periodically born, but a small number can survive. I have called this principle, by which each slight variation, if useful, is preserved, by the term natural selection, in order to mark its relation to man's power of selection.*

Before giving a closer look at biological evolution, we must first introduce some concepts which are used in a similar manner in the field of evolutionary algorithms.

- **Gene:**
  The gene is a segment of chromosomes that constitutes the smallest unit of information. Genes consist of long strands of deoxyribonucleic acid (DNA) and can be defined as the blueprints for constructing life.

- **Allele:**
  Each gene can have different alleles. Sometimes, different DNA sequences (alleles) can result in different traits, such as color. Sometimes, different DNA sequences (alleles) will have the same result in the expression of a gene.

- **Chromosome:**
  This is a single, large set of genes.

- **Genome:**
  The genome of an organism represents the whole hereditary information that is coded in the DNA. The word was coined by Hans Winkler by combining the words **gen**e and chromos**ome**.

- **Phenotype:**
  This is the complete physical appearance and constitution of the individual.

- **Genotype:**
  The genotype is the composition of the individual genes. If there is a change in the genotype, i.e. in the genes, there can be also a change in the phenotype, the appearance, but this does not necessarily occur

But what is evolution and when does the change in individuals occur? With every generation, genes from the parents are recombined and an offspring is formed. The most important terms will be explained shortly:

- **Mutation:**
  Mutation is based on "copying errors" during the reproduction of the DNA. They are responsible for a steady change in the form of a species; even though most of the single mutations have no direct impact on the phenotype, a change will occur by summing up minor mutations.

- **Recombination:**
  Recombination takes place at the sexual mating, where the genotypes of the parents are combined. Even if it is only a combination that does not create something new the fact that a new genotype is created from the mass of possibilities makes the recombination more important in nature than the mutation.

- **Selection:**
  During selection, the ratio of the allele is changed in the population. This is caused, for example, by a better adaptation to the environment of individuals with that special allele.

This stage has the most influence on the future generation. Only the fittest individuals create offspring and can reproduce their genotypes. But nature does not work towards a specific goal, such as making longer necks for giraffes. What counts is the fitness and how well the individuals are adapted in that specific moment. However, there are always minorities in a population: this is called polymorphism. It is not yet completely understood where it comes from and why it is there, but it keeps diversity in a population.

- **Genetic Drift:**
  During a sequence of generations, some alleles can die out because of a random chain of events.

4.3   Genetic and Evolutionary Algorithms

Evolutionary algorithms (EAs) have been invented independently by different researchers: by John Holland (77) who was working at the University of Michigan and introduced genetic algorithms (GAs), and also by Ingo Rechenberg (141) from the Technical University of Berlin, who discovered evolutionary strategies. Both approaches are based on the theory of evolution and belong to evolutionary algorithms. Nevertheless, it was not before the mid 80's, with the advent of the faster computers that evolutionary algorithms were tested on practical problems. Through Goldberg's book "'Genetic Algorithms in Search, Optimization, and Machine Learning" (64) the topic finally attracted notice to the scientific community. Even if today most EAs cannot be characterized clearly as genetic or evolutionary algorithms, a difference was perceived at the beginning. Evolutionary algorithms usually work with a real value representation of the solution; the shift in the generation is mainly driven through mutation. In contrast, genetic algorithms use a binary encoding for the solutions, which directly represent the genes of an individual.

4.3.1   Evolutionary Optimization

Evolutionary Algorithms try to imitate the natural evolutionary principles according to Darwin while preserving a global search potential. The peculiarity of EAs is the maintenance of a set of elements *(the population)* that are searched parallel to one another. The fitness function assigns a *'fitness'* to every solution according to the optimization problem. Based on this fitness value the algorithm evaluates the solutions. The decoding function translates the individuals to the *real world optimization problem*. We will now define the two basic spaces, the fitness function, decoding function and the feasible and infeasible set of solutions.

Definition 4.3.1 (Search Space, Solution Space)

The Solution Space G represents the feasible solutions in the real optimization problem.

The Search Space S is the set that is searched by the optimization algorithm.

Definition 4.3.2 (Fitness Function)

The Fitness Function $f : S \rightarrow \mathbb{R}$ is defined on S and assigns a real value to the solutions.

Definition 4.3.3 (Decoding Function)

The Decoding Function $d : S \rightarrow G$ maps the elements of S into G

Furthermore, an EA contains a set of genetic operators that work on the population. They perform the basic principles of evolution *selection* and *variation*. The selection shifts the focus of search towards better solutions and better regions in the search space, while variation operators create new elements in the search space. This is done with the mutation and crossover operator and also maintains diversity in the population.

- **Initialization:**
  The initial generation is created. This can be done randomly or by using any heuristical knowledge.

- **Evaluation:**
  EAs work with some kind of representation of the solution. For that the solutions have to be evaluated according to the objectives. In most cases these are the objective functions of the *real problem*. If there are constraints, we can also define some metrics using the objective function and the constraint violations to assign a fitness value to the solution.

- **Selection:**
  The selection operator has the task of deciding which solutions are chosen for the mating pool. The individuals from the mating pool are used to generate new offsprings, and by doing this they form the new generation. Since the individuals in the mating pool are those from which genes are recombined and passed on to the next generation, it is desirable that only good solutions are chosen. For that the selection operator basically changes the selection probability p_i of the individual i with the result that good solutions are picked with higher probability than bad solutions (63). The selection operator has to guide the population in the right direction. By doing that, the optimization can gradually concentrate on the relevant areas of the search space. The basis of the evaluation of the individuals is mostly the objective function. As a theoretical measure and for the comparison of different methods, we can define the selection intensity:

Definition 4.3.4 (Selection Intensity)

The intensity I of the selection operator is defined as

$$I = \frac{\bar{F}_{sel} - \bar{F}}{\sigma} \tag{4.8}$$

Here $\bar{F}_{sel}$ is the average fitness of the population before and $\bar{F}$ after the selection. To get a normalized measure which does not depend on the search space, the difference is divided by the standard deviation σ. The selection pressure has a great influence on the convergence rate of the algorithm (115). A high intensity indicates a lot of selection pressure and fast convergence.

There exist many well known methods for achieving those goals. Here are the most important ones:

– **Tournament Selection**
   This method introduces the selection pressure by holding a tournament between s solutions, where s is the tournament size. The individual with the highest fitness out of the s competitors is the winner and will be removed from the set of solutions and put into the mating pool. This step is repeated until enough individuals are inserted into the mating pool. Since only the best individuals of the tournament rounds are inserted, the average fitness in the mating pool will be superior to the fitness in the original population. The selection pressure can be easily increased by increasing the tournament size s, since being the best individual among a larger set is always harder than to be the best out of a smaller set.

– **Proportional Selection**
   Here the selection probability of each individual is proportional to its fitness value f_i.

$$p_i = \frac{f_i}{\sum_{i=1}^{I} f_i} \tag{4.9}$$

   A good illustration for this approach is a roulette wheel with slices for every solution in an size according to the selection probability p_i. The solution where the wheel stops is selected for the mating pool and then removed from the wheel. This is repeated until enough individuals are selected.

– **Linear Ranking Selection**
   Here every individual is ranked according to its fitness value. The rank of the least fittest individual is defined to be zero. The selection probability of the others are proportional to their rank $r_i \in (1, \dots, I)$:

$$p_i = \frac{b}{n} - \left(\frac{2b - 2}{n} \right) \left(\frac{r_i - 1}{n - 1} \right) \tag{4.10}$$

   where $b \in [1, 2]$ defines the selection pressure.

- **Crossover:**

  This operator is capable of creating new individuals by combining the selected solutions. The idea behind performing a crossover is that new individuals may be better than their parents if they choose the best characteristics from each parent. For that, it is important that the design of the operator concerns itself with the structure of the individuals. Genetic information which belongs together should not be destroyed and should be used by the offspring. We introduce some operators for both binary and real-value coded individuals.

  For binary coded individuals the crossover is more intuitive and can be performed with:

  - **k-Point Crossover**

    Here k breaking bids are chosen and between the breaking bids the binary strings of the two individuals are exchanged. Mostly one or two-point crossover is used.

  - **Uniform Crossover**

    Here for each gene or binary digit the operator decides from which parent it is taken.

  In case of real value coded individuals there are:

  - **Blend Crossover (BLX-α)**

    Assuming that $x_{1,i}^t$ and $x_{2,i}^t$ are two parent solutions with $x_{1,i}^t < x_{2,i}^t$ then the BLX-α operator creates an offspring with:

    $$x_{1,i}^{t+1} = (1 - \gamma_i)x_{1,i}^t + \gamma_i x_{2,i}^t, \tag{4.11}$$

    where $\gamma_i = (1 + 2\alpha)u_i - \alpha$ and u_i is a random number between 0 and 1. The offspring then is in the range of $\left\{ x_{1,i}^t - \alpha(x_{2,i}^t - x_{1,i}^t), x_{2,i}^t + \alpha(x_{2,i}^t - x_{1,i}^t) \right\}$. The location of the child depends on the difference between the parent solutions. If the difference between the parents is small the offspring will be respectively similar to the parents (52).

  - **Simulated Binary Crossover (SBX)**

    As the name suggests, this operator wants to simulate the principle of a singe-point crossover on a binary string for real-coded solutions (45). First, a random number u_i between 0 and 1 is created. According to that, β_i is calculated with the following equation:

    $$\beta_i = \begin{cases} (2u_i)^{\frac{1}{\eta+1}} & \text{if } u_i \leq 0.5; \\ \left(\frac{1}{2(1-u_i)}\right)^{\frac{1}{\eta+1}} & \text{otherwise,} \end{cases} \tag{4.12}$$

    The distribution index η is any nonnegative real number. With a large value of η close solutions have a higher probability of being chosen and with a smaller η

distant solutions will be chosen with higher probability. Then the offsprings are given as follows:

$$x_{1,i}^{t+1} = 0.5 \left[(1 + \beta_i)x_{1,i}^t + 1 - \beta_i)x_{2,i}^t \right],$$
$$x_{2,i}^{t+1} = 0.5 \left[(1 - \beta_i)x_{1,i}^t + 10\beta_i)x_{2,i}^t \right]$$

(4.13)

Here, for each gene or binary digit the operator decides from which parent it is chosen.

- **Mutation:**
  The mutation operator slightly changes the genotype of an individual. The degree of modification and the impact on the phenotype depends on the mutation operator. If the mutation operator creates only solutions or phenotypes in the immediate neighborhood, then the goal can only be the fine-tuning of the solution. If the mutation has a big impact on the individual, the goal is the exploitation of the search space. Again, there is a difference between real-coded and binary-coded solutions. For a binary-coded system the mutation can be a randomized bit flip. For a real-value solution you can just add a normal distributed random variable to the solution ($x = x + N(0, \sigma)$). A difficulty is the choice of the probability and the distribution of the mutation. Some work has already been done on this aspect - for this we refer readers to Rechenberg (141) and Schwefel (152). Normally, not all individuals are mutated in every generation. The probability for each individual of mutation occurring is set by the mutation probability p_m. $M''(t)$ represents the mutated population.

- **Update Population:**
  Here the new generation is formed out of the parent and offspring population. Here we apply *survival of the fittest* and the best μ individuals are chosen for the next generation. It can be based only on the offspring generation or on both, the parent and the offspring generation.

4.3.1.1 NSGA2: A Multi Objective EA

The non-dominated sorting genetic algorithm (NSGA) has been proposed by Deb et al. (46). In this section, we introduce the NSGA2 which is used throughout this work. The NSGA2 is based on a normal GA; however there are some modifications to adapt the algorithm to the multi-objective case. There are basically two features:

1. Non-dominated sorting

2. Crowding distance sorting

Algorithm 1 Evolutionary Algorithm

1: $t \leftarrow 0$

2: *initialization:* initialize population $P(0)$

3: **while** termination condition $\neq$ true **do**

4:      evaluate $P(t)$

5:      selection: mating pool $M(t) \leftarrow select(P(t))$

6:      crossover: $M'(t) \leftarrow crossover(M(t))$

7:      mutation: $M''(t) \leftarrow mutation(M'(t))$

8:      update population: $P(t+1) \leftarrow update(P(t) \cup M''(t))$

9:      $t \leftarrow t + 1$

10: **end while**

Initially, a feasible, uniformly distributed random population P_0 with size N is created. Then we create a child population Q_0, also of size N, with the usual binary tournament selection, recombination and mutation. The combined population $R_0 = P_0 \cup Q_0$ is formed. Then the non-dominated Pareto front is identified and all solutions in that front are assigned to F_1. After that, F_1 is removed from R_0 and the new non-dominated set is assigned to F_2. This operation is repeated until R_0 is empty. Now all solutions are ranked in different subsets, with R_0^1 being the subset with the best solutions. For the next generation, we have to reduce the population from $2N$ to N individuals. Since our solutions are already sorted, we start filling the new generation with R_0^1, then R_0^2 and so on until the population size of N is reached. For the last subset, we cannot choose all solutions, so we need a second criterion, the crowding distance. If it is not possible to take all solutions and we cannot rank them according to each other, at least the diversity of the solutions should be emphasized. To do this, the solutions are sorted according to the crowding distance and P_1 is filled up with the most widely spread solutions.

The basic algorithm is shown in Figure 4.3 and algorithm 2:

4.4 Fuzzy logic theory

Consider the problem of assigning cars to the two sets *old cars* or *new cars*. Consider classical set theory where an element is either a member of a set or not. If you define an old car is older than 5 years clearly a car which is 13 years old belongs to the set *old cars*. But what is with a car in good shape which has an age of six years; it has to go to the group with old cars. Consequently, using two-valued set theory there is no distinction in a set, meaning that there is no difference between the 13 year old car and the six year old one, they belong equally to the set.
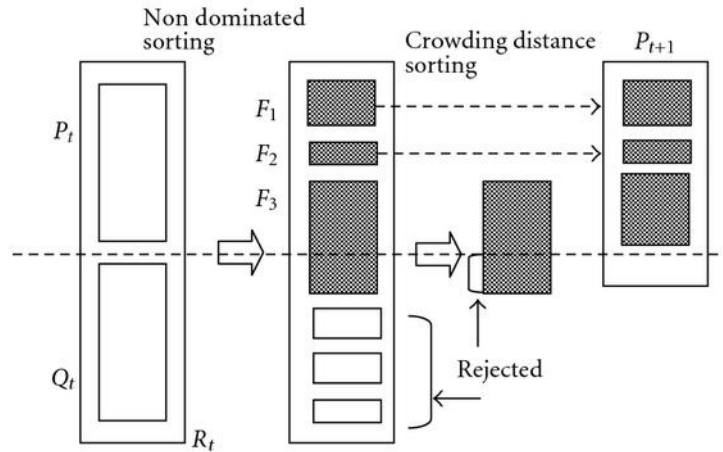
Figure 4.3: Scheme fot the NSGA II algorithm.

Algorithm 2 NSGA2 update population

1: combine parent and child population $R_0 = P_0 \cup Q_0$

2: perform non-dominated sorting into multiple subsets $F = (F_1, F_2, \ldots)$

3: set $P_{t+1} := null, i = 1$

4: **while** $(|P_{t+1}| + |F_i| \leq N)$ **do**

5: $\quad P_{t+1} = P_{t+1} + F_i$

6: $\quad i = i + 1$

7: **end while**

8: Sort F_i according to crowding distance

9: choose the first $(N - |P_{t+1}|)$ element out of F_i

10: use selection, crossover and mutation to create a new population Q_{t+1}

11: $t = t + 1$

However, fuzzy sets have no problem with this situation. The two cars will be both members of the set *old cars* but both to a different degree. For example, a 13 year old car may be a member to that set to a degree of 0.95, whereas the 6 year old car belongs to the set to a degree of only 0.3.

Throughout this work the concept of fuzzy logic is used, especially for our control. For that we introduce the basic concepts in this section.

4.4.1 Formal definitions

In contrast to classical sets, elements of fuzzy sets have degrees of membership which indicate the certainty (or uncertainty) that this element belongs to that set. Suppose X is the domain, or universe of discourse, and $x \in X$ is a specific element of the domain X. Then the fuzzy set A is characterized by a membership mapping function:

$$\mu_A : X \rightarrow [0, 1] \tag{4.14}$$

Therefore, for all $x \in X$, $\mu_A(x)$ indicates the certainty to which element x belongs to fuzzy set A. Fuzzy sets can be defined for discrete or continuous domains.

4.4.2 Membership functions

A membership function, also referred to as the characteristic function, is the essence of fuzzy sets and defines it. The function is used to assign a degree of membership to each of the elements of the domain to the corresponding fuzzy set. Also two valued sets can be characterized by membership functions. For example, consider the domain X of all floating-point numbers in the range $[0, 10]$. Define the crisp set A in the range $[2, 3]$, then $\mu_A(x_i) = 1$ for all $x \in [2, 3]$ and $\mu_A(x_i) = 0$ for all the others.

Membership functions can be of any shape as determined by experts in the domain over which the set is defined, nevertheless they have to satisfy the following constraints:

- The range of a membership function has to be in $[0, 1]$

- For each $x \in X, \mu_A(x_i)$ must be unique.

Many different functions can be used, for example:

- Triangular functions:

$$\mu_A(x; a, b, c) = \begin{cases} (x - a)/(b - a), & a \leq x \leq b \\ (c - x)/(c - b), & b \leq x \leq c \\ 0, & x < a \vee x > c \end{cases} \tag{4.15}$$

- Logistic functions:

$$\mu_A(x; \gamma) = \frac{1}{1 + e^{-\gamma x}} \tag{4.16}$$

- Γ-membership functions:

$$\mu_A(x; \alpha, \gamma) = \left\{ \begin{array}{ll} 0, & x \leq \alpha \\ 1 - e^{\gamma(x-\alpha)^2}, & x > \alpha \end{array} \right. \quad (4.17)$$

- Gaussian-membership functions:

$$\mu_A(x; \beta, \gamma) = e^{-\gamma(x-\beta)^2} \qquad (4.18)$$

It is up to the human expert to choose the one which capture the characteristics of the fuzzy set in the most appropriate way.

4.4.3 Fuzzy operator

As for crisp sets, relations and operators are also defined for fuzzy sets. For the below defined relations and operators let X be the domain or universe, and A and B are the fuzzy sets defined over the domain X.

Definition 4.4.1 (Equality of fuzzy sets)

Two fuzzy sets are equal if and only if the sets have the same domain and $\mu_A(x) = \mu_B(x) \forall x \in X$. That is $A = B$.

Definition 4.4.2 (Containment of fuzzy sets)

Fuzzy set A is a subset of fuzzy set B if and only if $\mu_A(x) \leq \mu_B(x) \forall x \in X$. That is, $A \subset B$.

Definition 4.4.3 (Complement of fuzzy sets (NOT))

Let $\bar{A}$ denote the complement of set A. Then for all $x \in X$, $\mu_{\bar{A}}(x) = 1 - \mu_A(x)$.

The intersection of two sets is the set of elements occurring in both sets. Operators that implement intersections are referred as t-norms. The result of a t-norm is a set that contains all the elements of the two fuzzy sets, but proportional to the degree of membership that depends on the t-norm.

Definition 4.4.4 (t-norms)

A binary operation $\Delta : [0, 1] \times [0, 1] \to [0, 1]$ is a t-norm if it satisfies the following:

1. $1 \Delta x = x$

2. $x \Delta y = y \Delta x$

3. $x \Delta (y \Delta z) = (x \Delta y) \Delta z$

4. If $w \leq x$ and $y \leq z \Rightarrow w\Delta y \leq x\Delta z$

These operators are important for defuzzification of the variables. The first point states that 1 act as an identity, the second states that Δ has to be commutative, the third that Δ has to be associative, and the last says that Δ is increasing in each argument. Some examples are (132):

- Product operator: $\mu_A(x)\Delta_0\mu_B(x) = \mu_A(x)\mu_B(x)$

- Min operator: $\mu_A(x)\Delta_1\mu_B(x) = min\{\mu_A(x), \mu_B(x)\}$

The most frequently used operators are given and for more we refer to Perdrycz (132):

- Summation operator: $\mu_A(x)\nabla_0\mu_B(x) = \mu_A(x) + \mu_B(x) - \mu_A(x)\mu_B(x)$

- Max operator: $\mu_A(x)\nabla_1\mu_B(x) = max\{\mu_A(x), \mu_B(x)\}$

4.4.4 Fuzzy logic

In the previous section we discussed the theoretical aspects of fuzzy sets. In this section we introduce the reasoning about facts with the help of fuzzy set operators. Now consider three fuzzy sets *young*, *goodShape* and *highValue* and assume the following:

$$\mu_{young}(Auto1) = 0.9 \text{ and } \mu_{goodShape}(Auto1) = 0.7$$
$$\mu_{young}(Auto2) = 0.3 \text{ and } \mu_{goodShape}(Auto2) = 0.5$$

If you know that a good shape and a low age influence positive the value of a car then by application of the Δ_1 t-norm it is possible to determine which car has the higher value:

$$\mu_{highValue}(Auto1) = min\{0.9, 0.7\} = 0.7$$
$$\mu_{highValue}(Auto2) = min\{0.3, 0.5\} = 0.3$$

It is also possible with the Δ_0 t-norm which would result in the following:

$$\mu_{highValue}(Auto1) = 0.9 \times 0.7 = 0.63$$
$$\mu_{highValue}(Auto2) = 0.3 \times 0.5 = 0.15$$

It depends on the expert to determine which t-norm reflects better the reality. Although the example above shows a simplistic situation which will be not found in real world it makes clear the basic assumptions used here. For real world applications it is possible that more than one situation, as described by *if-then* rules, are simultaneously active, with different actions. The problem is to determine the best action to take and therefore a mechanism is needed to infer an action based on the set of activated situations.

Fuzzy logic, therefore is a system, which forms together with an inferencing system a tool for approximate reasoning. Zadeh (175) defined fuzzy logic (FL) as a logical system, which is an extension of multivalued logic that intended to serve as a logic for approximate reasoning. The most important concepts used are that of linguistic variables and the fuzzy rules.

4.4.5 Fuzzy rules

For fuzzy systems in general, the dynamic behavior of that system can be characterized by a set of linguistic fuzzy rules. These rules can be based on the knowledge and experience of a human expert or can be built by analysis of data. The general form of fuzzy rules is:

$$\text{if A is a and B is b then C is c,}$$

where A and B are fuzzy sets with the universe X_1, X_2 and C a fuzzy set with the universe X_3. Therefore the antecedent of a rule form a combination of fuzzy sets through application of the logic operators. The consequent part of a rule is usually a single fuzzy set with corresponding membership function or can also be directly the outcome of the logic operator.

Fuzzy rules together with fuzzy sets form the knowledge base of a fuzzy rule-based reasoning system. In addition there are three other important components necessary; the fuzzyfication, inference and defizzyfication which will be explained in the following section.

4.4.6 Fuzzy inferencing

4.4.6.1 Fuzzyfication

The fuzzyfication is concerned with finding a fuzzy representation of non-fuzzy input values. This is achieved through application of the membership functions for each fuzzy set in the rule space. In the car example the fuzzyfication mapped the age of *Auto1* which is one year via $\mu_{young}(Auto1) = 0.9$ to the degree of membership for fuzzy set *young*.

4.4.6.2 Inferencing

The task of the inferencing system is to map the fuzzified inputs to the rule base and produce a fuzzified output for each rule (see Figure 4.4). The degree of membership to the output fuzzy set is determined with the degrees of membership in the input sets and the relationship between input sets. These relationships are defined by logic operators that combine the sets in the antecedent.

Assume again the car example and the fuzzy sets *young* and *goodShape* and the output fuzzy set *highValue* which are connected by the following rule:

$$\text{if \textit{young} is a and \textit{goodShape} is b then \textit{highValue} is c,}$$

from the fuzzyfication process we know $\mu_{young}(a)$ and $\mu_{goodShape}(b)$. The first step is then to calculate the firing strength of each rule in the rule base. This is achieved with the operators discussed in Section 4.4.3. For example assuming the min operator the firing strenght α_k for rule k is:

$$\mu_{young}(x)\Delta_1\mu_{goodShape}(x) = min\left\{\mu_{young}(x), \mu_{goodShape}(x)\right\} \qquad (4.19)$$
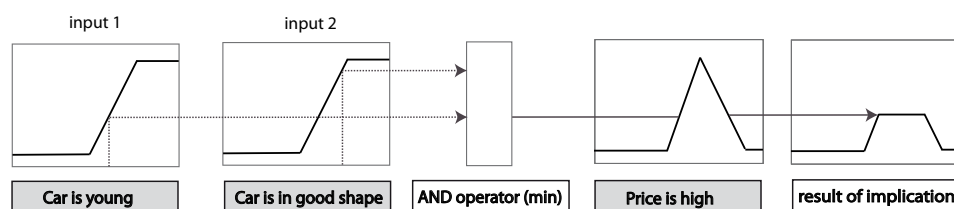
Figure 4.4: Graphical demonstration of the Fuzzy inferencing

The next step is to accumulate all activated outcomes. During this step one single fuzzy value is determined for each $c_i \in C$. Usually the final fuzzy value β_i is computed with the max operator:

$$\beta_i = \max_{\forall k} \{\alpha_{k_i}\} \tag{4.20}$$

The end result of the inferencing process is a vector of fuzzyfied output values with a zero for rules with no firing strength.

4.4.6.3 Defuzzyfication

Given a set of activated rules the defuzzification process is to convert the output of the fuzzy rules into a scalar, non-fuzzy value. Several inference methods (t-conorms) exist to find an scalar value to represent the action to be taken, for example:

max-min Method The rule with the largest firing strength is selected, and it is determined which consequent membership function is activated. The centroid of the area under that function is calculated and the horizontal coordinate of that centroid is taken as the output of the control.

4.5 Fuzzy logic control system

One of the largest applications for fuzzy logic can be found in the area of controls. It can be said that fuzzy control is a *control with sentences rather than equations*. Thus instead of describing the control strategy with a system of differential equations, the control is expressed with a set of linguistic rules. The first application of fuzzy control comes from the work of Mamdami and Assilian (113) in 1975, with the design of a fuzzy control for a steam engine. Fuzzy logic, is much closer to the human thinking and natural language than traditional mathematical logic. Therefore it provides an effective means of capturing the inexact nature of real worlds and human thinking. The essential part of every fuzzy logic control (FLC) is a set of linguistic
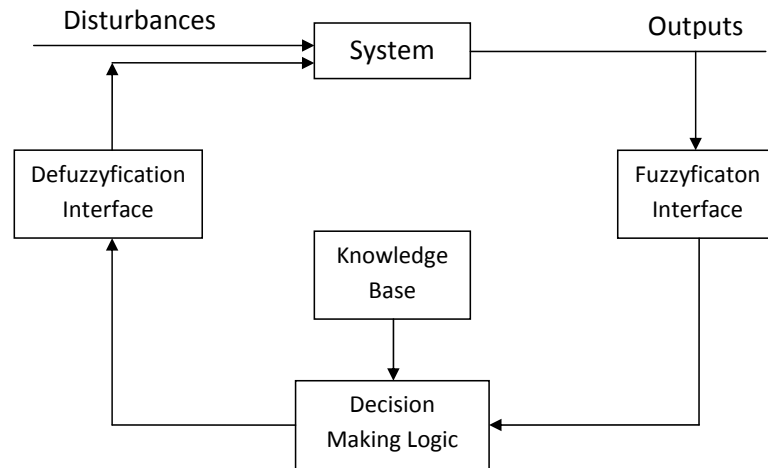
Figure 4.5: The structure of a fuzzy control.

control rules related by the dual concepts of fuzzy implication and the compositional rule of inference. In essence, the FLC provides an algorithm which can convert the linguistic control strategy based on expert knowledge or data mining into an automatic control strategy. The methodology of FLC appears very useful when the processes are too complex for analysis by conventional quantitative techniques or when the available sources of information need to be interpreted qualitatively, inexactly, or uncertainly. Thus FLC can be seen as a step toward a rapprochement between conventional precise mathematical control and human-like decision making (1).

A fuzzy control can be seen as a nonlinear static function that maps control inputs onto control outputs. This nonlinearity is mainly caused by:

- The fuzzyfication process if nonlinear membership functions are used,

- the rule base,

- the inference engine depending on the operator which is used,

- the defuzzification process.

To highlight the issues involved, Figure 4.5 shows the basic configuration of an FLC, which comprises four principal components: a fuzzification interface, a knowledge base, decision-making logic, and a defuzzification interface.

1. The fuzzification interface involves the following functions:

    (a) measuring of input variables,

(b) performing a scale mapping that transfers the range of values of input variables into corresponding universes of discourse,

(c) performing the fuzzification that converts input data into suitable linguistic values which may be viewed as labels of fuzzy sets

2. The knowledge base comprises a knowledge of the application domain and the attendant control goals. It consists of a data base and a linguistic (fuzzy) control rule base:

   (a) the data base provides necessary definitions, which are used to define linguistic control rules and fuzzy data manipulation in an FLC,

   (b) the rule base characterizes the control goals and control policy of the domain experts by means of a set of linguistic control rules.

3. The decision-making logic is the kernel of an FLC; it has the capability of simulating human decisionmaking based on fuzzy concepts and of inferring fuzzy control actions employing fuzzy implication and the rules of inference in fuzzy logic.

4. The defuzzification interface performs the following functions:

   (a) a scale mapping, which converts the range of values of output variables into corresponding universes of discourse,

   (b) defuzzification, which yields a non-fuzzy control action from an inferred fuzzy control action.

4.6   Hierarchical fuzzy systems

With applying the standard fuzzy control to more complex systems a serious limitation was discovered. The number of rules increases for a complete fuzzy control exponentially with the number of variables (138; 173). With n variables and m fuzzy sets defined for each variable we need m^n rules to construct a complete fuzzy control (this would correspond to rules of the form: *IF* x_1 *is* A_x^1 *and* z_1 *is* A_z^1 *THEN* $y_1 = C_1$ with $(x_1, ..., x_n)$, $(z_1, ..., z_n)$ and $(A_{x,z}^1, ..., A_{x,z}^m)$). As the number of variables increases the control will be difficult to implement, not well understandable and overload the memory. To avoid this rule-explosion problem hierarchical fuzzy systems (138) have been proposed. These systems consist out of a number of low-dimensional fuzzy systems which are connected in a hierarchical fashion. The topology is shown in Figure 4.6. We define m fuzzy sets for each input variable, that results in m^2 rules per fuzzy set which leads to $(n-1)m^2$ rules for the complete fuzzy system, which is linear dependent to the number of input values n.
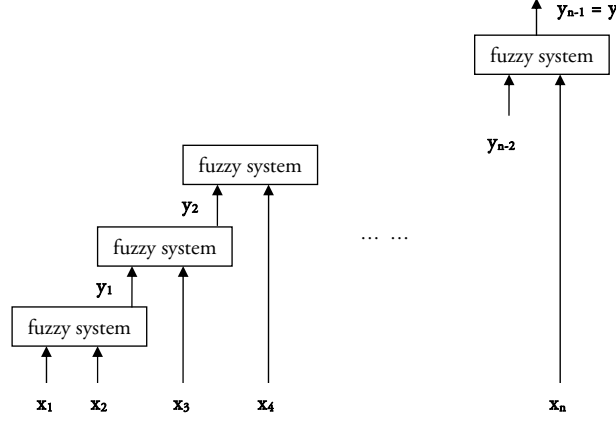
Figure 4.6: Example of an n-input hierarchical fuzzy system based on $n - 1$ two input fuzzy systems.

4.6.1 Analysis of hierarchical fuzzy systems

4.6.2 Takagi-Sugeno-Kang fuzzy system

The Takagi-Sugeno-Kang (TSK) rule based model requires only a small number of rules to describe complex, highly non-linear models with a smaller number of rules than Mamdani fuzzy systems would require (28; 100). Another difference between the Mamdani and TSK fuzzy structures is the fact that the consequents are, respectively, fuzzy and crisp sets. Suppose that m fuzzy sets A_i^p are defined for each variable x_i, where $i = 1, \ldots, n$ and $p = 1, \ldots, m$. Then the fuzzy model is represented by m rules of the following type:

IF x_1 *is* A_1^1 *and* x_2 *is* A_2^1 *and* $\ldots$ *and* x_n *is* A_n^1 *THEN* $\hat{y}_1 = h^1(x_1, ...x_n)$

IF x_1 *is* A_1^2 *and* x_2 *is* A_2^2 *and* $\ldots$ *and* x_n *is* A_n^2 *THEN* $\hat{y}_2 = h^2(x_1, ...x_n)$

$\vdots$

IF x_1 *is* A_1^p *and* x_2 *is* A_2^p *and* $\ldots$ *and* x_n *is* A_n^p *THEN* $\hat{y}_p = h^p(x_1, ...x_n)$

then the system for two inputs x_1, x_2 and one output y_1 can also be written as:

$$f_1(x_1, x_2) = \frac{\sum_{p=1}^{m} \sum_{q=1}^{m} h_1^{pq}(x_1, x_2) \left[\mu_{A_1^p}(x_1) \mu_{A_2^q}(x_2) \right]}{\sum_{p=1}^{m} \sum_{q=1}^{m} \left[\mu_{A_1^p}(x_1) \mu_{A_2^q}(x_2) \right]}, \tag{4.21}$$

where $h_1^{pq}(x_1, x_2)$ are linear or nonlinear functions. In general the fuzzy system at level l is:

$$f_l(y_{l-1}, x_{l+1}) = \frac{\sum_{p=1}^{m} \sum_{q=1}^{m} h_l^{pq}(y_{l-1}, x_{l+1}) \left[\mu_{C_{l-1}^p}(y_{l-1}) \mu_{A_{l+1}^q}(x_{l+1}) \right]}{\sum_{p=1}^{m} \sum_{q=1}^{m} \left[\mu_{C_{l-1}^p}(y_{l-1}) \mu_{A_{l+1}^q}(x_{l+1}) \right]}, \qquad (4.22)$$

where m membership functions $\mu_{C_{l-1}^p}$ $(p = 1, \ldots, m)$ are defined for the intermediate variable y_{l-1} and $h_l^{pq}(y_{l-1}, x_{l+1})$ are linear or nonlinear functions.

In a mathematical way the whole hierarchical fuzzy system can be stated as:

$$\begin{aligned} f_1(x_1, \ldots, x_n) &= y \\ &= f_{n-1}\left\{ x_n, f_{n-2}\left[x_{n-1}, f_{n-3}(x_{n-2}, \ldots) \right] \right\}. \end{aligned} \qquad (4.23)$$

4.6.3 Universal approximation

When we use the proposed hierarchical fuzzy logic (HFL) for optimization we have to ensure that the optimization is not restricted by adapting the response surface. If this would be the case our optimization cannot find the optimal solution. For that we have to prove that our HFS can serve as an universal approximator to any continuous function on a compact set.

The hierarchical fuzzy system is a nonlinear mapping from $(x_1, \ldots, x_n) \in R^n$ to $y \in R$. An important question is whether this mapping can be represented by the hierarchical style of the system. Therefore the following has to be true:

$$f(x_1, x_2, x_3) = f_2(f_1(x_1, x_2), x_3), \qquad (4.24)$$

Theorem 1: For any continuously differentiable function $g(x_1, x_2, x_3)$ on $U = [\alpha_1, \beta_1] \times [\alpha_2, \beta_2] \times [\alpha_3, \beta_3]$, there exists a hierarchical fuzzy system $f(x_1, x_2, x_3)$ in the form of (4.24) such that

$$\|g - f\|_\infty \leq \sum_{i=1}^{3} \left(\left\| \frac{\delta g}{\delta x_i} \right\|_\infty + \left\| \frac{\delta f}{\delta x_i} \right\|_\infty \right) b_i, \qquad (4.25)$$

where the infinite norm $\|*\|_\infty$ is defined as $\|h(x)\|_\infty = sup_x \in U |h(x)|$ and $b_i = (\beta_i - \alpha_i)/(m-1)$.

A proof of this theorem is given by Wang (163). For completeness of this work we also put it in the Appendix B.

4.6.4   Sensitivity analysis of hierarchical fuzzy systems

To use a hierarchical fuzzy system we need a sequence of the input variables $x_1, ..., x_n$. From Fig. 4.6 we see that the sequence determines through how many 2D-fuzzy systems the variables go through. For example is x_n only passed through one, however x_1 and x_2 pass all $n-1$ fuzzy systems. For the design of such system the question arises: Should be x_1 or x_n the most important variables? For that question one has to analyze whether the output y is more sensitive to x_1 or x_n. If y is more sensitive to x_1 we put the most important variables as x_1 and the least important to x_n else we allocate the variables in reverse order. Therefore Wang (164) analyzed the sensitivity of the system output with respect to small perturbations in input variables. For that it is adequate to analyze a low-dimensional fuzzy system since in a hierarchical fuzzy system the sub-systems have the same structure and are connected in a regular fashion. If a perturbation of an input is intensified after passing through a low-dimensional fuzzy system then the more often it goes through the system the more intense it gets. Consequently, it is sufficient to concentrate the analysis on a $f_1(x_1, x_2)$ fuzzy system.

When a small perturbation δx_1 is added to the input x_1 we want to analyze the change of the output of $f_1(x_1, x_2)$ which can be computed according to the Mean-Value Theorem as follows:

$$
\begin{aligned}
\delta f_1 &= f_1(x_1 + \delta x_1, x_2) - f_1(x_1, x_2) \\
&= \left. \frac{\delta f_1}{\delta x_1} \right|_{\bar{x}_1, x_2} \delta x_1
\end{aligned}
\tag{4.26}
$$

where $\bar{x}_1$ is some point in $[x_1, x_2 + \delta x_1]$. From Formula (4.26), we see that if $|\delta f_1/\delta x_1|$ is larger than one, the perturbation δf_1 will be smaller than δx_1. Therefore the analysis is equivalent to the analysis of the magnitude of $(\delta f_1/\delta x_1)$.

To obtain constructive conclusions the fuzzy system has to be specified more precisely. For that we choose equally spaced triangular membership functions defined as follows:

$$
\mu_A(x; a, b, c) = \begin{cases}
(x-a)/(b-a), & a \leq x \leq b \\
(c-x)/(c-b), & b \leq x \leq c \\
0, & x < a \lor x > c
\end{cases}
\tag{4.27}
$$

The two functions $\mu_{A_1^q}$ and $\mu_{A_2^p}$ cover respectively the domains $[\alpha_1, \beta_1]$ and $[\alpha_2, \beta_2]$ and for h_1^{pq} we use a constant value $\bar{y}_1^{pq}$, then as fuzzy system we obtain:

$$
f_1(x_1, x_2) = \frac{\displaystyle\sum_{p=1}^{m}\sum_{q=1}^{m} \bar{y}_1^{pq} \left[\mu_{A_1^p}(x_1)\mu_{A_2^q}(x_2) \right]}{\displaystyle\sum_{p=1}^{m}\sum_{q=1}^{m} \left[\mu_{A_1^p}(x_1)\mu_{A_2^q}(x_2) \right]},
\tag{4.28}
$$

For those type of fuzzy systems Wang (164) found three observations regarding the sensitivity against perturbations of one of the input variables.

Observation 1 For hierarchical fuzzy systems there is no general conclusion about which inputs are more influential to the system output.

Observation 2 The sharper the membership functions $\mu_{A_1^p}(x_1)$, the larger the sensitivity function $|\delta f_1/\delta x_1|$.

Observation 3 The smaller the values for $\bar{y}_1^{pq}$, the smaller the sensitivity function $|\delta f_1/\delta x_1|$.

Concluding from the first observation we do not have to order the inputs $(x_1, ..., x_n)$ according to preferences. This is advantageous because at this stage we do not know which input variables are important for our blind control, in fact exactly this we want to find out. Indirectly this also implies that the size of our hierarchical fuzzy system has no influence on the outcome. The second observation goes deeper into detail and gives us an instrument for modifying the perturbation of an input. If one wants to increase the perturbation $|\delta x_1|$ after passing through $f_1(x_1, x_2)$ more membership functions should be defined in the interval $[\alpha_1, \beta_1]$; and vice versa for less perturbation. Given the third observation larger values of $\bar{y}_1^{pq}$ would amplify the perturbation $|\delta x_1|$ and smaller $\bar{y}_1^{pq}$ reduce $|\delta x_1|$ when it is passed through the fuzzy system.

4.7 Layout of the optimization

Here we describe how throughout this work the optimization of any system in combination with our simulation environment is handled.

4.7.1 Choice of Optimization Algorithm

If we consider an optimization problem of the following form

$$\underset{\mathbf{(x)}}{\text{Minimize}} \qquad f(\mathbf{x}),$$

$$(4.29)$$

where the cost function $f : \mathbb{R}^m \to \mathbb{R}$ cannot be evaluated, but can be approximated by approximating the cost functions $f^* : \mathbb{R}_+^p \times \mathbb{R}^n \to \mathbb{R}$. This kind of approximation can be found in most of the thermal building simulation programs, such as IDA ICE 3.0 (3), EnergyPlus (50), or TRNSYS (90). In such a case the computation of the cost function involves solving a system of partial and ordinary differential equations that are coupled to algebraic equations. In general, one cannot obtain exact solutions, but an approximate numerical solution. Hence, the cost function $f(\mathbf{x})$ can only be approximated by an approximation cost function $f^*(\epsilon, \mathbf{x})$, where $\epsilon \in \mathbb{R}_+^q$ is a vector that contains discontinuities. That can cause optimization algorithms which need smooth cost functions to get stuck far from the *best* solution. Nonlinear programming algorithms can only be used if the approximate cost functions, defined on the numerical approximations to the state variables, converge to a smooth function as the precision

of the simulation increases (134), or if the approximation error goes to zero sufficiently fast as the optimization algorithm approaches a solution (27). Yet, not all building simulation programs satisfy this requirement and it has been observed (166; 167) that solvers which require smoothness on the cost function can end up far from the global minimum.

In our work it is important that a solution close to the global minimum is found without verifying each run. Since the optimization is also used on a control it has to function independently with different cost functions and simulation settings. Probabilistic optimization algorithms do not require a smooth cost function and have already been used effectively together with building simulation programs, see for example (21; 41; 166; 168; 170). The drawback with these stochastic methods is that they need generally many iterations to converge (65), which may cause problems if the simulation for evaluating the fitness function is expensive. In our case, we evaluate a simple thermal model[1], which needs not that much time to evaluate even on an embedded system.

Wetter and Wright (168) compared several deterministic and probabilistic optimization algorithms. The best results for their test problems have been achieved with a hybrid particle swarm and Hooke-Jeeves algorithm. The drawback is that especially with that method many iterations are necessary. Second best result (0.05% worse) was achieved with a simple GA which needed much less iterations before converging. In literature GA's showed already strong performance in combination with building simulation software (for example in (21; 170; 171)). Given that we will cope with two objectives, the energy consumption and the thermal comfort, a multi-objective evolutionary algorithms (MOEA) will be used for the optimization of the blind control.

4.7.2 Combination with the building simulation program

To perform the optimization we combined two independent programs. The NSGA-II[2] (Non-dominated Sorting Genetic Algorithm) (43) optimization algorithm and the IDA ICE 3.0[3] (IDA Indoor Climate and Energy) program (147).

The IDA ICE simulation tool is iteratively called by the NSGA-II via batch mode whenever there is a evaluation of the fitness function needed. The results from the optimization are given back to NSGA-II which is evaluating the fitness functions and changing the design variables according to its crossover and mutation operators. With the new design parameters the IDA ICE is called again until termination criteria is fulfilled. The operation diagram is given in Fig. 4.7.

To fit the IDA ICE software to the specific needs of the user it is possible to write your own components and connect them to the simulation process. They are written in the *"neutral model format"* (NMF) from which it is also possible to call functions written in C. For that reason our blind control with the fuzzy logic system is written in C embedded in a NMF module which

---

[1]The model is explained in more detail in Chapter 7

[2]The NSGAII algorithm is explained in Section 4.3.1.1.

[3]The IDA/ICE simulation software is explained in more detail in Section 3.1.
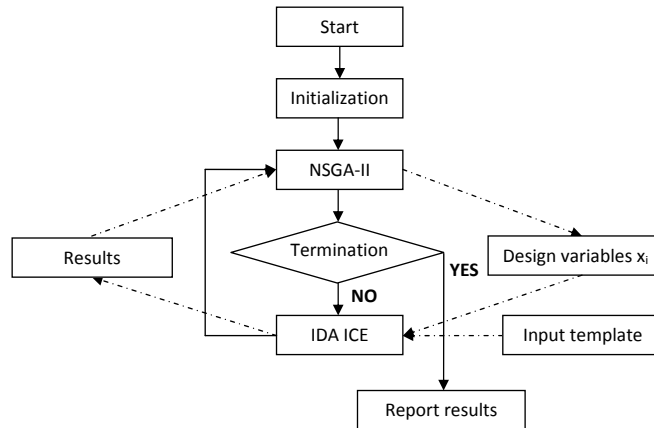
Figure 4.7: Operation diagram of NSGA-II and IDA ICE.

is connected to the window model of IDA ICE. In order to verify the functionality the fuzzy-logic control was also implemented in MATLAB and compared to the results obtained by our algorithm.

4.8   Adaptation of the fuzzy control

The performance of fuzzy logic control (FLC) depends on its control rules and membership functions. Consequently these parameters have to be adjusted to the process that is controlled. In most cases, fuzzy systems have been used to incorporate human expert knowledge. In the 1990's the lack of learning capabilities of those systems generated an interest in coupling fuzzy logic with learning methods. The two most successful directions are neuro-fuzzy systems (86; 120) and genetic fuzzy systems (9; 37; 149). A detailed overview of the field of genetic fuzzy systems is given by Cordon (36). The genetic learning process can cover different levels of complexity according to structural changes, which can range from the altering of parameters to structural changes where the set of rules is changed by the algorithm (47). An overview of the design parameters for an FLC is given by Lee (100).

First of all there is a difference between tuning and learning:

The main idea is to employ an evolutionary optimization to automate the design of the knowledge base (KB). For that it is necessary to parameterize the fuzzy KB, and to find the parameter values which are optimal according to a defined cost function. The parameters constitute the optimization space, that is considered by the optimizer. The decision which part of the KB will be subject of adaptation is itself a multi-objective problem; the conflicting objectives are the dimensionality and efficiency. A search space with less parameters results in a faster adaptation process, while the obtained solutions may be suboptimal. A larger search space may lead to a too expensive optimization that is not executable due to time constraints.

First of all there is a difference between tuning and learning:

- Learning processes act on higher levels of complexity, consequently the search space is bigger. During the process they can change the rule base or even the whole KB and therefore do not depend on predefined rules.

- A tuning process performs the optimization of an existing fuzzy rule base system. The goal is only to find suitable parameters for the membership functions or scaling functions.

Since we have already knowledge about the state variables and also about the rule base we only change the parameters of the system. For defining the set of parameters it is important to see the structure of our fuzzy logic, which can be described as follows[1]:

$$f_1(x_1, x_2) = \frac{\sum_{p=1}^{m} \sum_{q=1}^{m} \bar{y}_1^{pq} \left[\mu_{A_1^p}(x_1) \mu_{A_2^q}(x_2) \right]}{\sum_{p=1}^{m} \sum_{q=1}^{m} \left[\mu_{A_1^p}(x_1) \mu_{A_2^q}(x_2) \right]}, \tag{4.30}$$

Where x_1, x_2 are the inputs to the system, the membership functions μ_A are defined in Formula 5.5, and $\bar{y}_1^{pq}$ are constant values. As parameters to be changed we have the choice between:

- the membership function μ_A,

- the scaling factors $\bar{y}_1^{pq}$.

The membership functions for the different state variables are defined according to the occurrence of the variables, see Section 6.2.2. This guarantees that the whole spectrum of the state variables is covered regularly by the functions. Furthermore for each function μ_A we have to define 3 parameters, see Formula 5.5, which results in 3 variables per membership function, consequently we get in total $3*(p+q)$ variables. With changing only the scaling factors $\bar{y}_1^{pq}$ we get $p*q$ variables. More important is that with changing the shape of the membership function we have an uncontrollable influence on the hierarchical fuzzy systems (see Section 4.6.4) that could change the sensitivity of the system regarding some state variables. For these reasons we use the parameter $\bar{y}_1^{pq}$ for adaptation, which results in a matrix of parameters for each fuzzy system:

$$\begin{pmatrix} \bar{y}_1^{11} & \cdots & \bar{y}_1^{1q} \\ \vdots & \ddots & \vdots \\ \bar{y}_1^{p1} & \cdots & \bar{y}_1^{pq} \end{pmatrix}, \tag{4.31}$$

Actually the parameters $\bar{y}_1^{pq}$ can be understood as a weight assigned to the single rules according to their degree of meaningfulness. The practical implication is that by changing the parameters the response surface of the control changes.

---

[1]The same formula is printed in Section 4.6.2 but for convenience the formula was reprinted.

4.9   Chapter Summary

In this chapter, first we explained the basic principles of optimization and genetic algorithms. After that we gave an introduction of fuzzy logic and the hierarchical fuzzy systems. Furthermore we explained the optimization of our hierarchical fuzzy system with genetic algorithms. In the following chapter this scheme will be used for optimizing the controls and for assessing its saving potential.

5

Preliminary Studies

Part of the work described in this chapter has already been published in (39; 40):

D. DAUM AND N. MOREL. **Assessing the saving potential of blind controller via multi-objective optimization**. *Building Simualtion*, 2 (3):175-185, 2009.

D. DAUM AND N. MOREL. **Assessing the total energy impact of manual and optimized blind control in combination with different lighting schedules in a building simulation environment**. J*ournal of Building Performance Simulation*, 3 (1):1-16, 2010.

This chapter shows the first results and conclusions obtained by case studies with the optimization and simulation test bed. The first question we have to answer is, if we can optimize an existing control with this approach, identify the optima, and show the potential of this control. For that we take a control algorithm (66), recently developed at LESO, and try to increase its performance. After that we assess the influence of shading devices on the energy consumption. For that we combine different control strategies for blinds and artificial lighting to show the influence of the energy consumption and also the saving potential of the different measures.

5.1   Optimization of an existing control strategy

Until now, it was shown in literature that the proposed controls in terms of energy consumption are superior to an on-off controlled counterpart (60; 93; 95). Unfortunately, the maximal saving potential has as far as we know not been evaluated. Our goals are to optimize the energy efficiency of an existing control and on the other hand to introduce a second objective, an

assessment of thermal comfort. This gives us the possibility to identify the complete saving potential and furthermore establish a trade-off between user-comfort and energy-efficiency. For a more realistic simulation we introduce stochastic models to handle occupancy, internal loads and artificial lighting which influences the energy consumption directly.

5.2 Case study setting

In this section we consider two different settings, the first consists of a room from the LESO experimental building in Lausanne and the second is a flat located in a residential apartment building in Lucerne.

5.2.1 LESO experimental building

The ground floor of the test building can be seen in Figure 5.1. Room number 002 was modeled with IDA ICE according to its properties. With the regards to the window, we did not model a day lighting system with an anidolic[1] system. Instead we used only a normal window with the combined size of these two windows. For a thorough introduction of the LESO anidolic system we refer to Altherr (8) and Linhart (107). The model room has no exterior walls except for the South oriented wall with the window. From the North and South we assume that there are no surrounding buildings that could potentially block the sunlight. It is located in Lausanne, Switzerland at a latitude of $46.53°$, longitude of $6.67°$ and altitude of 410 m. For the simulation the 2007 weather data from Lucerne is used as the second building is located in Lucerne (Switzerland at a latitude of $47.03°$, longitude of $8.18°$ and altitude of 456 m) and we wanted to make the results comparable. The specifications of the building are given in Table 5.1.

5.2.1.1 Heating system

The room is equipped with one electric radiator that is positioned below the window and has a setpoint of 21 $°C$. The LESO building is not equipped with an air conditioning unit but we introduced one in the simulation to assess the cooling needs in terms of energy consumption.

5.2.1.2 Occupation

As each human being emits heat and pollutants, her/his presence directly changes the indoor environment. In addition to that, the interaction with electrical appliances as well as the use of artificial lighting increases the internal heat gains and the consumption of electricity. In an office building it is mostly the computer and, for example, the coffee machine that are responsible, while in residential buildings the focus will be on the dishwasher and dryer as

---

[1]The upper window in each LESO room has an anidolic mirror to provide sufficient illumination during overcast skies as well as illuminate the back of each room.

Table 5.1: Specifications of the LESO building

Blind	External blind, total shading coefficient: 0.14, short wave shading coefficient 0.2, no influence on the U-value
Room	Floor area of a room: $15.7\,m^2$ Room height: $2.8\,m$
External Wall	Facade wall (to South): $5.4\,m^2$, light wall ($1\,cm$ plaster panel + $12\,cm$ thermal insulation + $1\,cm$ wood)
Internal Wall	light partition wall ($1\,cm$ plaster panel + $4\,cm$ thermal insulation +$1\,cm$ plaster panel)
Floor	$15.7\,m^2$ ($1\,cm$ rubber coating + $6\,cm$ screed + $6\,cm$ thermal insulation + $25\,cm$ concrete slab)
Window	$3.8\,m^2$ net area (double glazing with IR coating, U-value: $1.4\,W/m^2K$)
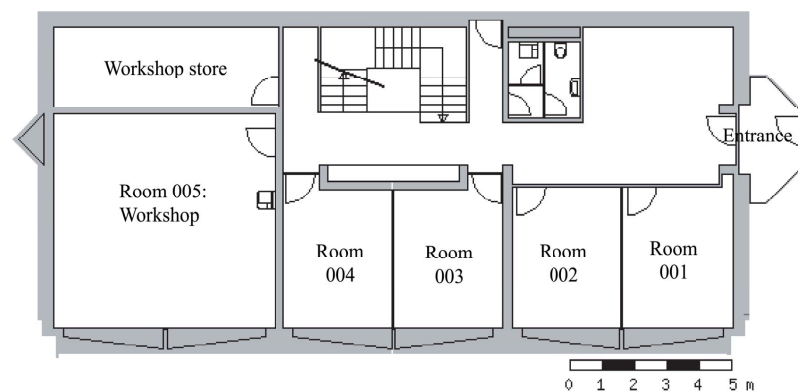
Figure 5.1: Floor plan of the LESO building

Table 5.2: Probabilities for occupancy on weekdays and weekend for the LESO office building based on studies from Jessen Page (130).

Hour	1	2	3	4	5	6	7	8	9	10	11	12
Weekday	0.00	0.00	0.00	0.00	0.00	0.00	0.05	0.10	0.70	0.70	0.70	0.70
Weekend	0.00	0.00	0.00	0.00	0.00	0.00	0.01	0.01	0.05	0.05	0.05	0.05

Hour	13	14	15	16	17	18	19	20	21	22	23	24
Weekday	0.20	0.60	0.70	0.70	0.70	0.70	0.70	0.10	0.01	0.01	0.01	0.00
Weekend	0.01	0.01	0.01	0.00	0.00	0.00	0.00	0.00	0.00	0.00	0.00	0.00

the biggest consumers. Additionally occupants also interact with the building to manage their thermal and visual comfort by using the windows, doors and blinds. These interactions will in turn affect the energy consumption of the buildings HVAC unit. We use the stochastic models developed at LESO by Jessen Page (130) that are described in Section 3.2.

In our simulation the occupant has direct influence on:

- Productions of internal metabolic heat gains and pollutants

- Use of appliances (additional heat gains)

- Use of artificial lighting (additional heat gains)

The occupancy density for the LESO room is $7.5\ m^2$ net area/person with a metabolic rate of 1.2 met and heat emissions of 70 W/person. The probabilities of occupancy are given in Table 5.2, 5.4.

5.2.1.3 Electric equipment

In the LESO office rooms the appliances consist mostly out of PCs which was incorporated in the model for appliances explained in Section 3.2.2.

5.2.1.4 Artificial lighting

How artificial lighting is used depends mostly on the occupant and whether there are automated schedules already installed in the building. To simulate the attitude towards the usage of artificial lighting we implemented the Lightswitch 2002 algorithm (142) which simulates the switching behavior of occupants. This gives us a realistic feeling of the periods where artificial lighting is most probably used. The installed nominal power in the LESO room is

Table 5.3: Specifications of the Elfenau building

Rolling shutters	External blind, total shading coefficient: 0.17, short wave shading co-efficient 0.17, U-value coefficient: 0.9 (that means that with lowered blinds, the U-value of the window is multiplied with 0.9).
Appartement	Floor area of flat: 65.4 m^2, Room height: 2.3 m.
External Wall	Facade wall: 5.4 m^2, light wall (1 cm plaster panel + 30 cm brick masonry + 1.5cm mineral render) U-value: 1.19 W/m^2K.
Internal Wall	light partition wall (1 cm plaster panel + 4 cm thermal insulation +1 cm plaster panel).
Floor	65.4 m^2 (2 cm wood parquet + 8 cm cast cement + 30 cm reinforced concrete).
Window	10.95 m^2 net area (U-value 2.9 W/m^2K), Living room south-west: 1.95 m x 1.32 m, Bedrooms north-east and south-east: 1.25 m x 1.32 m, Bathrooms north-east and south-east: 1.0 m x 1.0 m, Balcony door kitchen north-east: 1.13m x 2.23m, Balcony door bedroom south-west: 0.70 m x 2.23 m.

4.5 W/m^2 with an efficacy of 55.2 lm/W. The exact algorithm can be found in Section 3.2.3 under *Light4*.

5.2.2   Residential apartment building

The second experiment setup consists of a flat located in a residential apartment building (see Fig. 5.2). The whole building was modeled with IDA ICE according to its real dimensions but only one flat in the third floor was equipped with the blind controls for optimization (see listing). The building is surrounded by other buildings which have been integrated in the computational model (see Fig. 5.3, 5.4). It is located in Lucerne, Switzerland at a latitude of $47.02°$ North, longitude of $8.19°$ East and altitude of $477\ m$. For simulation, the data is from the SIA climatic data collection for the station Lucerne, which is located at a latitude of $47.02°$, longitude of $8.18°$ and altitude of $456\ m$.

5.2.2.1   Heating system

The building is equipped with three radiators per apartment which are positioned below the windows. Thermostatic valves with a set point of 21 $°C$ control them. An oil boiler with 0.8 annual efficiency is used for heating and domestic hot water.
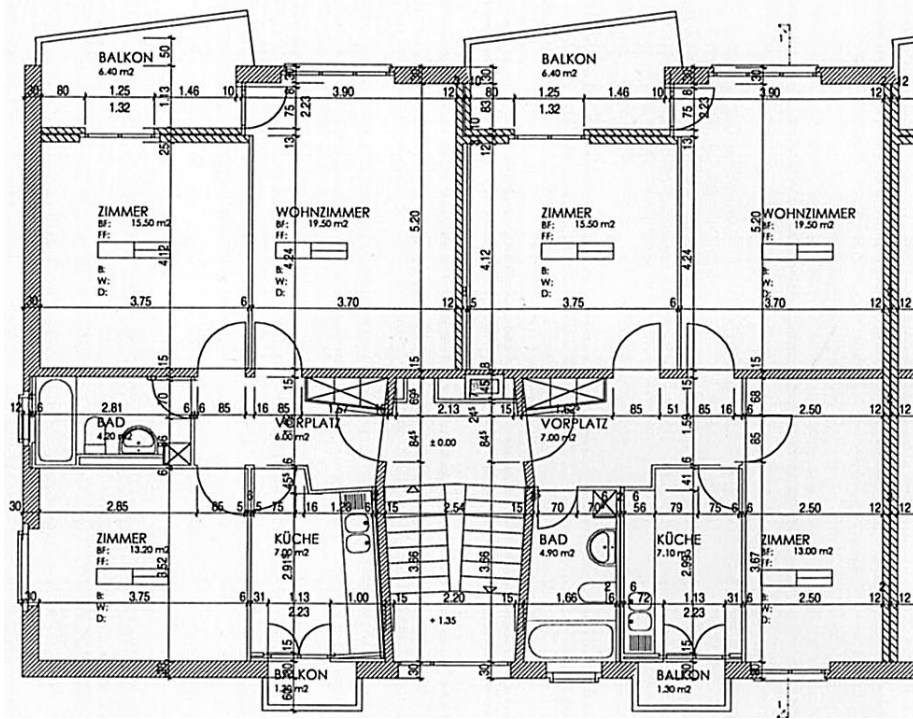
Figure 5.2: Floor plan of the Elfenau building
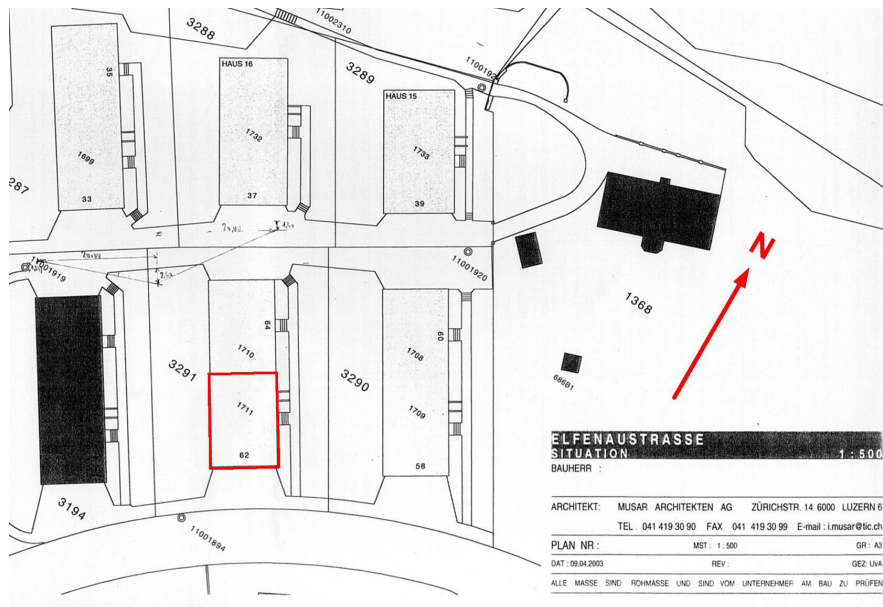
Figure 5.3: Layout of the surrounding buildings, floor plan of Fig. 5.2 is market with a red line
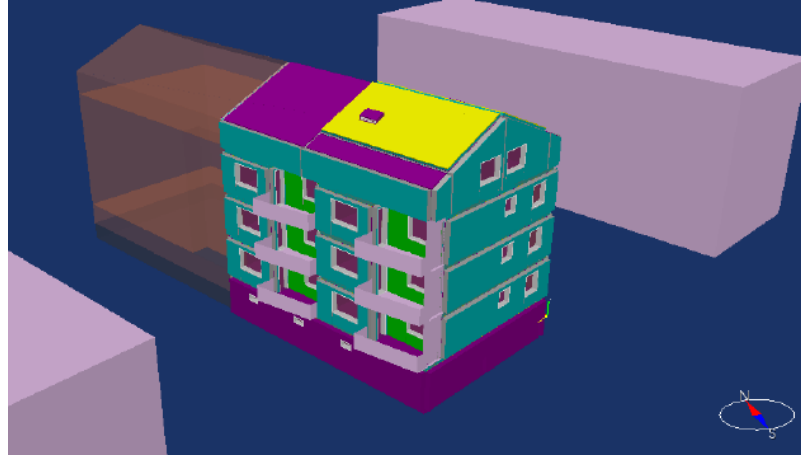
Figure 5.4: 3D view of the building in the IDA ICE software

5.2.2.2 Occupation

For modeling the inhabitants the same stochastic model employed in the first setting is used (see Section 5.2.1.2). The Occupancy density in our flat is $32 \ m^2$ net area/person with a metabolic rate of $1.2 \ met$ and heat emissions of 70 W/person. The probabilities of occupancy are given in Table 5.4.

5.2.2.3 Electric equipment

The same stochastic model used in the first case is applied, the description can be found in Section 3.2.2.

5.2.2.4 Artificial lighting

The installed nominal power is $9.4 \ W/m^2$ with an efficacy of $65 \ lm/W$. The lighting is controlled the same way as in the LESO building, via Lightswitch 2002. The exact algorithm can be found in Section 3.2.3 under *Light4*.

5.3 The optimized control

The control is based on Fuzzy Logic with two state variables and the following rules:

1. If T_e *is winter* and E_{glob} *is night* then $\alpha = x_1$

2. If T_e *is winter* and E_{glob} *is high* then $\alpha = x_2$

3. If T_e *is winter* and E_{glob} *is mid* then $\alpha = x_3$

Table 5.4: Probabilities for occupancy on weekdays and weekend for the Elfenau residential building

Hour	1	2	3	4	5	6	7	8	9	10	11	12
Weekday	1.00	1.00	1.00	1.00	1.00	1.00	0.80	0.70	0.60	0.01	0.01	0.01
Weekend	1.00	1.00	1.00	1.00	1.00	1.00	0.80	0.70	0.60	0.40	0.40	0.40

Hour	13	14	15	16	17	18	19	20	21	22	23	24
Weekday	0.01	0.01	0.01	0.01	0.01	0.60	0.70	0.80	1.00	1.00	1.00	1.00
Weekend	0.40	0.40	0.40	0.40	0.40	0.60	0.70	0.80	1.00	1.00	1.00	1.00

4. If T_e *is winter* and E_{glob} *is low* then $\alpha = x_4$

5. If T_e *is summer* and E_{glob} *is night* then $\alpha = x_5$

6. If T_e *is summer* and E_{glob} *is high* then $\alpha = x_6$

7. If T_e *is summer* and E_{glob} *is mid* then $\alpha = x_7$

8. If T_e *is summer* and E_{glob} *is low* then $\alpha = x_8$

E_{glob} is the global vertical illuminance in [lux] on the window plane, and T_e the current outside temperature in [$°C$]. The output values α correlate directly with the blind setting, where $\alpha = 0$ means the blind is closed, and $\alpha = 1$ stands for blind is open. The membership functions are shown in Fig. 5.5, 5.6. The optimizer is acting the same way as explained in Chapter 4.7 by changing the crisp values of each rule. For example if x_6 is set to $\alpha = 0$ this means that if T_e is *summer* and E_{glob} is *high* then the blinds should be closed.

Since we measure the illuminance at different positions we get different blind movements for every window.

5.4 Objectives of the optimization

The fuzzy logic control is responsible for attempting optimal use of the blinds during occupancy and without occupancy. During this time we want to optimize the energy consumption and the thermal comfort in the rooms. Of course blinds also have a strong bearing on visual comfort. To optimize a shading algorithm it is important to quantify objectively the visual comfort. The two main causes of visual discomfort are glare and insufficient illuminance. While insufficient illuminance can be evaluated easily with a illuminance sensor glare is, by far, more
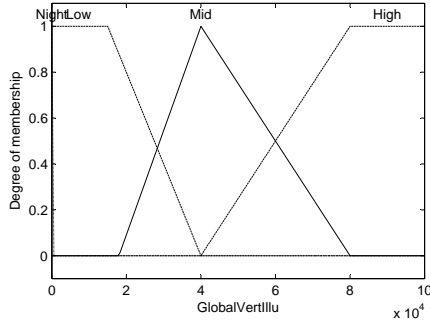
Figure 5.5: Membership function of E_{glob}
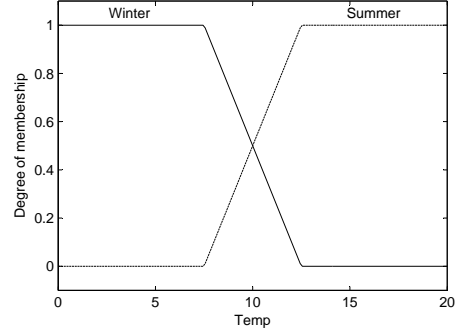
Figure 5.6: Membership function of T_e

difficult to evaluate. To evaluate every blind position for glare is not in the scope of this work and is particularly difficult for residential buildings. The level of illuminance is included indirectly in the optimization: If the illuminance is insufficient the Lightswitch2002 algorithm will switch on the artificial lighting with a high probability and we consume energy which will negatively influence the first objective.

5.4.1 Energy consumption

Objective one is the cumulated energy that has been used for the HVAC and the artificial lighting:

$$f_1(\mathbf{x}) = \int_T (P_H + P_L)\, dt \qquad (5.1)$$

Where P_H [W] is the Power of the HVAC, P_L [W] the power of artificial lighting and T the duration.

5.4.2 Thermal comfort

The main purpose of installed heating and air-conditioning systems is to provide an environment that does not impair performance or the health of the occupants. In finding a suitable solution it also has to be taken into account that comfort depends on the context. People who work in naturally ventilated buildings where they are able to open the windows may be able to adjust to the changing environment throughout the year. On the other hand people that work in air-conditioned offices will feel uncomfortable with slightest changes to their usual environment.

The most common standards are the ISO/DIS 7733 (2003) and the ASHRAE Standard-55 (2004), which since the last revision do not greatly deviate from each other. A good overview and comparison of the international standards is given by Olesen (128).

71

Input variables accounting for the thermal environment are: temperature (air, radiant, surface), humidity, air velocity, clothing and activity level. In our study we concentrate on satisfying the general thermal comfort, so minimizing the PPD[1] (53) is an appropriate objective. Nevertheless there are a number of points which need to be noted:

1. The subjective data on which Fanger's model is based, were obtained exclusively from climate chamber studies where a steady state had been reached when the subjects had been in constant conditions in the chamber for three hours.

2. Prediction of conditions for optimal comfort, PMV or PPD require a knowledge of the clothing insulation and the metabolic rate. Normally assumptions are made for these parameters. If they deviate too much from reality they can influence heavily the results. Especially clothing has a large influence on PMV.

3. Value of clothing insulation used is obtained by the practitioner from tables in which clothing insulation is listed against descriptions of items or ensembles of clothing. The values of clothing insulation have been determined in experiments using heated manikins.

4. Metabolic rate is similarly obtained from tables of activities for which the appropriate metabolic rate is given.

Some possible sources of error in the assumptions underlying the analytical method suggest themselves.

The tables of clothing insulation values assume that the insulation for a particular ensemble is independent of climate or culture. Systematic errors can occur due to:

1. the interpretation of a particular description of a clothing ensemble

2. climatically-determined effects such as the wetting of the clothing by sweat from the skin and

3. the different ways in which clothing is actually used in different climates and cultures.

Metabolic rate could also be affected by climate in a systematic way. People used to hot conditions may undertake particular activities in a more economical way. Metabolic rates determined simply on the basis of an activity descriptor would not pick up this effect. Individual response to different environments depends on the order in which they happen, a mean vote predicted by a steady-state model would not reflect this.

---

[1]The Predicted Percentage Dissatisfied (PPD) is the predicted percent of dissatisfied people at each PMV. It depends on the metabolic rate [met], the cloth index [clo], air velocity [m/s], mean radiant temperature [$^{\circ}C$], ambient air temperature [$^{\circ}C$], and vapor pressure of water in ambient air [Pa]. PPD is the predicted percent of dissatisfied people at each PMV. As PMV changes away from zero in either the positive or negative direction, PPD increases.
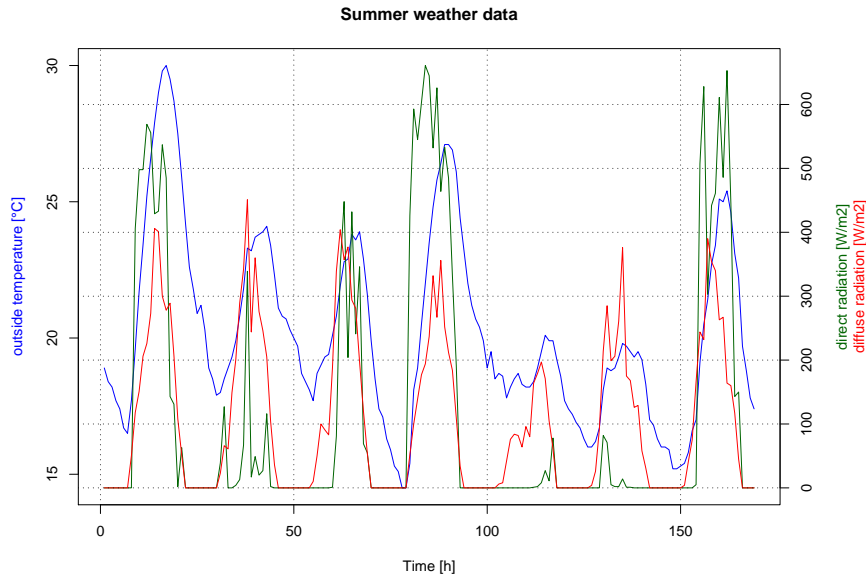
Figure 5.7: Profile of the outside temperature, direct radiation and diffuse radiation of the test data: *Summer*

The way in which people react to an environment depends on their experience with it. People presented with the same environment in a climate chamber have no such expectations or experiences. As a result people in the real situation will be comparing their actual sensation with their expected sensation, and not with some 'absolute' scale as would climate chamber subjects. People will use environmental controls at their disposal to modify the environment to their liking. Given that there is a natural variation between people in the conditions they find desirable, the conditions people choose will be closer to their desired temperature than some imposed standard.

All these effects arise from the inability of the heat-balance model to take into account social and climatic factors that are included by field surveys.

Nevertheless the PPD is a suitable measure for us because we use it not for evaluating the absolute thermal comfort of that environment rather than for identifying the difference of thermal comfort provided by different control strategies. The occupants do not change their clothing (0.75 clo) during the optimization. Although this may not reflect real behavior, it makes the results of the simulation comparable and does not influence the procedure we present for optimization of a blind control. For that reason, our second objective is as follows:

$$f_2(\mathbf{x}) = \frac{\int_T PPD\,dt}{T} \tag{5.2}$$

For the control suggested in Chapter 7 we discuss again the problem and propose also a solution for a personal measure of thermal comfort in Section 7.5.
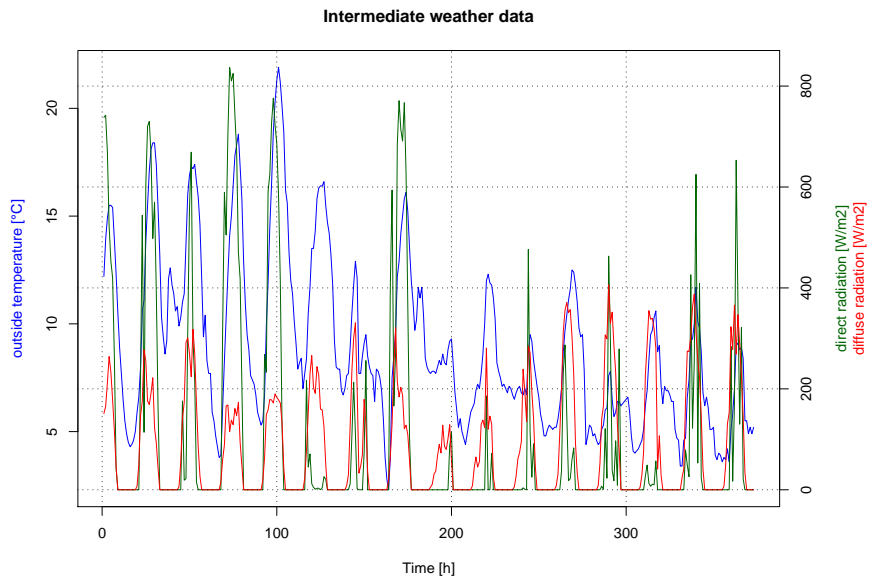
Figure 5.8: Profile of the outside temperature, direct radiation and diffuse radiation of the test data: *Intermediate*
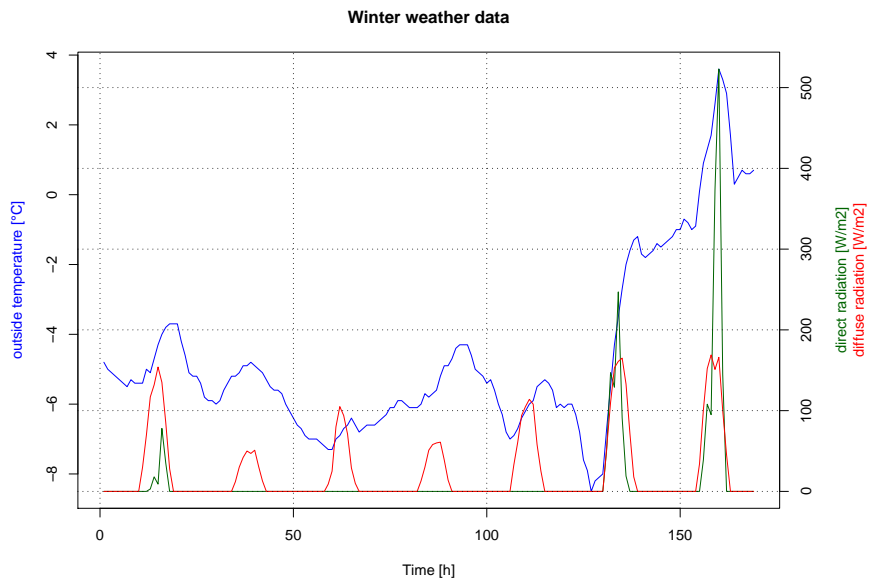
Figure 5.9: Profile of the outside temperature, direct radiation and diffuse radiation of the test data: *Winter*

5.5 Simulation results

For the LESO room we run the NSGA-II for 80 generations with a population size of 80. One evaluation of the fitness function in IDA ICE takes about 15 s on a 3.00 GHz Pentium PC, which results in an execution time of about 27h. For the Elfenau building we run the NSGA-II for 100 generations with a population size of 60 and one evaluation takes about 180 s on a 3.00 GHz Pentium PC which causes an execution time of about 300h. The SBX (Simulated Binary Crossover) recombination probability is set to 0.9 and a distribution index of 15, the mutation probability is 0.1 with a distribution index of 20 (42). The simulation covers seven cold days, 14 intermediate, and five warm days. These synthetic periods are chosen to cover all kinds of climate conditions and keep the simulation time manageable. To take into account the internal heat reservoir, the dynamic simulation repeats the first 24h until all conditions have balanced out and only after this the main simulation begins. Although this takes computational time it increases accuracy significantly. The temperature, direct radiation and diffuse radiation for the three sets of weather data are shown in Fig. 5.7, 5.8, 5.9. In both cases we compared the optimal solution found with our procedure with the results (L_{ref}, E_{ref}) achieved with the original parameters which have been proposed by a human expert (67).

5.5.1 LESO Room

To achieve comparable results we first analyze the parameters that have been originally proposed along with the two extreme cases: blinds are always lowered, blinds are always open (see Table 5.6). The Pareto-front of the best population is shown in Figure 5.10(b) together with L_{ref}. The solution with the reference setting L_{open} and L_{closed} are not shown because of the scale.

In Figure 5.10(a) we show how the optimization is advancing from population to population and converging towards the Pareto-front. In the first generations the population is moving fast towards the optimal Pareto-front whereas at the end the movement is dramatically slowing down. With this knowledge the number of generations for future optimizations can be estimated to avoid useless iterations.

The best setting in terms of energy consumption, with the condition $21° \leq T_i \leq 25°$, is L_{best}^{f1}, which consumes 34.35 $[kWh]$ and has an average PPD of 10.36%. One can see that L_{ref} is relatively close to the ideal energy consumption but is lacking average PPD. On the other hand L_{best}^{f2}, which is the best setting for objective f_2 (average PPD), does not improve average PPD thus much, creating a flat trade-off between the two objectives. It is worth noting again that the occupant does not change his clothing in order to adapt to the changes and for that reason the PPD reaches high values.

In Table 5.5 we show how energy consumption (objective f_1) is distributed over the periods. One can see that the minimum energy consumption for the winter can be reached with leaving the blinds open all the time. This makes sense as the solar gains are maximized and the blinds have no influence on the insulation, which is the opposite result to the Elfenau case. The high-energy consumption during the winter period is due to low radiation and cannot be compensated
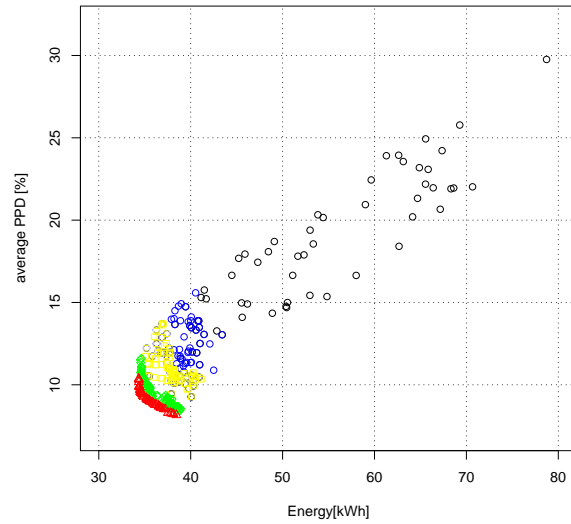
(a) Developement of the solutions during the optimization. The initial population is shown in black, the second in blue, the third in yellow, the 10th in green and the final population in red which is also shown in Figure 5.10(b).
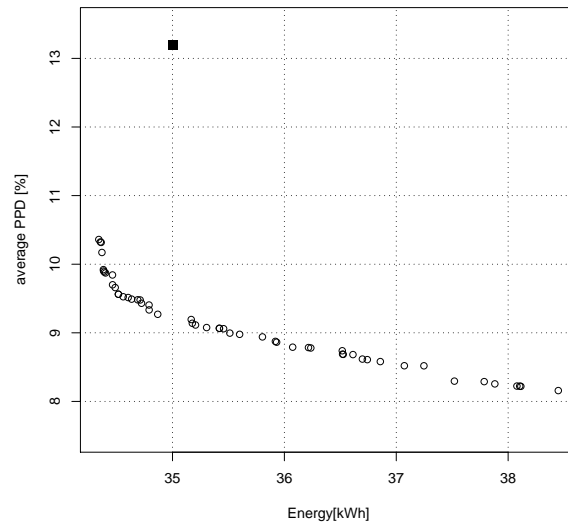
(b) Pareto front of the LESO optimization with a population of 80 individuals and 80 iterations. The case L_{ref} is shown as a filled quadrat, L_{open} and L_{closed} are not shown because of scale.

Figure 5.10: Pareto fronts for the LESO case.

Table 5.5: Results for the LESO case separated by periods.

Case	f_1^{winter}[kWh]	$f_1^{intermediate}$[kWh]	f_1^{summer}[kWh]	f_2^{winter}[%]	$f_2^{intermediate}$[%]	f_2^{summer}[%]
L_{open}	31.15	36.20	16.11	11.60	8.27	5.98
L_{closed}	39.86	17.12	0.59	8.30	43.78	13.14
L_{ref}	33.02	1.57	0.40	13.47	15.09	9.11
L_{best}^{f1}	33.30	0.96	0.09	9.97	12.38	6.71
L_{best}^{f2}	31.16	7.14	0.00	7.84	9.33	6.09

by any blind control. In the intermediate and summer case, one can better see the impact of an advanced control system. The energy consumption in L_{best}^{f1} is reduced 98% in the intermediate and 99% in the summer period compared to L_{open}. By comparing L_{best}^{f1} and L_{ref} there is still an improvement of 39% in the intermediate and 77% in the summer period.

5.5.1.1 Influence of the parameters

For designing fuzzy systems it is interesting to investigate the influence of the fuzzy parameters on the results. In Figure 5.11 we plotted all 8 parameters and the two objectives against each other. Attention must be given to the scale that is individually adapted to the intervals. The parameters, which are strongly correlated to the objectives are x_2, x_3, x_4 and x_7, where x_2 is significant as it is not close to 1.00 but rather varies according to the objectives. That means that x_2 which corresponds to

If T_e *is winter* and E_{glob} *is high* then $\alpha = x_2$,

is a crucial parameter for adapting the objectives. On the other hand the parameters x_1, x_5 seem to be more randomly distributed. The two rules for the parameters are:

If T_e *is winter* and E_{glob} *is night* then $\alpha = x_1$,

If T_e *is summer* and E_{glob} *is night* then $\alpha = x_5$.

Both parameters correspond to E_{glob} *is night*; as the textile blinds do not have any affect on the insulation of the building a change in the parameters would not change the result, and so the optimization procedure finds no pressure in moving the parameters in any direction.

5.5.2 Residential apartment building in Elfenau

The comparable results can be found in Table 5.7. The Pareto-front of the best population is shown in Figure 5.12 together with E_{ref}, the solution with the reference setting and E_{open}. In the most energy efficient solution, E_{best}^{f1}, only 661.73 kWh of energy are consumed for heating during the defined period and the average PPD was at 11.36%. The best value for the average PPD is reached at 9.67% with E_{best}^{f2} and a Energy consumption of 718.48 kWh.

77

Table 5.6: Sets of x values with the results for the LESO case

Case	$f_1[kWh]$	$f_2[\%]$	x_1	x_2	x_3	x_4	x_5	x_6	x_7	x_8
L_{open}	83.46	8.53%	1.00	1.00	1.00	1.00	1.00	1.00	1.00	1.00
L_{closed}	57.57	27.25%	0.00	0.00	0.00	0.00	0.00	0.00	0.00	0.00
L_{ref}	35.00	13.19%	1.00	0.60	0.80	1.00	1.00	0.30	0.50	0.70
L_{best}^{f1}	34.34	10.36%	0.19	0.49	1.00	1.00	0.23	0.23	0.97	0.50
L_{best}^{f2}	38.44	8.15%	0.31	0.99	0.99	1.00	0.68	0.18	0.33	0.74

Table 5.7: Sets of x values with the results for the Elfenau case

Case	$f_1[kWh]$	$f_2[-]$	x_1	x_2	x_3	x_4	x_5	x_6	x_7	x_8
E_{open}	695.53	11.46%	1.00	1.00	1.00	1.00	1.00	1.00	1.00	1.00
E_{closed}	832.54	13.54%	0.00	0.00	0.00	0.00	0.00	0.00	0.00	0.00
E_{ref}	756.67	12.16%	1.00	0.60	0.80	1.00	1.00	0.30	0.50	0.70
E_{best}^{f1}	661.72	11.36%	0.08	0.95	0.70	0.92	0.26	0.95	0.99	0.84
E_{best}^{f2}	718.48	9.67%	0.07	0.99	0.97	0.92	0.09	0.87	0.36	0.64

Table 5.8: Results for the Elfenau case separated by periods.

Case	$f_1^{winter}[kWh]$	$f_1^{intermediate}[kWh]$	$f_1^{summer}[kWh]$	$f_2^{winter}[\%]$	$f_2^{intermediate}[\%]$	$f_2^{summer}[\%]$
E_{open}	493.37	193.91	8.24	10.57	13.27	8.73
E_{closed}	495.85	293.51	43.17	11.28	17.30	8.27
E_{ref}	501.09	239.51	15.97	10.55	14.94	8.21
E_{best}^{f1}	491.88	192.74	6.81	10.32	13.41	8.29
E_{best}^{f2}	486.87	203.83	11.83	8.67	11.64	6.73
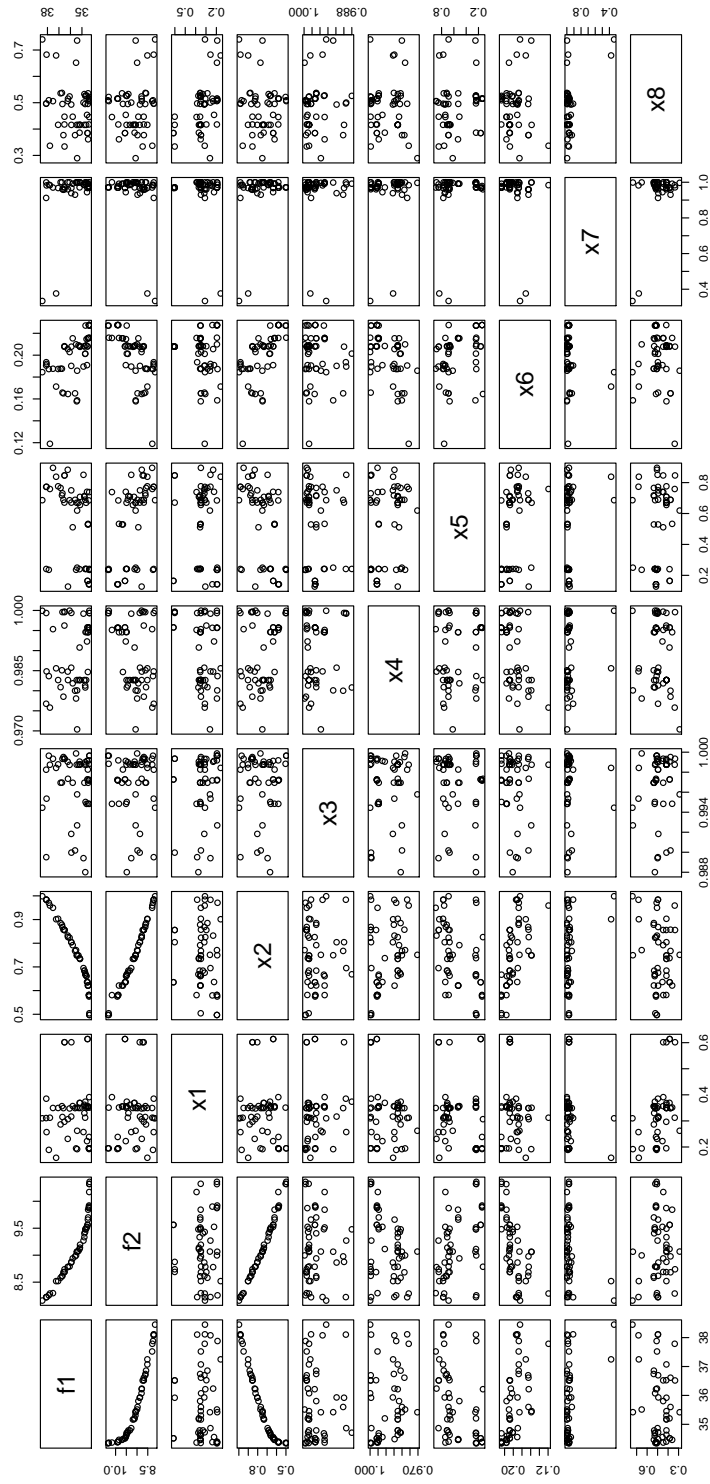
Figure 5.11: All 8 variables of the LESO optimization and the two objectives of the final population are plotted against each other. This helps to find relations between the decision variables and the objectives. For example there is a connection between f_1, f_2 and x_2 and also f_1, f_2 and x_7 are related. One has to take care about the scale which is adapted to each set of data
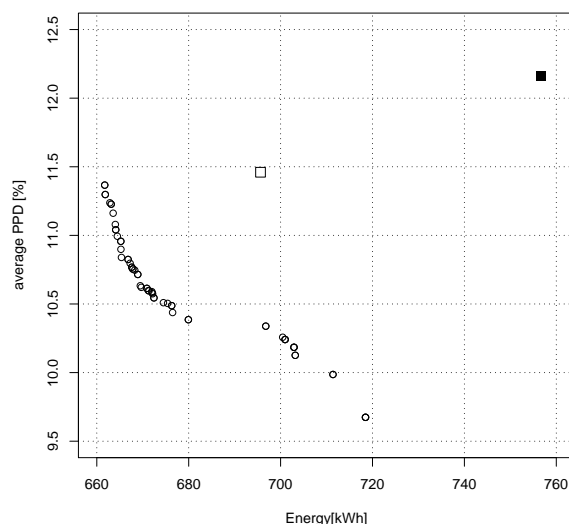
Figure 5.12: Pareto front of the Elfenau optimization with a population of 60 and 100 iterations. The case E_{ref} is shown as a filled quadrat and E_{open} as a blank one, E_{closed} is not shown because of scale.

The distribution of energy consumption among the three periods is shown in Table 5.8. Because of a U-value of 0.9 of the roller blinds it is possible to achieve less energy consumption than in the E_{open} setting, this is implemented in E_{best}^{f1} and E_{best}^{f2}. In the Elfenau case energy savings are lower than in the previously discussed LESO case. By comparing E_{best}^{f1} with E_{open} there are savings of 1.3% (winter), 0.6%(intermediate) and 17.3%(summer) for the single periods. This may be due to the fact that the windows are not all facing the south facade, which is the case at the LESO room. Furthermore the minimal energy consumption for the winter period is not reached by E_{best}^{f1} rather by E_{best}^{f2}. This means, that a combination of these two controllers that would behave like E_{best}^{f2} in winter and E_{best}^{f1} in the other two periods would be better and if possible should be found through the optimization procedure. Not finding such a solution means that the fuzzy system is not optimally adaptable to its needs and cannot utilize the full saving potential of the blinds.

5.6 Assessing the energy consumption of manual and automated blinds in combination with different lighting schedules

In Chapter 2.4 we cited some studies which tried to quantify the amount of savings for different schemes of lighting and blind usage. This case study was mainly motivated to test our simulation test bed but also to better quantify the influence of different blind controls on different

combinations of artificial lighting and orientations of the building.

Controlling blinds and lighting not only changes the consumption of electric energy for lighting, but also that of heating and cooling. To assess the real influence of controls this had to be taken into account. We not only tested the control models against a worst-case scenario but also against a best-case, which is represented by an optimal solution for controlling the blinds in a special setup.

5.7 The different control strategies tested in this case study

In this case study we apply the control models we introduced in Section 3.2.3 for artificial lighting and in Section 3.2.4 for the blinds. Furthermore we introduce an optimized control that is described in the following section.

5.7.1 Blind4 an optimal blind control

With this control we want to asses the maximum saving potential of a blind control in this setup. As a basis we use a fuzzy logic system[1] with two inputs, the inside and outside temperatures. An optimization process then tunes the fuzzy system to control the blinds in an energy efficient way. It can be said that fuzzy control is *control with sentences rather than equations*. Thus instead of describing the control strategy with a system of differential equations, the control is expressed with a set of linguistic rules. These linguistic rules define the properties of the fuzzy system. For example:

If T_e *is winter* and E_{glob} *is high* then $\alpha = C$

Often in literature the rules are defined by experts of that domain and express their knowledge, for example in Kolokotsa (93) and Lah et al. (99). In our approach we define only a structure of rules but the conclusions of these rules are changed by the optimizer and evolve over time, with a final set of parameters that are optimal in respect to the defined objectives. A human expert who is defining the rule base cannot guarantee this advantage. Also an evaluation of the rule base is difficult because the optimal case it not known.

In this context, the fuzzy system can be seen as a non-linear function

$$f(x_1, x_2) = C, \tag{5.3}$$

where x_1, x_2 are the inputs (inside and outdoor temperature) and C the actual setting of the blinds. To fit the movements of the blinds to the specific needs of that room we may change the parameters of the fuzzy system to produce an outcome C that satisfies our needs defined in Chapter 5.7.1.3. In the following we explain the inside of the function $f(x_1, x_2)$ and how we change the properties with parameters.

---

[1]The fuzzy system that is used is explained in more detail in Section 4.6.

5.7.1.1 The fuzzy logic control

We selected a Takagi-Sugeno-Kang (TSK) rule based model[1], which requires only a small number of rules to describe complex, highly non-linear models (28; 100). Another benefit of the TSK fuzzy structure is the fact that the consequents are crisp sets. Suppose that 5 fuzzy sets A_i^p are defined for each variable x_i, where $i = 1, 2$ is the number of inputs and $p = 1, \ldots, 5$ the number of membership functions defined per input. Then a complete fuzzy system[2] is represented by 5×5 rules of the following type:

IF x_1 *is* A_1^1 *and* x_2 *is* A_2^1 *THEN* $\alpha = C_1$
IF x_1 *is* A_1^2 *and* x_2 *is* A_2^1 *THEN* $\alpha = C_2$
$\vdots$
IF x_1 *is* A_1^1 *and* x_2 *is* A_2^2 *THEN* $\alpha = C_6$
IF x_1 *is* A_1^2 *and* x_2 *is* A_2^2 *THEN* $\alpha = C_7$
$\vdots$
IF x_1 *is* A_1^1 *and* x_2 *is* A_2^3 *THEN* $\alpha = C_{11}$
IF x_1 *is* A_1^2 *and* x_2 *is* A_2^3 *THEN* $\alpha = C_{12}$
$\vdots$
IF x_1 *is* A_1^1 *and* x_2 *is* A_2^4 *THEN* $\alpha = C_{16}$
$\vdots$
IF x_1 *is* A_1^1 *and* x_2 *is* A_2^5 *THEN* $\alpha = C_{21}$
$\vdots$
IF x_1 *is* A_1^5 *and* x_2 *is* A_2^5 *THEN* $\alpha = C_{25}$,

where $C_1, ..., C_{25} \in [0, 1]$ are the crisp outputs of each rule. Basically this rule set is dividing the input space for the two variables into small rectangles and it is up to the optimization to define an output, which corresponds to the blind setting, for each of these rectangles. The system for two inputs x_1, x_2 and one output $f(x_1, x_2)$ can also be written as:

$$
f(x_1, x_2) = \frac{\sum_{p=1}^{5} \sum_{q=1}^{5} \bar{y}^{pq} \left[\mu_{A_1^p}(x_1) \mu_{A_2^q}(x_2) \right]}{\sum_{p=1}^{5} \sum_{q=1}^{5} \left[\mu_{A_1^p}(x_1) \mu_{A_2^q}(x_2) \right]}, \tag{5.4}
$$

where $\bar{y}^{pq}$ are the parameters used for tuning the fuzzy system and $\mu_{A_i^p}$ are the membership functions.

---

[1]For a detailed introduction we refer to Chapter 4.6.2

[2]A complete fuzzy system consists out of a rule base which includes all combinations of membership functions. In out case we have two variables with five membership functions each which will result in 25 rules.

Table 5.9: The tables in the `lesoeib` database which we use in our data mining together with the domains for the membership functions

Name	Symbol	Description	Domain	e_i^1	e_i^2	e_i^3	e_i^4	e_i^5
`Ti`	T_i	Indoor temperature [° C]	[15.3,29.7]	15.3	22.2	23.2	24.6	29.7
`Te`	T_e	Outdoor temperature [° C]	[-6.7,34.5]	-6.7	5.6	15.3	21.7	34.5

As membership functions we chose equally spaced triangular functions defined as follows:

$$\mu_A(x; a, b, c) = \begin{cases} (x-a)/(b-a), & a \leq x \leq b \\ (c-x)/(c-b), & b \leq x \leq c \\ 0, & x < a \vee x > c \end{cases} \quad (5.5)$$

For each input (x_1, x_2) we use five triangular membership functions, defined in (5.5):

$$\begin{aligned}
\mu_{A_i^1}(x_i) &= \mu_{A_i^1}(x_i; e_i^1 - \epsilon, e_i^1, e_i^2) \\
\mu_{A_i^2}(x_i) &= \mu_{A_i^2}(x_i; e_i^1, e_i^2, e_i^3) \\
\mu_{A_i^3}(x_i) &= \mu_{A_i^3}(x_i; e_i^2, e_i^3, e_i^4) \\
\mu_{A_i^4}(x_i) &= \mu_{A_i^4}(x_i; e_i^3, e_i^4, e_i^5) \\
\mu_{A_i^5}(x_i) &= \mu_{A_i^5}(x_i; e_i^4, e_i^5, e_i^5 + \epsilon)
\end{aligned} \quad (5.6)$$

where ϵ is an arbitrarily small positive constant to prevent that term $(x - a)$ or $(c - x)$ in (5.5) is divided by 0. The parameters e_i^m, $m = 1, ..., 5$ define the position of the triangular shaped functions and are given in Table 5.9 for our two inputs. The membership functions for inside and outside temperature are shown in Figure 5.13(a), 5.13(b).

5.7.1.2 The tuning process

The tuning process is explained in Section 4.8.

5.7.1.3 The objectives

One goal of this case study is to show the interplay of different control models for blinds and artificial lighting our objectives for the optimization are:

1. Heat load introduced by artificial lighting

2. Heat, cooling load introduced by heating and cooling

The use of energy loads of the zone instead of energy consumed by heating, cooling and lighting may change the absolute values of the optimization but does not influence the optimization since there is a linear ratio between these quantities. The advantage of a multi-objective
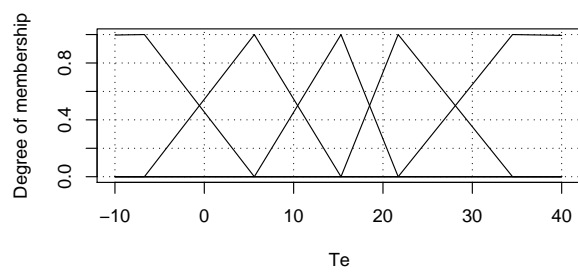
(a) Membership functions for the outside temperature
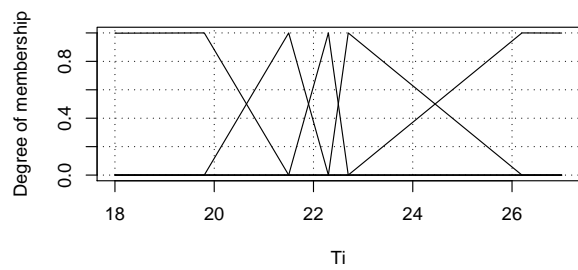
(b) Membership functions for the inside temperature

Figure 5.13: The two membership functions for the fuzzy control

optimization is that no information about the two objectives is lost and at the end a trade off between these two objectives can be identified. To maintain thermal comfort, constraints regarding the indoor temperature (max: $25°C$, min: $21°C$) are given. For the optimization the *Light4* control model is used. Glare is not considered in this work. The result of the optimization is a blind control that keeps the temperature and the illuminance level within the defined bandwidth as long as possible to minimize the energy consumption.

5.8 The case study setup

As experimental setup we used again our model of the LESO building, which is described in Section 5.2.1. The model for occupancy and the appliances was also integrated in the model.

This time we run the simulation for a period of one year for each of the combinations of lighting and blind control schemes. We used weather data from Lausanne of the year 2007. One simulation took about 300 s on a 3.00 GHz Pentium PC. In contrast to the optimization, where we repeat the simulation many times, here the simulation was carried out once which each combination, which made it possible to take one year as simulation horizon.

5.9 Simulation results

5.9.1 Results of the optimization process

Unlike in Section 5.2 we run the simulation in each iteration of the optimization for a whole year. We reduced the population size to 40 and run it for 60 generations resulting in an execution time of 200h. The results of the optimization for the South oriented office room of the LESO building are shown in Figure 5.14. Each point shows the energy consumption of the same control with a different set of parameters. For the case study we choose the solution with the minimal overall energy consumption for the South and North setup. The set of parameters used for the South and North case are given in Table 5.10. Additionally to that, the response surfaces for both optimized fuzzy controllers are shown in Figures 5.15(a), and 5.16(a). As the optimization algorithm only explores areas where an input is measured, the actual response in the other areas, for example $T_e = -10$ ° C and $T_i = 25$ ° C, is random and may not be explained with common sense. However as long as this state does not appear during the run it will be no limitation. The outcomes in terms of shading fraction are given as weekly boxplots[1] together with the weekly average outside temperature in red, and the weekly inside temperature in blue for the North (Figure 5.16(b)) and South (Figure 5.15(b)) facade.

---

[1]A boxplot is a tool of the descriptive statistic to graphically depict groups of numerical data through their five-number summaries: the smallest observation (sample minimum), lower quartile (Q1), median (Q2), upper quartile (Q3), and largest observation (sample maximum). In the Figures the median is shown by the black point, the box shows the lower and upper quartile and the lines show 1.5 times the interquartile range.
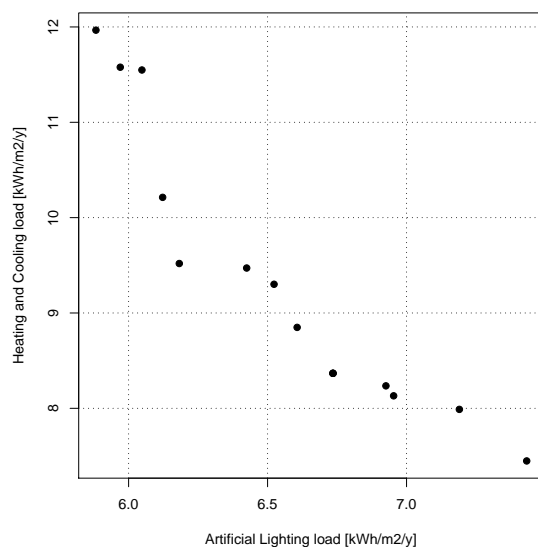
Figure 5.14: The Pareto-front of the control optimization with the trade-off of lighting load against heating, and cooling load. Each point represents the solution of a different control with a different parameter set.

5.9.2   Results of the case study

Allover we tested four different control strategies for blinds along with four for lighting, which resulted in 16 different setups. These, were simulated with a South-facing and a North-facing facade that resulted in a total of 32 different setups. Annual energy simulations have been carried out with IDA ICE for all setups and the energy loads have been split in heating, cooling and lighting energy which are shown in Figure 5.18 for the North facing setup and in Figure 5.17 for the South facing setup. The aim of this was to compare different control strategies and their influence on the energy consumption. The only thing these strategies change is the load of energy, which has to be introduced into the room by heating, or extracted by cooling. The consumed electric energy of artificial lighting and the heat load that it introduced are equal. We think that this is a suitable measure for comparing different control strategies. Of course, heating load is normally derived directly from a primary energy source, which makes it more efficient than electric energy. However, in taking this into account a simple conversion efficiency will not provide an insight into the problem as the power generation strongly depends on the country and therefore gives us no clear rule in how to favor energy used for heating. In France, for example, the electric energy originates almost 78% (26) from nuclear power plants so a comparison of green house gas (GHG) emissions would mislead the reader. The concepts of primary energy and energy cost have the same problems that they are highly dependent on the given conditions. To calculate the energy of mechanical cooling the coefficient of performance (CoP) has to be defined which varies greatly between countries. In northern
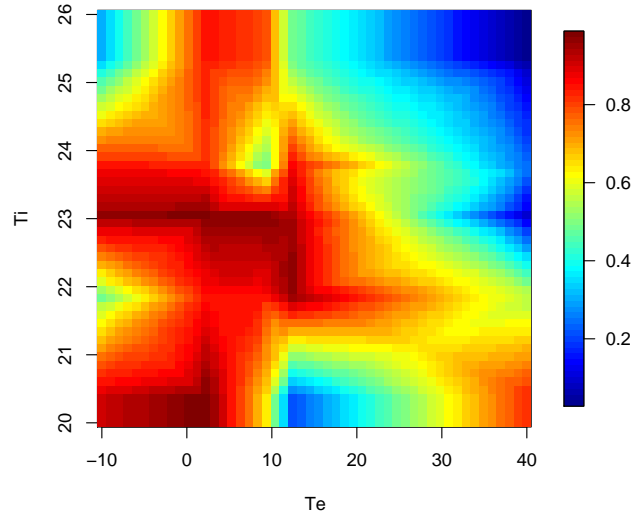
(a) The response surface for the *South* case after optimization. For high and low temperatures the optimizer may not have sufficient data for the optimization. Therefore, values in these areas may not be explained by common sense. Nevertheless, it does not bias the results if these values do also not occur in the future.
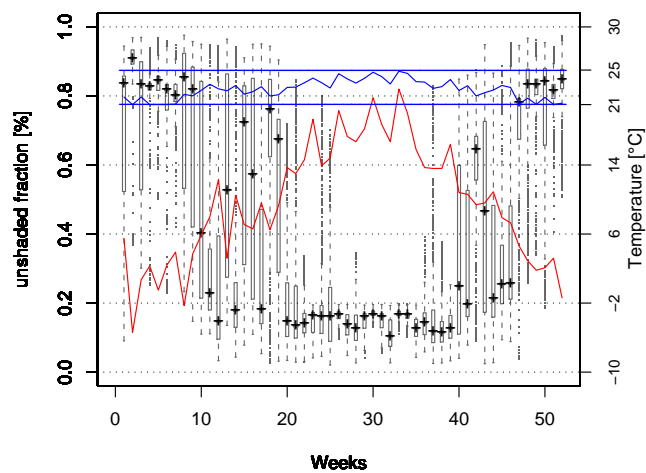
(b) Weekly boxplots of the unshaded fraction for the Blind4 control in the *South* setup together with the weekly average inside temperature (blue) and outside temperature (red) on the second y axis

Figure 5.15: The response surface for the Blind4 control together with the outcome in the *South* setup
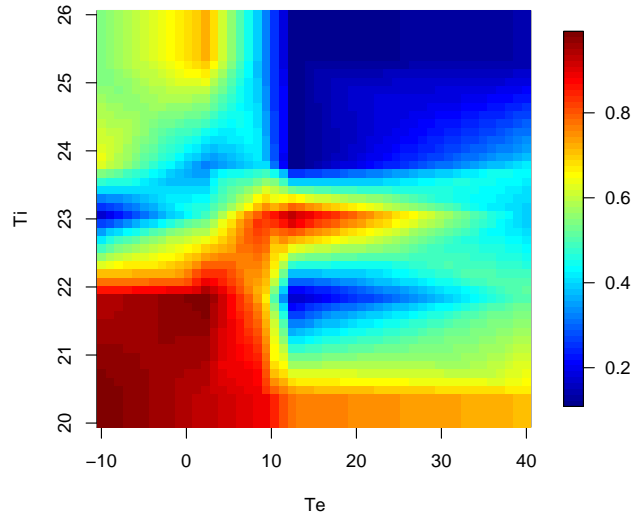
(a) The response surface for the *North* case after optimization.
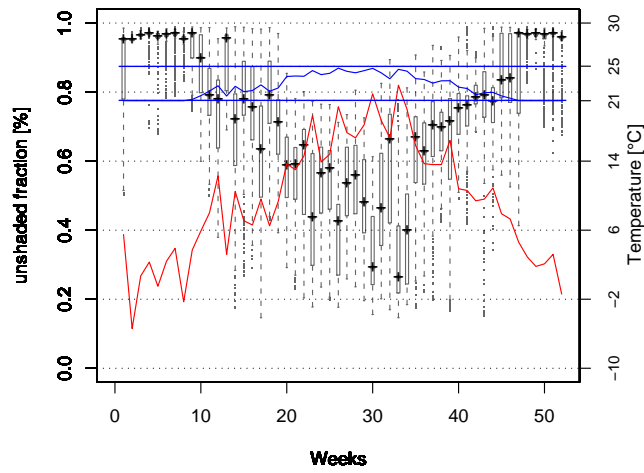
(b) Weekly boxplots of the unshaded fraction for the Blind4 control in the *North* setup together with the weekly average inside temperature (blue) and outside temperature (red) on the second y axis

Figure 5.16: The response surface for the Blind4 control together with the outcome in the *North*
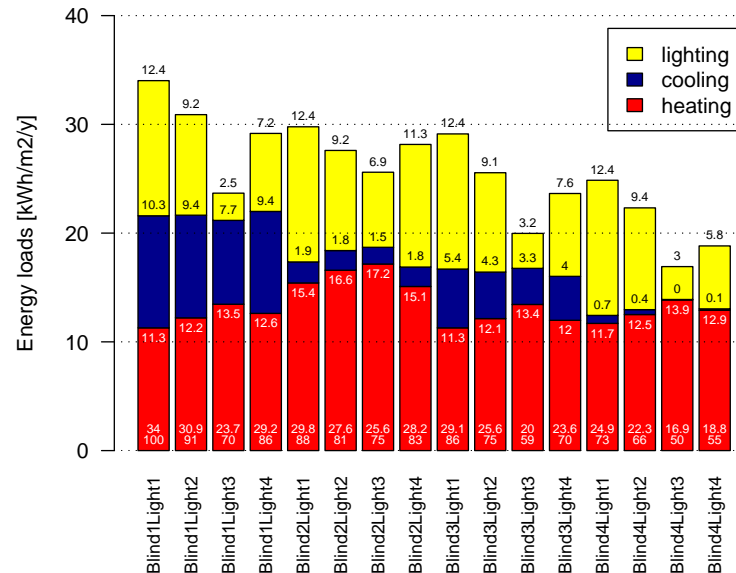
Figure 5.17: Results for different combinations of controls in the North case. On every part of the bar the load is shown and additional to that the combined consumption in percent and absolute values is shown at the bottom of every bar.

Europe many buildings have no air conditioning and, of course, temperatures here above $26\,^{\circ}C$ are also uncomfortable. With stating the cooling load, the degree of overheating is shown and comparable for the different control models. Furthermore the calculation of primary energy is only a linear transformation of the results without providing more information. If this conversion rate is known, thanks to the two objectives of the optimization, a set of parameters could easily be chosen to favour the use of primary energy, see Figure 5.14.

Out of the single results it is not clear which control plays a larger role for energy savings. To get a feeling of that, the single average energy usage is given in Figures 5.19, 5.20. For example, the lighting usage of 7.8 $kWh/m^2/y$ of *Blind1* is calculated as the average of all the setups where *Blind1* one was used.

5.9.2.1 Blinds

In the *Blind1* case the blinds stay open all the time, which significantly increases the solar gains during the summer and winter periods. In the *North* case the results found, show a global energy load of 29.4 $kWh/m^2/y$, which is 29% greater than the best average case. In the *South* case the load is 64.4 $kWh/m^2/y$, which is very different to the other blind controls. This is due to the massive cooling needs during the summer time, which is about 4 times higher compared to the average *Blind2* control model and 38 times higher than the cooling load with the optimized *Blind4* control.
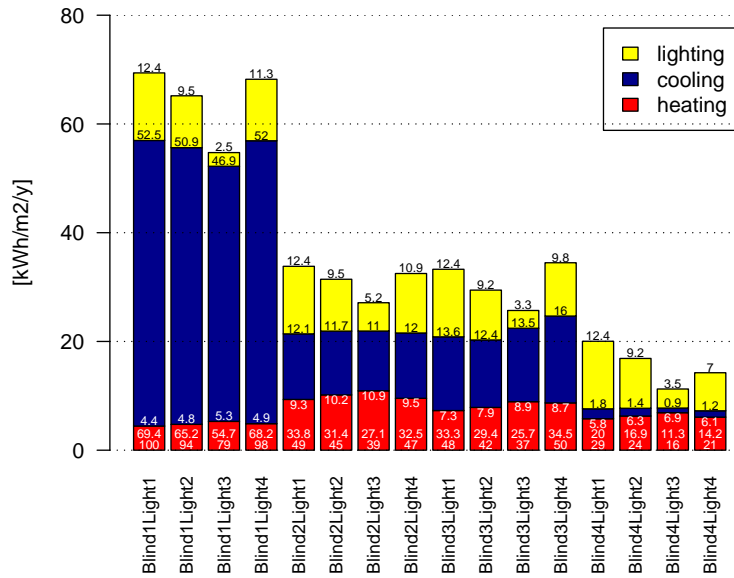
Figure 5.18: Results for different combinations of controls in the South case. On every part of the bar the load is shown and additional to that the combined consumption in percent and absolute values is shown at the bottom of every bar.

Table 5.10: Set of parameters for the controls for the south and north case

North	$\bar{y}^{p1}$	$\bar{y}^{p2}$	$\bar{y}^{p3}$	$\bar{y}^{p4}$	$\bar{y}^{p5}$	South	$\bar{y}^{p1}$	$\bar{y}^{p2}$	$\bar{y}^{p3}$	$\bar{y}^{p4}$	$\bar{y}^{p5}$
$\bar{y}^{1q}$	1.00	0.93	0.10	0.68	0.52	$\bar{y}^{1q}$	0.93	0.62	0.25	0.87	0.55
$\bar{y}^{2q}$	0.93	0.99	0.50	0.32	0.72	$\bar{y}^{2q}$	0.95	0.81	0.51	0.96	0.75
$\bar{y}^{3q}$	0.89	0.70	0.87	0.41	0.34	$\bar{y}^{3q}$	0.99	0.94	0.20	0.04	0.76
$\bar{y}^{4q}$	0.77	0.13	0.97	0.10	0.11	$\bar{y}^{4q}$	0.72	0.27	0.02	0.19	0.01
$\bar{y}^{5q}$	0.71	0.52	0.36	0.43	0.14	$\bar{y}^{5q}$	0.79	0.33	0.24	0.20	0.22

The blinds of the next blind control remain closed from 8 am to 6 pm during the week-days. In the *North* and *South* cases the cooling loads are significantly reduced (-81%, -77%). The energy required for lighting increased by 2 $kWh/m^2/y$ in the *North* case and only 0.5 $kWh/m^2/y$ in the *South* case. Overall there is a reduction of 52% in the *South* case along with just 6% in the *North* case.

The *Blind3* does not change that much compared with the *Blind2* case, for both orientations.

The *Blind4* control was most efficiently able to reduce the energy demand. It achieved the lowest loads for lighting and cooling and was also able to reduce the heat loads compared with *Blind2* and *Blind3* for both orientations. In the North case a global average load of 20.7 $kWh/m^2/y$ was measured compared to 29.4 $kWh/m^2/y$ in the worst case. In the South case the reduction was even greater with 15.6 $kWh/m^2/y$ compared to 64.4 $kWh/m^2/y$, which is a reduction of 76 %. Looking at the single cases in Figures 5.20 and 5.19 the control is almost able to bring the cooling loads down to zero with all of the four lighting schemes. Furthermore the heating can be reduced below the level of the *Blind2* and *Blind3* setups. By comparing the boxplots of the shading (Figures 5.16(b), 5.15(b)) one can see that the shading factors in the South oriented setup are much higher than in the North orientation, especially during the summer time. The northern shading during the summer time is more dependent on the temperature, whereas on the South facade only little interaction can be seen and blinds remain closed for more than 80% of the time. During the wintertime both setups have significantly lower shading factors to increase the solar gains.

5.9.2.2 Lighting

As expected, the *Light1* control generates a constant energy consumption of 12.4 $kWh/m^2/y$ in all combinations, as it is completely independent of any environmental conditions. By comparing this control to the others in the *North* case we ascertain the largest load for lighting, the second highest for cooling, but the lowest for heating (see Figure 5.19); this is due the heat gains produced by the lighting during the wintertime. This also applies to the South case even though the cooling loads are quite similar in this setup regarding the different choices of artificial lighting controls (see Figure 5.19).

In *Light2*, the lighting is only switched on if an occupant enters the room. This reduces, on average, the load in the *North* case for lighting by about 26% and for cooling about 13%. In all three measures the reduction is just 10% as more heating is required during the wintertime. In the *South* case, lighting loads are similar whereas the loads for cooling are only reduced by 4%. This is due to the fact that during the summer time the absolute value of cooling is higher, which reduces the percentile savings of changing the lighting control in respect to the *North* case.

The *Light3* was shown to be the most energy efficient by reducing the lighting loads by about 69% and the overall loads by about 27% in the *North* case. In the *South* case almost similar values were reached.

The realistic behavior of an occupant was modeled using *Light4*. It was shown in the *North* case that a manual control by an active occupant is 36% better than leaving the light switched
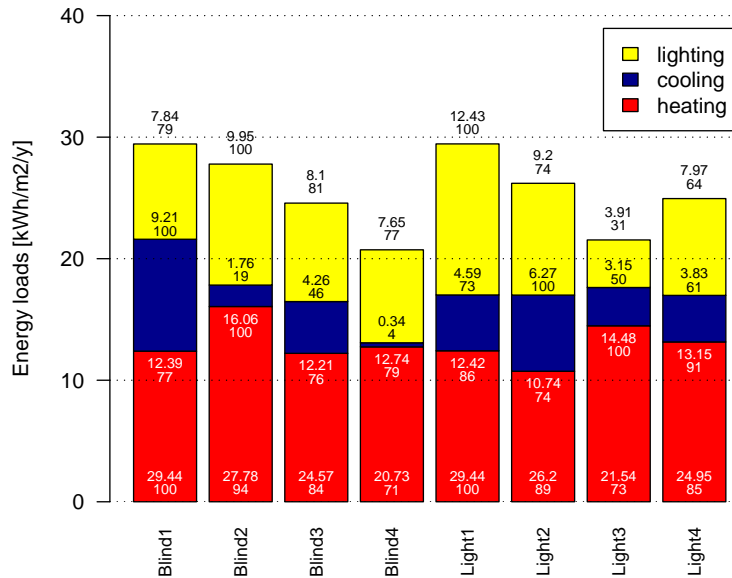
Figure 5.19: Average loads of the light and blind controls for the North case. The load for every type of energy is indicated on the bars as well as the percental from the highest consumption separately for blind and light controls. The overall consumption is indicated at the bottom of every bar.

on for the whole day. The other way around the lighting load was reduced by 21%, which is similar to the *North* case, but the global usage is only reduced by 9% compared with 15% in the *North*.

5.9.2.3 Overall balance

The different energy consumptions for the North oriented case vary between 33%:30%:37% (lighting, cooling, heating) (complete load of 34.0 $kWh/m^2/y$) in the *Blind1Light1* case and 18%:0%:82% (total of 16.9 $kWh/m^2/y$) in the *Blind4Light3* case. This means that it is possible to keep temperatures below 25 $°C$ without cooling. The variations on the South oriented facade move from 6%:76%:18% (total of 69.4 $kWh/m^2/y$) for *Blind1Light1* to 30%:8%:61% (total of 11.3 $kWh/m^2/y$) for *Blind4Light3*. The variations on the South facade are much higher, but with an optimal control it is possible to reach lower levels of energy consumption than on the North facade.

The setup closest to an active occupant was *Blind3Light4*. In both orientations this setup faired worse then the best controlled setup, which proved to be *Blind4*. However it did better than *Blind1Light1*, which referred to an inactive occupant

Generally, it can be said that blinds on a South oriented facade have a greater influence on
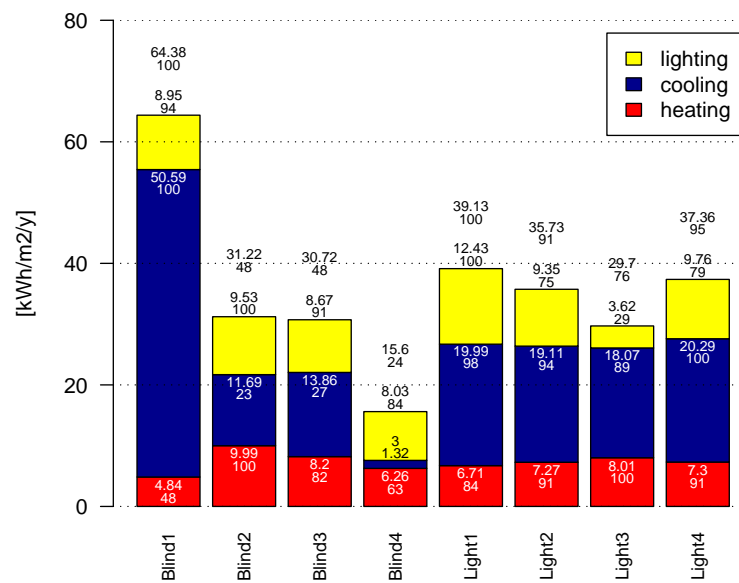
Figure 5.20: Average loads of the light and blind controls for the South case. The load for every type of energy is indicated on the bars as well as the percental from the highest consumption separately for blind and light controls. The overall consumption is indicated above every bar.

the overall energy consumption than artificial lighting. On the North facade both systems have more or less the same saving potential. Using occupancy detectors and dimmable automatic lighting controls can significantly reduce the lighting consumption. The blind control also influences lighting loads since they change the indoor illuminance. The best results can be achieved if a good blind control works together with dimmable lights. Then savings between 45% and 79% (*North* and *South* setup) are possible.

5.10   Chapter summary

In this section we wanted to prove the following two points:

- Our simulation test bed is capable of optimizing a given control and depending on the objectives showing the maximum energy savings that may be possible.

- With the combination of different lighting and blind controls we showed that the saving potential of an advanced blind control systems outreaches by far the saving potential of lighting control.

We showed that a combination of a simulation program and an optimizer based on evolutionary algorithms can find an "'optimal control'" for both, the LESO office room case and the residential apartment, that are significantly better than the used reference case. The energy savings found showed the necessity for optimization in this field, and the superiority of the resulting solutions in terms of energy and thermal comfort to the *man made* counterpart. Also the results are only suitable for that specific setup, whereas this approach is capable of assessing the saving potential while evaluating also the comfort of occupants. This makes it possible to benchmark different systems and make a statement about their theoretical saving potential. One can also compare different types of controllers and may receive a combined Pareto-front consisting of the best results by different systems.

Regarding our second point we investigated the interplay and influence of lighting and blind control algorithms on the heating, cooling and lighting energy loads of an office room. It is important to include all relevant factors in simulation since a decrease in one type of load may lead to an increase in another type of load. We tested all combinations of four blind and four lighting control models in a South-facing, and a North-facing office. The results show, that regarding the use of blinds and lighting, the active inhabitants can easily improve their energetic footprint by 30% to 50% electric energy when compared to the worst case. It also shows that the energy efficiency can be further improved by introducing advanced control algorithms that can reduce energy loads between 45% and 79% compared to the on/off schedules. This massive energy reduction is mainly reached through an advanced control of blinds, which highlights the importance of research in this area.

We expressed the thermal and visual comfort in terms of energy. The advantage of this procedure is that results can be more easily compared. However, the drawback is that one cannot assess the energy savings that may occur if the occupant tolerates temperatures above 26°C.

6

Identifying the state variables

Part of the work described in this chapter has already been published in (41):

D. DAUM AND N. MOREL. **Identifying important state variables for a blind controller**. *Building and Environment*, 45 (4):887-900, 2010.

6.1 Introduction

In literature many different blind controls have been suggested; it has been shown in most cases, that they can provide energy savings and better comfort. In the early approaches they where based only on one state variable, but over time more variables have been taken into account and the structure got more sophisticated. With an increasing number of state variables the performance may rise but also the cost and complexity (see also Section 2.3). The handling of several state variables might not be a problem in a scientific setting, however in the real world, the additional sensors often make the controls expensive, complicated to install and hence unattractive for users.

Therefore, for designing a blind control it is important that the state variables provide enough information for setting the blinds in a beneficial position given the environment. On the other hand too much information does not improve the result but adds dispensable costs and complexity.

In this chapter we present a systematic way to identify the important state variables for a blind control by comparing the performance of the same control with different sets of state variables. It is based on an adaptable hierarchical fuzzy[1] control that gets optimized with our optimization environment (Chapter 4) in terms of energy consumption and thermal comfort,

---

[1]An introduction is given in Section 4.6

and is then tested in our simulation test bed. With the resulting information a statement can be made about the importance of a state variable regarding energy efficiency and the comfort. For assessing the saving potential we use a model of a LESO office room that we modeled in the IDA ICE building simulation software[1]. This allows us to test different types of blind control strategies in a fast and exact manner.

With the same system we also investigate the properties of our fuzzy system regarding the number membership functions that are necessary for a good adaptation performance.

In Section 6.2 the number of membership functions for our fuzzy system is determined. The framework in which we test the different controls is explained in Section 6.3, and Section 6.4 presents the results and findings.

6.2 Construction of the hierarchical fuzzy system

The concept of hierarchical fuzzy systems (HFS) is introduced in Section 4.6 together with the general introduction of fuzzy logic.

To fill our HFL, which can generally be described as follows[2]

$$f_l(y_{l-1}, x_{l+1}) = \frac{\sum_{p=1}^{m} \sum_{q=1}^{m} h_l^{pq}(y_{l-1}, x_{l+1}) \left[\mu_{C_{l-1}^p}(y_{l-1}) \mu_{A_{l+1}^q}(x_{l+1}) \right]}{\sum_{p=1}^{m} \sum_{q=1}^{m} \left[\mu_{C_{l-1}^p}(y_{l-1}) \mu_{A_{l+1}^q}(x_{l+1}) \right]}, \qquad (6.1)$$

we have to define the following items:

- the functions $h_l^{pq}(y_{l-1}, x_{l+1})$,

- the type of membership function,

- the number of membership function for each variable.

6.2.1 The functions $h_l^{pq}(y_{l-1}, x_{l+1})$

The properties of the functions $h_l^{pq}(y_{l-1}, x_{l+1})$ affect the approximation ability of the HFL and the number of parameters which are used for the adaptation of the HFL. In Section 4.6.3 it was shown that a HFL is an universal approximator if the function is a $m-1$'s polynomial of y_{l-1}:

$$h_{pq}(y_1) = d_{0pq} + d_{0pq}y_1 + \cdots + d_{(m-1)pq}y_1^{m-1} \qquad (6.2)$$

where m is the number of membership functions defined per variable that results in m^3 parameters for each fuzzy system. Given the limited computer time for calculations and to

---

[1] In Section 5.2.1 we provide a detailed description of the LESO room

[2] this formula was already introduced in Section 4.6.2 as Formula 4.22 but has been reprinted here for better understanding. For a detailed explanation we refer to the mentioned position.

Figure 6.1: An example of fuzzy sets defined for each variable (the $m = 4$ case).

exclude redundant sets of parameters it is advantageous to decrease the number of parameters substantially. On the other hand a decrease will result in loss of the approximation capabilities. If we replace $h_l^{pq}(y_{l-1}, x_{l+1})$ with a single parameter $\bar{y}_l^{pq}$ we reduce the number of parameters to m^2 for each fuzzy system. The observations made during the sensitivity analysis in Section 4.6.4 are still valid. The approximation capabilities are now only determined by the number of membership functions for each variable; the HFL for the first system can be described as follows:

$$f_1(x_1, x_2) = \frac{\sum_{p=1}^{m} \sum_{q=1}^{m} \bar{y}_1^{pq} \left[\mu_{A_1^p}(x_1) \mu_{A_2^q}(x_2) \right]}{\sum_{p=1}^{m} \sum_{q=1}^{m} \left[\mu_{A_1^p}(x_1) \mu_{A_2^q}(x_2) \right]}, \tag{6.3}$$

For better understanding of the approximation capabilities of our HFL we split each fuzzy system in domains. In Figure 6.1 the domains are shown for the $m = 4$ case. Always, only two of these domains are active at one time, for example the two gray ones. The result for the first domain $f_1(x_1, x_2)$ can be calculated according to Formula 6.3 as follows:

$$
\begin{aligned}
f_1(x_1, x_2) &= \bar{y}_1^{22} \quad \mu_{A_1^2}(x_1) \quad\quad \mu_{A_2^2}(x_2) \\
&+ \bar{y}_1^{23} \quad \mu_{A_1^2}(x_1) \quad\quad (1 - \mu_{A_2^2}(x_2)) \\
&+ \bar{y}_1^{32} \quad (1 - \mu_{A_1^2}(x_1)) \quad \mu_{A_2^2}(x_2) \\
&+ \bar{y}_1^{33} \quad (1 - \mu_{A_1^2}(x_1)) \quad (1 - \mu_{A_2^2}(x_2))
\end{aligned}
\tag{6.4}
$$

We use triangular membership functions where $\mu_{A_1^p}(x_i) + \mu_{A_1^{p+1}}(x_i) = 1$ (see also Figure

6.4). In this case also $\mu_{A_1^p}(x_1) \geq 0$, $\mu_{A_1^q}(x_2) \geq 0 \ \forall p = 2,3$ is true. All other membership functions are zero and are not considered. By simplification one obtains

$$
\begin{aligned}
f_1(x_1, x_2) \ &= \ \bar{y}_1^{22}\mu_{A_1^2}(x_1)\mu_{A_2^2}(x_2) \\
&+ \bar{y}_1^{23}\mu_{A_1^2}(x_1) \\
&- \bar{y}_1^{23}\mu_{A_1^2}(x_1)\mu_{A_2^2}(x_2) \\
&+ \bar{y}_1^{32}\mu_{A_2^2}(x_2) \\
&- \bar{y}_1^{32}\mu_{A_1^2}(x_1)\mu_{A_2^2}(x_2) \\
&+ \bar{y}_1^{33} \\
&- \bar{y}_1^{33}\mu_{A_2^2}(x_2) \\
&- \bar{y}_1^{33}\mu_{A_1^2}(x_1) \\
&+ \bar{y}_1^{33}\mu_{A_1^2}(x_1)\mu_{A_2^2}(x_2)
\end{aligned}
\tag{6.5}
$$

and

$$
\begin{aligned}
f_1(x_1, x_2) \ &= \ \mu_{A_1^2}(x_1)\mu_{A_2^2}(x_2)(\bar{y}_1^{22} - \bar{y}_1^{23} - \bar{y}_1^{32} + \bar{y}_1^{33}) \\
&+ \mu_{A_1^2}(x_1)(\bar{y}_1^{22} - \bar{y}_1^{33}) \\
&+ \mu_{A_2^2}(x_1)(\bar{y}_1^{32} - \bar{y}_1^{33}) \\
&+ \bar{y}_1^{33}
\end{aligned}
\tag{6.6}
$$

which has the general form of

$$
f_1(x_1, x_2) = a + bx_1 + cx_2 + dx_1 x_2
\tag{6.7}
$$

For visualization we plot in Figure 6.2(a) a possible outcome with parameters $\bar{y}_1^{22} = 0$; $\bar{y}_1^{23} = 1$; $\bar{y}_1^{32} = 0$; $\bar{y}_1^{33} = 1$. In Figure 6.2(b) the whole response surface is shown when all parameters are by turns $1, 0$. As variables we have chosen T_e and E_{esn}. By down scaling of the raster (increasing the number of membership functions) any resolution could be achieved. It can already be seen that the resolution for irradiance for lower values is higher as it is the case with the density of the data.

6.2.2 The membership functions

In this Section we discuss the type of the membership functions as well as the number and the distribution on the interval. For our hierarchical fuzzy system $n = 5$ state variables $(x_1, ..., x_5)$ will be considered, which are shown in Table 6.1. The state of occupancy will not be considered here because it changes nothing at the approximation ability of a control. However, in real world the control strategy can be changed completely if nobody is in the room and the control can act regardless of visual and thermal comfort. First, we have to assign domains $[\alpha_i, \beta_i]$, $i = 1, ..., 5$ for each variable that will be covered by the membership function. As a starting point we use the data which was collected in the LESO experimental building.
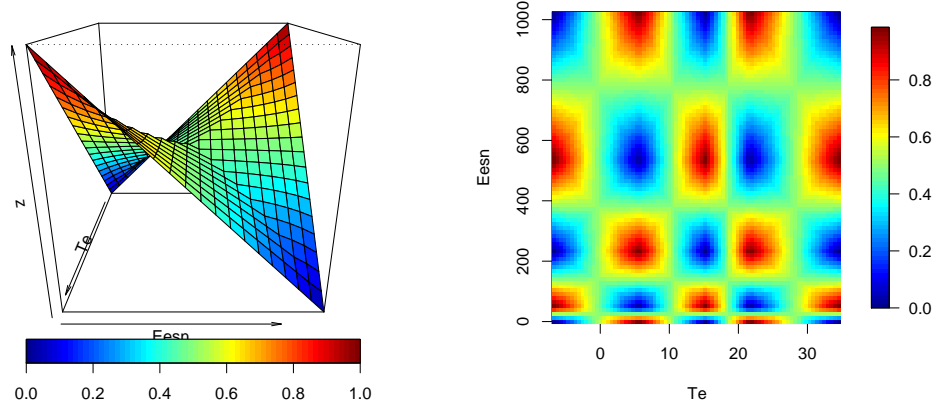
(a) Possible outcome of one field of the response surface.

(b) The whole response surface with the state variables T_e and E_{esn} and five membership functions per variable. The parameters are by turns $1, 0$.

Figure 6.2: The single cell and a complete response surface

6.2.2.1 Description of monitored data

The LESO building is equipped with a building management system based on the commercial EIB bus, which can read out the status of the building's sensors and actuators. The system was installed in 1999; about 240 sensors and actuators are connected to the system. The available data which is used for our study is shown in Table 6.1.

The benefit of this data is the ability to assign domains $[\alpha_i, \beta_i]$, $i = 1, ..., 5$ and adapt our membership functions according to the density of the data. The histograms of all five variables are plotted in Figure 6.3. The assumption is that in intervals with high density of data more membership functions are placed for a more precise control than in intervals with less records. For that we chose the distribution according to the density of the monitored data. Since it is not yet clear how many membership functions will be used per variable we plotted in Figure 6.5 the variables split in different quartiles with the resulting membership functions.

6.2.2.2 Type of membership function

Regarding the type of membership functions there are many different possibilities that are described in Section 4.4.2. It cannot be determined exactly which type of membership is the best for our task. In literature triangular membership functions have proven to be adequate for many different applications. Furthermore our analysis of the HFL in Section 4.6.4 is partly based on triangular shaped membership functions. For those reasons we use triangular based membership functions for the HFL.
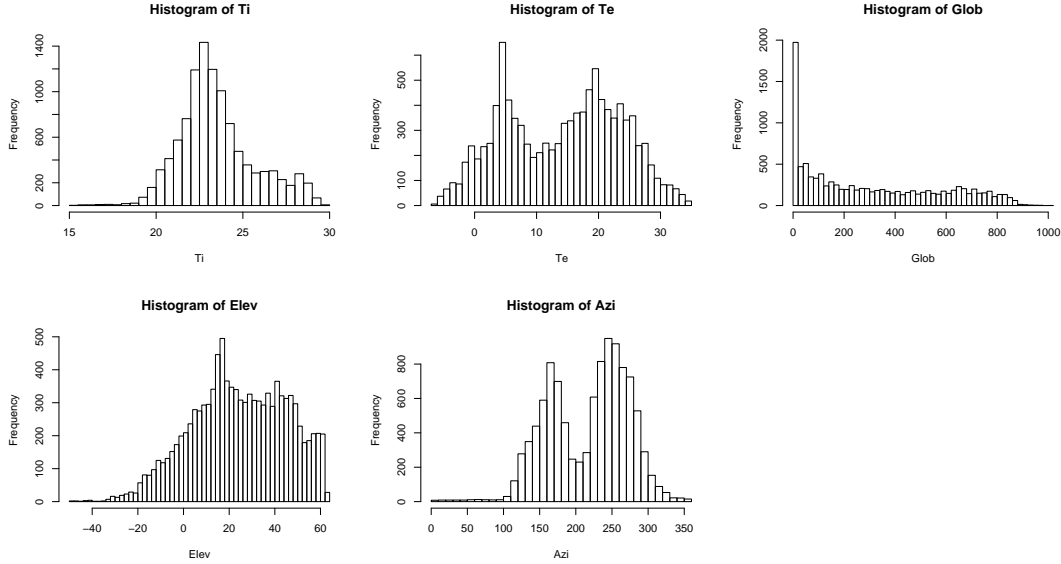
Figure 6.3: Histogram of all decision variables.

We need two types of membership functions for our hierarchical fuzzy system. Five $(\mu_{A_1^q}, ..., \mu_{A_5^q})$, $q = 1, ..., m$ sets of membership functions for our variables and one set $\mu_{A_Y^q}$, $q = 1, ..., m$ for passing the information $f(x_1, x_{i+1}) = y_i$, $y_i \in [0, 1]$ to the next fuzzy system. The triangular are membership functions that defined in (5.5) and are respectively for every x_i:

$$\begin{aligned}
\mu_{A_i^1}(x_i) &= \mu_{A_i^1}(x_i; e_i^1 + \epsilon, e_i^1, e_i^2) \\
\mu_{A_i^j}(x_i) &= \mu_{A_i^j}(x_i; e_i^{j-1}, e_i^j, e_i^{j+1})
\end{aligned}$$
(6.8)

for $j = 2, 3, ..., m - 1$, and

$$\mu_{A_i^m}(x_i) = \mu_{A_i^m}(x_i; e_i^{m-1}, e_i^m, e_i^m + \epsilon),$$
(6.9)

where $i = 1, .., 5$ and ϵ is an arbitrarily small positive constant to prevent that term $(x - a)$ or $(c - x)$ in (5.5) is divided by 0. Two important characters of this kind of functions are: First, at any point $(x_1, ..., x_5) \in [\alpha_1, \beta_1] \times ... \times [\alpha_5, \beta_5]$ at most two membership functions among $\mu_{A_i^p}(x_i)$, $(p = 1, ..., m)$ will be nonzero; second, the summation of the two nonzero membership functions equals always one $\mu_{A_i^p}(x_i) + \mu_{A_i^{p+1}}(x_i) = 1$.

For every variables $(x_1, ..., x_5)$ we have to define e_i^j, $j = 1, ..., m$. A general membership function is shown in Figure 6.4.

6.2.2.3 Number of membership function

The number of membership functions m per state variable is more difficult to assess. Based on the analysis carried out in Section 4.4.2 we want to use the same number of membership
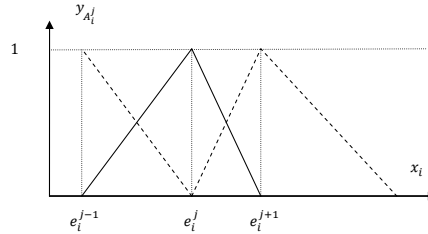
Figure 6.4: Membership function according to Formula 6.9 and 5.5.

functions for each variable.

By increasing the number of membership functions the resolution will be increased and the control strategy can be better adapted to its task. However, an increase in membership functions will directly increase the number of parameters of the HFL which have to be adapted by the optimization.

Finding the necessary resolution and herewith the number of membership functions cannot be obtained from calculations. We implemented a fuzzy system that we test with different number of membership functions (MFs). No matter how many MFs we define they are always distributed according to the density of the data. In Figure 6.5 all variables are divided in different quantiles and according to that the MFs are shown.

For finding the optimal number of membership function we suggest the same procedure we will use for finding the optimal set of state variables:

1. Preparation of five fuzzy systems with 2, 3, 4, 5 and 6 membership functions which are all distributed according to the collected data and shown in Figure 6.5. Each HFL consists of all state variables shown in Table 6.1.

2. Optimizing the five fuzzy systems with a multi-objective optimizer on three periods with weather data explained in Section 6.3.1.

3. Evaluating the final population of solutions for each control on one year weather data to find out about the general capability of the single control.

In the first row of Figure 6.6 the Pareto-front[1] is shown after the optimization where the results do not differ that strong. For better comparison we show in Figure 6.7(a) the boxplot of the two objectives for the five controls. Also the performance is increasing with the number of MF's, the results are not significant as the notches indicate. In the second row of Figure 6.6 we show the results where each set of parameters was run for one year. Of course the scale of the energy consumption changed because in one year more energy was used, though comparability remains coherent. Looking at the one year simulations the difference between the outcomes

---

[1]The concept of Pareto-front is explained in Section 4.1.2.3.
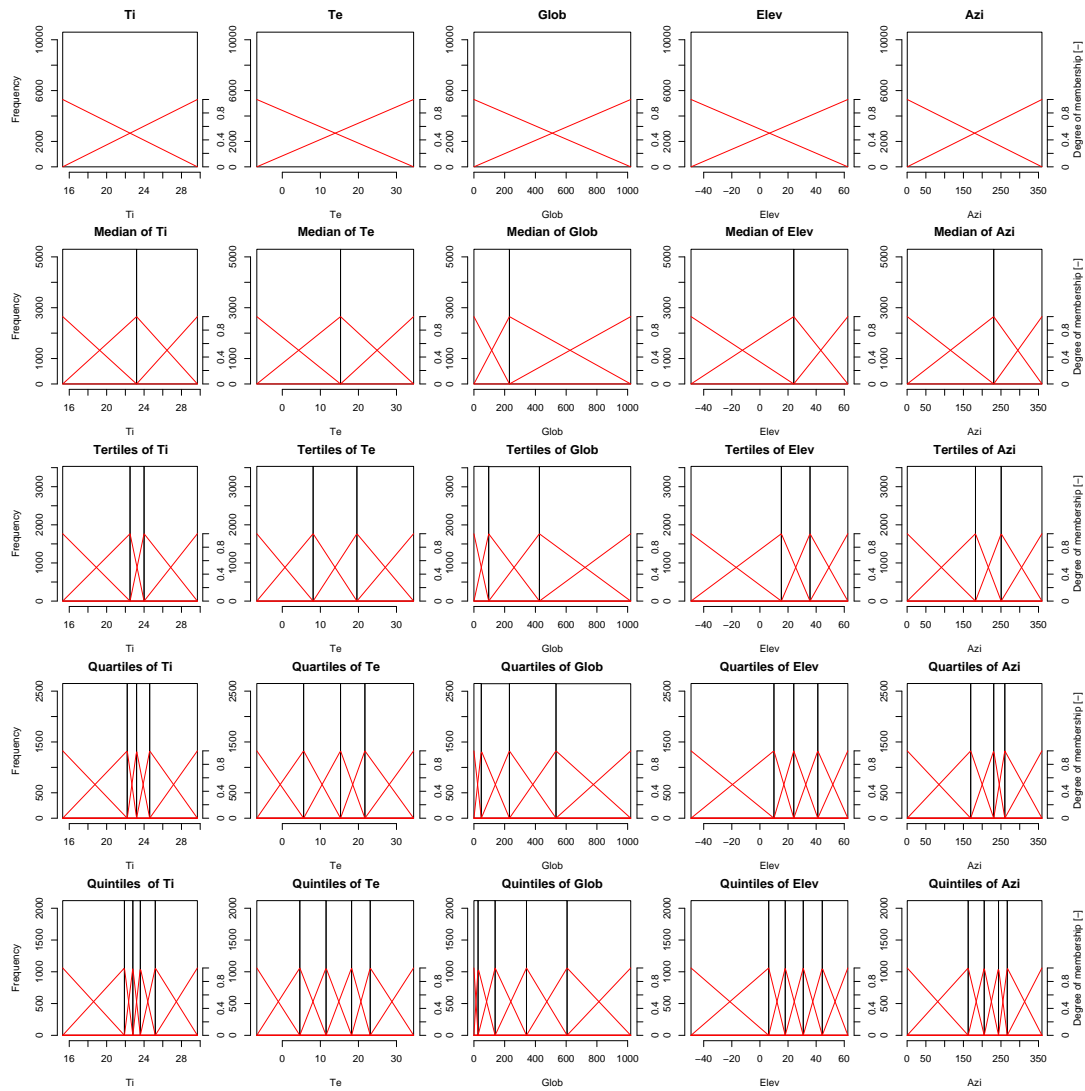
Figure 6.5: All variables are split into different quantiles together with the resulting membership functions.
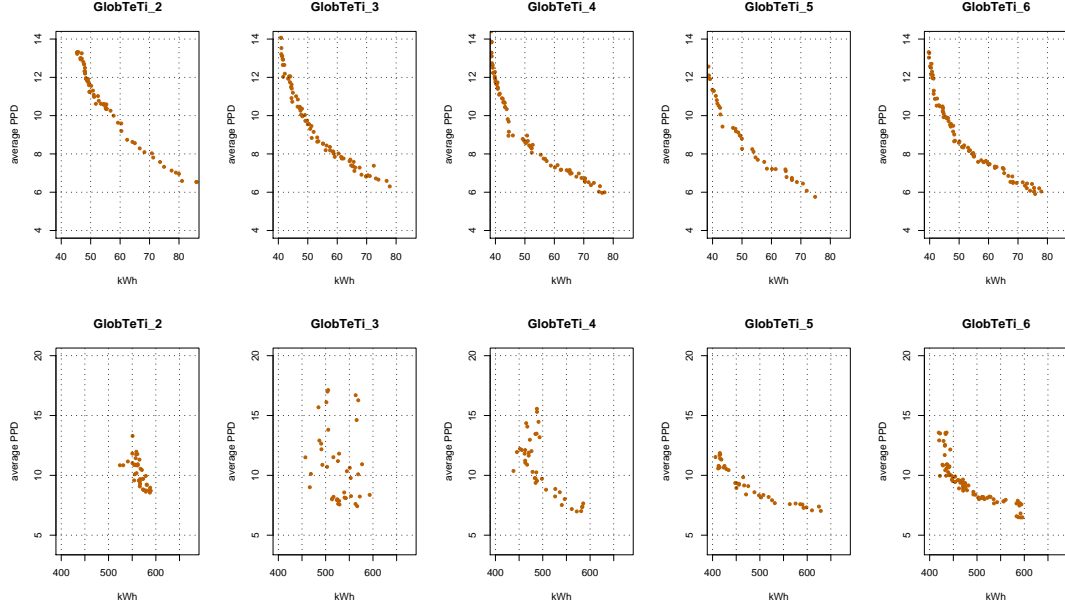
Figure 6.6: Solutions for the simulations with different number of membership functions in the fuzzy systems. The first row shows the results after the optimization and the second row after the one year run with the found parameters.

is already more evident. Aided by the boxplot in Figure 6.7(b) it can be clearly seen that the control models with 2 and 3 MF's are significantly worse than the one with 4, 5 or 6 MF's. Especially for 2 and 3 MF's the results for the one year run are more widely distributed and look more random. It is the consequence of less MF's, which makes it hard to let the control distinguish between different situations.

Five MF's will result in 25 parameters, which is reasonable for our control system and with six MF's we do not get any better. Consequently, five MF's represent a good trade off between correctness and computational costs. A drawback is that we do not test all kind of different combinations of state variables, but nevertheless we think it gives a sound estimate.

Summing up, as declared before, we use $m = 5$ triangle shaped membership functions which are distributed on the intervals $[\alpha_i, \beta_i]$. For that task we divide the data according to the 0.25 quartiles into four domains with an equal number of data points. This is shown in Figure 6.5 and the cutoff points are displayed in Table 6.1.

For passing the information $f(x_1, x_{i+1}) = y_i$ to the next fuzzy system, we define $\mu_{A_Y^q}$, $q = 1, ..., 5$ as equally spaced triangular membership functions in the interval $[0, 1]$ which results in $e_Y^1 = 0$, $e_Y^2 = 0.25$, $e_Y^3 = 0.50$, $e_Y^4 = 0.75$, $e_Y^5 = 1$, and is shown in Figure 6.8.

(a) Optimization phase.

(b) One year optimization.
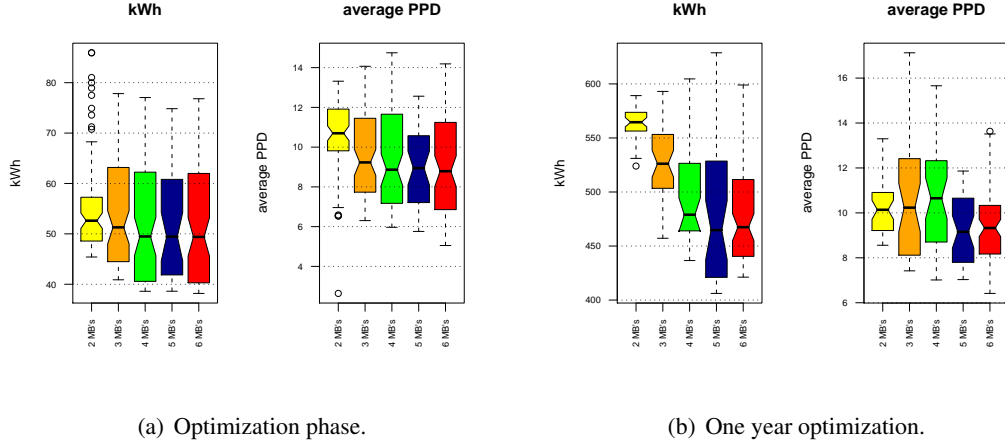
Figure 6.7: Boxplot of the two objectives for the optimization phase and the one year evaluation. The notches refer to the 95% confidence interval for the difference in two medians. If the notches of two plots do not overlap this is a *strong evidence* that the two medians of the sample differ.
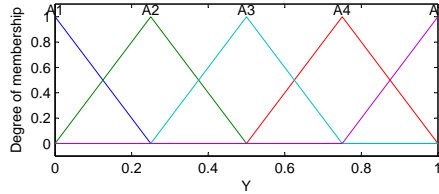
Figure 6.8: Membership function for passing the information $f(x_1, x_{i+1}) = y_i$ to the next fuzzy system.

6.3 Identifying the state variables

We perform the optimization with our simulation environment presented in Chapter 3 and as virtual building we use the LESO room which is described in Section 5.2.1.

We consider the five variables that are listed in Table 6.1. Because we work with a complete fuzzy logic system we have automatically ($5^2 = 25$) rules for the first category system. As explained in Section 6.2.2 the parameters $\bar{y}_1^{pq}$ are subject of the optimization. So, for the first category our optimizer has to determine the following matrix:

$$\begin{pmatrix} \bar{y}_1^{11} & \cdots & \bar{y}_1^{15} \\ \vdots & \ddots & \vdots \\ \bar{y}_1^{15} & \cdots & \bar{y}_1^{55} \end{pmatrix},$$ (6.10)

with 25 optimal values for $\bar{y}_1^{pq} \in (0, 1)$ with $q, p = 1, ..., 5$. In the second category the optimization has 25 parameters for $\bar{y}_1^{pq}$ and 25 parameters for $\bar{y}_2^{pq}$, which is a total of 50; in the

Name	Symbol	Description	Domain	e_i^1	e_i^2	e_i^3	e_i^4	e_i^5
Ti	T_i	Indoor temperature [° C]	[15.3,29.7]	15.3	22.2	23.2	24.6	29.7
Te	T_e	Outdoor temperature [° C]	[-6.7,34.5]	-6.7	5.6	15.3	21.7	34.5
Glob	E_{esn}	Vertical outdoor irradiance [W/m^2]	[0.0,1020.0]	0	48	231	534	1020
Elev	γ_s	Elevation of the sun [°]	[-49.02,62.55]	-49.02	9.97	24.08	41.18	62.55
Azi	α_s	Azimuth of the sun from due north in a clockwise direction[°]	[0.40,359.18]	0.40	169.39	230.73	260.28	359.18

Table 6.1: The tables in the `lesoeib` database which we use in our data mining together with the domains for the membership functions

third a total of 75 and in the fourth of 100 parameters. Since $0 < \bar{y}_1^{pq} < 1$ and $f_1(x_1, x_2)$ is a weighted average of the values $\bar{y}_1^{pq}$ we have always $y_1 \in [0, 1]$.

6.3.1 The weather data

The simulation covers seven cold days, 14 intermediate, and five warm days. These synthetic periods are chosen to cover all kind of climate conditions and to keep the simulation time manageable. Since all the results are evaluated also for a one year period this does not influence the final results. To take the internal heat storage into account the simulation for every different period starts not until all conditions have balanced out. Although this takes computational time it increases accuracy significantly. The temperature, direct radiation, and diffuse radiation for the three sets of weather data are shown in Figures 5.7, 5.8, 5.9.

6.3.2 Occupancy and appliances

The goal of the simulation is to find out about the adaption capabilities of the single controls. Optimizing 26 different fuzzy systems takes already days, hence we had to identify sources to increase the speed of the optimization without limiting the validity. In previous simulations we included stochastic models for appliances and occupancy to create realistic settings. For testing the adaption capabilities they only slow down the simulation and maybe even disturb the results as they add noise. Hence we do not include stochastic processes for this specific simulations. IDA/ICE uses variable time steps in order to increase the accuracy of the model. Sometimes they can be as small as some seconds. This is incredibly slowing down the simulations. We set the shortest time step to 300s to gain speed without loosing accuracy as we do not want to set the blinds more frequently.

6.4 Simulation results

To obtain comprehensive results we have to include every combination of the five variables in our study. The order does not matter as we have shown in Section 4.6. Given that we have

$n = 5$ state variables $(x_1, ..., x_5)$ for our hierarchical fuzzy system we obtain

$$\binom{5}{2} = \frac{5!}{(5-2)!2!} = 10, \tag{6.11}$$

different combinations of variables for the first category, $\binom{3}{5} = 10$ different combinations for the second category, $\binom{4}{5} = 5$ different combinations for the third category and $\binom{5}{5} = 1$ for the fourth category. This results in 26 different fuzzy systems that have to be tested. We implement every single fuzzy system in our simulation environment and then optimize the parameters of the fuzzy systems with the procedure described in Section 4.7. Consequently we obtain 26 Pareto-fronts that show the result of the optimized fuzzy systems regarding the average PPD and the energy consumption during the three test periods (see Figures 5.7, 5.8, 5.9). However the result of the optimization does not say too much about the quality of the controls since all parameters of the fuzzy system are well adapted to exactly this special period. Also a dummy variable which has enough variance to distinguish between different situations would look good as indicator if the control is well adapted to this specific variance. To find out if the control works in general and the state variables really include information, we take the parameters $\bar{y}_m^{pq}$ (see Formula 5.4) for all the solutions of the final population and run the simulation for the whole year.

In summary the procedure can be basically divided in four different steps:

1. Fitting of the membership function to the 5 different state variables $x_1, ...x_5$ and building of the 26 different fuzzy logic controls as explained in Section 6.2.

2. Optimizing the 26 fuzzy systems with a multi-objective optimizer on three periods as explained in Section 4.7.

3. Evaluating the final population of solutions for each control on one year weather data to find out about the general capability of the single control.

4. Evaluating the optimal solution regarding the energy for all directions. The experimental setup will be explained together with the results.

6.4.1 Results of the optimization of the fuzzy systems

The 26 different fuzzy systems are distributed over four categories, where every category has a different number of state variables. The names of the fuzzy systems match always with their state variables. For the single categories we get the following fuzzy systems:

Category1 `ElevAzi, GlobAzi, GlobElev, GlobTe, GlobTi, TeAzi, TeElev, TeTi,`
`TiAzi, TiElev.`

Category2 `GlobElevAzi, GlobTeAzi, GlobTeElev, GlobTeTi, GlobTiAzi,`
`GlobTiElev, TeElevAzi, TiAziTe, TiElevAzi, TiElevTe.`
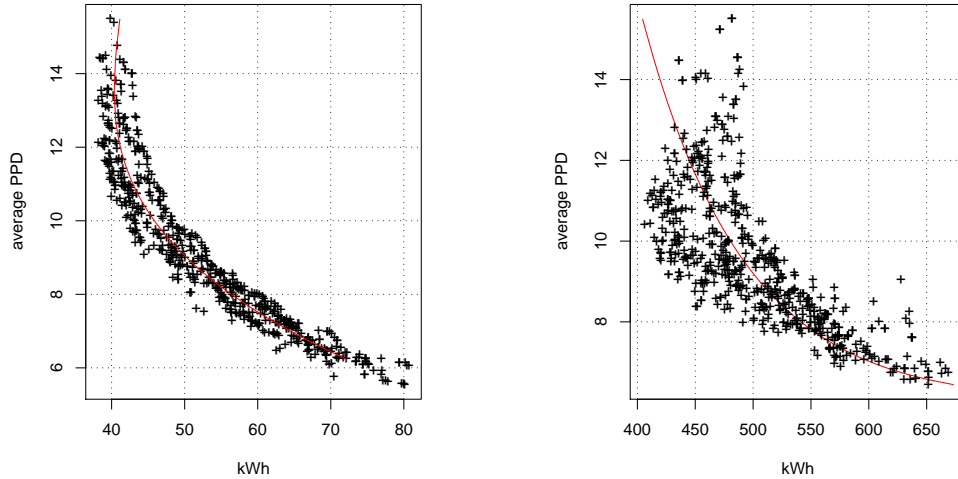
(a) All solutions of the first category fuzzy system from the optimization. The red line is the result of a linear model of the form $y = x + x^2 + x^3$. It serves as reverence for all one year evaluations.

(b) All solutions of the first category fuzzy system evaluated for one year. The red line is the result of a linear model of the form $y = ln(x)$. It serves as reverence for all one year evaluations.

Figure 6.9: Solutions of the first category with reference line

Category3 `GlobTeAziElev, GlobTeAziTi, GlobTeTiElev, GlobTiAziElev, TeTiAziElev`

Category4 `GlobTeAziElevTi`

The observed Pareto-front for the single controls are shown in Figure 6.11 for the first category, in Figure 6.12 for the second, in Figure 6.13 for the third, and in Figure 6.14(a) for the fourth category. Every dot represents the result of a control regarding the two objectives and has a specific set of parameters. The results are plotted together with a fitted linear model[1] of the combination of all data from the first category. Figure 6.9(a) shows the combined data of the first category: the fitted curve which is only for visualization makes it easier to compare the results. By looking at the data it should be kept in mind that the parameters are all optimized to suit best the situation given by the simulation. It was expected that the results are quiet close. In general that means, that if we could fit the parameters exactly to our conditions it would be possible to achieve good results regardless of the input factors we use. Nevertheless by comparing the results of the first and second category it is obvious that most of the points are below the fitted line. So it was possible to adapt the control a little better then with only two state variables. In the third and fourth category there is no significant improvement compared to the second category.

---

[1]The linear model has the form $y = x + x^2 + x^3$
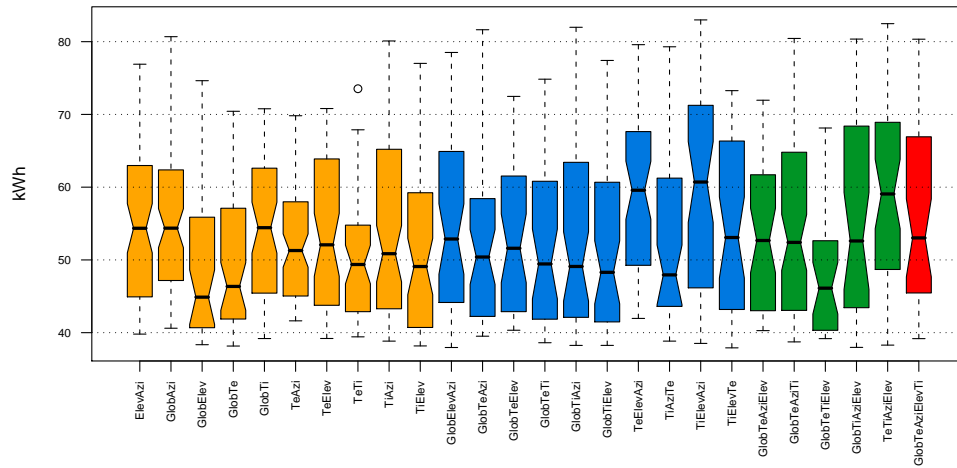
(a) Boxplot of the energy consumption of all fuzzy controls for the optimization phase
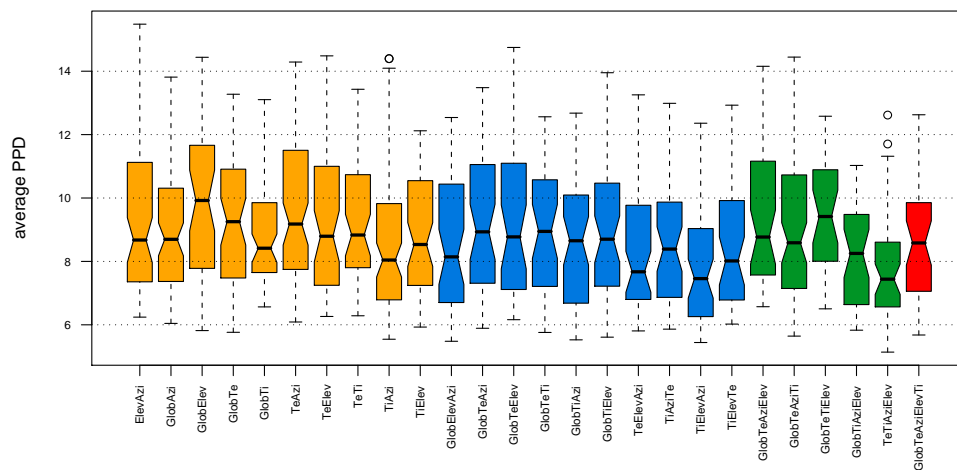
(b) Boxplot of the average PPD of all fuzzy controls for the optimization phase.

Figure 6.10: The two objectives in the optimization phase
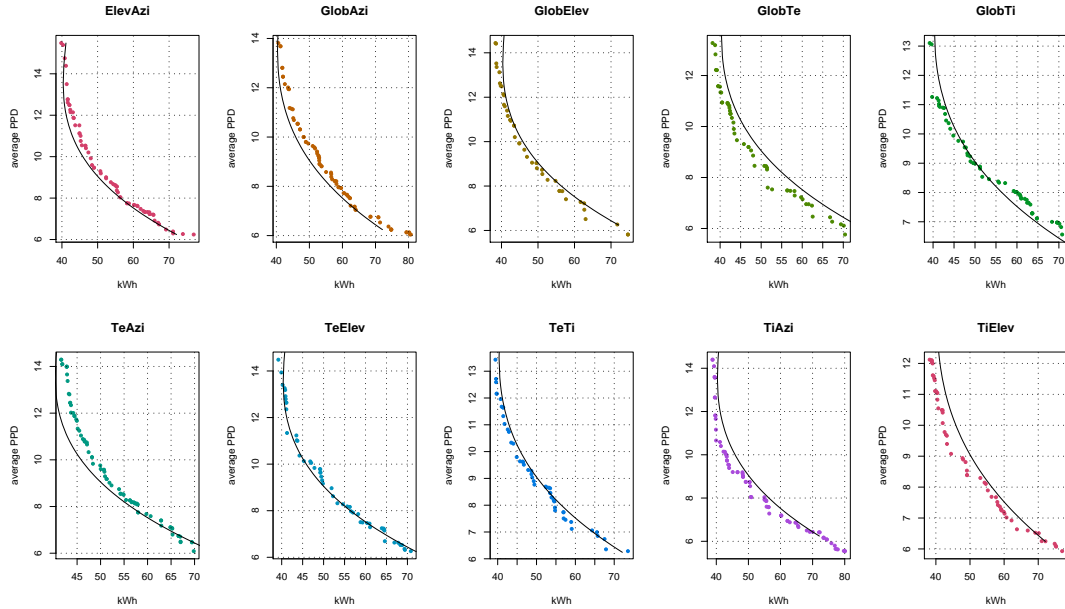
Figure 6.11: All Pareto-fronts from the different controls. To better evaluate them a black line is plotted which is the result of the fit of a third order model of all results combined.

Boxplots of the two objectives for the single controls are given in Figures 6.10(a) and 6.10(b). The notches refer to the 95% confidence interval for the difference in two medians. That means if the notches of two plots do not overlap this is *strong evidence* that the two medians of that sample differ.

One has to keep in mind that the median of single objectives cannot directly be converted into the performance of the control. Especially since the results may not be equally distributed within the interval and therefore do not give a combined measure of both objectives.

6.4.2 Results of one year run of the fuzzy systems

For the evaluation of the obtained fuzzy control we take the parameter of the optimization and simulate for each control the performance over one year.

The results are shown in Figures 6.15, 6.16, 6.17, 6.14(b). This time we did not obtain a Pareto-front since not only Pareto-optimal solutions are shown rather than all solutions from the optimized set of parameters. Again we fit a linear model of the type $y = ln(x)$ to the solutions of the first category. The result together with the obtained solutions of the first category is shown in Figure 6.9(b).

With one year evaluation of all hierarchical fuzzy systems we test how good the parameters have been fitted to achieve good thermal comfort and low energy consumption. This gives us informations about the importance of the variables used in the controls. For example by comparing the results of `TeElev` (Figure 6.15) and `TeElevAzi` (Figure 6.16) no improvement
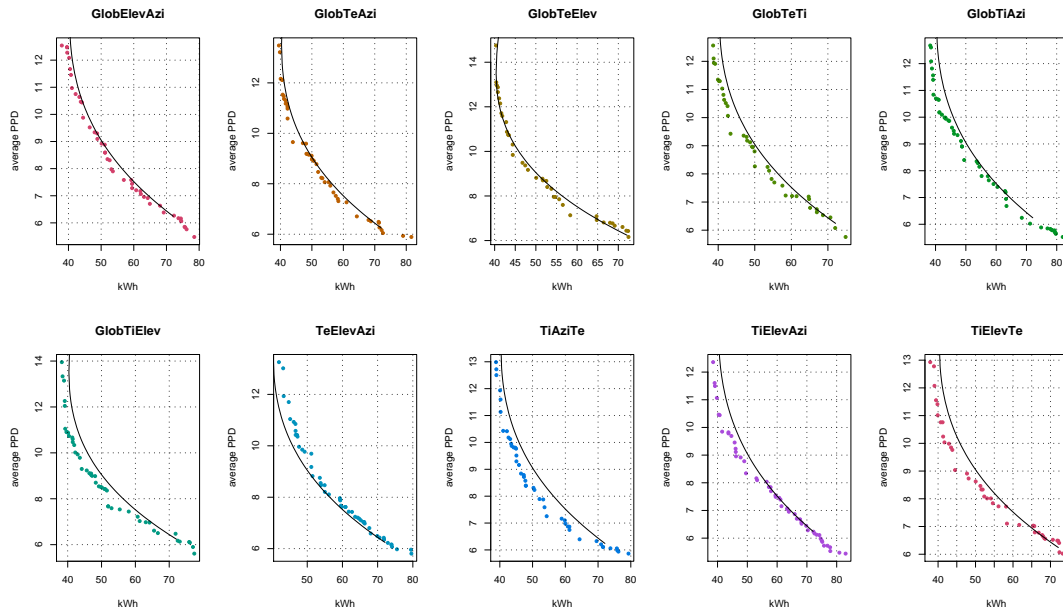
Figure 6.12: All Pareto-fronts from the different controls of the second category. As reference the same black line as in Figure 6.11 is drawn.
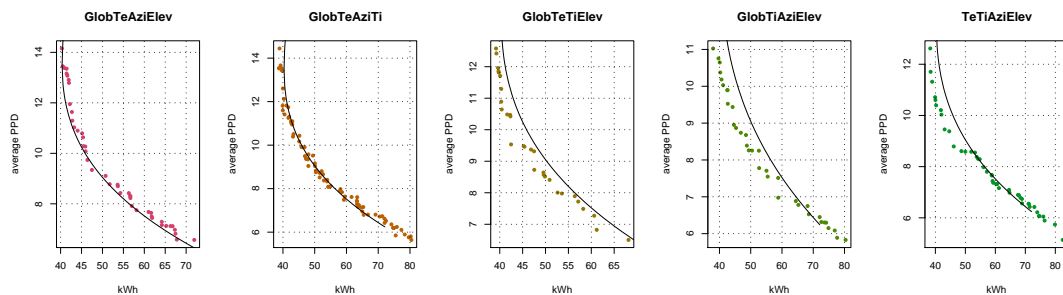
Figure 6.13: All Pareto-fronts from the different controls of the third category. As reference the same black line as in Figure 6.11 is drawn.

(a) Pareto-front of the test phase.

(b) Pareto-front from the one year evaluation
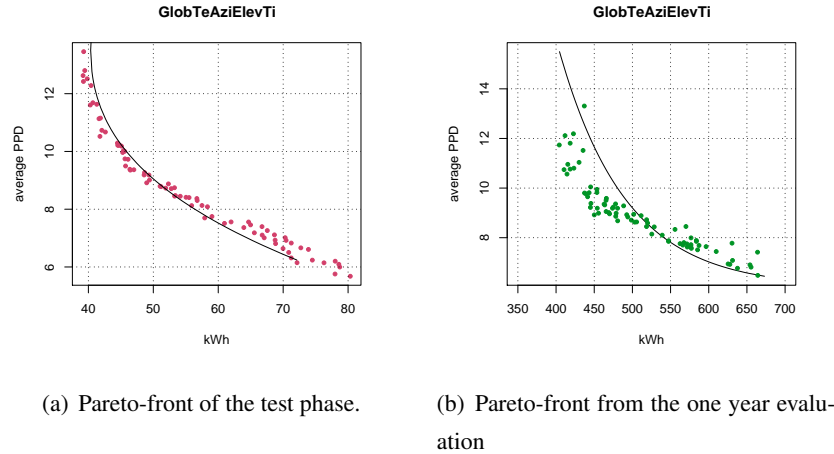
Figure 6.14: Pareto-fronts from fourth category fuzzy system. As reference the same black lines as in Figures 6.9(b), 6.9(a) is drawn.

in performance can be seen. The conclusion is: Adding information about the azimuth to this set of variables does not provide additional information to increase performance. But in case of `ElevAzi` (Figures 6.15) and `GlobElevAzi` (Figure 6.16) the performance increases by adding the variable `Glob` to the control.

After comparing boxplots of the first and second objective we used a combined measure of the two objectives. It is the relative euklidian distance from each solution to the line of the fitted model (see Figure 6.18). This has the advantage that the mean of the solutions can be used as an indicator for the performance. Again the notches refer to the 95% confidence interval for the difference in two medians. It can be seen that the best control from the first category is `GlobTe` which is also better than many of the controls of Category2, Category3 and Category4. That means that even a small number of input factors already provide sufficient information to build a good control. If a control is realized with only two variables, selection of those is especially important since most of the other two-variables controls in Category1 are considerably worse.

In Figure 6.19(a) the relative performance per category is plotted. The increase from Category1 to Category2 fuzzy systems is significant. The increase from Category1 to Category3 systems is as well significant but from Category2 to Category3 a decrease is reported that is also significant. Category4 is increasing the performance again but not above the level of Category2.

In Figure 6.19(b) all controls are grouped to the single state variables. The first boxplot contains all controls where `Ti` is used. By doing that, finally the variables can be ranked according to their importance. It shows that controls which include `Ti` are significantly better than the rest. If controls include `Te` or `Glob` they are significantly better than controls which
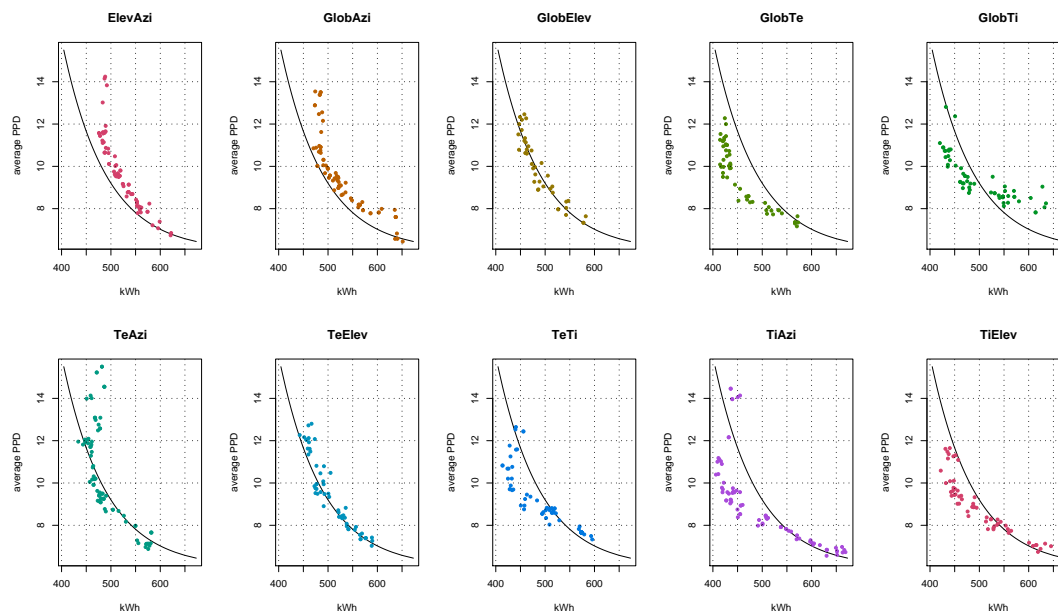
Figure 6.15: All results from the one year evaluation of the different controls of the first category. For a better evaluation a black line is plotted which is the result of the fit of a model of the combined results.

contain `Azi` or `Elev`. Between `Glob` and `Te` there is no evidence which are better, the same applies to `Azi` and `Elev`.

In Figure 6.20(a) the same principle for the objective energy consumption is used as in Figure 6.19(b). It can be said that controls which contain the variables `Ti` and `Te` are significantly better in terms of energy consumption than controls that include `Azi` and `Elev`. The variable `Glob` is not significant better or worse than the other four.

The second objective the average PPD for the single variables is shown in Figure 6.20(b). Since the meadians of all samples are close there cannot be made a statement according to the 95% confidence interval. Here, for the first time, the variables `Azi` and `Elev` are not worse than the others. Even though the variable `Ti` seems to be important and has the best mean, it is not significantly better than any other variable.

The results can be summarized as follows:

1. Including more than three variables yields in no further improvement in the performance.

2. Two state variables provide sufficient information for good blind control.

3. According to our investigations the importance of the state variables can be stated as:

   1. T_i

   2. T_e ,E_{esn}

112
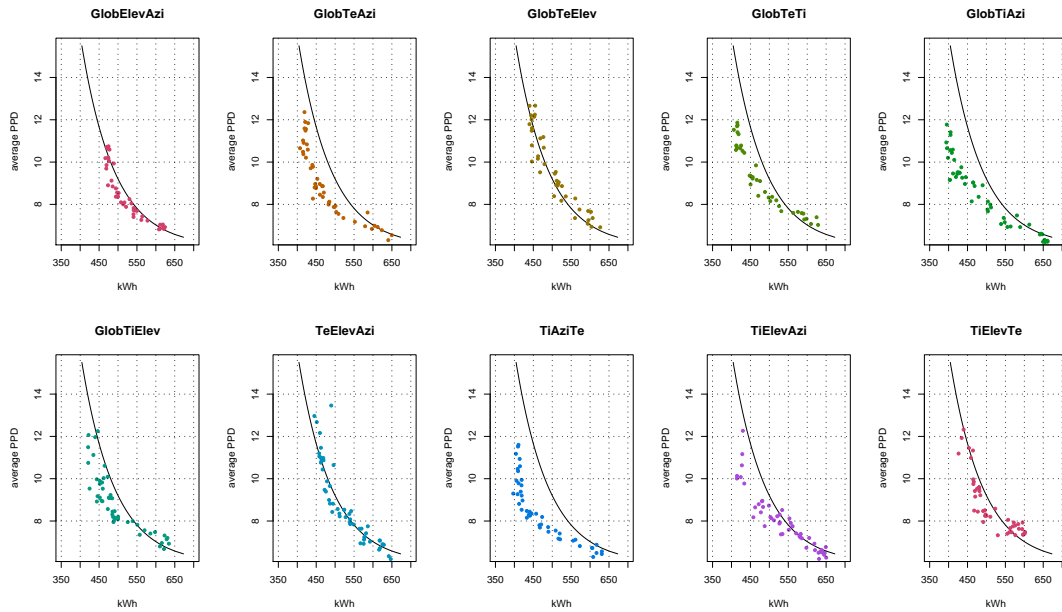
Figure 6.16: All results from the one year evaluation of the different controls of the second category. To better evaluate them a black line is plotted which is the result of the fit of a model of all results combined.
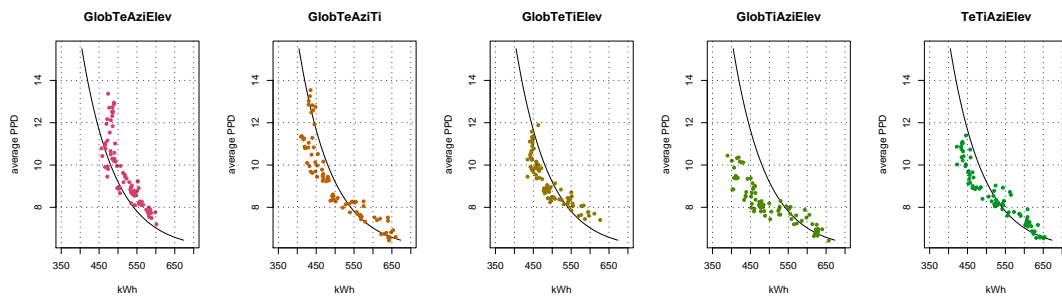
Figure 6.17: All results from the one year evaluation of the different controls of the third category. To better evaluate them a black line is plotted which is the result of the fit of a model of all results combined.
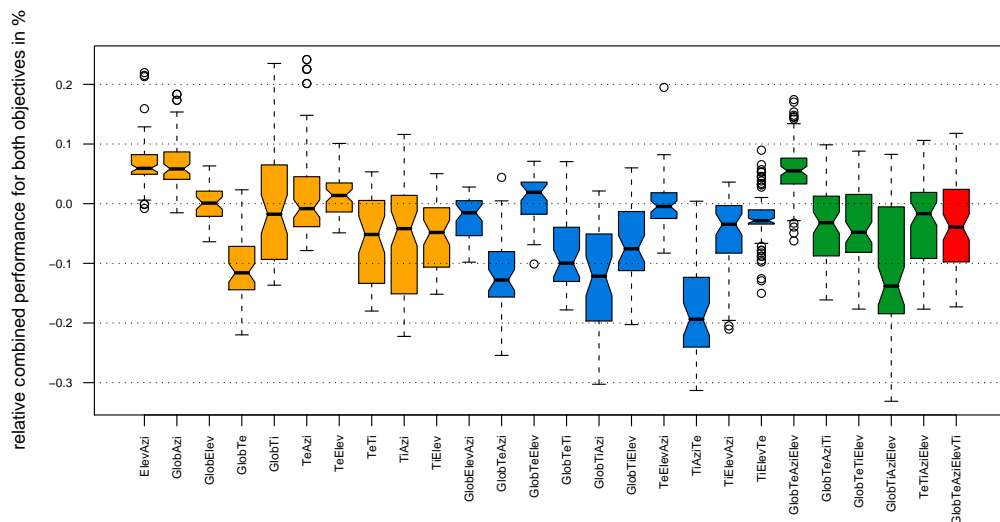
Figure 6.18: Boxplot of the relative performance (minimization of both objectives) of both objectives for all fuzzy controls for the one year evaluation. The notches refer to the 95% confidence interval for the difference in two medians. That means if the notches of two plots do not overlap this is *strong evidence* that the two medians of that sample differ.

    3. α_s, γ_S

4. The importance of the variables regarding energy consumption is:

    1. T_i, T_e

    2. E_{esn}

    3. γ_s, α_S

5. About the importance regarding the average PPD no significant statement can be made.

6.4.3 Results of different orientations

After testing the performance of the optimized controls on yearly data we also want to assess the efficiency regarding different orientations. Until now only the south oriented case was simulated. We use the same office room but incorporated it 12 times into a imaginary dodecagonal building. We chose this alternative over rotating the building for the single orientation because with this method we obtain data for all 12 orientations with one optimization run. Since the inner walls are adiabat, no heat flux from the rest of the building can influence the results. This further investigation has two goals:

- To identify the robustness of our control regarding a modification of orientation.
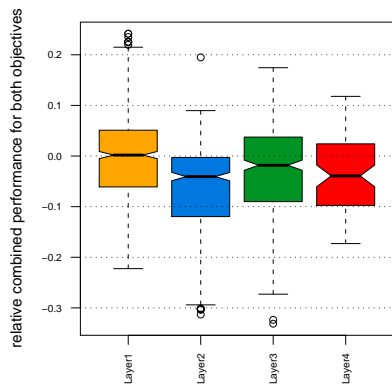
(a) Boxplot of the relative performance of both objectives for the single layers for the one year evaluation.
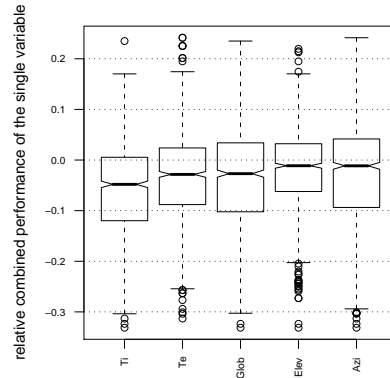
(b) Boxplot of the relative performance (minimization of both objectives) of both objectives for the single variables for the one year evaluation.

Figure 6.19: The notches refer to the 95% confidence interval for the difference in two medians. That means if the notches of two plots do not overlap, this is *strong evidence* that the two medians of that sample differ.
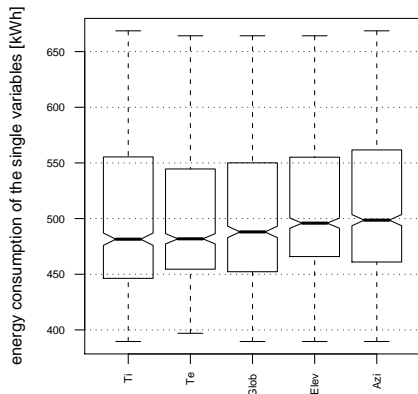
(a) Boxplot of the energy consumption for the single variables for the one year evaluation.
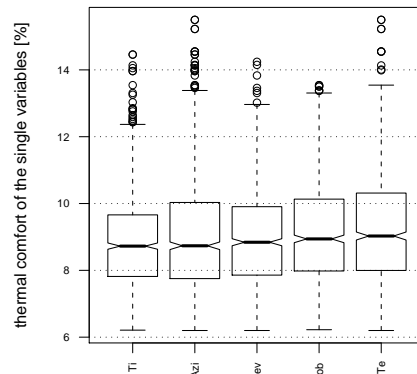
(b) Boxplot of the thermal comfort for the single variables for the one year evaluation.

Figure 6.20: The average of each variable for the one year evaluation

115

- To provide reference cases for our future adaptive control.

The results are shown in Figures 6.21, 6.22, 6.23. This time no Pareto-front can be given since only one solution is evaluated for one year. The energy consumption is given for each of the 12 orientations, which represents a measurement each $30°$ where $0°$ refers to south. The red stands for heating energy, the blue for cooling and the yellow for electric lighting. The latter was only switched on during occupancy and for illuminance levels lower than 300 lux on the work plane.

The result for $0°$ should always match with the lowest energy consumption of the associated controls in Figures 6.15, 6.16, 6.17, 6.14(b). There we also find the lowest energies consumed compared to the other orientations which is due to the fact that they have been optimized for the south case. For example in the case of `TeTi` the best energy consumption was reached with 413.64 kWh. The corresponding set of parameters is:

$$\begin{pmatrix} 0.90 & 0.42 & 0.97 & 0.85 & 0.23 \\ 0.99 & 0.85 & 0.99 & 0.82 & 0.85 \\ 0.66 & 0.85 & 0.98 & 0.47 & 0.80 \\ 0.21 & 0.97 & 0.95 & 0.86 & 0.48 \\ 0.86 & 0.53 & 0.01 & 0.20 & 0.00 \end{pmatrix}, \qquad (6.12)$$

which are inserted in the control of every of the 12 blind controls and then run for a yearly simulation.

It shows that non of the controls are able to provide optimal control in any other case than the south case and that independent of the state variables; no controls are adapted for different orientations.

In the first category clearly the controls with indoor temperature (`Ti`) and outside temperature (`Te`) show more efficacy than the others. This is an expected outcome since the energy used for heating and cooling depend heavily on the indoor temperature.

The worst controls are those taking into account data that is not directly related to the temperature as elevation and azimuth. Also they show good performance at $0°$ the informations encapsulated in the fuzzy rules are not general enough to serve on a global basis. As a reference we show in Figure 6.21 the outcome of a simulation run with random parameters and the `TeTi` control. The `ElevAzi` control performs for some direction worse than the random one. Especially in the east directions it has a lot of cooling needs.

In Category2 (shown in Figure 6.22) the picture is basically the same. Controls that include the information about temperature perform well but if not, they differ a lot in performance.

From the obtained results one can see that performance regarding the orientation of the tested controls was quite bad. No control could satisfy the needs for all directions, though controls that include the inside or outside temperature did observable better. Summing up this final experiments shows that the robustness of the optimized controls was not sufficient regarding different orientations. This brings us to the result that none of the tested static controls can deliver sufficient control performance regarding the energy consumption without adaptation to the building characteristics.
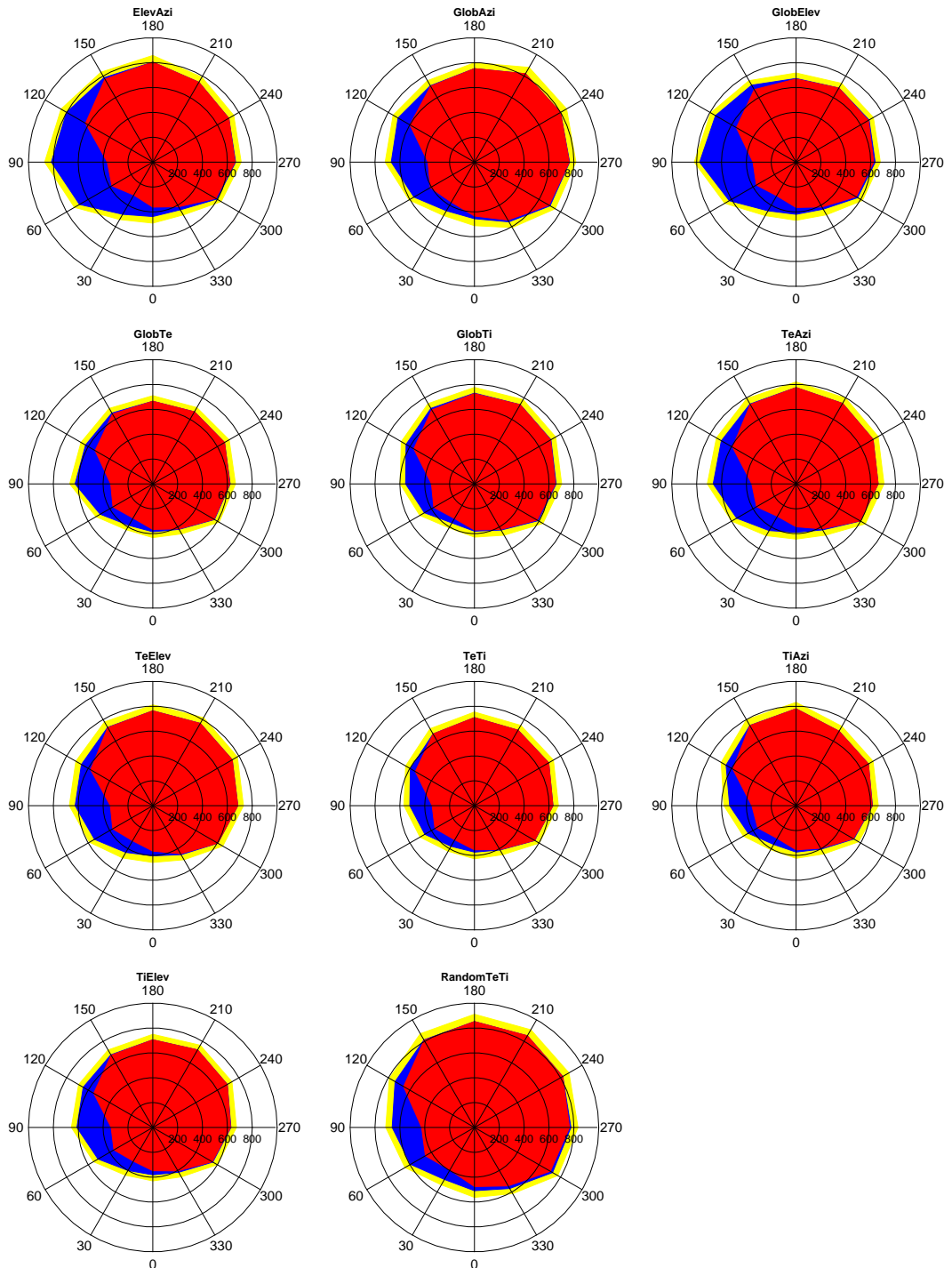
Figure 6.21: All results for Category1 with different orientations for each blind control with the most energy efficient energy consumption. The energy consumption is given for each of the 12 orientation which represents a measurement each 30° where 0° refers to south. The red stands for yearly heating energy the blue for cooling energy and the yellow for electric lighting in [kwh/year].
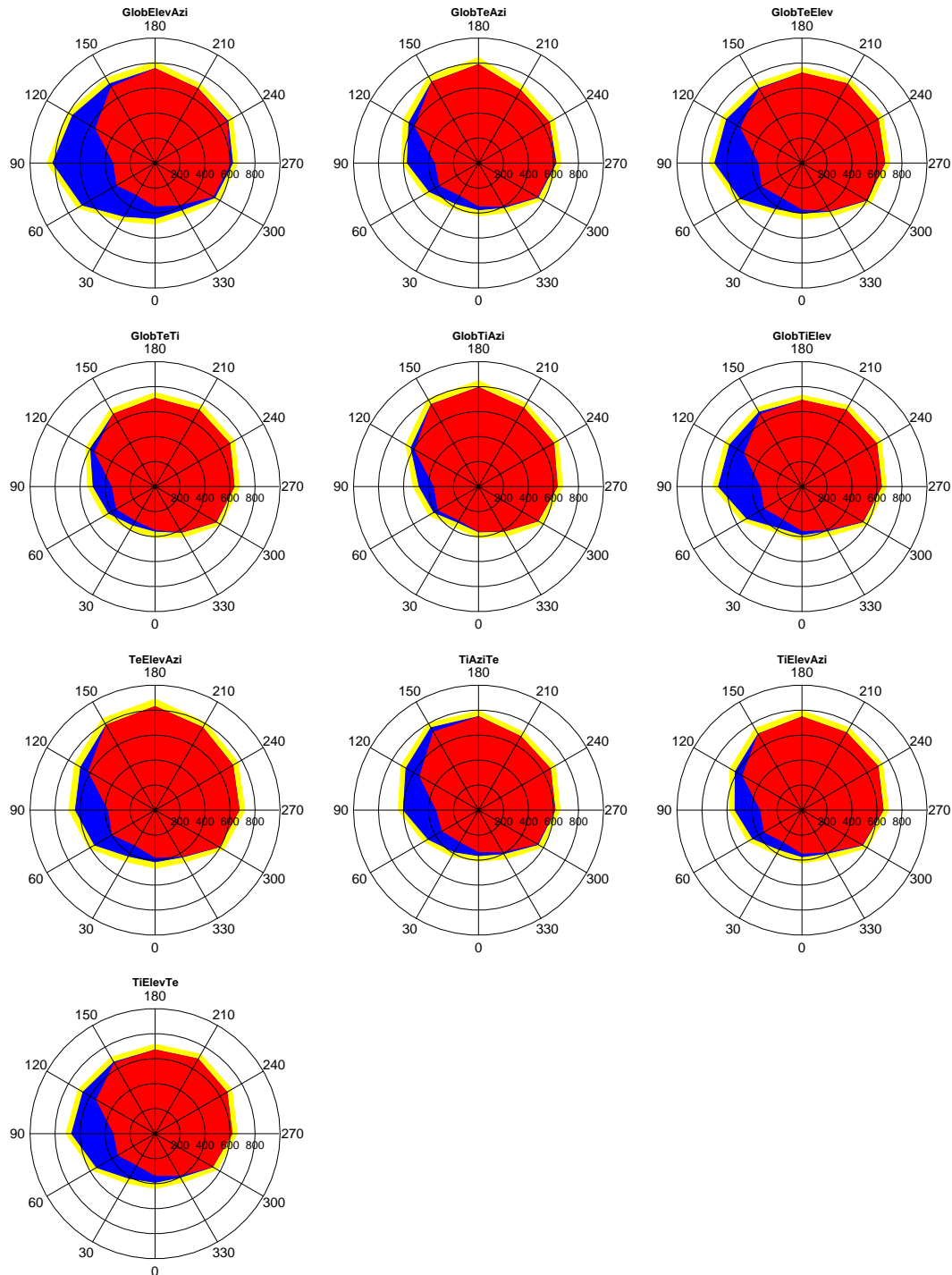
Figure 6.22: All results for Category2 with different orientations for each blind control with the most energy efficient energy consumption. The energy consumption is given for each of the 12 orientation which represents a measurement each 30° where 0° refers to south. The red stands for yearly heating energy the blue for cooling energy and the yellow for electric lighting in [kwh/year].
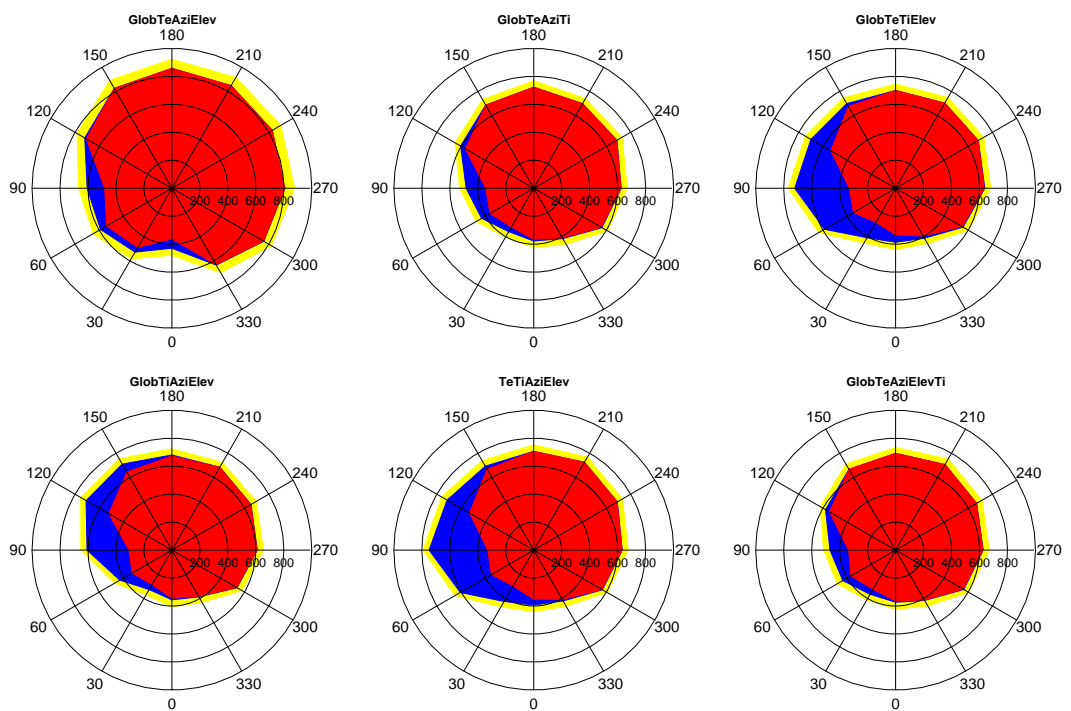
Figure 6.23: All results for Category3 with different orientations for each blind control with the most energy efficient energy consumption. The energy consumption is given for each of the 12 orientation which represents a measurement each 30° where 0° refers to south. The red stands for yearly heating energy the blue for cooling energy and the yellow for electric lighting in [kwh/year].

6.5 Chapter Summary

In this Chapter we proposed a combination of a high level simulation program and an optimizer based on evolutionary algorithms. First, we determined the number of membership functions for our hierarchical fuzzy system. Then, we compared 26 different fuzzy logic blind controls which have been all based on a hierarchical fuzzy system with different numbers of layers. The 26 controls represented every possible combination of the five state variables we wanted to test on there importance regarding two objectives: the energy efficiency and the thermal comfort. The main findings are:

- The results show significant differences regarding the importance of the single variables and that already two variables can supply enough information for a sound blind control.

- The robustness of the obtained controls is insufficient in regard to other building characteristics.

- To deliver sound results regarding the energy efficiency a control has to adapt itself to the building by learning during its use.

Of course not all variables which could be interesting have been included in this study, as a result it might be interesting to include also other variables especially if they are easy to collect.

7

The adaptive control system

In the previous chapters we laid the basis for our adaptive control by introducing hierarchical fuzzy systems, a performance measure and by giving an analysis about the state variables. In this chapter we will introduce the functioning of our adaptive control. The central element is the predictive control with its models, the optimization and the adaptation to the environment. For that we will discuss the single modules in detail, and than link them together.

We begin with stating the goals of the control in Section 7.1. In Section 7.2 we explain the general functioning of a predictive control; the single parts of it are described in Section 7.4 (The prediction model) and Section 7.5 (The objective function). The fuzzy logic control which we use for our control is introduced in Section 7.3.

7.1 Goals of the control

As we already mentioned the control strategy should fulfill the following items:

- It should be adaptable to the building in which it is installed.

- It should adapt to the thermal preference of the user.

- The control should use as little state variables as possible.

- The implementation has to be efficient to work on small embedded systems.

The control will be based on a model predictive control (MPC) that is able to fulfill all the predefined goals. The adaptivity to the environment, we reach by collecting the data of our sensors and fitting a thermal model according to these data. The adaptation to the occupant will be carried out by including occupant votes into a thermal profile for each inhabitant. Then, according to the latter the fuzzy logic will be optimized. The optimal set of state variables was already determined in Chapter 6.

7.2 Model Predictive Control

Model predictive controls (MPC) have been used in industry for three decades already, especially in the process industry (23; 103; 116). The term *predictive control* does not refer to a special type of control strategy rather to a wide range of control algorithms which use explicitly a predictive process model for minimizing a cost function to obtain a control action (62). A model predictive control (MPC) performs two central tasks:

- explicit prediction of future process behavior,

- computation of appropriate control action required to drive the predicted output as close as possible to the desired target values.

The overall objectives of a model predictive control (MPC) may be summarized as (153):

- Prevent violations of input and output constraints.

- Drive some output variables to their optimal set-points.

- Prevent excessive movement of the input variables.

- Control as many process variables as possible when a sensor or actuator is not available.

Basically, predictive control is well known to everybody and used in our daily live for walking and driving. For example, consider a good chess player who is always planning a few steps ahead:

1. *Predict:* When you play chess you want to reach something that cannot be reached within one move. So you try to predict the moves of your opponent according to your moves.

2. *Plan:* Compare the predicted performance with your target. If at the end of the sequence you are not satisfied with the predicted situation you have to change some of your moves and predict again the moves of your opponent.

3. *Act:* If you find a sequence with a good predicted outcome for you the move will be carried out. Although there may be already a plan for the next five moves only one move will be carried out and based on the response the procedure of prediction and planning is repeated. This process proceeds until the end of the game.
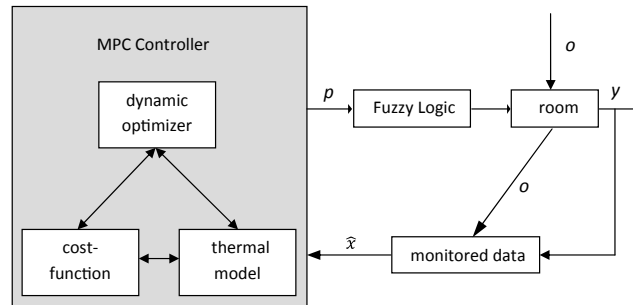
Figure 7.1: Basic MPC control loop

In general a model predictive control is formulated as solving on-line a finite horizon open-loop optimal control problem subject to system dynamics and constraints involving states and controls. Based on the measurements obtained at a time t or time steps before, the control predicts the future dynamic behavior of the system over a prediction horizon T_p and determines over a control horizon T_c (in general $T_c < T_p$) the input such that a penalty function gets minimized. If there are no disturbances the optimization could be performed only for the initial state at time $t = 0$ for all the following states $t > 0$, however this is not possible normally. The time difference δ between the measurements and recalculation can vary but will take place every δ time-units. It starts a new procedure of prediction and optimization for finding new parameters for the input function. A basic control loop is shown in Figure 7.1.

Analog to the demonstrative example, the methodology of MPC's can be characterized by the following steps (75):

1. The future outputs for a predetermined horizon T_p, called the prediction horizon, are predicted at each instant t using the process model. These predicted outputs $\hat{y}(t + i|t)$ for $i = 1...T_p$ depend on the known values up to instant t (past inputs and outputs) and on the future control signals u_{t+i}, $i = 0...T_p - 1$, which are those to be sent to the process and to be calculated.

2. The set of future control signals is calculated by optimizing a determined criterion in order to keep the process as close as possible to the reference trajectory. The criterion usually based on the quadratic error between the predicted output signal and the reference trajectory. The control effort is included in the objective function in most cases. An explicit solution can be obtained if the criterion is quadratic, the model is linear and there are no hard constraints; otherwise an iterative optimization method has to be used. Some assumptions about the structure of the future control law are also made in some cases, such as that it will remain constant after a given instant.

3. The control signal u_t, the control action calculated for the current time, is sent to the process whilst the calculated future control actions are discarded because in the next sampling instant y_{t+1} is already known; step 1 is repeated with the new value and all the sequences are brought up to date. Thus u_{t+1} is calculated at time instant $t + 1$ (which in principle will be different from u_{t+1} calculated at time instant t because of the new information available) using the receding horizon concept.

All MPC algorithms possess common elements which are mainly (23):

- prediction model,

- objective function,

- algorithms for identifying the control law of our fuzzy logic control[1].

In our case we add:

- fuzzy logic control

In standard MPC the control action is directly predicted. Meaning that during the prediction horizon T_p the predicted outputs $\hat{y}(t + i|t)$ consist, in our case, directly out of blind settings for each time step t. Unfortunately, the weather is not predictable for the next time steps without including external information which would in turn complicate the control. Normally, the solution is to define a sufficient short time step in which the weather is not changing that much and as in classical MPC theory to reiterate the process of prediction after each time step.

The drawback is that the computational cost for an embedded system may be to high and furthermore the connection to a power source would be obligatory.

With the inclusion of the fuzzy logic we do not optimize the deterministic movements of blinds in the future, we optimize a set of parameters $R = (\hat{y}_i^{pq})$, $p, q \in (1, \ldots, 5)$, $i \in (1, 2)$ based on current knowledge for applying in the future. The idea behind is that the building has to act the same way as it acted in the past if the outdoor, indoor conditions are the same as in the past.

Consequently, we can chose a much longer time step after restarting the optimization because the rules stay valid.

7.3 The Fuzzy Logic Control

The fuzzy logic is the centerpiece of our control algorithm. Ones fed with the optimized parameter it will directly respond with a setting for the blind according to the variables. The behavior and bodywork of the fuzzy logic was already investigated in former chapter. Goals of these preliminary studies have been:

---

[1]Generally, you can obtain the control law for any control, in our case the optimizer finds optimal rules for a fuzzy logic control
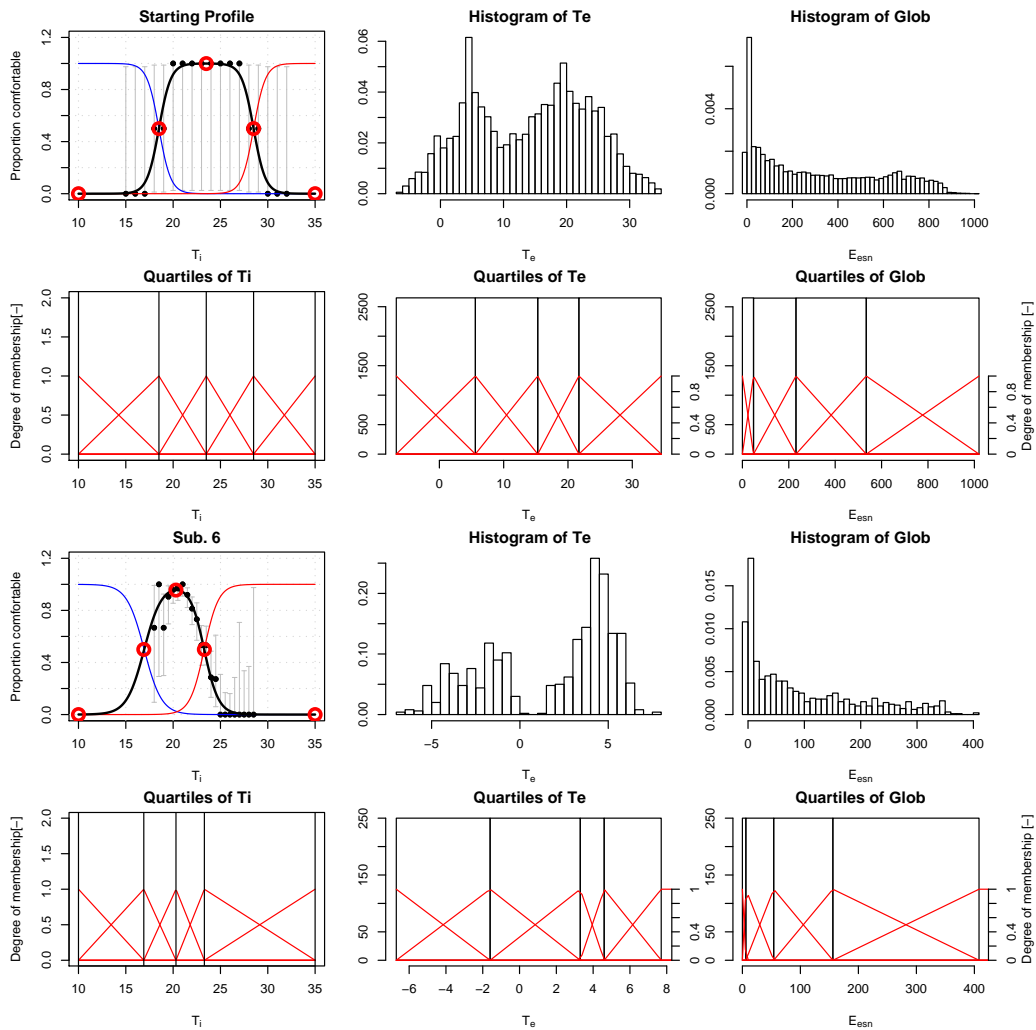
Figure 7.2: The membership functions for E_{esn} (vertical outdoor irradiance $[W/m^2]$), and Te (outdoor temperature $[^\circ C]$) are distributed according to monitored data. The MF for Ti (indoor temperature $[^\circ C]$) is distributed according to the thermal profile of the occupant. As example we show the distribution according to the starting profile and the profile from Subject 6 out of the field study explained in Section 7.5.

125

7. THE ADAPTIVE CONTROL SYSTEM

1. to find a suitable fuzzy logic control,

2. to detect the efficient state variables.

The first point is discussed in Section 4.5 where we explicitly explained the advantages of hierarchical fuzzy logic which is the basis of our control. The second point is addressed in Chapter 6 where we showed a systematic way of identifying the important variables for our control. The results of these preliminary studies are:

- We use a hierarchical fuzzy logic (HFL) control as a basis.

- As variables we integrate the E_{esn} (vertical outdoor irradiance $[W/m^2]$), T_i (indoor temperature $[°C]$) and T_e (outdoor temperature $[°C]$).

The construction of the HFL is described in Section 6.2. There the distribution of the membership functions was on collected data. This data is specific for this room and therefore cannot be used as general guideline for the distribution of the membership function (MF). On the other hand it makes sense to have more MF's in areas where the density for the state variable is also higher. For that reason we have to adapt the distribution of the membership functions according to the input of the control. Since we collect the three variables anyway for the fitting of the thermal model we can also use this data for the distribution of the MF's. The shortest period we could use for fitting the distribution is one week, the longest depends on how long the control has already collected data. Practically, during summer time we want a higher density of MF's for higher values of T_e, in winter the opposite. But we want also a more balanced representation during time when high differences in temperature may occur. Furthermore an adaptation with a long period of data is increasing the requirements of our embedded system in terms of memory. On that account we choose to adapt the distribution of the MF's always according to the weather data of the last 90 days.

This method works well for E_{esn} and Te. For the indoor temperature however, the distribution of the measured values is not identical with the areas where an exact control is necessary. The areas of a fine control are where the occupant starts feeling too cold or too warm. In Section 7.5 we will introduce an adaptive thermal profile of the occupant (see Figure 7.2: first figure in second and fourth line), where the probability of *too hot* (red line), *too cold* (blue line) and *comfortable* (black line) according to the indoor temperature T_i is shown. The centered MF should peak at the highest probability of comfort $P_0(T_i)$. The two adjacent MF's should peak when thermal comfort declines the most, which is given in the turning points of the probability of feeling too hot $P_1(T_i)$ and probability of feeling too cold $P_{-1}(T_i)$. Consequently we define
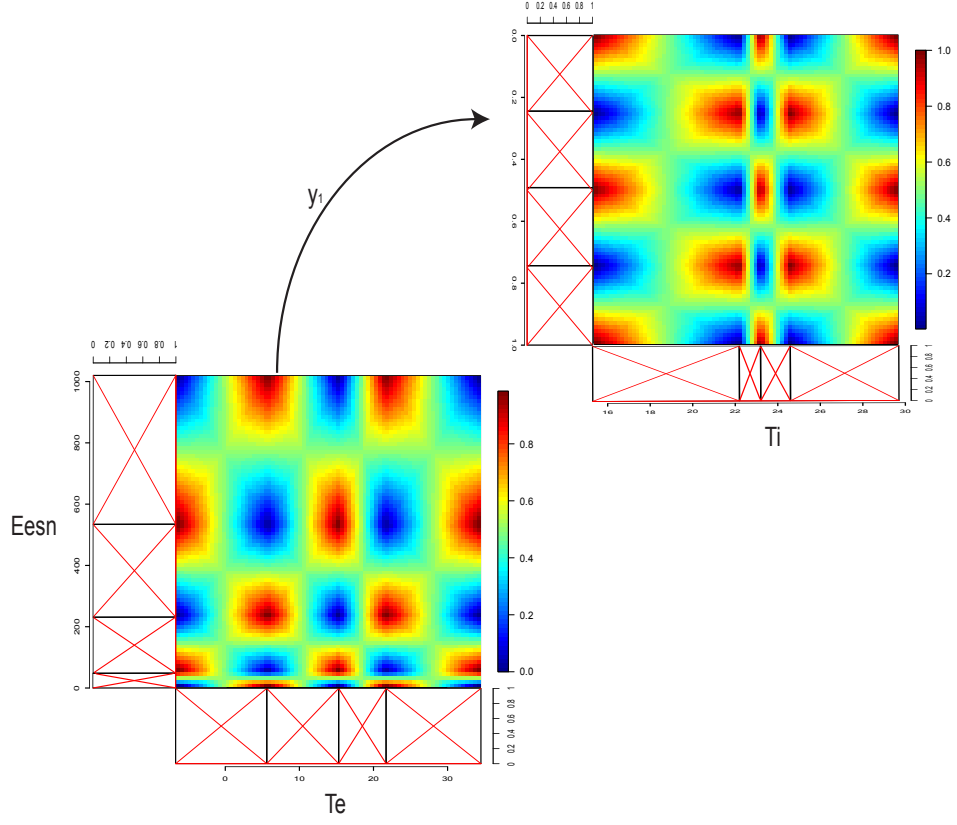
Figure 7.3: The layout of our HFL. The response surface with the four membership functions is shown. For better visibility of the response surface the parameter are by turn 0 and 1.

the MF's for the variable T_i according to Formula 6.9 as follows:

$$e_{Ti}^1 = 10 \tag{7.1a}$$

$$e_{Ti}^2 = \left\{ Ti \left| max(P'_{-1}(Ti)) \right. \right\} \tag{7.1b}$$

$$e_{Ti}^3 = \left\{ Ti \left| max(P_0(Ti)) \right. \right\} \tag{7.1c}$$

$$e_{Ti}^4 = \left\{ Ti \left| max(P'_1(Ti)) \right. \right\} \tag{7.1d}$$

$$e_{Ti}^5 = 35 \tag{7.1e}$$

All five points are marked in Figure 7.2 with red circles.

In Section 6.2 we already plotted the MF's according to the data distribution; in Fig. 7.2 we plot them again for $m = 5$ and our three variables E_{esn}, T_i, T_e together with the outcome if we assume another distribution and another thermal profile .

Summing up our HFL has the layout shown in Fig. 7.3.

7.4 The predictive model

An essential part of a MPC is the predictive model that is used for prediction of the system states. Our model has to predict the energy needs and temperature of a part of the building, for which we use a simplified thermal model.

Several simulation models and simulation tools have been developed to evaluate the energy use in indoor environments. These range from simplified calculation procedures to detailed dynamic simulations. The simplified calculations are based on only a few parameters describing the building for estimation of energy for heating and cooling over one period. On the other hand there exist many detailed simulation tools as BSim (20), esp-r (127), and IDA ICE (3). For the implementation in our control the model needs to fulfill three main criteria:

- dynamic calculation of the temperature

- easy adaptation to any building with few parameters

- low computational efforts

The first point is important because we will need to calculate the heating and cooling at any time depending on the setting of our blinds in order to find a efficient strategy. For that steady-state simulations are not applicable. We have to fit our model to the building in which it predicts the future energy consumption. There, it is important that the set of parameters is as small as possible with no redundancies. Otherwise the optimization of the system during the adaptation consumes more time or may not converge. The third point is also essential for an embedded system where computational power is restricted.

On that account we use a simplified thermal model based on Nielsen (126) and Kämpf (89). In the following the dynamic model and the calculation procedures are described.

7.4.1 The thermal model

The thermal model was developed for the assessment of heating and cooling needs according to different blind control strategies. The calculations are based on a basic dynamic two-node model, taking into account the heat capacity of the walls and of the room air. The room air heat capacity C_i exchanges heat with the internal surfaces and external air, it receives heat via solar radiation which depends on the weather and the setting of the blinds. The equivalent electric network is shown in Figure 7.4. The heat capacities of the internal building elements are lumped into one heat capacity C_i, that exchanges heat with the internal surfaces.
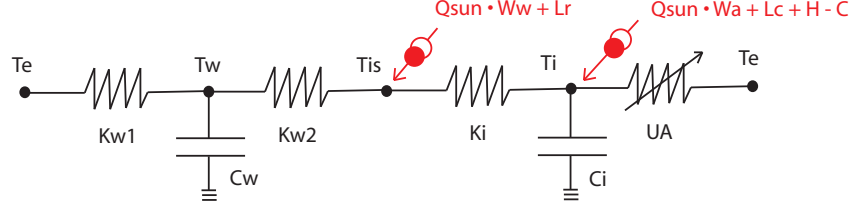
Figure 7.4: The thermal model as an equivalent electric circuit.

7.4.1.1 The mathematical description

Based on Kirchhoff's current law the equation system of the thermal model consists of two differential equations for the heat capacities and one algebraic equation for the internal surfaces:

$$C_i \frac{dT_i}{dt} = UA \cdot (T_e - T_i) + K_i \cdot (T_s - T_i) + S \cdot w_a \cdot Qsun + L + H - C \tag{7.2a}$$

$$C_w \frac{dT_W}{dt} = K_{w2} \cdot (T_{is} - T_w) + K_{w1} \cdot (T_e - T_w) \tag{7.2b}$$

$$0 = K_{w2} \cdot (T_w - T_{is}) + K_i \cdot (T_i - T_{is}) + S \cdot w_w \cdot Q_{sun} \tag{7.2c}$$

With external temperature T_e $[°C]$, indoor air temperature T_i $[°C]$, temperature on surfaces T_s $[°C]$, temperature of the wall T_w $[°C]$, internal heat capacity C_i $[JK^{-1}]$, heat capacity of constructions C_w $[JK^{-1}]$, conductance between exterior surface and capacity of building element K_{w1} $[WK^{-1}]$, conductance between capacity of building element and internal surfaces K_{w2} $[WK^{-1}]$, conductance between internal surfaces and air K_i $[WK^{-1}]$, conductance to external environment UA $[WK^{-1}]$, fraction of solar energy absorbed by furniture w_a $[W]$, fraction absorbed by surfaces w_w $[W]$, transmitted solar energy Q_{sun} $[W]$, internal loads L $[W]$, heating loads H $[W]$, cooling loads C $[W]$, shading S $[-]$ and time t $[s]$.

The first order differential equation system (7.2a), (7.2b), (7.2c) may be written in the form

$$\mathbf{C} \cdot \vec{T}'(t) = \mathbf{A}(t) \cdot \vec{T}(t) + \vec{u}(t) \tag{7.3}$$

with the positive diagonal thermal capacity matrix $\mathbf{C}$, the temperature at the nodes $\vec{T}(t)$ and the derivate upon time $\vec{T}'(t)$, the symmetric heat transfer matrix $\mathbf{A}(t)$, and the different source terms from each node $\vec{u}(t)$. In that form we get:

$$\begin{pmatrix} C_i & 0 \\ 0 & C_w \end{pmatrix} \begin{pmatrix} T_a'(t) \\ T_w'(t) \end{pmatrix} = \begin{pmatrix} -UA(t) - \kappa & \kappa \\ \kappa & K_{w1} \end{pmatrix} \begin{pmatrix} T_a(t) \\ T_w(t) \end{pmatrix} + \begin{pmatrix} u_a(t) \\ u_w(t) \end{pmatrix} \tag{7.4}$$

with the source terms

$$\begin{pmatrix} u_a(t) \\ u_w(t) \end{pmatrix} = \begin{pmatrix} UA(t) \cdot T_e(t) + \frac{\kappa}{K_{w2}} \cdot (Q_{sun}(t) \cdot w_w + L_r(t)) \\ \frac{\kappa}{K_i} \cdot (Q_{sun}(t) \cdot w_w + L_r(t)) \end{pmatrix}$$

$$+ \begin{pmatrix} Q_{sun}(t) \cdot w_a + L_c(t) + H(t) - C(t) \\ K_{w1} \cdot T_e(t) \end{pmatrix}, \tag{7.5}$$

and the conductance κ between T_a and T_w

$$\kappa = \left(\frac{K_i \cdot K_{w2}}{K_i + K_{w2}} \right) \tag{7.6}$$

Different approaches have been discussed in literature to solve such an equation system, for example in Carter (24). These include explicit Euler methods, implicit Euler methods, modal spectral methods (98), and Fourier series methods. In the case of a two node model also an analytical solution can be found (126), however this method is time consuming and hence not applicable for an embedded system. The first order differential equation (Formula 7.4) is solved with the implicit Euler scheme with a discrete time step Δt. To derive $\vec{T}^n$ we need to solve the linear equation system with $\vec{T}_a^n$ and $\vec{T}_w^n$ as unknowns.

$$C \cdot \vec{T}^{n-1} + \Delta t \cdot \vec{u}^n = (C - \Delta t \cdot A^n) \cdot \vec{T}^n \tag{7.7}$$

where the upper case index displays the corresponding time step. A LU decomposition/back-substitution scheme was used to solve the linear system. In order to save computing time and given the fact that A changes little within a time step we keep the LU decomposition and use only the back-substitution.

In order to determine for the next time step the heating needs to reach the T_a^n set point temperature we write Equation 7.7 with everything on the left-hand site:

$$C \begin{pmatrix} T_a \\ T_w \end{pmatrix}^{n-1} - C \begin{pmatrix} T_a \\ T_w \end{pmatrix}^n + \Delta t \cdot \mathbf{A} \begin{pmatrix} T_a \\ T_w \end{pmatrix}^n + \Delta t \cdot \begin{pmatrix} u_a \\ u_w \end{pmatrix}^n = 0, \tag{7.8}$$

where T_a^n is the only unknown. Finally we isolate H^n from Equation 7.5 and obtain the heating value at time step n:

$$\begin{aligned} H^n = & \frac{C_i}{\Delta t} \cdot (T_a^n - T_i^{n-1}) - (-UA^n - \kappa) \cdot T_a^n - u_a^n + \kappa \\ & \cdot (\Delta t \cdot (-\kappa - K_{w1}) - C_w)^{-1} \\ & \cdot (C_w \cdot T_w^{n-1} + \Delta t \cdot \kappa \cdot T_a^n \cdot + \Delta t \cdot u_a^n) \end{aligned} \tag{7.9}$$

The value for the cooling C^n is obtained in the same way.

7.4.2 The solar radiation model

Windows are a direct source of solar energy for every building. It is important to get an estimate of the transmitted solar energy Q_{sun} dependent on the setting of the blinds. As stated before, we want to reduce the input information of the control to a minimum. Hence, our model has to calculate Q_{sun} with information monitored by a sensor. The source of energy, the solar radiation, can be separated into two basic components: direct beam component and

diffuse solar component. Direct solar component is the solar radiation arriving at the Earth's surface with the sun's beam. Some of the radiation removed from the beam is redirected or scattered towards the ground - the diffuse solar component. Global solar radiation E_{esn} is the total incoming solar energy (both direct and diffuse) on a plane and can be measured by a pyranometer[1], which is placed outside the window. The unknown factors on which the transmitted energy depends-on can be divided in:

- angle dependent transmittance,

- non-angle dependent transmittance.

7.4.2.1 Non-angle dependent transmittance

The correction for non-angle dependent transmittance $F_{non-angle}$ includes mainly the blinds which will be an input to our thermal model. Different blinds can have different properties for that we have to include the Solar Heat Gain Coefficient (SHGC) of the blind into our calculations as follows:

$$F_{blinds} = \alpha + (1 - \alpha) \cdot SHGC \quad [-] \tag{7.10}$$

where $\alpha \in [0, 1]$ is the fraction of the window that is not shaded by the blinds. In other words: $\alpha = 1$ means blinds are open, $\alpha = 0$ means blinds are lowered. For the effective fitting of this parameter it is important that the blinds are not completely opened all time because then the parameter has no effect, a fitting is not possible and during the optimization of the fuzzy logic the calculations with an arbitrary SHGC parameter might be wrong.

For a window there are three basic parameters regarding its energy performance which are the U-value for the thermal transmission, the g-value giving the total solar energy transmittance and the visual transmittance, T_{vis}, expressing the fraction of daylight flux through the window.

For our daylight model only the g-value is of importance, since the thermal leakage of the window is already included in the thermal model. The g-value depends not only on the window. It is also connected to the incident angle of sun light, but since we do not have enough data for an exact fit we assume a constant value.

Finally the solar heat gains depend on the size of the window A_w. For avoiding redundancies in the parameters we merge the A_w and the g-value to one parameter:

$$F_w = g \cdot A_w \quad [m^2] \tag{7.11}$$

In summary the non-angle dependent transmittance can be given as:

$$F_{non-angle} = F_{blinds} \cdot F_w \quad [m^2] \tag{7.12}$$

---

[1]A pyranometer is a type of actinometer used to measure broadband solar irradiance on a planar surface and is a sensor that is designed to measure the solar radiation flux density (in watts per metre square) from a field of view of 180 degrees.

7.4.2.2 Angle dependent transmittance

In this section we want to include all factors that influence the solar radiation dependent on the incident angle, explicitly the shading for far objects and building overhangs.

The corrections for far objects are based on a shadow horizon defined by the azimuth and the height of obstructions relative to the window. Since this effects, in most of the time, are recognized by the solar radiation sensor we do not account for them.

For building overhangs we take only into account the horizontal shadow which depends on the elevation γ_s, the proportion of the height h of the window, the depth d of the overhang (see Figure 7.5(a)) and the current setting of the blind α. We have to distinguish two different cases: 1. The beam radiation is already blocked by the blind and there is no additional influence of the overhang (see Figure 7.5(b)); 2. The overhang blocks additional beam radiation (see Figure 7.5(a)).

We account only for direct beam radiation since the diffuse solar radiation is not blocked by the overhang. We assume that 50% of radiation is the direct component and 50% is the diffuse one.

$$P_w = \frac{d}{h} \quad [-] \tag{7.13}$$

$$F_{angle} = \left\{ \begin{array}{ll} 1 - (P_w \cdot tan(\gamma_s) - (1 - \alpha)) \cdot 0.5, & (P_w \cdot tan(\gamma_s)) > (1 - \alpha) \; [-] \\ 1, & (P_w \cdot tan(\gamma_s)) \leq (1 - \alpha) \; [-] \end{array} \right. \tag{7.14}$$

7.4.2.3 The solar heat gains

For each time step the transmitted solar energy Q_{sun} is calculated by:

$$Q_{sun} = F_{angle} \cdot F_{non-angle} \cdot E_{esn} \quad [W] \tag{7.15}$$

with the correction factor for angle dependent transmission F_{angle}, the correction factor for angle independent transmission $F_{non-angle}$, and global solar radiation E_{esn}.

7.4.3 Model validation

For validation of thermal models many techniques have been developed, including code checking, analytical tests (16), inter model comparison (88), and empirical comparison (109). An overview is given in Bloomfield et al. (17). The thermal model is based on Nielsen (126) and Kämpf (89); already thorough validations of the models have been carried out. Nevertheless we check our model with case studies against the IDA ICE software to ensure that the code works.

As case study we use a hypothetical room which has been modeled in IDA ICE see Figure 7.6 and Table 7.1. To exclude the ground conductance the body floats free inside the building

(a) Overhang has influence on the shading calcula-
tion.

(b) Overhang has no influence on the shading calcu-
lation.
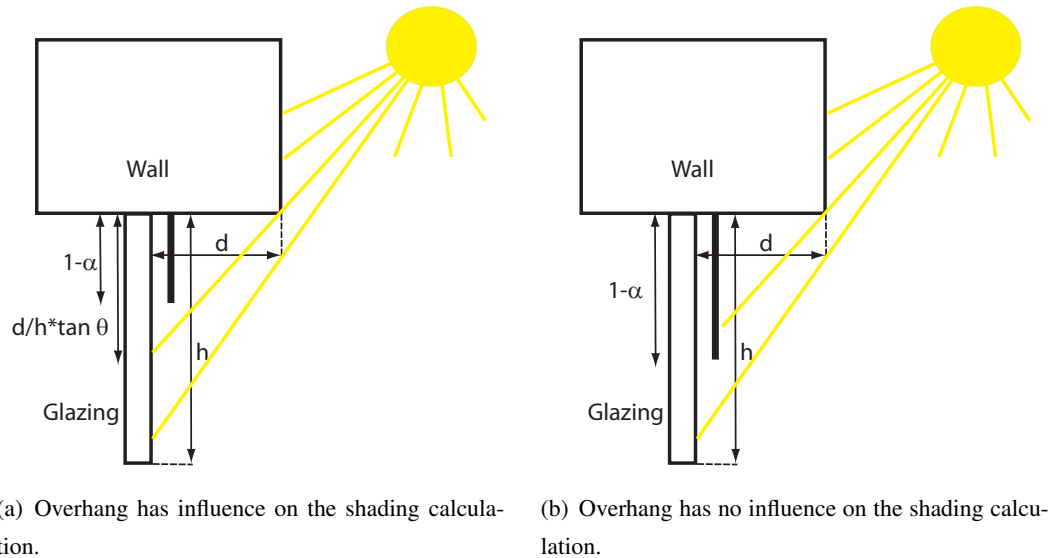
Figure 7.5: Definition of the geometry used for the horizontal shadow

and is connected to the outside with only one external wall. The indoor walls are adiabatic, the room is not occupied, there are no furniture and no internal loads in the room. The infiltration rate is set to a constant value of $0.25h^{-1}$ and the windows stay closed all the time. We use the weather data from Lausanne of the year 2007. The solar gains through the window, which is an input to our model, is calculated with IDA ICE. For the other inputs such as outdoor temperature we use the same input file as for IDA ICE.

To verify the dynamic behavior of our model we plot two time series, one calculated by our model, one by the IDA ICE software, for the internal temperature and the heating power. The deviation of the two curves for the heating power is also plotted. For the time series we show 14 days of a cold period where mainly heating is needed (set point temperature for heating $20°C$).
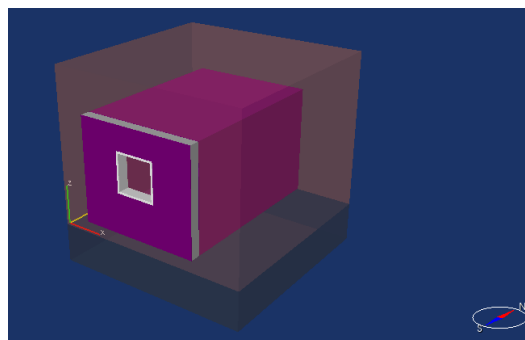
Figure 7.6: The test room with a window of $1m^2$, and dimensions of $3m$ x $4m$ x $2.6m$

Table 7.1: Specifications of the test chamber

Component	Description
Rolling shutters	External blind, total shading coefficient: 0.17, short wave shading coefficient 0.17, U-value coefficient: 0.9 (that means that with lowered blinds, the U-value of the window is multiplied with 0.9).
Appartement	Floor area of flat: $12m^2$, Room height: $2.6m$.
External Wall	Facade wall: $6.8m^2$, light wall ($1cm$ plaster panel + $30cm$ brick masonry + $1.5cm$ mineral render) U-value: $1.19W/m^2K$.
Internal Wall	light partition wall ($1cm$ plaster panel + $4cm$ thermal insulation +$1cm$ plaster panel).
Window	$1m^2$ net area (U-value $2.0W/m^2K$), south oriented
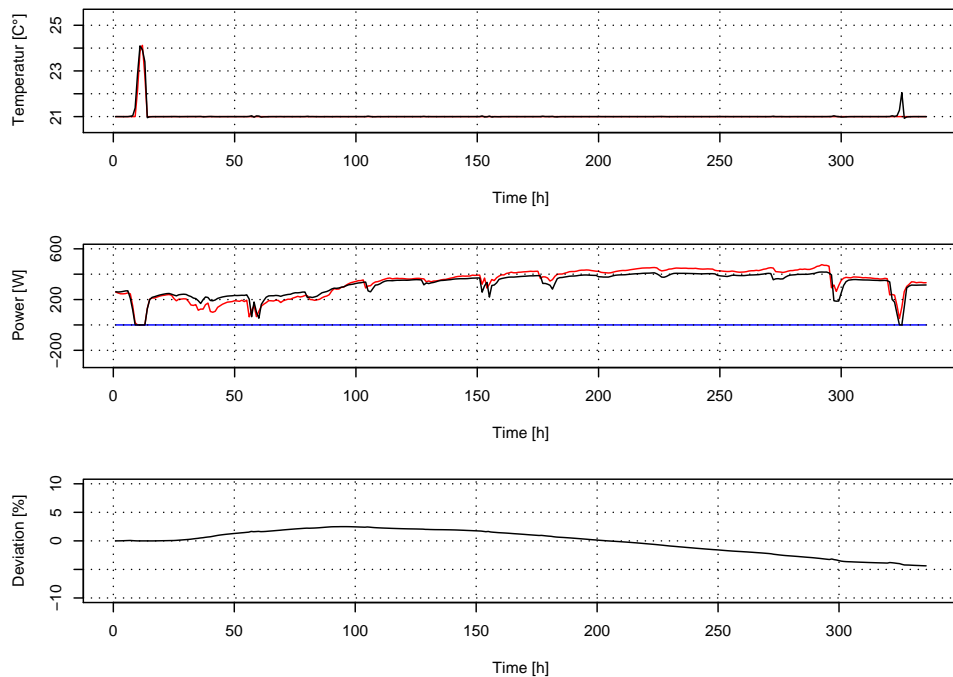
Figure 7.7: The dynamic behavior of indoor temperature T_i, heating power H, cooling power C, and percental deviation of the heating power. The black line reflects IDA ICE.
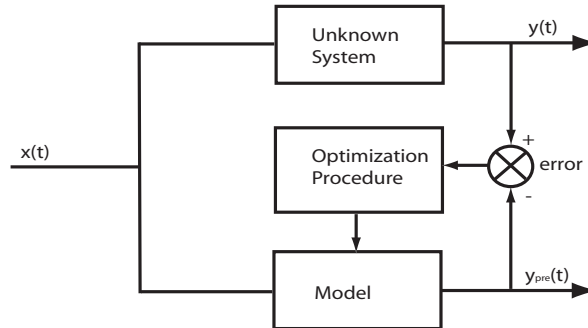
Figure 7.8: Representation of the model reference approach for the system identification.

Table 7.2: Parameters for the fitting of the thermal model

Name	Unit	Description
C_w	$[JK^{-1}]$	heat capacity of the heavy wall material
C_i	$[JK^{-1}]$	heat capacity of the heavy wall material
K_{w1}	$[WK^{-1}]$	conductance of external part of the wall
K_{w2}	$[WK^{-1}]$	conductance of internal part of the wall
K_i	$[WK^{-1}]$	conductance of thin layer of air
UA	$[WK^{-1}]$	conductance to the external environment through windows and ventilation
$SHGC$	$[-]$	Solar Heat Gain Coefficient for the blind
F_w	$[m^2]$	size of the window and g-value
P_w	$[-]$	shading through building overhangs

The graphs are shown in Figure 7.7. The difference between IDA and our model in total heating energy consumption during those 14 days of simulation is 4.7% which is acceptable.

7.4.4 Fitting of the process model

The goal is to fit the parameters of our thermal model according to previously monitored data to get a basis for determining an optimal strategy for the blinds for the next period. A similar approach was proposed by Dewson (48).

The optimization problem to solve can be stated as follows:

$$\begin{aligned}
\underset{(C_w,...,W)}{\text{Minimize}} \quad & \sum_{q \in (H,C,T_i)} \sum_{t=1}^{T} \Big(q_t \left(C_w, C_i, K_{w1}, K_{w2}, K_i, UA, SHGC, F_w, P_w \right) - q_t^{ref} \Big)^2 , \\
\text{Subject to} \quad & 1 \leq C_w \leq C^U \\
& 1 \leq C_i \leq C^U \\
& 0 < K_{w1} \leq K^U \\
& 0 < K_{w2} \leq K^U \\
& 0 < K_i \leq K^U \\
& 0 < UA \leq UA^U \\
& 0 < SHGC \leq 1 \\
& 0 < F_w \leq F_w^U \\
& 0 < P_w \leq 1
\end{aligned}$$

$$(7.16)$$

Where $q_t(C_w, ..., W)$ is the function of heating load, cooling load and indoor temperature during the time interval t and q_t^{ref} the reference value. Our lumped thermal model depends on differential equations, if the parameters are altered during the fit discontinuities in the fitness function can occur. For that we also use genetic algorithms[1] for fitting the parameters in our limped thermal model. The configuration of the adaptation is shown in Figure 7.8.

7.4.4.1 Data provided for the fitting

Our model has nine parameters that we need to fit, they are given in Table 7.2. Regarding the input for fitting our model, we are restricted to the data we can obtain from sensors, which we have to install in the apartment (in any case we get T_e, T_i, and E_{esn}). We discriminate between three cases of additional information:

1. The heating/cooling power can be determined (Results in Figure 7.9).

2. Temperature sensors on the radiators can display if the heating is switched on (Results in Figure 7.10).

3. No information is given about heating or cooling (Results in Figure 7.11).

In the ideal case we can determine the heating or cooling load and can use this as an input for fitting. For example in the LESO building the heating power of each room can be accessed via the EIB bus system. Since this is not the normal case and installing sensors for

---

[1]For the single objective problems we used a standard GA from the Kanpur Genetic Algorithms Laboratory that can be downloaded at the following address: http://www.iitk.ac.in/kangal/codes.shtml

monitoring the exact amount of supplied heat to each room is complicated we use only a sensor for temperature at one radiator, which makes it is easy to get binary information about the state of the radiators.

If we want to reduce further the use of sensors we can restrict our fitting on times where normally no heating is used. That means we are only using data to fit our model when the average outdoor temperature of the last 24h is above $18C°$.

For our first setting we are allowed to use all the data given in Table 7.3. That means that our fitness function is Formula 7.16. The initial parameter and the assessed one are shown in Table 7.4. In Figure 7.9 the output of the model with optimized parameters is shown. In the upper chart of Figure 7.9, T_e is shown (black for real data, red for model output), the second chart shows heating H and cooling C demand, and in the third E_{esn} (black) is shown together with Q_{sun} (green) that was assessed by the model; furthermore the non-shaded fraction of the blinds α is shown in red, which corresponds always with the blind parameters during the recording of the input parameters. The deviation (shown in chart 4 and 5 of Figure 7.9) in terms of indoor temperature is lower than 1%. Heating and cooling loads are also in an acceptable range given the fact that nearly no heating was needed and the absolute values are negligible.

In the second case we will not have the exact values for the heating and cooling but we know when the heating or cooling is switched on or off. This will result in the following objective function where we only have binary values for H_q, C_q:

$$\underset{(C_w,...,W)}{\text{Minimize}} \quad \sum_{q\in(H_b,C_b,T_i)} \sum_{t=1}^{T} \Big(q_t\left(C_w, C_i, K_{w1}, K_{w2}, K_i, UA, SHGC, F_w, P_w\right) - q_t^{ref} \Big)^2, \tag{7.17}$$

The results of these runs are shown in Figure 7.10 and Table 7.4. The fit of the temperature is sound but the size of the window was overestimated, which leads to larger solar gains.

In the third case we will not have any information about heating and cooling. This will result in the following objective function:

$$\underset{(C_w,...,W)}{\text{Minimize}} \quad \sum_{t=1}^{T} \Big(q_t\left(C_w, C_i, K_{w1}, K_{w2}, K_i, UA, SHGC, F_w, P_w\right) - q_t^{ref} \Big)^2, \tag{7.18}$$

The result is shown in Figure 7.11. The building we used for the fitting is equipped with an air conditioning unit which keeps the temperature below $25C°$.

The results show that the fitting of our simple model is working also without information of the heating and cooling.

Figures 7.12 and 7.13 show the behaviour of the model with optimized parameters.

Table 7.3: Input for the fitting of the thermal model

Name	Unit	Description
E_{esn}	$[Wm^{-2}]$	irradiance on the window plane
T_e	$[C°]$	outdoor temperature
T_i	$[C°]$	indoor temperature
C	$[W]$	cooling load
H	$[W]$	heating load
α	$[-]$	window fraction not shaded by the blinds

Table 7.4: Values of the parameter for the simple test case

Name	Original values	Values case 1	Values case 2
C_w	671,757.00	578,970.43	604,961.92
C_i	761,758.00	635,129.40	754,801.07
K_{w1}	5.79	6.18	8.29
K_{w2}	2.72	6.88	3.43
K_i	20.40	58.88	1.33
UA	13.40	9.38	15.47
$SHGC$	0.15	0.12	0.16
F_w	1.00	2.05	3.99
P_w	0.00	0.89	0.82
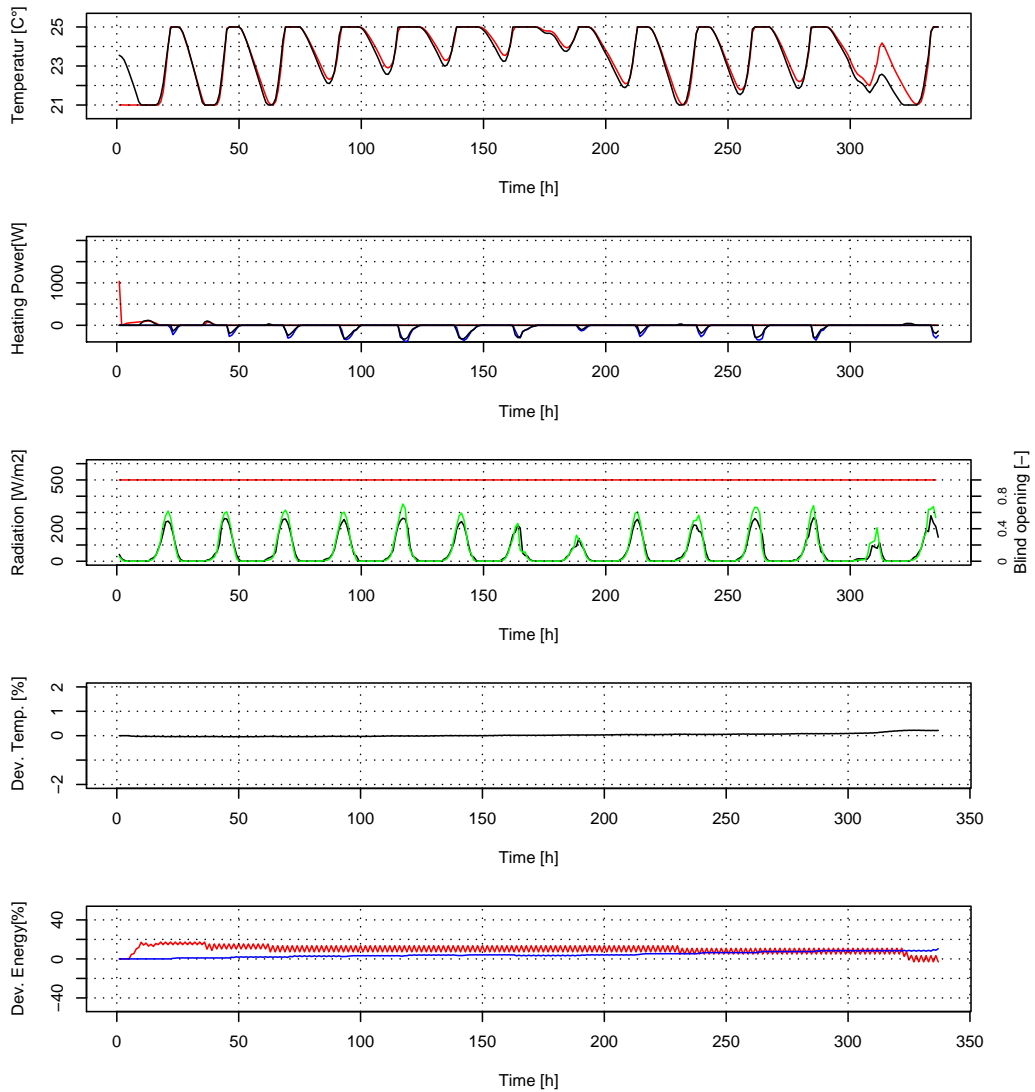
Figure 7.9: Information given: heating/cooling load, T_e, T_i. The dynamic behavior of indoor temperature T_i for the fitted model (red) and the real temperature (black), heating power H, cooling C, the real consumption is given in black, the one of the fitted model in red (heating) and blue (cooling). In the third chart the radiation is shown: real in black, model radiation in green, and the blind setting in red. The next two charts show the percental deviation in indoor temperature, and percental deviation of the heating, cooling power.
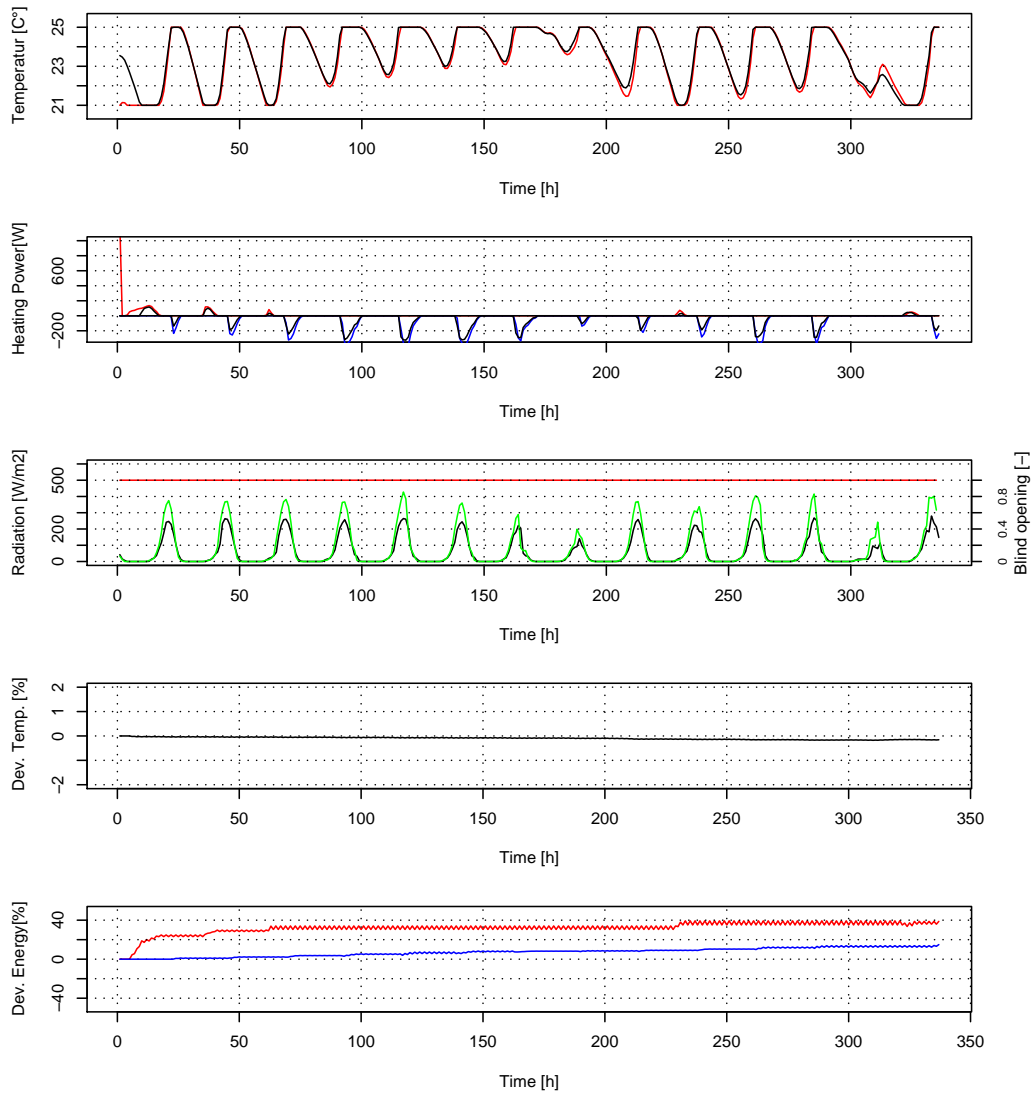
Figure 7.10: Information given: binary heating/cooling load, T_e, T_i. The dynamic behavior of indoor temperature T_i for the fitted model (red) and the real temperature (black), heating power H, cooling C, the real consumption is given in black, the one of the fitted model in red (heating) and blue (cooling). In the third chart the radiation is shown: real in black, model radiation in green, and the blind setting in red. The next two charts show the percental deviation in indoor temperature, and percental deviation of the heating, cooling power. This time the model was fitted only with the indoor temperature and binary data for heating and cooling.
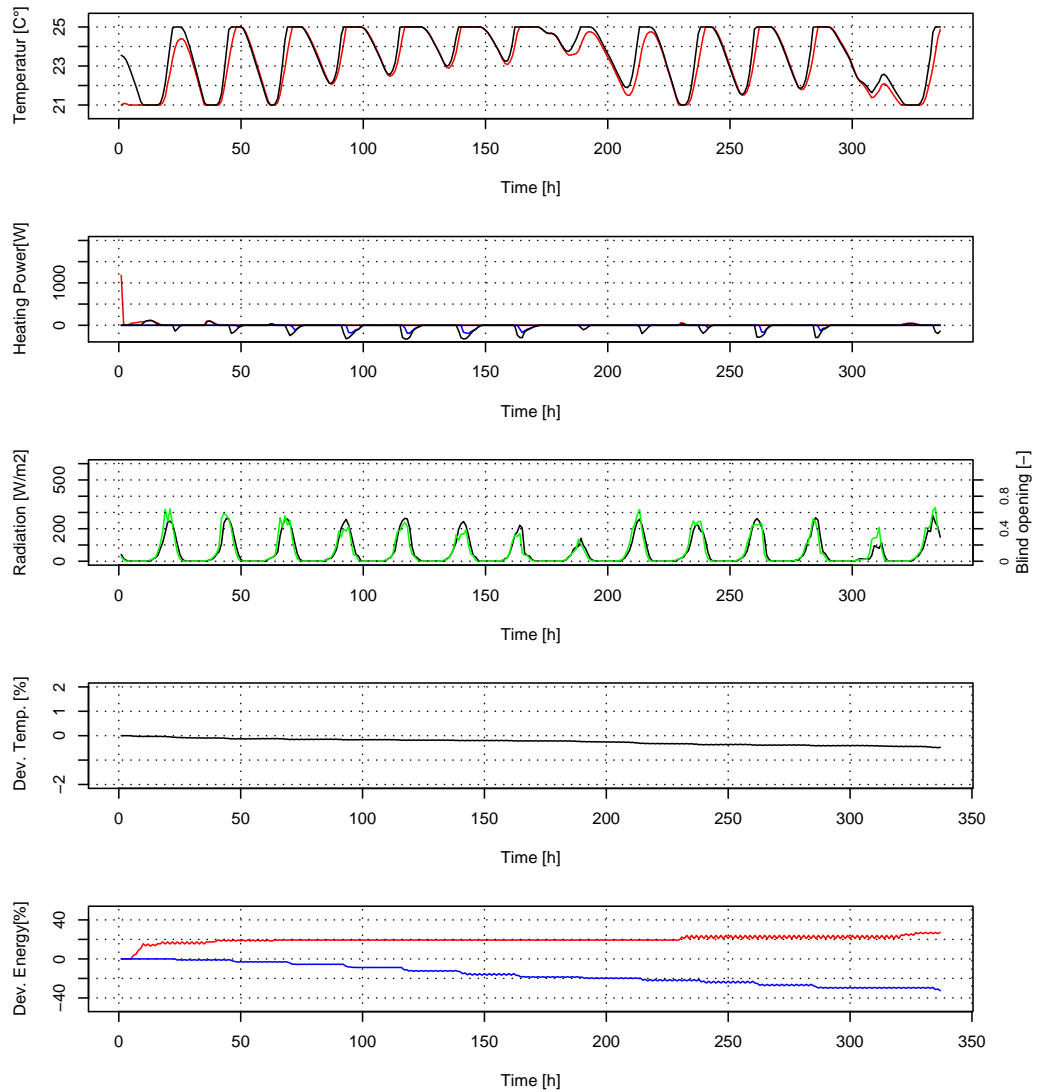
Figure 7.11: Information given: T_e, T_i. The dynamic behavior of indoor temperature T_i for the fitted model (red) and the real temperature (black), heating power H, cooling C, the real consumption is given in black, the one of the fitted model in red (heating) and blue (cooling). In the third chart the radiation is shown: real in black, model radiation in green, and the blind setting in red. The next two charts show the percental deviation in indoor temperature, and percental deviation of the heating, cooling power. This time the model was fitted only with the indoor temperature.
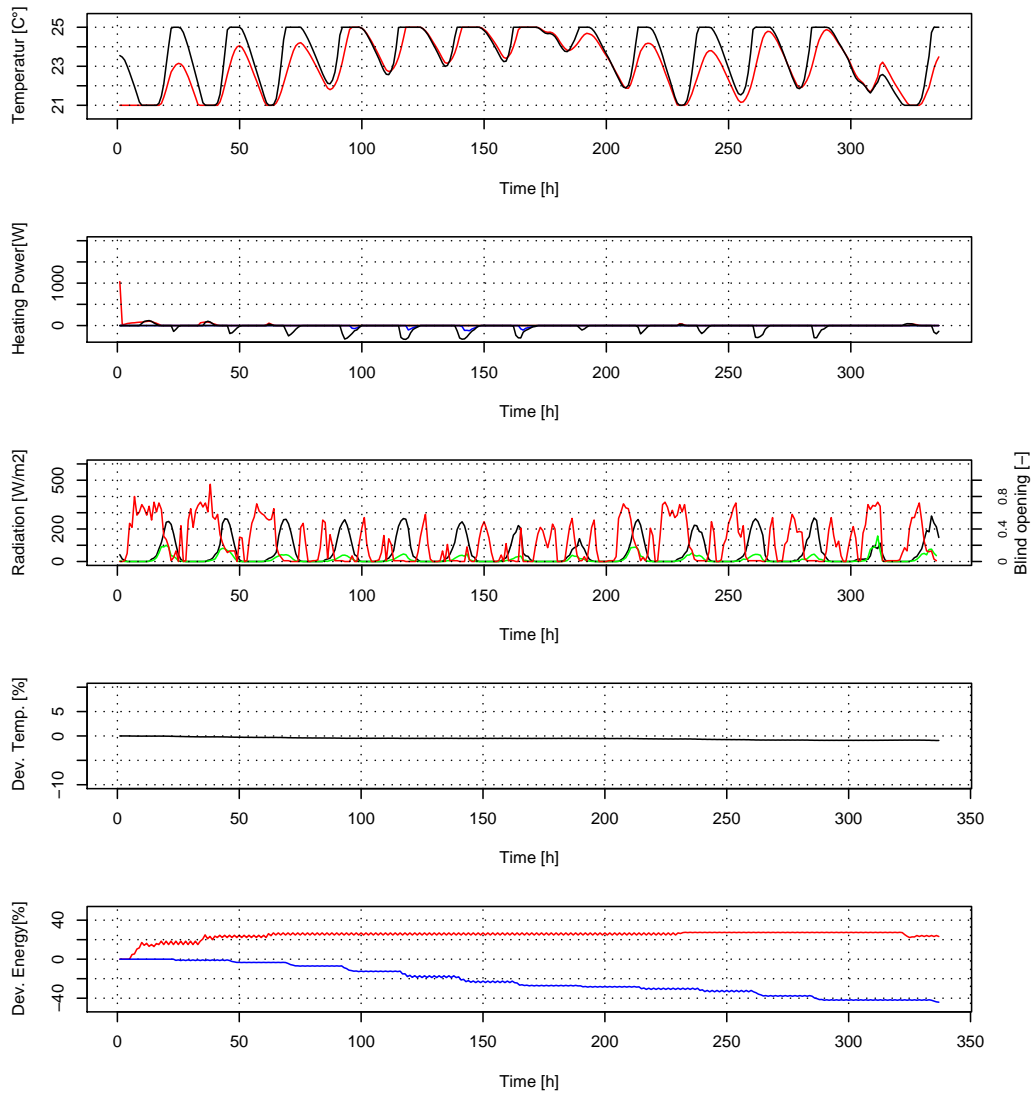
Figure 7.12: This Figure shows the behavior of the model with optimized blind parameters and an active cooling: The predicted indoor temperature T_i of the model after optimization of the blinds (red) and the measured temperature (black), heating power H, cooling C, the real consumption is given in black, the one of the fitted model in red (heating) and blue (cooling). In the third chart the radiation is shown: real in black, model radiation in green, and the blind setting in red. The next two charts show the percental deviation in indoor temperature, and percental deviation of the heating, cooling power.
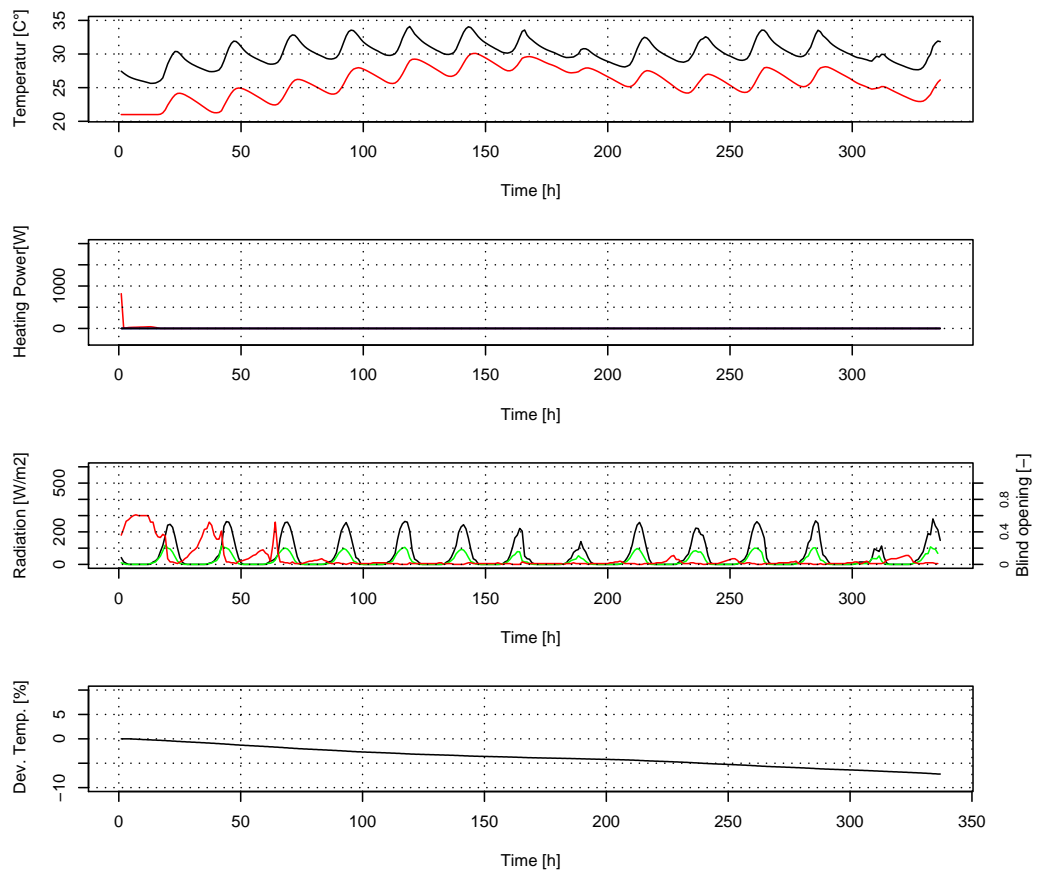
Figure 7.13: This Figure shows the behavior of the model with optimized blind parameters without cooling: The indoor temperature T_i for the model (red) and the real temperature (black), heating power H, cooling C, the real consumption is given in black, the one of the fitted model in red (heating) and blue (cooling). In the third chart the radiation is shown: real in black, model radiation in green, and the blind setting in red. The next two charts show the percental deviation in indoor temperature, percental deviation of the heating and cooling power is not shown because it is not applicable. The advantage of an intelligent blind control is in this case only measurable in terms of indoor temperature.

7.5   The objective function

The objective function has to make the performance accountable for different solutions via assigning a value. Therefore we have to choose a criteria that suits well the goals we want to reach. The main goals are:

- providing thermal comfort,

- providing visual comfort,

- saving energy

The control will only drive the blinds, we have to state clear in which situations the thermal comfort depends on the blinds; only in these situations it can be improved. This is the case:

- During summer time, the blinds have to eliminate dispensable solar gains through windows.

- During winter time, the blinds have to maximize the solar gains and contribute to heat the space. Thermal comfort is only influenced if the heating is to weak or not switched on during spring or autumn.

The blinds cannot improve thermal comfort when the heating is providing too much heat. In Chapter 5 we used the Predicted Percentage Dissatisfied (PPD) introduced by Fanger (53) for evaluation of different controls. To evaluate the difference of comfort in an environment where everything is stable, but the blind control, this delivers appropriate results. The evaluation of thermal comfort in a real environment with incomplete information is more sophisticated.

Many methods for comfort evaluation have been proposed; a good overview is given by Olesen (128). All the proposed methods have in common that they need detailed information of the thermal environment to perform statements. These include, among other variables, temperature (air, radiant, surface), humidity, air velocity, clothing and activity level. For a control these informations are only accessible via sensors. These can be installed easily in a labratory, but for real applications it is essential that the control is easy to install and also not too costly. Hence, a small number of sensors is more favorable. Furthermore there are no sensors for variables such as clothing and activity level. Again, there is a big difference between an office and a residential building. While in offices the activity level and clothing are rather constant throughout the year it may change often in living spaces.

Measures of thermal comfort are typically based on field data. Researchers gather data on the thermal environment and the simultaneous thermal response of subjects. That is usually measured by asking them for a 'comfort vote' on the ASHRAE or Bedford scales (13). Then, statistical methods are used to link thermal variables (temperature, air velocity, humidity) together with states which are considered as *neutral* by the subjects. Based on that analysis the thermal comfort is predicted in other situations. The problems with this approach is that the

environment is inherently changing and hard to explain accurately with some variables; measurement errors for the input can rise to errors in the relationship predicted by the statistical analysis (79).

Current standards such as the ISO 7730 (4) (PMV) and ASHRAE 55 (155) are also based on the response of subjects assessed in stable conditions in climate chambers. The results from surveys should therefore be predicted by the index. When rational indices are used for predicting thermal comfort of subjects during field studies, the range of conditions that are found comfortable in field surveys is much wider than the rational indices predict. Nicol and Humphreys (124) suggested that this effect could be a result of internal adaptation of the subjects and their behavior towards the climate conditions in which the field study was carried out.

Humphreys and Nicol (80) explored the manner in which the discrepancy between PMV and the actual vote depends on the variables from which PMV is calculated. They came to the conclusion that a prediction made with one variable is not inferior to using the PMV with all the necessary data of the thermal environment. This also suggests that with less sensors a prediction regarding the thermal comfort can be made.

The results of the aforementioned studies are based on the accumulated results of many individuals. Consequently another question is arising if we want to guarantee thermal comfort to a single occupant: Can any method without direct user feedback predict the thermal comfort? To address this question an analysis of field survey data is valuable.

7.5.1 Field survey methodology

During the years 2006 to 2009 a detailed field survey of the adaptive actions of occupants, their thermal satisfaction, and the coincident environmental conditions were carried out in the LESO-PB[1] building (70). For a detailed description of the building we refer to Altherr and Gay (8). It is located on the EPFL campus, Switzerland at a latitude of $46.53°$, longitude of $6.67°$ and altitude of 410 m. The building has 14 south-facing rooms that are occupied by senior researchers, research assistants, technical staff and secretaries. During the surveyed period between five and eight offices have been occupied by two persons. An electronic survey was activated on the PCs of all occupants on a rotation basis. The questionnaire appeared up to 4 times a day and recorded in total 6851 entries from 28 different participants with the following evaluations:

- clothing and activity level,

- thermal sensation on the ASHRAE scale, which is based on the Fanger scale, is shown in Table 7.5,

- adaptive opportunities exercised.

---

[1]Laboratoire d'énergie solaire et physique du bâtiment (LESO-PB)
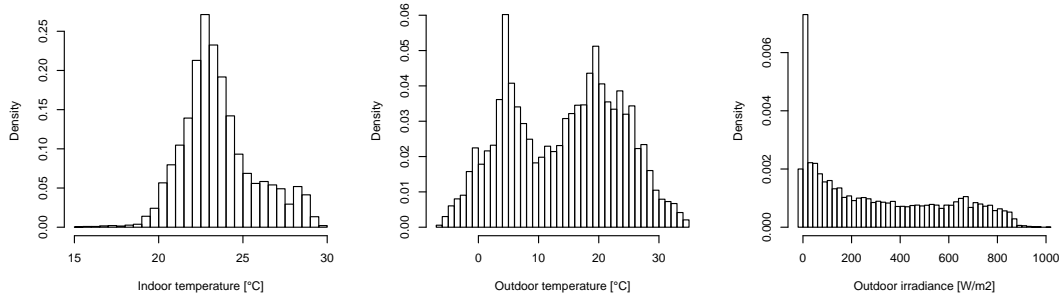
Figure 7.14: Distribution of outdoor and indoor temperature, outdoor illuminance during occupied periods of the study.

Table 7.5: Thermal sensation and satisfaction scales

Thermal sensation (PMV)	How do you feel this time? (ASHRAE)	Bedford scale	Votre impression thermique actuelle?	event
3	Hot	Much too warm	Très chaud	*too hot*
2	Warm	Too warm	Chaud	*too hot*
1	Slightly Warm	Comfortably warm	Légèrement chaud	*too hot*
0	Neutral	Comfortable	Comfortable	*comfortable*
-1	Slightly cool	Comfortably cool	Légèrement frais	*too cold*
-2	Cool	Too cool	Froid	*too cold*
-3	Cold	Much too cool	Très froid	*too cold*

Outdoor (T_e), indoor (T_i) temperatures and solar irradiation (E_{esn}) have been collected through sensors connected to the EIB-system, installed in the LESO building, and then linked to the monitored data. The sensors for indoor temperature are installed at a shaded position in each room. The distributions of the observed variables during the study are shown in Figure 7.14.

Regarding the adaptive opportunities the subjects were asked to indicate whether they opened the window, changed the clothing, lowered a blind, switched-on a fan, opened the office's door or had a cold drink during the preceding hour.

7.5.2 Statistical analysis

The first goal of this statistical analysis is to identify the individual distributions of the thermal comfort votes of single subjects for the whole range of indoor temperatures. To infer a probability distribution for the thermal sensation S_{th} from responses of subjects we use the

multinomial logistic model, which is a straightforward extension of logistic models[1]. The probability $p(S_{th}|T_i)$ of a given sensation S_{th} (here: *too hot*:+1, *comfortable*: 0, *too cold*:-1) to be reported relative to the physical stimulus T_i (indoor temperature in our case) can be formulated as:

$$p(S_{th} = S_i) = \frac{\exp(a_i + b_i T_i)}{\sum_{j=-1}^{+1} \exp(a_j + b_j T_i)}, \tag{7.19}$$

where S_i is the thermal sensation and a_i and b_i are regression parameters obtained through multinomial logistic. S_0 is the reference level with $a_0, b_0 = 0$.

This regression analysis was performed considering the thermal comfort of the subjects depending on the indoor temperature T_i. For the multinomial logit regression we divided the events in three groups, which are *too hot*, *comfortable* and *too cold*. According to the BS EN ISO 7730 (85) the accepted range of comfort is defined as PMV $\in [-0.5, 0.5]$. According to that we define the answers Très chaud, Chaud, Légèrement chaud as *too hot*; the answers "'Très froid"', "'Froid"', "'Légèrement frais"' as *too cold*; and the central answer "'Comfortable"' as *comfortable* [2]. (Table 7.5).

7.6 The personalized thermal profile

To create the objective function the inhabitant will only have one button for indicating that an environment is too hot or too cold.

Following Equation 7.19 the probability to be comfortable $P_{S_0}(T_i)$ can be written as:

$$P_{S_0}(T_i) = \frac{1}{1 + \exp(a_{S_1} + b_{S_1} T_i) + \exp(a_{S_{-1}} + b_{S_{-1}} T_i)} \tag{7.20}$$

This results in a individual thermal profile of the occupant for evaluation of his thermal comfort according to the indoor temperature. In Fig. 7.15(b) we show results of the logistic regression for all occupants. The red line denotes $P_{S_1}(T_i)$, the probability that the subject feels too hot given a specific indoor temperature. The blue line denotes $P_{S_{-1}}(T_i)$, the probability that the subjects feels too cold. The black line is indicating the probability of comfort $P_{S_0}(T_i)$.

The first question we want to answer is whether it is sufficient to use one objective function for all possible users or whether we need different functions for each user. In Fig. 7.15(c) the aggregated probability of comfort is shown together with the comfort profiles of single subjects, which are also shown in Fig. 7.16 in more detail. It can be seen that the single comfort profiles

---

[1]For an introduction into statistical modeling we refer to Powers (135).

[2]Naming the central category "Comfortable" instead of "neutral" according to the ASHRAE scale will not change the location where the highest probability of comfort is reached. It can only steepen (central category may cover a smaller semantic range) or flatten (central category may cover a wider semantic range) the curve, which makes no difference in regard of controlling decisions.

(a)

(b)

(c)
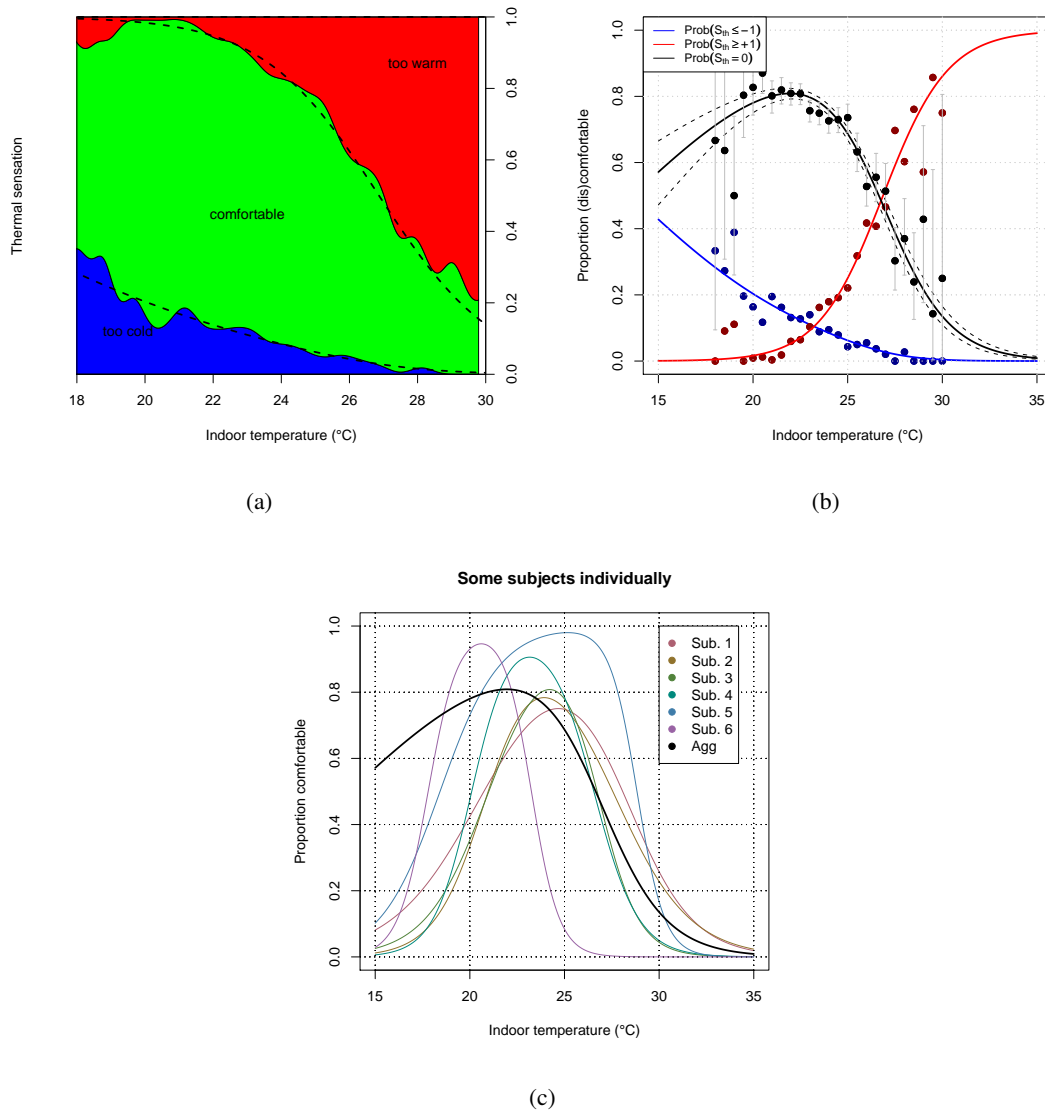
Figure 7.15: (a) Distribution of observed thermal sensation votes conditional on indoor temperatures, with fitted multinomial logistic models. (b) Fitted thermal comfort (black line) and discomfort probabilities (blue and red lines) with standard errors (dashed lines) for the aggregated data. The flat curve between 15 °C and 20 °C can be explained by many opposite votes between 18° C and 22° C that occur in the aggregated data. (c) Probability of thermal comfort for single subjects and the aggregated line for all six subjects.
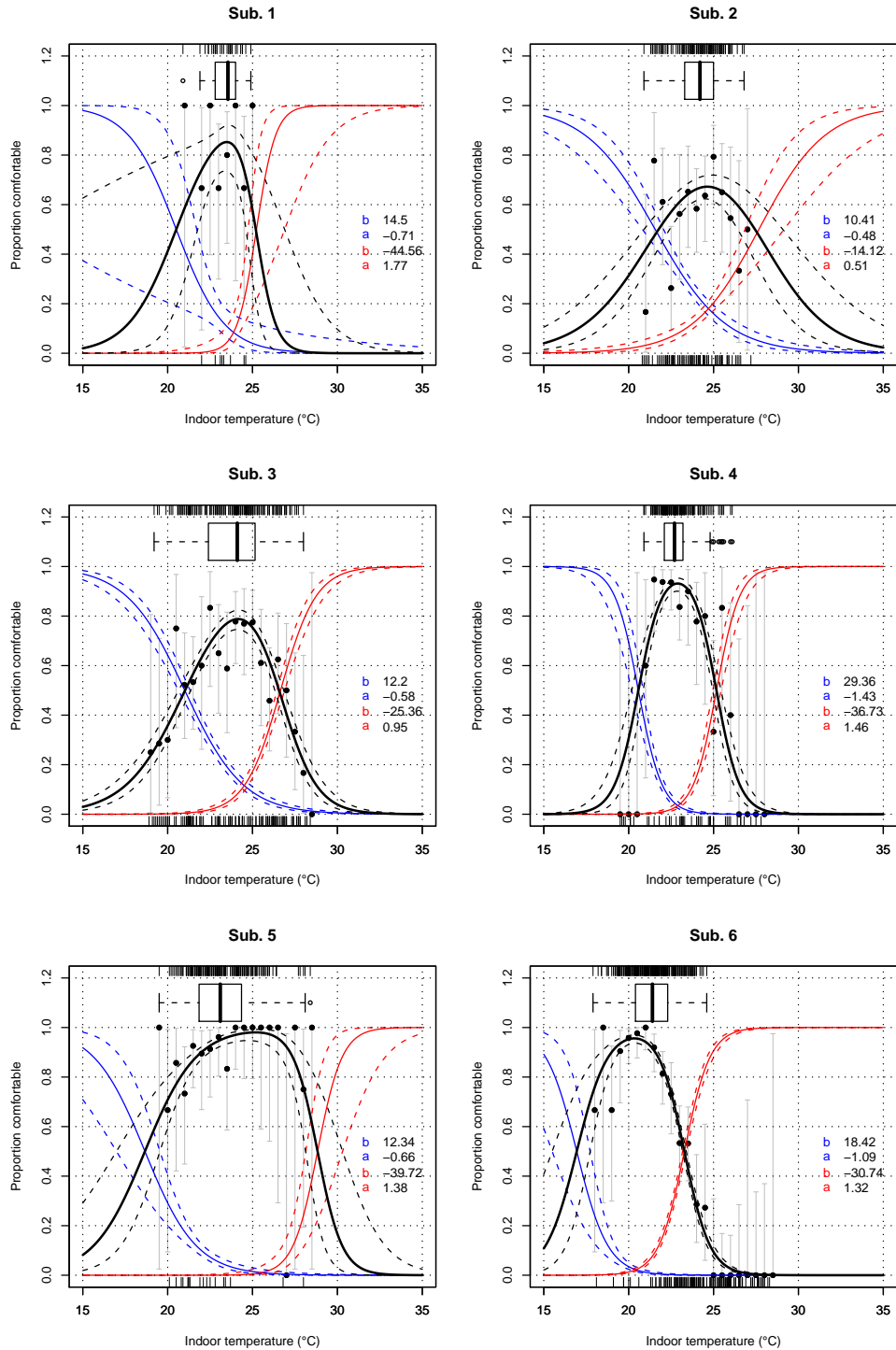
Figure 7.16: Fitted thermal comfort (black line) and discomfort probabilities (blue and red lines) with standard errors (dashed lines).
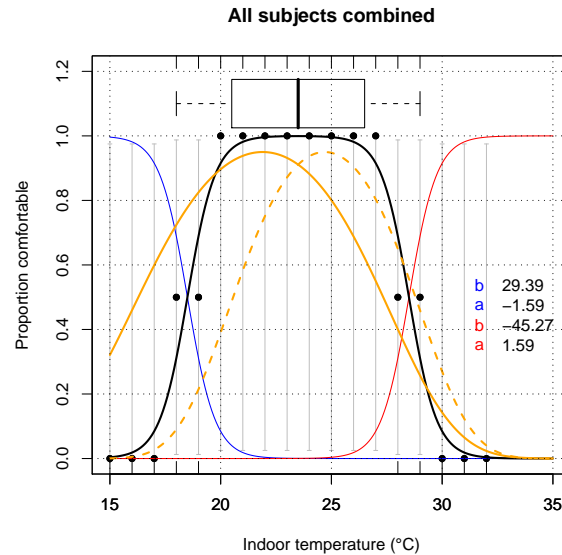
Figure 7.17: The starting thermal profile that is activated as default (black line: thermal comfort probability, blue and red lines: discomfort probabilities). The orange line shows as reference the PPD with following settings (relative humidity: $RH = 60\%$, mean radiant temperature: $T_{mrt} = T_i$, ambient velocity: $V_a = 0$, activity level: $met = 1$, clothing level: $clo = 1$, $clo = 0.5$ (dashed line)).

can differ much from the aggregated profile. For example, the subject 6 has his peak of comfort around 21 °C and is relatively intolerant against increases and decreases of this temperature. Subject 5 has the highest probability of feeling comfortable at 25 °C with a higher tolerance in both directions. By using a standard objective function that would be based on aggregated data many people would not be satisfied. The flat curve between 15 °C and 20 °C can be explained by many opposite votes between 18° C and 22° C that occur in the aggregated data. Figure 7.15(a) shows the distribution of the observed thermal sensation votes and Figure 7.15(b) the aggregated thermal profile of all subjects. Due to opposed votes the profile can never have a well defined peak as it is possible for single users; following it is advantageous to personalize the comfort profiles.

7.6.1 Adaptation of the thermal profile

With the monitored data we have shown that the perception of comfort strongly depends on single occupants. In this section we will now introduce the method for adapting the thermal profile to the wishes of a given occupant.

7.6.1.1 Incorporation of user wishes

Every adaptive control has to incorporate the feedback of the occupant. Two different possibilities exist:

- The information comes from the user directly.

- The information comes from the heating or air cooling unit operated by the user.

The first case occurs mainly if there is no heating or cooling and the occupant is pushing a button to indicate it is too cold or too warm. In reality this will be the case in summer when there is no air cooling as in the case in most residential buildings in Switzerland and north Europe. The second case occurs when the heating or air cooling is switched on by the user. In this case we evaluate this as a user wish because she is starting the heating/cooling, which indicates that she feels uncomfortable, and use it directly as a vote. By doing that, automatically the thermal profile does not conflict with the set-points of the heating or cooling. If the thermal profile is used directly to control a HVAC unit, only information from the user will be considered.

It is clear that the occupant will interact with the environment to avoid unpleasant situations as overheating. But if she is satisfied with the thermal comfort it is hard to believe that she will push a button to indicate that. Furthermore it goes not along our concept of a user friendly device. Hence, once a day between 8.00 am in the morning and 11.00 pm in the evening, we placed one artificial vote for the event *comfortable* with the average temperature of this period. If we have occupancy information, this will be performed for occupied days only.

7.6.1.2 The starting profile

After installing a control system in an unidentified environment, with unidentified user we do not know anything about the thermal profile, still we need an objective function. For that we have to define a standard thermal profile that is used as default at the beginning. It has to fulfill the following two points:

- adapts quickly to the individual profile of the occupant.

- allows the control to perform already at the beginning.

A first possibility is to take the profile from the aggregated data. But the problem is that high temperatures are already penalized, although the occupant is still comfortable with them. Also there are many opposite votes in the aggregated data, we want to avoid this by adapting the profile to each occupant. For that reason we need a curve with a high comfort probability on a wide range of temperature. Furthermore we need a curve which is based on few data points to ensure that the entries made by occupants have a high weight right from the outset and the curve quickly converges to the *real* individual curve of the occupant.

The comfort profile shown in Figure 7.17 satisfies these basic requirements. It is constructed from points shown in Table 7.6. For comparison we also plot the PPD in Figure 7.17 to show that the starting profile deviates not to much from a well known comfort measure.

Table 7.6: Data created for the starting default profile, -1 denotes *too cold*, 0 denotes *comfortable*, 1 denotes *too hot*

Description	1	2	3	4	5	6	7	8	9	10	11
T_i	15	16	17	18	19	18	19	20	21	22	23
event	-1	-1	-1	-1	-1	0	0	0	0	0	0
	12	13	14	15	16	17	18	19	20	21	22
T_i	24	25	26	27	28	29	28	29	30	31	32
event	0	0	0	0	0	0	1	1	1	1	1
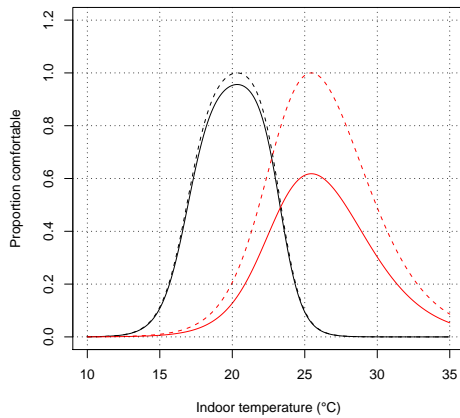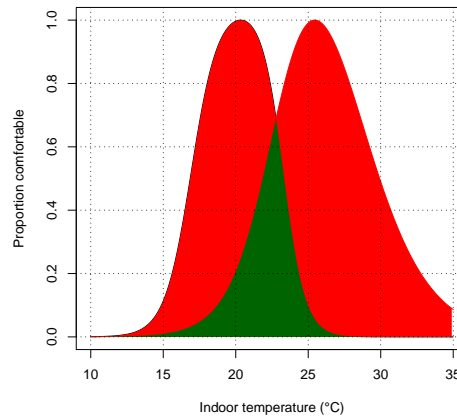
(a)   (b)

Figure 7.18: (a) Two thermal profiles, the rescaled profiles are shown with dashed lines. (b) Two thermal profiles, with the overlapping surface (green) and the non-overlapping surface (red).

The time of convergence against the *real* thermal profile is crucial for an adaptive procedure. For measuring the congruency of two thermal profiles we first normalize them to one. By rescaling a thermal profile no modification is made since the control always will try to reach the optimal point. If this is at 0.8 or 1 is equivalent for the result. Figure 7.18(a) shows two thermal profiles with their rescaled counterparts (dashed lines).

As a measure for congruency we take the ratio of non-overlapping surface to overlapping surface of two thermal profiles.

Two thermal profiles $f_i(T_i), f_j(T_i)$ are congruent $f_i(T_i) \cong f_j(T_i)$ if $A_{ij} = 1$ and not congruent if $A_{ij} = 0$, with:

$$A_{i \cap j} = \int_{\infty}^{f_j(T_i)=f_i(T_i)} f_j(T_i)dT_i + \int_{f_j(T_i)=f_i(T_i)}^{\infty} f_i(T_i)dT_i, \qquad (7.21)$$

$$A_{i \Delta j} = \left(\int_{\infty} f_i(T_i)dT_i - A_{i \cap j} \right) + \left(\int_{\infty} f_i(T_i)dT_i - A_{i \cap j} \right), \qquad (7.22)$$

$$A_{ij} = 1 - \frac{A_{i \Delta j}}{A_{i \cap j} + \int_{\infty} f_i(T_i)dT_i + \int_{\infty} f_j(T_i)dT_i}, \qquad (7.23)$$

where A_{ij} is the congruency, $A_{i \cap j}$ denotes the overlapping surface (green in Figure 7.18(b)) and $A_{i \Delta j}$ the non-overlapping surface (red in Figure 7.18(b)).

To show that the starting thermal profile converges towards the individual thermal profile in appropriate time and to clarify the procedure we generate votes according to the individual profile of subject 6. We first take the temperature, monitored in the office room of subject 6, for three months (January, April, August). Then we draw 30 random points in time each month and collect the corresponding T_i (upper three charts of Figure 7.19). For each temperature T_i we draw the state of comfort out of the comfort probability of Eqn. 7.20. We start with the thermal profile of Figure 7.17, after each vote a regression is conducted to derive the new parameters a_1, b_1, a_{-1}, b_{-1}. The development of the profiles are shown in Figure 7.19: the starting profile, thermal profiles after each 10 votes and the actual profile of subject 6. In the last chart of Figure 7.19 we show the congruency increasing from 0.66 to 0.87. This can be interpreted that at the beginning 66% of the surface have been overlapping and at the end 87% overlap, which is already a reasonable fit. In January the congruency of the curve between 22 °C and 30 °C cannot increase if temperatures in this range do not occur. There again, the curve between 18 °C and 22 °C is fitted quite quickly during January.

With changing outdoor weather conditions, the thermal profile of a human can be modified. Humphreys suggested even that the optimal comfort temperature could be expressed as,

$$T_C = aT_{e,rm} + b, \qquad (7.24)$$

where T_C is the comfort temperature [°C], $T_{e,rm}$ is the exponentially weighted running mean of the daily mean temperatures, and a and b are parameters. It is also intuitive that votes expressed closed to the present are more *important* than votes expressed 60 days in the past.
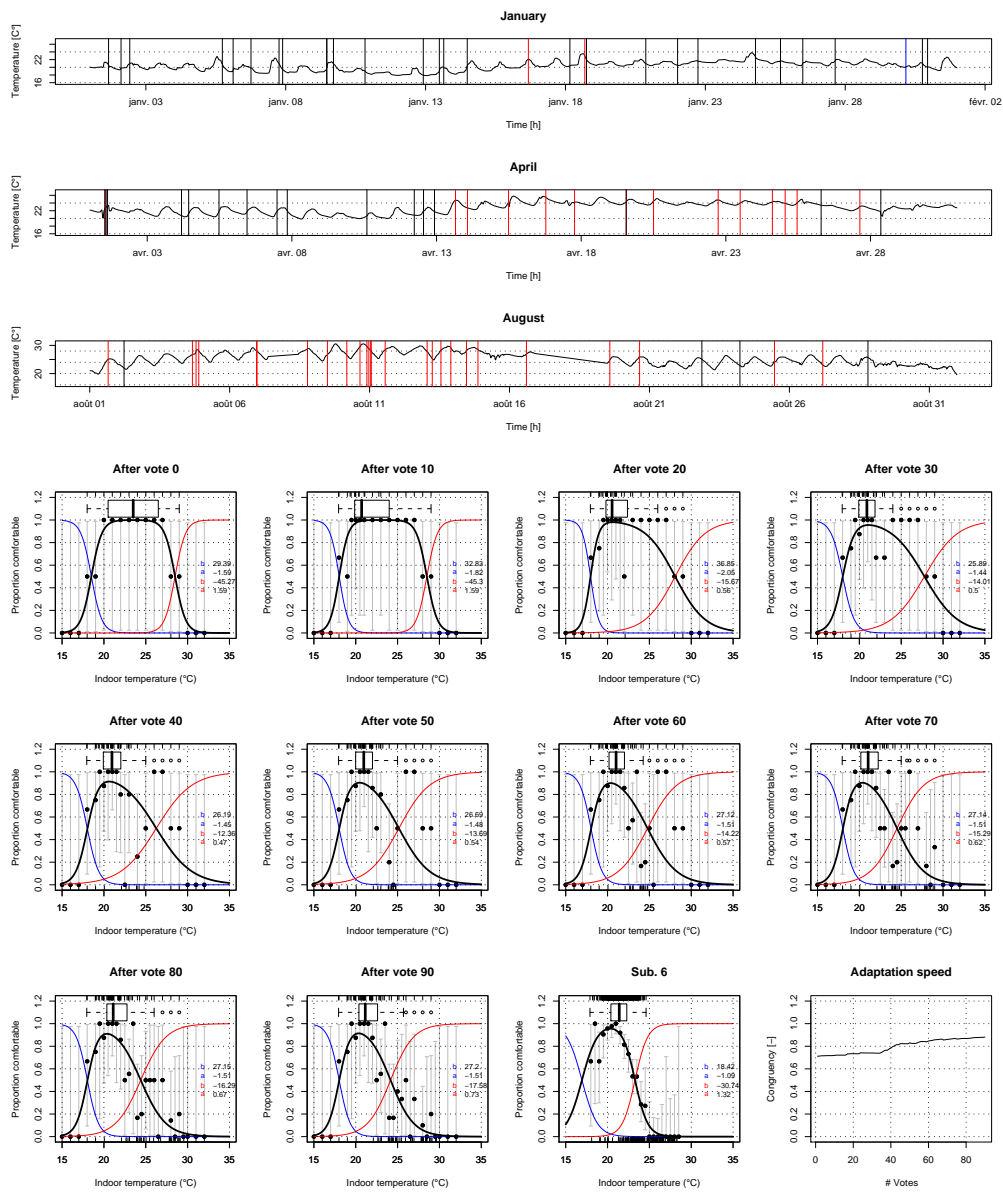
Figure 7.19: Top: The course of indoor temperature together with comfort votes for the month January, April and August. Black lines stand for events *comfortable*, red lines for events *too hot* and blue lines for the event *too cold*. Bottom: Thermal profile after each 10 votes. In the last chart the development of the congruency is shown.
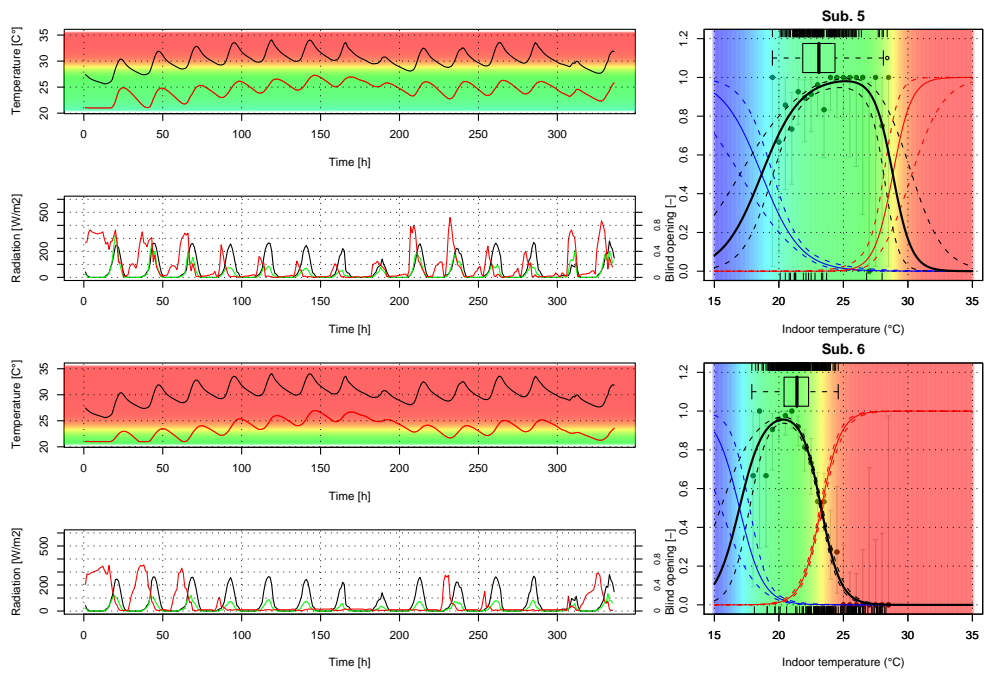
Figure 7.20: This figure shows the indoor temperature and blind movements resulting from two different thermal profiles.

For that we let the user override old votes. That means whenever a new vote is delivered at $\hat{T}_i$ we delete the votes older than 30 days in the vicinity of $\hat{T}_i$ defined as $\hat{T}_i \pm 0.25 \ C°$. With the suggested method the profile is steadily adapting to the occupant allowing also an adaptation to long term changes of the user such as changing clothing from winter to summer time.

7.6.2 Case study

Figure 7.20 shows the thermal profiles of two different users, derived from the LESO field study. Each of them have been implemented in the control and therefore used to optimize the parameters $\vec{F}$ for the fuzzy logic. Next to the thermal profiles we show in the upper part outdoor temperature T_e as a black line and indoor temperature T_i as a red line. In the lower part the black line corresponds to the irradiance E_{esn} before the blind, and the green line after the blind. Both lines belong to the left scale. The red line illustrates the unshaded fraction of the window, in other words, 0 stands for lowered blinds and 1 for raised blinds. It can be seen that with the thermal profile of subject 6 the indoor temperature is lower than with the profile of subject 5. This is due to the blind that is kept closed most of the time. Since only the blinds are controlled it is not possible to satisfy the thermal profile at all times, for that a cooling action is necessary. During spring the control for subject 5 would allow solar gains through the window to heat the room to around $25[C°]$, which would reduce the need of heating during the evening. With the profile of subject 6 this would not be possible because she is impaired by temperatures of $25[C°]$ and therefore would reject a control with this behavior.

7.7 Visual comfort

The main goal of this thesis is to set-up a control that is providing thermal comfort, is self adaptive, and is used in the residential environment. Of course we also know that the setting of the blinds is important for visual comfort. Since the objective of our control is to save energy it would be absurd to close the blinds and then switch on the artificial lighting. However we have chosen to account for the illuminance not in the main structure of our control algorithm.

Studies carried out by the LESO have shown that the most important stimuli of blind movement by occupants is visual comfort. For visual comfort a blind movement does directly change the lighting situation and the unpleasant situation is removed completely. Contrariwise, for thermal comfort the control needs to account for the inertia of the building; this is done poorly by human occupants and in the moment the stimuli for thermal comfort triggers a blind movement the effect on the thermal comfort stays limited.

Visual comfort is also only important if the occupant is present; if not, only thermal comfort should play a role in the setting of the blinds. For that, theoretically every algorithm for the visual comfort can be coupled with our control by including an occupancy sensor that switches between the two controls based on the state of occupancy.

7.7.1 Daylight

During most of the time daylight generates illuminance that exceeds by far the required workplane illuminance. By using daylight we can save energy and capitalize on the positive effects on the human body and occupants' wellbeing (160). It has also been identified as one of the major pacemaker of the internal clock (176). In 2002, Berson et al. (15) discovered, additional to the rods and cones, a third photo receptor, the retinal ganglion cells. It was shown that this additional so-called non-image-forming photoreceptor in the human retinal is important for the melantonin[1] supression and strongly influences our circadian system. For interested reader we refer to Linhart (106). It can be said, that using daylight for residential and office rooms is sound for the inhabitants and saves also energy if overheating is effectively prevented.

7.7.2 Quantification of visual comfort

The quantification of visual comfort has been a topic in science for many years; numerous publications show that most probably there is no universally accepted way of quantifying visual comfort. One of the first publications on this topic came from Luckiesh and Moss (110). After this numerous other publications tried to tackle the problem of visual comfort. A good overview is given by Lindelöf (105). The two main causes of visual discomfort are glare and insufficient or excessive workplane illuminance; where glare is, by far, the more difficult problem.

7.7.2.1 Quantification of glare

In 1983 the Commission International de l' Eclairage (CIE) (29) aggregated results of previous studies, and suggested the CIE Glare Index (CGI) based on Einhorn (51) to quantify discomfort glare, defined by:

$$CGI = 8\log_{10}\left[2 \cdot \frac{1 + E_d/500}{E_d + E_i} \sum_s \frac{L_s^2 \omega_s}{p_s^2}\right] \tag{7.25}$$

where E_d is the direct vertical illuminance [lux] at eye level from all sources, E_i is the eye-level indirect (excluding the glare source) illuminance [lux], L_s is the luminance [cd/m^2] of the bright part of each source s in the direction of eye, and ω_s is the solid angle [sr] of the latter. p_s is the Guth position index, defined by,

$$\begin{aligned}p_s \quad &= \exp[(35.2 - 0.31889 \cdot \alpha - 1.22 \cdot \exp(-2\alpha/9)) \cdot 10^{-3} \cdot \beta \\ &+ (21 + 0.26667 \cdot \alpha - 0.002963 \cdot \alpha^2) \cdot 10^{-5} \cdot \beta^2]\end{aligned} \tag{7.26}$$

It gives different weights to luminous sources according to their angular position. α is the angle [rad] from vertical of the plane containing the source and the line of sight and β is the angle [rad] between the line of sight and the line from the observer to the source.

---

[1]Melatonin is a hormone that has a major infuence on our sleep-wake pattern

Since the CGI is not easy to evaluate and therefore not applicable to derive general design rules, the CGI published a second report (30) in 1995, in which they defined the Unified Glare Rating (UGR):

$$UGR = 8\log_{10}\left[\frac{0.25}{L_b}\sum_s \frac{L_b^2\omega_s}{p_b^2}\right] \tag{7.27}$$

where $L_b = E_i/\pi$ is the background luminance [cd/m^2] perceived by the eye of the occupant. As a result, the UGR represents a simplification of the CGI. It is used, by luminaire manufacturers to provide design aids for their products. Parallel to the UGR the Visual Comfort Probability (VCP) was proposed in the United States by the *IESNA Lighting Handbook* (140). Both of these indexes have been developed for small electric light sources (161). They have unfortunately never been validated against daylight glare or glare from large light sources, therefore they are not applicable for large windows and daylight.

For quantification of glare from windows or large light sources, experiments have been originally carried out at the Building Research Station at the Cornell University in the USA, which led to the Daylight Glare Index (DGI) (25):

$$DGI = 10\log_{10}0.48\sum_s \frac{L_s^{1.6}\Omega_s^{0.8}}{L_b + 0.07\omega_s^{0.5}L_s} \tag{7.28}$$

where L_s is the source luminance [cd/m^2], L_b is the background luminance [cd/m^2], ω_s is the solid angle of the source [sr], and Ω_s is the solid angle [sr] of the source modified by its position in the field of view of the user. Chauvel et al. (25) found that the direct application of the DGI to a real daylight leads to an overestimation of glare. Newer research by Tuaycharoen and Tregenza (159) supports this opinion.

In a report of the CIE in 2002 (31), it is pointed out that the UGR is overestimated the glare for small (<0.005m^2) light sources and underestimated the glare for big (>1.5m^2) light sources. To overcome that weakness they defined the large room glare rating (GGR):

$$GGR = UGR + \left(1.18 - \frac{0.18}{CC}\right)8\log\left[\frac{2.55\left(1 + \frac{E_d}{220}\right)}{1 + \frac{E_d}{E_i}}\right] \tag{7.29}$$

where CC is the ceiling coverage, taking values between 0.15-1.

The afore mentioned indexes are more ore less dedicated to artificial light sources. In contrast to that, Nazal (121; 122) introduced the new daylight glare index method DGI$_N$ especially for the evaluation of daylight glare:

$$DGI_N = 8\log_{10}\left[0.25\left(\frac{\sum_s L_e^2\Omega_{pN}}{L_a + 0.07\left(\sum_s(L_w^2\omega_N)\right)^{0.5}}\right)\right] \tag{7.30}$$

where L_w is the average vertical luminance [cdm^{-2}] of the window, L_a the average vertical luminance [cdm^{-2}] of the surroundings and L_e the average vertical unshielded luminance of the outdoors.

The Daylight Glare Probability (DGP) index, suggested by Wienold and Christoffersen (169) evaluates the level of visual comfort in daylit office spaces, including glare, window luminances and luminance ratios within the field of view. It is defined as follows:

$$DGP = 5.87 \cdot 10^{-5} E_v + 9.18 \cdot 10^{-2} \log_{10}\left(1 + \sum_s \frac{L_s^2 \omega_s}{E_v^{1.87} p_s^2}\right) + 0.16 \qquad (7.31)$$

where E_v is the vertical eye illuminance [lux], L_s the luminance of source [cd/m^2], ω_s is the solid angle of the source and p_s is Guth's index. This index has been derived from real daylit spaces.

All these indices have been developed to rate mathematically and reproducible the risk of glare in an indoor environment. Unfortunately, for their calculation, a full knowledge of the luminance distribution in a room is necessary, making the indices difficult to integrate in control systems. Furthermore, in the residential environment the occupants has no place where he remains the most time as it is the case in an office environment; for that case also the whereabout of the person has to be detected, which is not an easy task.

7.7.2.2 Preferred illuminances

The second problem that can reduce visual comfort is insufficient or excessive workplane illuminance. Daylight illuminances can vary greatly during daytime but also within different sectors in a room. For example, daylight illuminances diminish rapidly with increasing distance from a window. Fortunately, our eye can adapt to different levels of illuminance by opening and closing the iris. Only if the illuminances exceed, the ability to adapt the visual comfort declines. Hence, we can always outline a range of preferred illuminances, rather than a single value. For determining the preferred range of illuminance many experiments have been conducted in the last 60 years, some with contrary results. In Fisher (55) an overview of research before 1970 is given. The UK Chartered Institution of Building Services Engineers (CIBSE) Code for Interior Lighting recommends that offices should have a design illuminance level of 500 lux. According to a field study conducted by the National Research Council Canada, illuminances larger than 150 lx were classified as appreciable daylight (143). In a field study at the Lawrence Berkeley National Laboratory (USA), office workers were allowed to control blinds and setting there own lighting. The recorded illuminances were in the range of 840-2146 lx in the morning and 782-1278 lx in the evening. This indicates that also higher illuminances have been tolerated (162). Michel (114) found that the workplane illuminance while reading or writing should not exceed 4000 lx, and while working in front of a computer it should not exceed 1000 lx; for both cases he assumed 80% surface reflection of the visual flux.

For working tasks including a computer screen, even lower illuminances can be sufficient. In a study of the Illuminating Engineering Society (IES) of North America it has been found that not more than 50 - 100 lx illuminance is required for working with CRT screens (83). Another study, conducted by a private company backed up these results by defining an illuminance value around 100 lx as comfortable (151). Regarding the upper level of illuminance

while working in front of a computer screen Roche et al. (145) reported limits of 1800 lx. Furthermore, they stated that the daylit illuminance range of 700-1800 lx appears comfortable for both computer and paper-oriented tasks. It has also been observed that under special conditions we tend to tolerate much lower lighting conditions. Baker (11) report that it is not unusual that people continue reading a newspaper with levels as low as 50 lx.

Nabil and Mardaljevic (117) concluded in the most recent overview the following illuminance levels:

- Workplane illuminances lower than 100 lx are generally considered insufficient to be either the sole source of illumination or to contribute significantly to artificial lighting.

- Workplane illuminances in the range of 100–500 lx are considered effective either as the sole source of illumination or in conjunction with artificial lighting.

- Workplane illuminances in the range of 500–2000 lx are often perceived either as desirable or at least tolerable.

- Workplane illuminances higher than 2000 lx are likely to produce visual discomfort.

Other studies showed that within the comfort zone of illuminance there is plenty of room for control systems to achieve also thermal comfort.

7.7.3 Control algorithm

As shown in the previous two sections, visual comfort can be divided into glare and illuminance. We have clearly seen that the evaluation of glare requires many informations that, for a control, have to be collected by sensors. One goal of our control was to keep the installation costs as low as possible. This would not be possible by including all sensors required for a glare assessment. Beyond that, in a residential building, in contrast to an office space, the whereabouts of the occupants are not easy to determine and are changing rapidly, as well as the action. For example you can watch TV on your couch or read a book. In the first case you will be extremely sensitive to glare, while in the second case it is not a problem. Since the control can never know exactly what task is performed, the error in prediction of the right blind setting is quite high. For these reasons we will not include an glare assessment into our system of control. However, a control for glare and illuminance levels, for example the control proposed by Lindelöf (105), can be added easily to ours in case it is used for offices and the additional sensors are installed.

Treating the insufficient or excessive illuminance is by far easier and a character that is essential for a good blind control. For this we only need two additional sensors:

1. an occupancy sensor,

2. an illuminance sensor placed at the point of interest

(a) Distribution for Subject 6.

(b) Distribution for Subject 5.
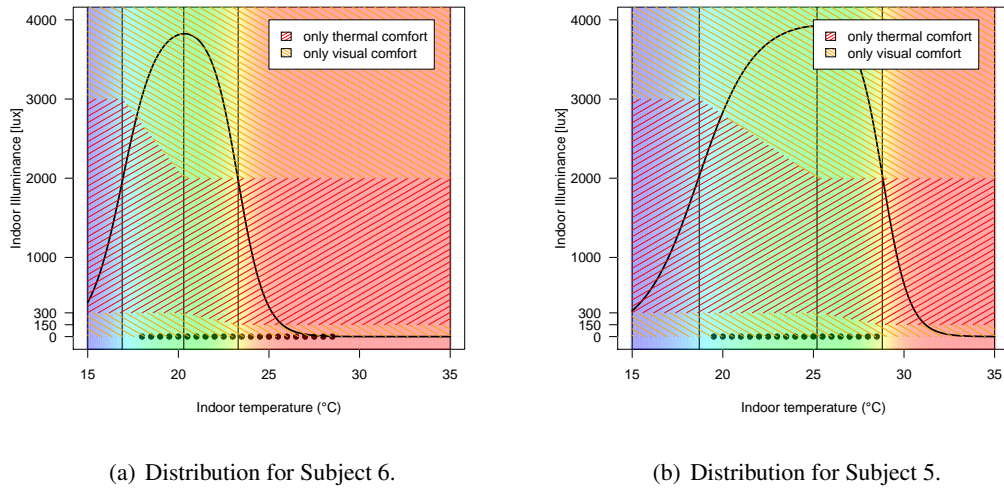
Figure 7.21: Distribution of the control strategies between thermal and visual comfort.

The occupancy sensor is important to distinguish clearly between periods where only thermal and energy aspects are considered by the control and periods where visual comfort plays also a role. The illuminance sensor is directly involved in the process of control. Without going into details we propose to use wireless sensors as they are easy to install, not expensive, and can be placed easily at any indoor place. This is especially important for the illuminance sensor, where different positions may be tested.

As we have seen, for the illuminance level there is no single target value, but rather a range of acceptable values. That means within this range we can follow our goal to reach thermal comfort, only on the edges we have to care about visual comfort. We propose the following control sequence for different values of E_v (horizontal illuminance on the workplane) [lux]:

- $E_v \leq 150$: only illuminance is considered.

- $150 < E_v \leq 300$: illuminance is considered together with the thermal comfort if the indoor air is too warm.

- $300 < E_v \leq 2000$: only thermal comfort is considered.

- $2000 < E_v \leq 3000$: illuminance is considered together with the thermal comfort if the indoor air is too cold.

- $3000 < E_v$: only illuminance is considered.

This control scheme is quite easy for the ranges $E_v \leq 150$, $300 < E_v \leq 2000$, and $3000 < E_v$ where either thermal or visual comfort plays a role. For the ranges $150 < E_v \leq 300$ and $2000 < E_v \leq 3000$ we have to find a balance between thermal and visual comfort. If, in
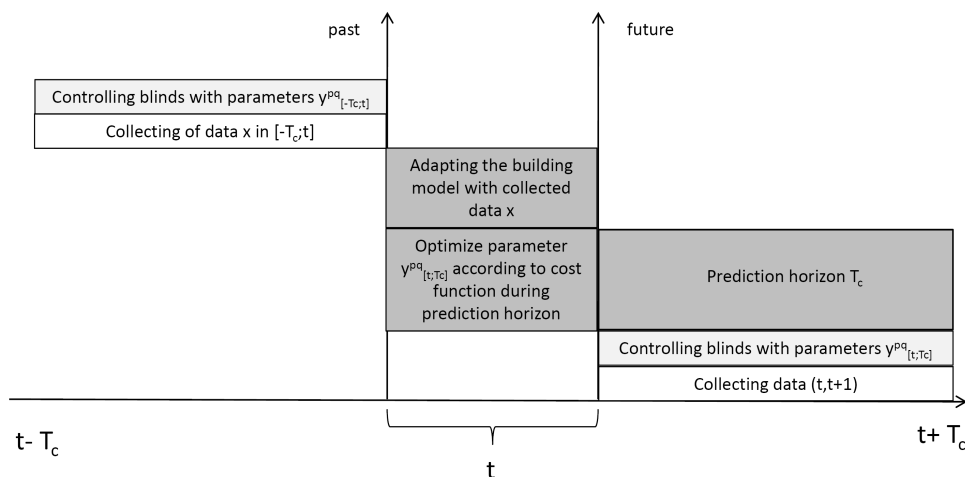
Figure 7.22: Structure of the MPC.

the range of $150 < E_v \le 300$ it is not *too hot* for the occupant, the blinds should be opened so that the target of $E_v > 300$ can be met. Thanks to the thermal profile we have an exact measure for *too hot*, we take the temperature where $P_1(T_i) = 0.5$. If the indoor temperature exceeds this value we allow the illuminance to drop to 150 lx. Below this temperature the minimal value is set 300 lx. For the range of $2000 < E_v \le 3000$ we apply the same scheme, but reversed. If the temperature is lower than T_i with $P_{-1}(T_i) = 0.5$; we allow illuminances until 3000 lx, otherwise only until 2000 lx. In Figure 7.21(a), 7.21(b) we visualized the scheme for two different thermal profiles.

7.8 Complete structure

The whole functioning of the MPC is shown in Algorithm 3 and Figure 7.22. Where t, T_c and i are measured in hours. In this setup every 168 hours, seven days the adaptation is carried out.

7.9 Chapter Summary

In this chapter we presented the different parts of our control strategy. We have shown that the control is adaptable to the building via the fitting of the thermal model and also via the adaptation of the membership functions regarding the monitored data, which makes the control applicable for different climate zones. We also showed that it can be adapted with the chosen parameters. Regarding the objective function for thermal comfort we gave an overview of the existing methodologies and pointed out the need of an adaptive thermal profile for different users based on the findings from a field study. To solve this issue we introduced a method

---
Algorithm 3 Non-linear Model Predictive Control

1: $t \leftarrow 0$

2: $T_c \leftarrow 168$

3: $i \leftarrow 0$

4: **while do**

5:     **while** $t \leq i * T_c$ **do**

6:         save $T_e(t)$ in $\vec{T_e}$

7:         save $T_i(t)$ in $\vec{T_i}$

8:         save $E_{esn}(t)$ in $\vec{E}_{esn}$

9:         save $T_{vote}(t)$ in $\vec{T}_{vote}(t)$

10:         delete $\vec{T_e}[j > (24 \cdot 90)]$

11:         delete $\vec{T_i}[j > (24 \cdot 90)]$

12:         delete $\vec{E}_{esn}[j > (24 \cdot 90)]$

13:         control with $y^{pq}_{[i \cdot T_c; i \cdot T_c + 168]}$

14:         $t \leftarrow t + 1$

15:     **end while**

16:     calculate $e^p_{\vec{T}_{vote}}, p \in [1, \ldots, 5]$ with $\vec{T_e}$

17:     calculate $e^p_{\vec{T_i}}, p \in [1, \ldots, 5]$ with $\vec{T_i}$

18:     calculate $e^p_{\vec{E}_{esn}}, p \in [1, \ldots, 5]$ with $\vec{E}_{esn}$

19:     $t_{Adaptation} \leftarrow 0$ {Start adaptation of the thermal model with the collected values in $\vec{x}(t)$}

20:     optimize $f(C_w, C_i, K_{w1}, K_{w2}, K_i, UA, SHGC, F_w, P_w)${Fit the model to measured values}

21:     save final parameters $C_w, C_i, K_{w1}, K_{w2}, K_i, UA, SHGC, F_w, P_w$

22:     $t_{Optimization} \leftarrow 0$ {Start optimization of the fuzzy logic}

23:     optimize $f\left(y^{pq}_{[i \cdot T_c; i \cdot T_c + 168]}\right)$ {Optimize parameters of fuzzy logic}

24:     save final parameters $y^{pq}_{[i \cdot T_c; i \cdot T_c + 168]}$

25:     $i \leftarrow i + 1$

26: **end while**

---

for adapting a thermal profile to the occupant with easy votes. This thermal profile is used as objective for the optimization of the Fuzzy Logic. Regarding the visual comfort we discussed the evaluation methods and implemented the an control sequence for illuminance levels.

8

Assessment of control system performance

In this Chapter we will describe the testing of our control strategy. The tests can be divided into two main parts:

- tests carried out in the simulation environment

- tests carried out in a real office, the LESO building

Section 8.1 comprises tests of the control carried out via simulation. The attention lies on the benchmarking of our control system against others. With the simulation it is also possible to asses the controls performance in many different settings. We will describe these settings and draw the conclusions regarding the performance.

Section 8.2 describes the monitoring that has been carried out in the LESO experimental building where our control has been implemented. For that we present the office rooms chosen for the test and also explain the EIB bus, its actuators and sensors, which facilitate the experimental implementation.

8.1 Tests in the simulation test bed

The goal in this section is to test our control. Therefore we use again our test bed described in Chapter 3. We tested two different setups, a residential building in Elfenau and an office room in the LESO building. We will now return to these setups to show the performance of our control relative to the Pareto-front we assessed in Chapter 3. Again these tests are carried out with the simulation software IDA/ICE with the same set-points as in Sections 5.5.2 and 5.5.1. The control described in Chapter 7 is implemented in C and C++ and then embedded in NMF modules that can be easily added to any simulation model via drag and drop.
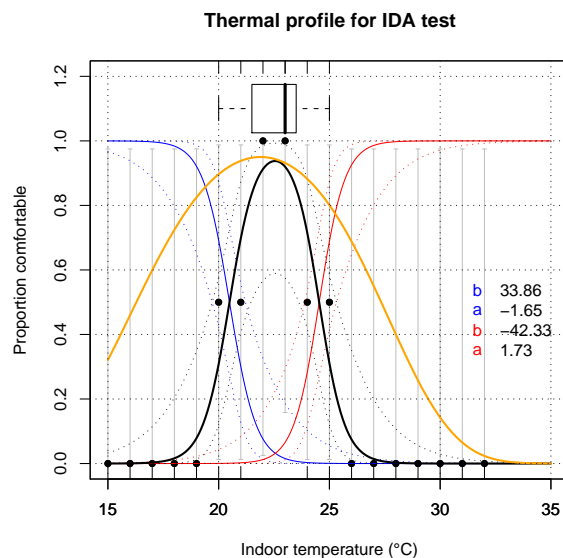
Figure 8.1: The artificial thermal profile that is activated during the IDA tests. The orange line shows as reference the PPD with following settings (relative humidity: $Rh = 60\%$, mean radiant temperature: $T_{mrt} = T_i$, ambient velocity: $V_a = 0$, activity level: $met = 1$, clothing level: $clo = 1$).

To make the data comparable we use the same weather data, shown in Figures 5.7, 5.8, 5.9, with the only difference that the control has 7 days before each period to collect data, adapt and optimize its parameters. As objectives we use the energy consumption and the PPD as measure for thermal comfort. For our control only the thermal profile defined in Section 7.5 is used. Normally we start with the initial profile shown in Figure 7.17 and let the users include their wishes to reach thermal comfort. In this case there are no users including their wishes and the relatively wide starting profile would not penalize temperatures above $25°C$ which would lead to poor energy performance. Since we do not want to compare apples to oranges we have to change the thermal profile that it penalizes temperatures above $25°C$ and under $21°C$. Hence we use the thermal profile shown in Figure 8.1 together with the PPD. Though, for comparing the controls to the Pareto-front we use the original two objectives.

8.1.1 Test in the Elfenau setup

As explained in Section 5.5.2, this setup consists out of a residential multi-family building and thus represents an ideal test case for our control. The results together with the Pareto-front from the optimization are shown in Figure 8.2(a). The results of the adaptive control system are shown as a green dot, the results of a former control developed at the LESO (66) is shown

as black square. It can be seen that our control is closer to the Pareto-front, capitalizing on most of the possible energy savings, while still providing good thermal comfort.

8.1.2   Test in the LESO setup

The settings for the LESO setup are introduced in detail in Section 5.5.1. As for the Elfenau case we run our control for the same period. The results (Figure 8.2(b)) show that also in this setup our adaptive control system is closer to the Pareto-front and therefore capitalizes on most of the potential.

To assess the control actions during one year we compare our control against an optimal blind control[1], namely Blind4 (explained in Section 5.7) in combination with the Light3 control (explained in Section 3.2.3). In Figure 8.3(a) we show the energy used for heating, cooling and electric lighting and how they add up for one year for an optimized control. In 8.3(b) weekly box plots of the shading factor together with the weekly average of indoor and outdoor temperatures for the optimized Blind4 Light3 combination are shown. Figures 8.4(a), 8.4(b) show the energy consumption and shading factors with our control[2]. By comparing the energy profiles of the two controls it can be said that in term of energy consumption both are equally good. Noticeable is that our control needs cooling energy in February[3]. This can be explained with the not yet adapted fuzzy logic at this stage because it is the first time that solar gains overheat the room and the control has not yet learned to handle this. After another adaptation cycle excessive solar gains are kept out.

8.1.3   Test for different orientations

In Chapter 6 we tested different setups of controls for different orientations. There we have seen that if we optimize the control for one direction[4] the performance will change for other directions, and more important, the result is not any more optimal. With our adaptive control we overcome that problem since the control is able to adapt to the subtleties of each orientation. In Figures 8.5(a), 8.5(b), 8.5(c) we show a radial diagram with the results of our control for different orientations. In the background of Figure 8.5(a) we show in limpid orange the performance of an optimized control, in Figure 8.5(b) the performance of the control suggested by Guillemin (66), and in Figure 8.5(c) the performance of the Lightswitch2002 algorithm.

The optimized control is not much better than our control showing that we capitalize on the whole potenzial.

While the control suggested by Guillemin (66) is showing a good performance on south oriented buildings it is weaker for north oriented buildings. This may be due to the fact that

---

[1]Optimal blind control means that we found the parameters for the fuzzy system coupling the IDA/ICE simulation with the genetic optimizer.

[2]Our control refers to the one suggested in Chapter 7.

[3]Normally in this situation we would open the window. Here, we use the cooling energy for quantifying the overheating.

[4]In Chapter 6 we optimized all controls for a south facing facade.

167
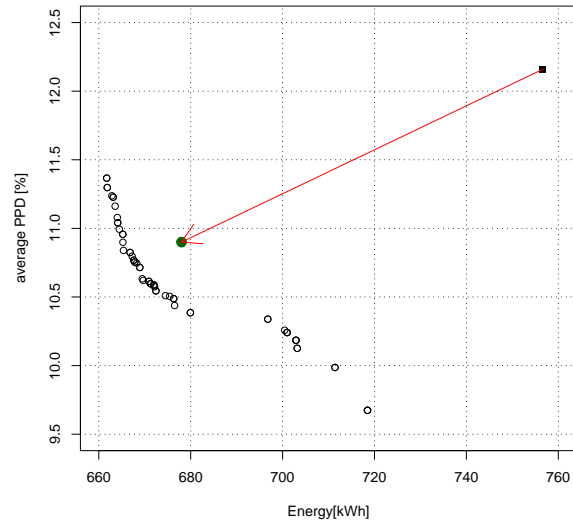
(a) Pareto-front of the optimization for the Elfenau case as already shown in Section 5.5.2 with the performance of another control shown as square and the performance of the adaptive control shown in green.
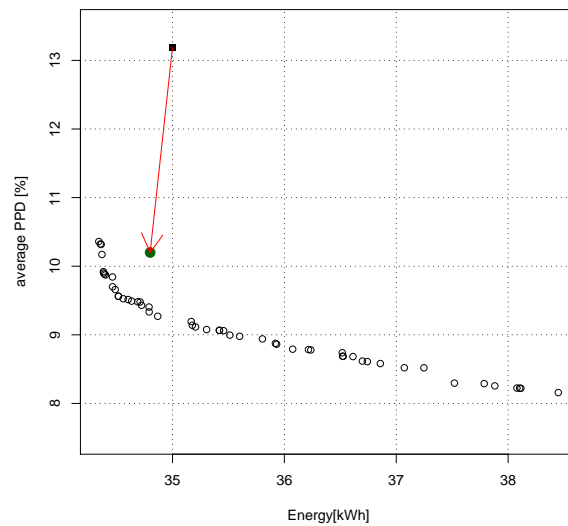
(b) Pareto-front of the optimization for the LESO case as already shown in Section 5.5.1 with the performance of another control shown as square and the performance of the adaptive control shown in green.

Figure 8.2: Plotting the Pareto-front and different types of controls allows a real comparison of the different controls.
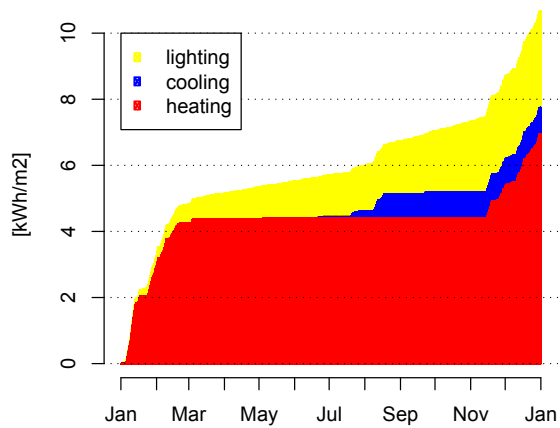
(a) The yearly accumulated energy consumption for heating, cooling and electric lighting.
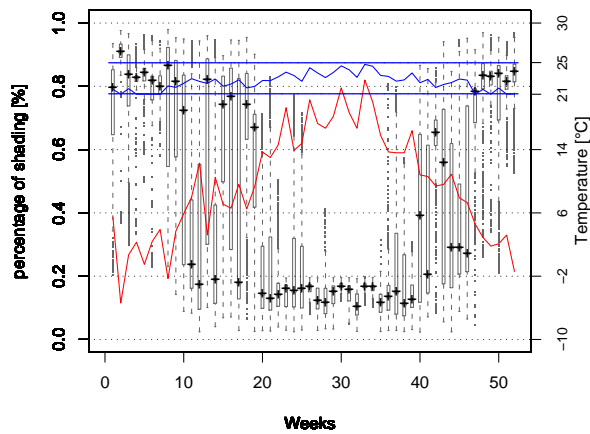
(b) The shading factor of the blind control shown in weekly box-plots together with the outdoor temperature shown in red and the indoor temperature shown in blue.

Figure 8.3: The blind control was set up with the most energy efficient parameters out of an optimization and was combined with the Light3 control for artificial lighting. For the test we use the LESO setup.
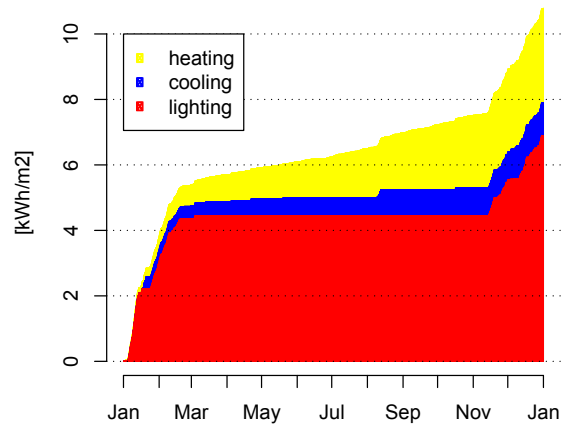
(a) The yearly accumulated energy consumption for heating, cooling and electric lighting.
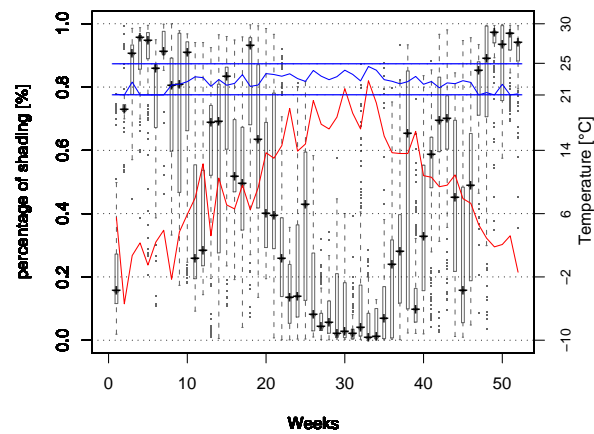
(b) The shading factor of the self adaptable blind control shown in weekly boxplots together with the outdoor temperature shown in red and the indoor temperature shown in blue.

Figure 8.4: In this setup the adaptable control explained in Chapter 7 in combination with the Light3 control for artificial lighting has been used. For the test we use the LESO setup.

solar gains are handled cautiously to prevent overheating, which leads to higher heating needs on north oriented facades.

The comparison with the Lightswitch2002 algorithm, that is supposed to act the same way occupants would do, shows how important a control for the south facade is; on the north facade they are basically identical.

8.2 Experiments in the LESO experimental building

The goal of the experiments described in this section is to study the behavior in a real experimental set up, additionally to the validation experiments carried out through simulation. We will measure the performance of the control through energy consumption and adaptation to the thermal profile.

In this section we will first describe the experimental set-up and the office rooms of the LESO experimental building, where our control was installed, as well as the sensors and actuators in combination with the EIB bus. After that we describe how the control was implemented and connected to the EIB bus. Finally we discuss the results gathered from these experiments.

8.2.1 Experimental Set-up

During design and execution of field experiments we deal with many different issues as procedure definition, hardware adaptation, software development, soft- and hardware testing and monitoring of the experiment.

Evaluating a control in the LESO building has many advantages: an installed EIB bus, hardware that eases the implementation, and also that the designer of the experiment can monitor it easily from his workplace. Nevertheless, the LESO is a building one-of-a-kind and during the experiment one has to account for this particularity and verify if the results also bear up under different conditions.

The main points are:

- Our control was primarily designed for usage in residential buildings (contrary to the building it is tested in).

- The LESO has a window front with an upper and lower window. The upper includes an anidolic daylighting system to channel more daylight to the interior of the room.

Regarding the first point the main difference is that in an office building occupants do predictable tasks that favors a blind control, which includes visual comfort and glare. In a residential building the occupants change often the task (watching TV needs completely different light than reading a book) or use the blinds for getting privacy. But the biggest difference is that residential buildings are often not occupied during daytime: the control can in consequence focus on thermal aspects. To overcome these differences the control will only deal with the upper blinds that are shading the anidolic system. The upper windows are the primary source of heat
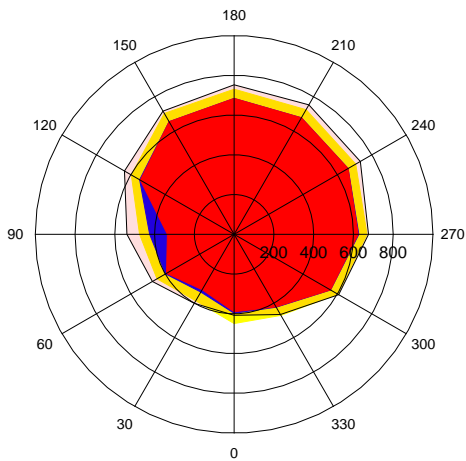
(a) The energy performance of the optimized control is shown in a limpid red.
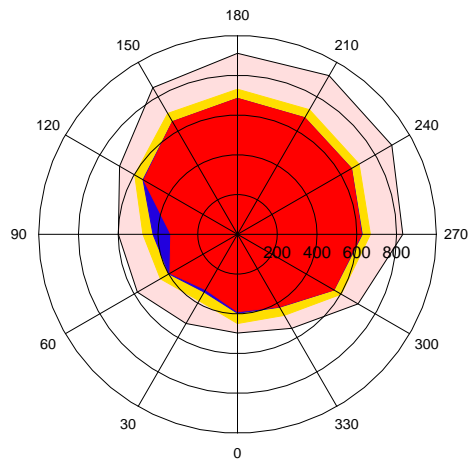
(b) The energy performance of the control of Antoine Guillemin (66) is shown in a limpid red.
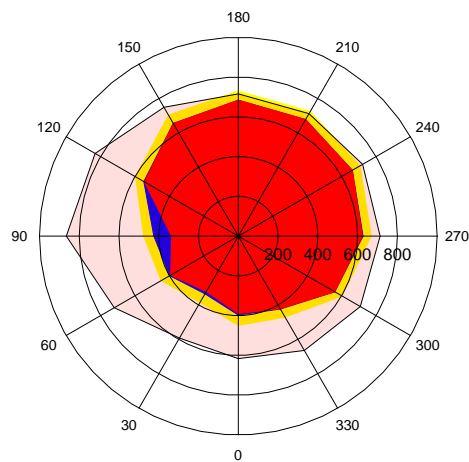
(c) The energy performance of blinds which are controled by the Lightswitch2002 algorithm is shown in a limpid red.

Figure 8.5: The energy consumption is given for each of the 12 orientation which represents a measurement each 30° where 0° refers to south. The red stands for yearly heating energy the blue for cooling energy and the yellow for electric lighting in [kwh/year] of our control. In the background the energy consumption of three other controls for comparison are shown.

gains in the south oriented rooms, essentially during summer time, and do not block the view to the outdoor of the occupant at any setting. This allows us to test the control system only for its primary objective: thermal comfort coupled with energy savings.

Our control was run for a period of six month starting in Mars and ending in August. With this period we cover cold, intermediate and warm climate conditions.

8.2.1.1 Compared settings

We compare only the differences resulting out of the use of the upper blinds. The lower blinds will only be controlled by the occupant. The backup heating is driven by the standard EIB[1] control system, which is a proportional-integral control without night setback. Artificial lighting is also only managed by occupants. Our control will run in the office room LE002.

8.2.1.2 Monitored Information

Between the 1st Mars and 31st August 2010 we recorded additional to the weather information:

- user interaction with the thermal set point for heating.

- energy consumption of the LESO office rooms and the work shop (heating and artificial lighting).

- indoor temperature of all LESO rooms.

Based on the measurements we compared the energy consumption, thermal comfort, and workplane illuminance of LE002 and the other office rooms.

8.2.2 The LESO building

We already described features of the LESO building, in Section 5.2.1, nevertheless, here we give additional informations about the technical features to give the reader a complete picture.

The LESO solar experimental building is a middle-size (1000 m^2) office building (Figure 8.8) with 14 south-facing office rooms that are occupied by senior researchers, research assistants, technical staff and secretaries. Each room has a height of 2.8m and a floor area of $15.7m^2$. The south facade was refurbished in 1999 and is now equipped with an anidolilic daylighting system[2] (Figure 8.9).

The building is divided in nine thermally isolated units. Most of these units are partitioned in two office rooms or accommodate either the conference room or the mechanical workshop.

---

[1]The European installation bus (EIB) is a standard according to EN 50090 and ISO/IEC 14543-3. It defines the connection and communication of sensors and actuators.

[2]The upper window in each LESO room has an anidolic mirror to provide sufficient illumination during overcast skies as well as illuminate the back of each room. A detailed description can be found in Altherr and Gay (8) and how it affects the use of artificial lighting is discussed in Linhart and Scartezzini (107)

The doors in each room have a surface of $3.0m^2$ and are made of $2cm$ thick wood. The lower windows are $2.1m^2$ and the upper one $1.7m^2$ in area, where the upper is tilted $45°$. All windows (Silverstar N 13020 S glazing) are double glazed with IR coating, U-value $1.4W/m^2K$ and g-value 0.54. The windows frame is made out of wood with a U-value $2.0W/m^2K$ and the surface is $0.9m^2$.

The total energy consumption of the building (including electric heating, lighting, computers and other appliances) is equal to $232\ MJ/m^2 \cdot year$, which includes $76\ MJ/m^2 \cdot year$ for heating and $42\ MJ/m^2 \cdot year$ for electric lighting during the period of October 1999 to March 2001. Altherr and Gay (8) reported that the energy signature of the building is $0.72\ W/m^2K$ when the outdoor temperature drops below $13°$ C. Above this temperature the free gains of the building are sufficient to heat it.

8.2.3 Control system implementation

In this Section we present the hardware and software set-up of the control. It is based on European Installation Bus (EIB), which is coupled with a hardware interface (ERGO3 myhomebox) that allows a quick data exchange. We also introduce the selection of sensors that are coupled to the EIB and important for our work. The control is implemented according to the explanations in Chapter 7; it runs partly on the ERGO3 box and on a Microsoft Windows based personal computer. The part implemented on the ERGO3 box is written in LUA[1], the one on the personal computer is written in C++.

8.2.3.1 The European Installation Bus (EIB)

Throughout the development of our control one main goal was that it can be installed with a small amount of sensors and is technically easy to implement. Nevertheless the use of a building management system as the EIB, although it is a technical overkill, makes it possible to implement our control without changing the hard-ware and gives us also opportunities for monitoring the performance. Furthermore we can control all blinds from one computer on which the different control strategies are running. Additional to the setting of the blinds we use an EIB interface that is installed in each room (see Figure 8.10) and includes a switch to indicate a higher or lower temperature set point, which is used to update the thermal profile. The electric radiators are also part of the EIB system and allow monitoring the heating energy of each single room.

8.2.3.2 Sensors

Three sensors are basically needed: E_{esn} (vertical outdoor irradiance $[W/m^2]$ on the plane of the facade), T_i (indoor temperature $[°C]$) and T_e (outdoor temperature $[°C]$). To measure T_i

---

[1]Lua is a lightweight, reflective, imperative and functional programming language, designed as a scripting language with extensible semantics as a primary goal. Lua has a relatively simple C API compared to other scripting languages.(Definition of Wikipedia)
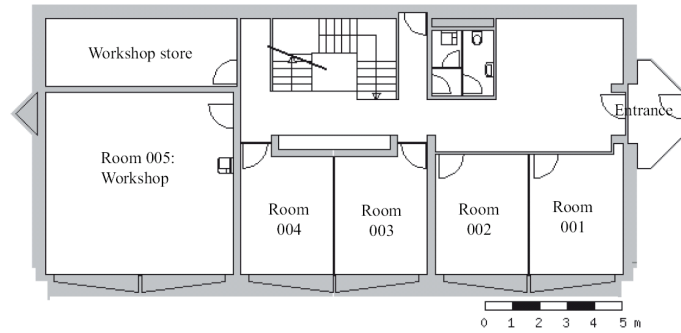
(a) Ground floor of the LESO building.
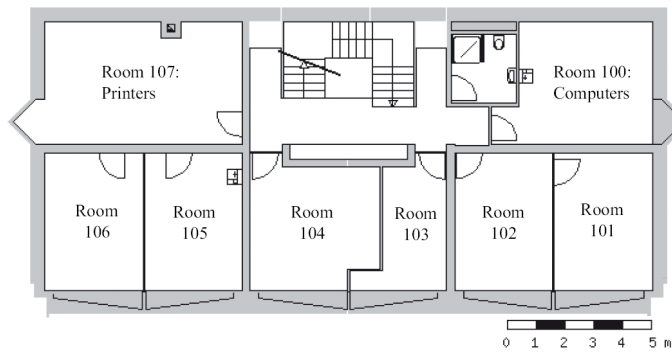
(b) First floor of the LESO building.
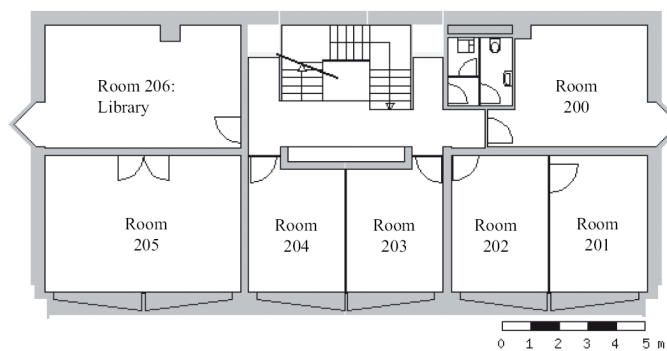
(c) Second floor of the LESO building.

Figure 8.6: The LESO building.
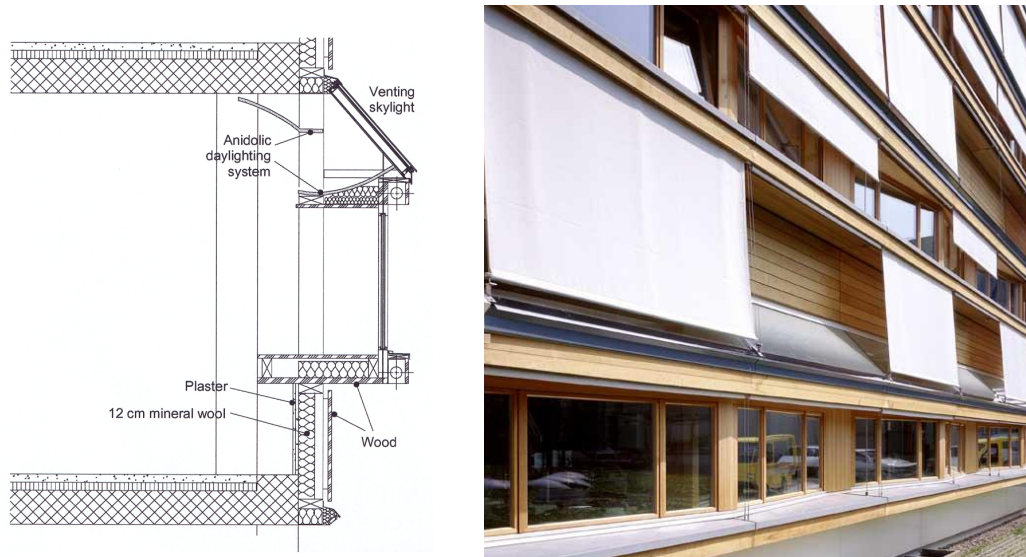
(a) Vertical section through the south facade, showing the anidolic system.

(b) The anidolic system and the upper blind from outdoor.

Figure 8.7: The LESO anidolic daylight system.

Figure 8.8: The LESO experimental building on the campus of EPFL, Switzerland.

Figure 8.9: The anidolic system that redirects daylight to the interior of the rooms.

Figure 8.10: Siemens UP 231/2: Electric lighting and temperature set point control box. The left rocker is used to indicate a higher or lower desired set point temperature.

we use the Siemens UP 231/2 Push button interface (see Figure 8.10) which has an integrated temperature sensor and is installed in each room. T_e is measured by a PT100 temperature sensor and vertical south outdoor irradiance with a pyranometer. The devices are summarized in Table 8.1.

8.2.3.3   The Ergo3 myhomebox

The Ergo3 myhomebox is generally a hardware box to visualize the information provided by the EIB building management system. It includes a firewall and IP connection and is therefore accessible from outdoor. Figure 8.11 shows the schema of the implementation of the control into the myhomebox.

Figure 8.11: Schema of the implementation with the ERGO Box.

Table 8.1: Specifications of the sensors

Manufacturer	Model	Type	Units	Error
Siemens	UP 231/2	Push-button interface and temperature sensor	$°C$	$±0.5°C$
Delta-T	BF3	Sunshine Sensor	W/m^2	12%
Phoenix Contact	MCR/PT100	Temperature sensor	$°C$	$±0.5°C$
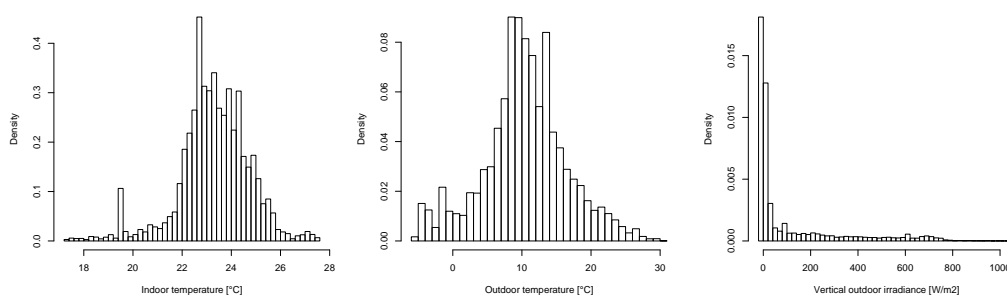
Figure 8.12: Distribution of the observed variables during the six month of field experiments.

8.2.4 Experimental Results

In this section we describe the results achieved during the six month of field experiments in the LESO experimental building.

8.2.4.1 First observations

We started the first measurements in succession at the beginning of March after testing the system and fixing bugs during February. Since the month of March has been extremely cold during the first weeks (see Figure 8.13), we were able to test the control in *winter* like conditions. Histograms of the observed outdoor, and indoor temperature as well as vertical outdoor irradiance, are given in Figure 8.12.

8.2.4.2 Energy Consumption

A major goal of our control system is energy saving. To compare the automatic controlled offices against offices that are not equipped with our control we measure the consumed heating energy H_{ij} and artificial lighting energy L_{ij}, where i denotes the room, and j the month. For that we define:

179
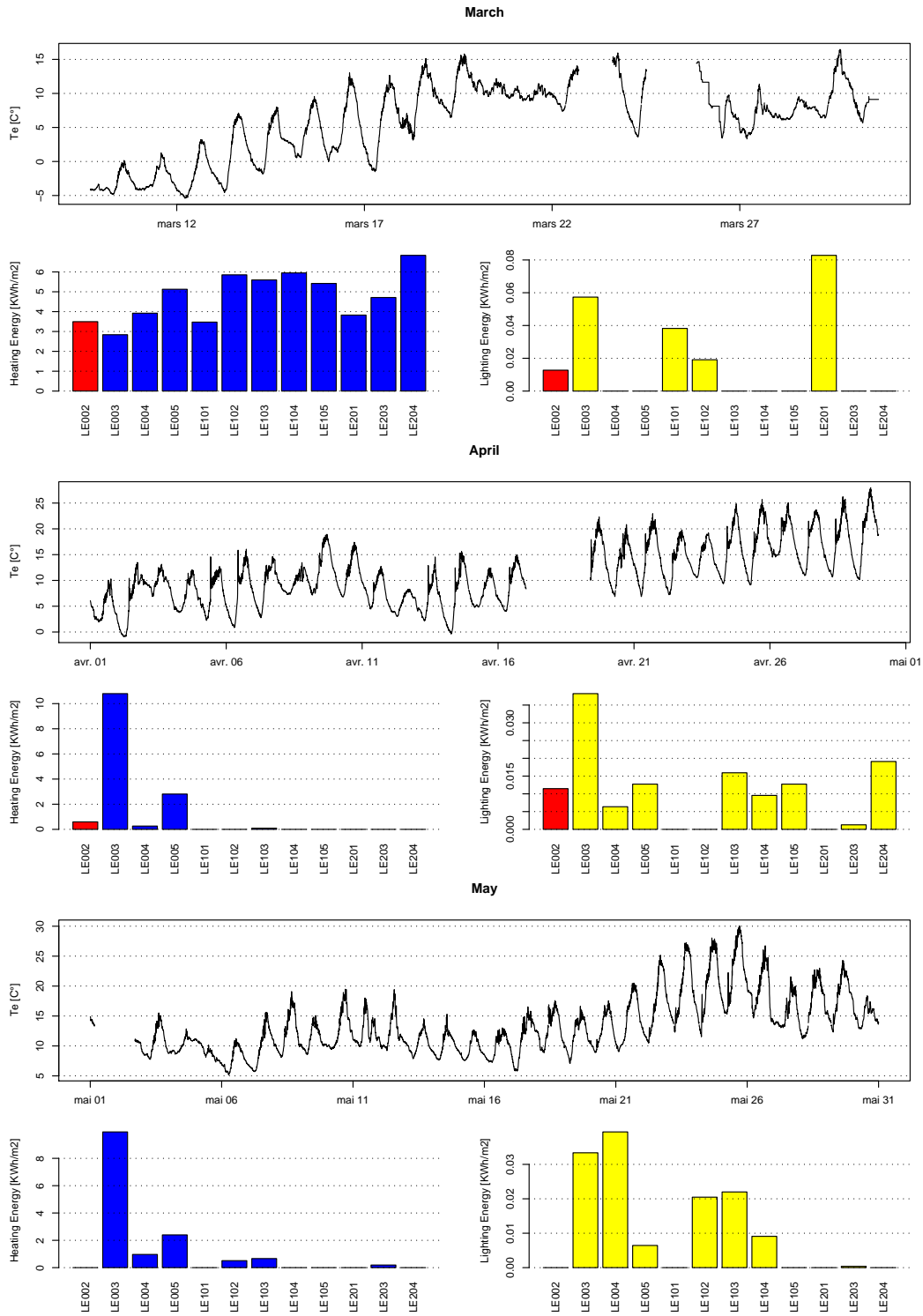
Figure 8.13: Monthly overview of outdoor temperature T_e, heating energy H, and artificial lighting energy L.
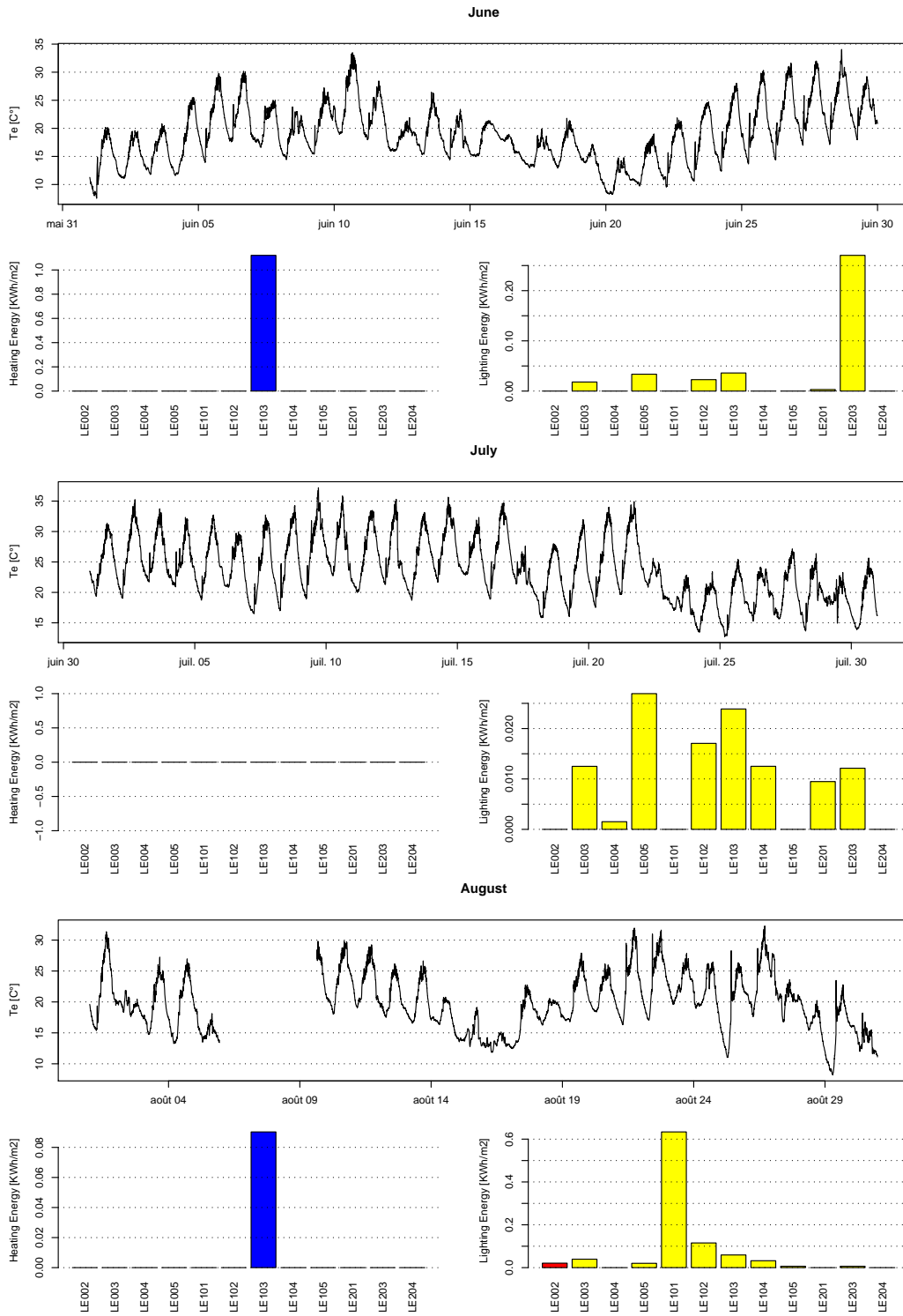
Figure 8.14: Monthly overview of outdoor temperature T_e, heating energy H, and artificial lighting energy L.
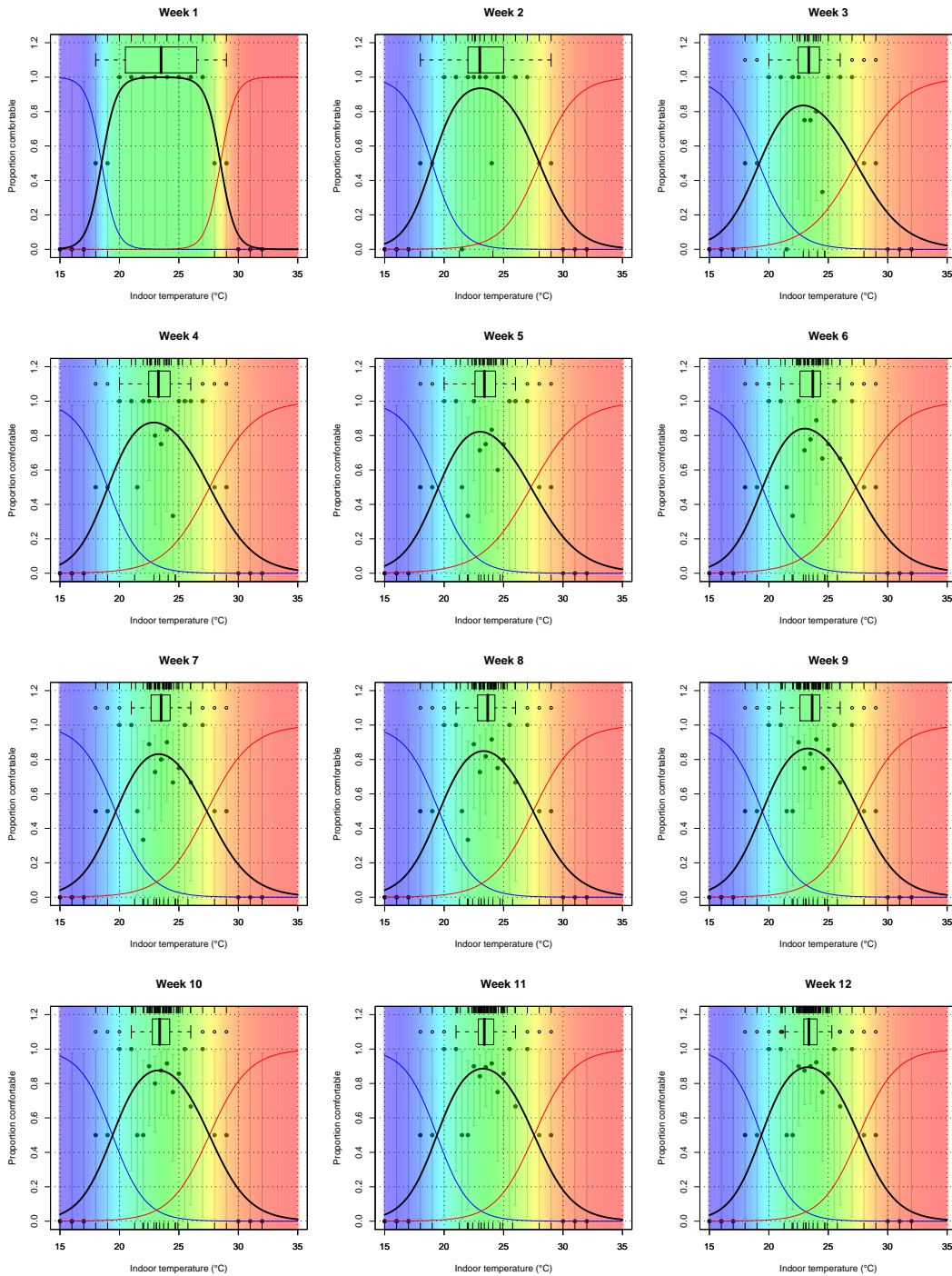
Figure 8.15: Weekly development of the thermal profile for room LE002; first part week 1-12.
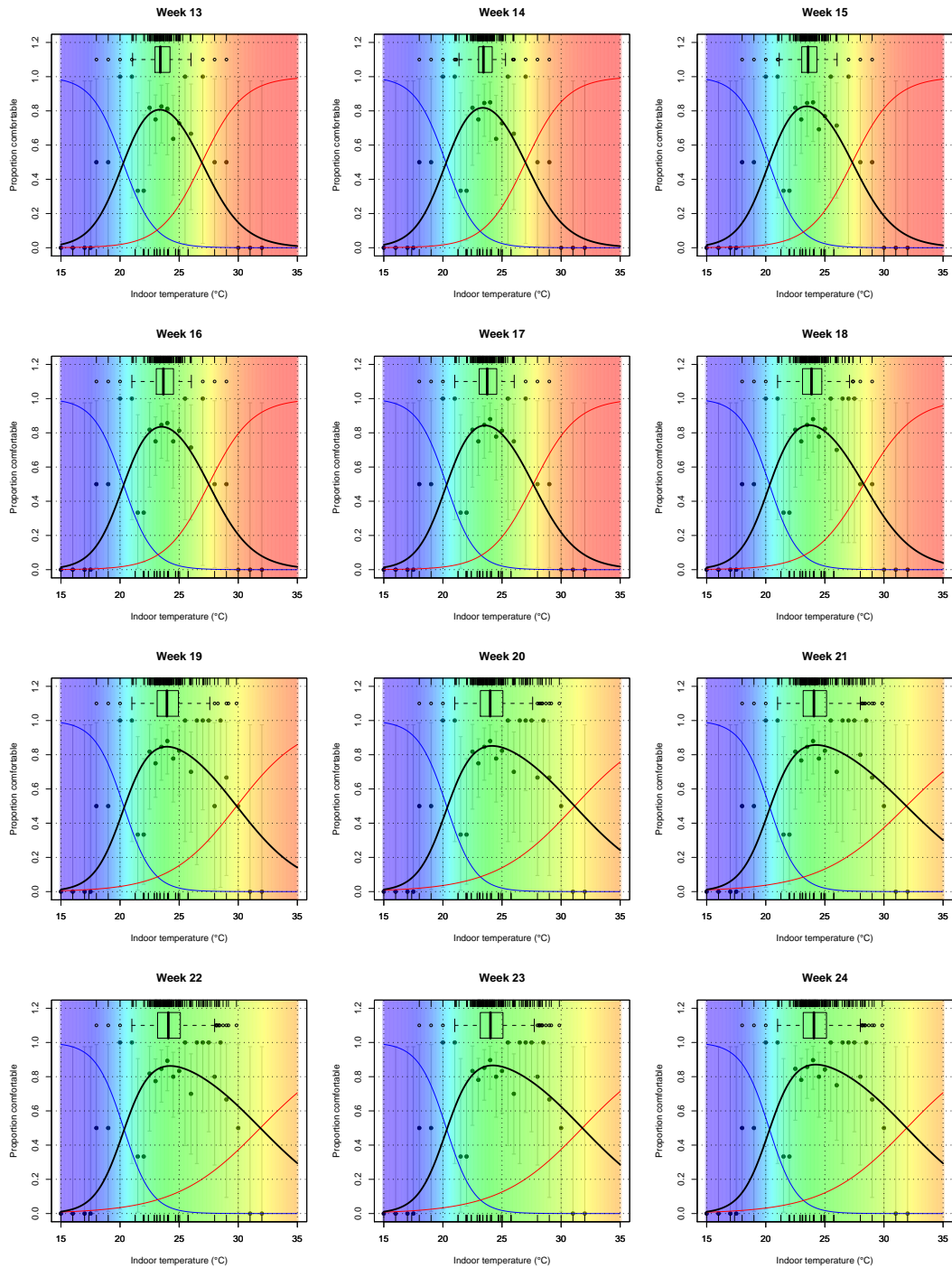
Figure 8.16: Weekly development of the thermal profile for room LE002; second part week 13-24

183

$$H^{tot} = \sum_i \sum_j H_{ij} \quad [KWh/m^2], \tag{8.1}$$

$$L^{tot} = \sum_i \sum_j L_{ij} \quad [KWh/m^2], \tag{8.2}$$

$$C_{ij} = H_{ij} + L_{ij} \quad [KWh/m^2], \tag{8.3}$$

$$C^{tot} = \sum_i \sum_j C_{ij} \quad [KWh/m^2], \tag{8.4}$$

where H^{tot} is the total consumed heating energy, L^{tot} is the total consumed artificial lighting energy and, C^{tot} the sum of heating and artificial lighting energy. Additionally C_i^{avg} denotes the average consumption of each room during all periods and, C_j^{avg} the average consumption of each month j for all rooms (I is the total number of rooms, J is the total number of periods). Definitions for heating H and lighting L energy are correspondent.

Table 8.2 shows the energy used for heating and artificial lighting for each month and each room. They are also shown graphically in Figures 8.13, 8.14. Initially we started the experiment with all standard office rooms of the LESO-PB building. Unfortunately in some office rooms the coupling of the EIB system and the heating did not work. Consequently we did not use the monitored data out of these rooms (LE001, LE202, LE205).

Table 8.3 shows the average energy consumptions for heating and artificial lighting, which is 11.08 [KWh/m^2] for the rooms with the conventional manual control and 4.06 [KWh/m^2] for the room with the adaptive control. The differences occur especially in the intermediate climate, where a solar gains can already effectively contribute to heat the office space.

The monitored savings of the control depends largely on outdoor conditions. Regarding the single periods the largest savings of the control can be seen during April and May, where the outdoor temperature was mainly in the range between $5°C$ and $20°C$. During these two month the heating energy consumption in the room LE002 was close to zero, while in the adjacent rooms energy use was much higher. Thanks to the large window area of the LESO building the room can be heated on a clear day only via solar gains. The reported savings of about 60% sound very ambitious. Looking at the simulation results from Section 5.9 in Figure 5.18 one can see that heating energy in the Blind2Light1 Setting was 9.3 KWh/m^2/y and in Blind4Light1 5.8 KWh/m^2/y which reflects also a reduction of about 40%. Nevertheless by only comparing one room with the other rooms special properties of LE002 (occupance rate, behaviour of the occupant) may leed to an influence of the results. This could have been corrected by applying the control to different offices which levels out the individual effects. Unfortunately the EIB system did strike at the beginning, not allowing us to implement the control in different offices. Since we executed many simulations regarding the energy savings we can cope with that.

8.2.4.3 Thermal comfort

The occupant was able to indicate at any time if it is too warm or too cold. These user wishes have been collected and according to the procedure desribed in Section 7.5, each week the

Table 8.2: Total heating and artificial lighting energy consumption during the experimental period (j = month index, i = room index).

H_{ij} [KWh/m²]	LE002	LE003	LE004	LE005	LE101	LE102	LE103	LE104	LE105	LE201	LE203	LE204	H_j^{tot} [-]
March	3.49	2.84	3.92	5.13	3.47	5.85	5.60	5.95	5.42	3.83	4.71	6.83	57.03
April	0.59	10.80	0.26	2.81	0.00	0.00	0.10	0.00	0.00	0.00	0.00	0.00	14.55
May	0.00	9.93	0.97	2.40	0.00	0.51	0.66	0.00	0.00	0.00	0.19	0.00	14.66
June	0.00	0.00	0.00	0.00	0.00	0.00	1.12	0.00	0.00	0.00	0.00	0.00	1.12
July	0.00	0.00	0.00	0.00	0.00	0.00	0.00	0.00	0.00	0.00	0.00	0.00	0.00
August	0.00	0.00	0.00	0.00	0.00	0.00	0.09	0.00	0.00	0.00	0.00	0.00	0.09
Total	4.09	23.56	5.15	10.33	3.47	6.36	7.57	5.95	5.42	3.83	4.90	6.83	87.46

L_{ij} [KWh/m²]	LE002	LE003	LE004	LE005	LE101	LE102	LE103	LE104	LE105	LE201	LE203	LE204	L_j^{tot} [-]
March	0.01	0.06	0.00	0.00	0.04	0.02	0.00	0.00	0.00	0.08	0.00	0.00	0.21
April	0.01	0.04	0.01	0.01	0.00	0.00	0.02	0.01	0.01	0.00	0.00	0.02	0.13
May	0.00	0.03	0.04	0.01	0.00	0.02	0.02	0.01	0.00	0.00	0.00	0.00	0.13
June	0.00	0.25	0.00	0.47	0.00	0.32	0.50	0.00	0.00	0.04	3.78	0.00	5.37
July	0.00	0.18	0.02	0.38	0.00	0.24	0.33	0.18	0.00	0.13	0.17	0.00	1.62
August	0.29	0.55	0.00	0.28	8.87	1.61	0.83	0.45	0.09	0.00	0.09	0.00	13.07
Total	0.32	1.11	0.07	1.15	8.91	2.21	1.70	0.64	0.10	0.26	4.05	0.02	20.54

Table 8.3: Average energy consumption per room of the different control systems. C^{rel} denotes the energy consumption of the automatic control relative to the manual one.

Control	C^{avg}_{March}	C^{avg}_{Apil}	C^{avg}_{May}	C^{avg}_{June}	C^{avg}_{July}	C^{avg}_{August}	$C^{tot/room}$	C^{rel}
	[KWh/m^2]	[KWh/m^2]	[KWh/m^2]	[KWh/m^2]	[KWh/m^2]	[KWh/m^2]	[KWh/m^2]	[-]
Manual	5.25	2.10	3.73	0.00	0.00	0.00	11.08	1.00
Automatic	3.49	0.59	0.00	0.00	0.00	0.00	4.09	0.37
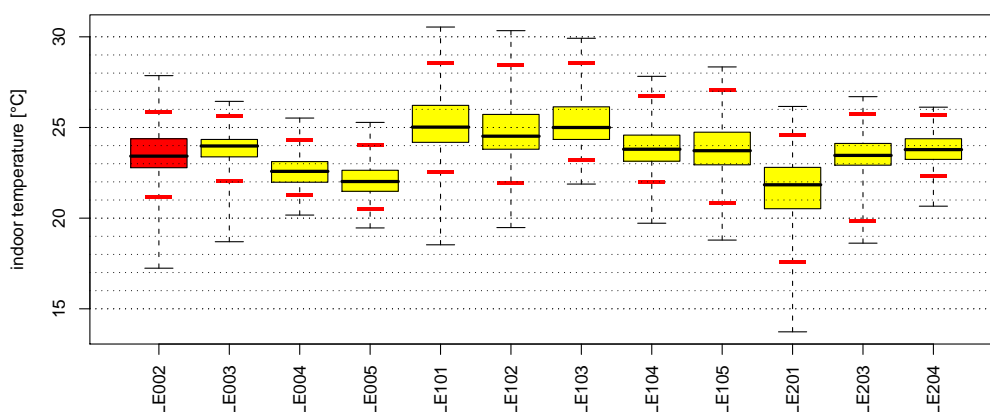
Figure 8.17: Distribution of indoor temperature T_i in the single rooms.

thermal profile was calculated. The evolution of the profile is shown in Figures 8.15, 8.16. It can be seen that the starting profile fades away quickly, adapting itself to the occupant. For degrees above $28°C$ the thermal profile is not changing much till week 19. Before hot temperatures are monitored no votes can be placed on them, consequently the profile does not adapt. The thermal comfort can be estimated using the monitored indoor temperatures in each room. In Figure 8.17 we see boxplots of the measured indoor temperatures for each room during the whole experiment. The boxplots indicate that in room LE002 50% of the time the temperatures have been between $22.78°C$ and $24.38°C$ (span of the box) in 95% of the time the temperature have been between $21.14°C$ and $25.88°C$ (span of the red lines) and the total range of temperature has been between $17.24°C$ and $27.86°C$ (span of the whiskers). In most other rooms the distribution of the temperature is broader, indicating a less efficient control.

With the thermal profile we do not only get an objective function for the control we get also a method for evaluation of thermal comfort with a personalized measure for each room. This delivers more precise results than the evaluation of thermal comfort with a standard measure that is the same for all the occupants. As thermal profiles for the room LE002 we take the

Table 8.4: Average thermal comfort according to the personal thermal profile

	LE002	LE004	LE104	LE105	LE201	LE204	avg.
Prop. comfortable [%]	86	87	82	46	74	81	76

one calculated out of the thermal wishes and for the other we take the profiles from the field study, explained in Section 7.5.1. We display these profile as background in Figure 8.18 and the measured indoor temperature as violin plot[1]. In room LE002, LE004, and LE204 in 95% of the time the temperature is in the *comfort zone*, meaning the probability of comfort is more than 80% according to the personla thermal profile. In the rooms LE001, LE104, LE105, and LE201 the environment is not that well controlled by the occupants and unpleasant situations occur. Our control was able to keep the temperature in the desired range. The average probability of comfort in room LE002 was 86% which is 10% better than average and the second best result of the compared rooms (see Figure 8.4). The outliers can be explained by the opening of a window during winter time, which does not really reduce the overall comfort, since it is an action chosen by the occupant herself. The rooms LE004 and LE204, where the occupants themself regulated the thermal environment, demonstrate that the concept of a thermal profile works in reality. The occupants adapted independently there thermal environment according to the votes they made. It also shows again how important an individual measure of thermal comfort is since the personal comfort temperature between these two subjects clearly differs.

8.2.4.4 Visual comfort

As we stated in Chapter 7.7 we restrict the control of the visual environment to the workplane illuminance levels. Only data monitored during occupancy of the single rooms and when artificial light was switched off are shown in the boxplots in Figure 8.19. The thick red lines at each box indicate the 95th percentile, the box the 50th percentile, and the total range is shown by the whiskers. The thin red lines show the control limits of 150 lx, 300 lx, and 2000 lx. It can be seen that in room LE002 the span of the 95th percentile is narrow compared to the others and furthermore it stays exactly inside the limits of 150 lx and 2000 lx. The box is centered around 500 lx, which lies perfectly in the desired range of workplane illuminances for paper based and computer based tasks.

---

[1]Violin plots are a method of plotting numeric data. A violin plot is a combination of a box plot and a kernel density plot. Specifically, it starts with a box plot. It then adds a rotated kernel density plot to each side of the box plot.
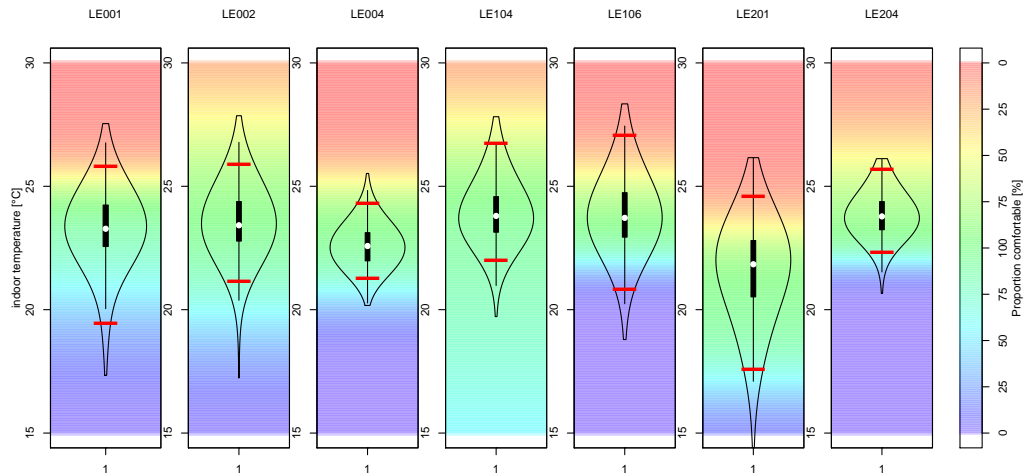
Figure 8.18: Distribution of measured indoor temperature T_i together with the thermal profile. The distribution of the temperature is shown via a violin plot, the red lines indicate the 95th percentile.
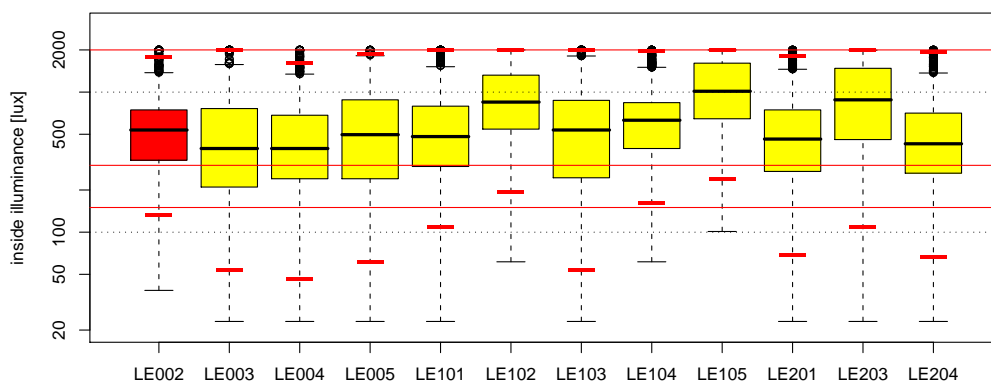
Figure 8.19: Distribution of workplane illuminance E_v in the single rooms.

8.3 Chapter Summary

We tested our control system on a real office room of the LESO building and in several computer simulations. In the simulations it was possible to compare our control with existing ones as well as an optimized control. For the simulation we used two different setup's: a simulation of a LESO office and a residential multi-family home. In both cases we show the Pareto-front of optimized controls and the performance of our control in respect to it. Furthermore other control strategies are compared to ours. The case studies show that with our control strategy a performance close to the Pareto-front was achieved that was also superior to the other implemented controls. With further simulations it was shown that the control system can also adapt to any orientation the facade may have. With the computational tests it was possible to test the control in many different setups, this was especially important to test the adaptation abilities of the control.

The second part of the tests consisted out of the on-site experiments in an occupied office room in the LESO building, where we monitored the energy consumption, and the environment variables. The occupants used the EIB interface for entering the thermal votes and altering their thermal profile. The results show that the temperature in the controlled office is more often in the comfort zone than in the other offices. The energy consumption for heating was reduced to 4.09 KWh/m^2 during the test period, while the other rooms used on average 11.08 KWh/m^2. The probability of thermal comfort of the inhabitants is 10% higher in the automatically controlled room compared to the other rooms. The distribution of the monitored workplane illuminance indicates that the values does not exceed the upper limit and do less often fall below the lower limit of workplane illuminance with our control. For further study we suggest applying the control randomly to different offices to exclude influences from the habits of the user.

Summing up, it can be said that the computational and experimental tests show the overall benefit of the control system for the occupants and for the energy consumption.

8. ASSESSMENT OF CONTROL SYSTEM PERFORMANCE

9

Conclusions

The aim of this doctoral thesis was to develop a blind control that could be built in prefabricated modules for easy renovation of existing buildings. To achieve this goal we identified three crucial properties that the control has to possess:

- The control should only require a minimum number of sensors.

- The automatic adaption should include the building as well as the occupants.

- The energy savings should be greater than the existing controls thanks to the adaptations made to the building.

Throughout this thesis we tried to substantiate each step of action to reach the aforementioned goals. For that, the first step of research was to create the simulation tools for tests and to investigate the theoretical properties of fuzzy logic controls and genetic algorithms. Subsequently, the gained knowledge was combined to create the controls system.

Reduction of state variables

The significance of different state variables for controls had not yet been assessed. The selection criteria were based on expert knowledge and statistical relations. We suggested an approach to identify the important state variables for a control system with an optimization that would quantify the performance of different sets of state variables. By selecting the best set a reduction of sensors without a loss of accuracy was possible. We applied this approach to our control and identified three state variables that allowed a similar control performance to a control with five state variables. Based on these results we included only the important sensors in the control system which made the installation more efficient and less expensive.

Automatic adaptation

The automatic adaption to its environment, including the occupant and the building, was a main objective of this thesis. As a base we used a fuzzy logic control with automated genetic rule optimization.

Adaptation to the occupant

By evaluating the occupants' queries we have shown that a general measure for thermal comfort is not possible for all occupants. Consequently, there is a need for a personalized measure of thermal comfort. In order to create this the occupant entered votes via the interface; from these we deduced statistically the probability of comfort relative to the indoor temperature. According to the profile the control sets its target temperature. Another advantage is that the profile is steadily adapting and with this we could also capture seasonal changes in comfort temperature. This guarantees that at each point in time the control system knows the desired temperature and will make the necessary changes to achieve it.

Adaptation to the building

The adaption to the building was achieved through the fitting of a simple thermal building model with data collected by the sensors of the control system. We showed that the monitored data was sufficient to fit the model. With the help of the simple model we evaluated different control strategies and optimized them according to the thermal profile.

Adaptation of the fuzzy logic

Normally the membership functions for fuzzy logic controls are defined during development, defining in which intervals the control has a fine resolution and in which it is more approximate. Inevitably, this would lead to a mismatch with the changing thermal profile. To avoid this we proposed for the state variable indoor temperature (T_i) an adaption for the membership function according to the thermal profile. The other two state variables were adapted according to the distribution of monitored values; automatically concentrating the fine resolution to intervals of interest.

Energy savings

Tests through simulation

In the test environment, developed in IDA/ICE, standard control modules were implemented that could now be used out of the box to evaluate different possibilities and show, the often underestimated, impact of a control system. We also implemented stochastic models mimicking the occupants' use of blinds and artificial lighting, to assess the absence of any control. Once we put this new tool into practice the following results were found:

- With preliminary studies in different settings we showed the influence of blind controls on energy consumption (heating, cooling, electric lighting) and the superiority of these over manually controlled blinds. With an optimized control it was possible to save up to 50% compared to manually controlled blinds.

- Choosing energy consumption and thermal comfort as objectives for multi-objective simulation we identified the Pareto-front, showing the trade-off between these two for different control strategies. By comparing our control system to the Pareto-front a comprehensive gage for the quality of the controls actions was found. Evaluating the control against the best possible outcome showed the unused potential and proved effective than evaluating it against a manual strategy.

- With the help of the simulation environment it was possible to test the control system during its development in various conditions. The final control system was tested in two different setups: a residential building and the LESO building. We showed that the suggested control capitalized on 96% of its potential regarding the energy consumption and 89% of its potential regarding thermal comfort when compared to an ideal control for the tested cases.

- Given that the orientation of the building is crucial for the irradiation intensity on its facades, we also tested the control system for all orientations. The results showed that our control system also achieved results close to the optimum.

Comprehensive field experiment

Despite the numerous computer simulations to verify the efficacy of the suggested control, they could not replace extensive field tests. Due to the EIB bus we could efficiently implement the control system and allow it to run for six month, covering winter, summer, and intermediate conditions. The system proved satisfactory in controlling the upper blinds. The first impacts were tangible after long absences during warm periods where solar gains were reduced and there was no overheating. When the blinds were not closed the temperature could easily reach 30°C after a sunny weekend. After analyzing the data it appeared that the automatically controlled office only needed about 50% of the average heating energy that was used in the manually controlled offices. Furthermore, the probability of thermal comfort was 10% higher in the automatically controlled office than that of the average probability of the manually controlled office. Over all, the control produced noticeable improvements to the occupant's comfort as well as the energy consumption.

9.1 Further Studies

The suggested methodologies in this doctoral thesis were not limited to the control of blinds.

Simulation optimization environment

- **Application of the simulation environment outside the scope of controls**
  With the help of this tool it was possible to carry out any optimization objective within the scope of the building simulation. With the option to define more than one objective a huge spectrum of applications were unlocked. For example, by choosing the two objective renovation costs and energy savings the result would be a Pareto-front showing different renovation options with the corresponding energy savings and costs. This would provide policy makers with a tool for finding the most efficient rules.

- **Identification of redundant state variables**
  The suggested methodology for the identification of state variables was also not bound to blind controls and it would be interesting to apply it to other fields of control.

Control system

- **Further steps towards a commercial control**
  The current version is not ready yet as a commercial control system. It is written in C/C++ which is a programming language used in industrially embedded controls. Throughout the development of the control we kept an eye on the compatibility with embedded systems. We chose only a simple thermal model, the monitored data was reduced to a minimum, the genetic algorithm was efficient, the optimization ran only once a week (it did not block the other tasks as it came on at night-time) and the implemented fuzzy logic did not consume much computational power. Nevertheless there is still room for improvement, for example, the optimization parameters for the genetic algorithm as well as in the fitting of the thermal model could be further fine tuned.

- **Application to new constructions**
  The focus was on the implementation into prefabricated modules. Nonetheless the control system might also be interesting for new constructions; the requirements for this new application have to be assessed and defined. Perhaps the use of wireless sensors and actuators could be integrated.

- **Interaction with visual comfort control systems**
  A priori the control system can be coupled with any system dedicated only to visual comfort. At any rate it would be interesting to assess the results of the interplay in terms of user satisfaction and energy consumption.

- **Including novel chronobiological research**
  As lighting engineers enter in the chronobiological research, the developers of blind and lighting controls also have to question themselves if the known objectives are to stay the same after including the results of the new field. Do we need different light levels at different times of the day? Or might it be good to change the color of light via color changing foil? We believe that besides energy performance and classic comfort measures a third objective will evolve to cover the chronobiological impact of daylight on humans.

References

[1] *Fuzzy logic controllers-A perspective*, San Francisco, 1980. 53

[2] *ASHRAE RP-839 NMF Translator - Users Guide*, 1996. 23

[3] *IDA INDOOR CLIMATE AND ENERGY*, Kyoto, Japan, 1999. 21, 58, 128

[4] ISO STANDARD 7730. **Moderate Thermal EnvironmentsDetermination of the PMV and PPD Indices and Specification of the Conditions for Thermal Comfort**. *International Organisation for Standardisation*, 1994. 145

[5] R. ALCALÁ, J. ALCALÁ-FDEZ, M. J. GACTO, AND F. HERRERA. **Improving fuzzy logic controllers obtained by experts: a case study in HVAC systems**. *Applied Intelligence*, **ISSN 0924-669X**, 2007. 12, 13

[6] R. ALCALÁ, J. M. BENÍTEZ, J. CASILLAS, O. CORDÓN, AND R. PÉREZ. **Improving fuzzy logic controllers obtained by experts: a case study in HVAC systems**. *Applied Intelligence*, **18(2)**:155–177, 2003. 13

[7] R. ALCALÁ, J. CASILLAS, O. CORDÓN, A. GONZÁLEZ, AND F. HERRERA. **A genetic rule weighting and selection process for fuzzy control of heating, ventilating and air conditioning systems**. *Engineering Applications of Artificial Intelligence*, **18(3)**:279–296, 2005. 12

[8] R. ALTHERR AND J. GAY. **A low environmental impact anidolic facade**. *Building and Environment*, **37(12)**:1409–1419, 2002. 64, 145, 173, 174

[9] P.P. ANGELOV. *Evolving Rule-Based Models. A Tool for Design of Flexible Adaptive Systems*. Physica-Verlag, Wuerzburg, 2002. 60

[10] M. ARIMA, E.H. HARA, AND J.D. KATZBERG. **A fuzzy logic and rough sets controller for HVAC systems**. In *Proceedings of the IEEE WESCANEX95 1*, pages 133–138, 1995. 12

[11] N. BAKER. **We are all outdoor animals**. *Architecture City Environment, Proceedings of PLEA*, pages 553–55, 2000. 160

[12] MANUEL BAUER. *Gestion biomimétique de l'énergie dans le bâtiment*. PhD thesis, Lausanne, 2007. 14

REFERENCES

[13] T. BEDFORD. **The Warmth Factor in Comfort at Work**. *MRC Industrial Health Board Report*, **No. 76**, 1936. 144

[14] D. M. BERSON, F. A. DUNN, , AND M. TAKAO. **Phototransduction by retinal ganglion cells that set the circadian clock**. *Science*, **259**:1070–1073, 2002. 14

[15] D. M. BERSON, F. A. DUNN, , AND M. TAKAO. **Phototransduction by retinal ganglion cells that set the circadian clock**. *Science*, **295**:1070–1073, 2002. 157

[16] B.H. BLAND. **Conduction in dynamic thermal models: analytical tests for validation**. *Building Services Engineering Research and Technology*, **13**:197–208, 1992. 132

[17] D. BLOOMFIELD, K.J. LOMAS, AND C.J. MARTIN. **Assessing programs which predict the thermal performance of building**. *BRE Information Paper*, **IP 7/92**, 1992. 132

[18] D. BOURGEOIS, C. REINHART, AND I. MACDONALD. **Adding advanced behavioural models in whole building energy simulation: A study on the total energy impact of manual and automated lighting control**. *Energy and Buildings*, **38**(7):814–823, 2006. 14

[19] DIMO BROCKHOFF AND ECKART ZITZLER. **Are All Objectives Necessary? On Dimensionality Reduction in Evolutionary Multiobjective Optimization**. In THOMAS PHILIP RUNARSSON, HANS-GEORG BEYER, EDMUND BURKE, JUAN J. MERELO-GUERVÓS, L. DARRELL WHITLEY, AND XIN YAO, editors, *Parallel Problem Solving from Nature - PPSN IX, 9th International Conference*, pages 533–542. Springer. Lecture Notes in Computer Science Vol. 4193, Reykjavik, Iceland, September 2006. 36

[20] DANISH BUILDING AND URBAN RESEARCH. *BSim2002*. http://www.bsim.dk, 2003. 128

[21] L.G. CALDAS AND L.K. NORFORD. **A design optimization tool based on a genetic algorithm**. *Automation in Construction*, **11 (2)**:173–184, 2002. 59

[22] F. CALVINO, M. LA GENNUSA, G. RIZZO, AND G. SCACCIANOCE. **The control of indoor thermal comfort conditions: introducing a fuzzy adaptive controller**. *Energy and Buildings*, **36(2)**:97–102, 2004. 12

[23] C. CAMACHO AND C. BORDONS. *Model Predictive Control*. Springer, London, 1999. 122, 124

[24] C. CARTER. **Computational methods for passive solar simulation**. *Solar Energy*, **45**:379–384, 1990. 130

[25] P. CHAUVEL, JB COLLINS, R. DOGNIAUX, AND J. LONGMORE. **Glare from windows: current views of the problem**. *Lighting Research & Technology*, **14**(1):31, 1982. 158

[26] S.K. CHO AND M. SZIKSZAINE-TABORI. **Country Nuclear Power Profiles**. *IAEA*, 2003. 86

[27] T.D. CHOI AND C.T. KELLEY. **Superlinear convergence and implicit filtering**. *SIAM Journal on Optimization*, **10 (4)**:1149–1162, 2000. 59

[28] F.L. CHUNG AND J.C. DUAN. **On multistage fuzzy neural network modeling**. *IEEE Trans. Fuzzy Syst*, **8 (2)**:125–142, 2000. 55, 82

[29] CIE. **Discomfort glare in the interior working environment**. *Technical report, Commission Internationale de lEclairage*, 1983. 157

[30] CIE. **Discomfort glare in interior lighting**. *Technical report, Commission Internationale de lEclairage*, 1995. 158

[31] CIE. **CIE collection on glare 2002**. *Technical report, Commission Internationale de lEclairage*, 2002. 158

[32] MICHAEL H. COEN. **Design Principles for Intelligent Environments**. In *Proceedings of the 1998 National Conference on Artificial Intelligence (AAAI-98)*, 1998. 18

[33] MICHAEL H. COEN. *Lecture Notes in Computer Science*. Springer Berlin / Heidelberg, New York, 1998. 18

[34] EUROPEAN COMISSION. **European Union Energy and Tranport in Figures**. *Directorate-General Energy and Tranport*, 2009. xiii, 4

[35] D. COOK, M. YOUNGBLOOD, E. HEIERMAN, K. GOPALRATNAM, S. RAO, A. LITVIN, AND F. KHAWAJA. **MavHome: An Agent-Based Smart Home**, 2003. 18

[36] O. CORDON, F. GOMIDE, F. HERRERA, F. HOFFMANN, AND L. MAGDALENA. **Ten years of genetic fuzzy systems: current framework and new trends**. *Fuzzy Sets and Systems*, **141 (1)**:5–31, 2004. 60

[37] O. CORDON, F. HERRERA, F. HOFFMANN, AND L. MAGDALENA. *Genetic Fuzzy SystemsEvolutionary Tuning and Learning of Fuzzy Knowledge Bases*. World Scientifc, Singapore, 2001. 60

[38] DAVID CORNE AND JOSHUA KNOWLES. **Some Multiobjective Optimizers are Better than Others**. In *Proceedings of the 2003 Congress on Evolutionary Computation (CEC'2003)*, **4**, pages 2506–2512, Canberra, Australia, December 2003. IEEE Press. 33

[39] D. DAUM AND N. MOREL. **Assessing the saving potential of blind controller via multi-objective optimization**. *Building Simualtion*, **2 (3)**:175–185, 2009. 21, 63

[40] D. DAUM AND N. MOREL. **Assessing the total energy impact of manual and optimized blind control in combination with different lighting schedules in a building simulation environment**. *Journal of Building Performance Simulation*, **3 (1)**:1–16, 2010. 63

[41] D. DAUM AND N. MOREL. **Identifying important state variables for a blind controller**. *Building and Environment*, **45 (4)**:887–900, 2010. 59, 95, 121

[42] K. DEB. *Multi-Objective Optimization Using Evolutionary Algorithms*. Wiley, 2000. 75

[43] K. DEB, A. PRATAP, S. AGARWAL, AND T. MEYARIVAN. **A fast and elitist multiobjective genetic algorithm: NSGA-II**. *Evolutionary Computation, IEEE Transactions on*, **vol.6, no.2**:182–197, 2002. 59

[44] K. DEB AND D. SAXENA. **Searching for pareto-optimal solutions through dimensionality reduction for certain large-dimensional multi-objective optimization problems**. *n Proceedings of the World Congress on Computational Intelligence (WCCI-2006)*, pages 3352–3360, 2006. 36

REFERENCES

[45] KALYANMOY DEB AND RAM BHUSHAN AGRAWAL. **Simulated Binary Crossover for Continuous Search Space**. *Complex Systems*, **9**:115–148, 1995. 44

[46] KALYANMOY DEB, AMRIT PRATAP, SAMEER AGARWAL, AND T. MEYARIVAN. **A Fast and Elitist Multi-objective Genetic Algorithm: NSGA–II**. *IEEE Transactions on Evolutionary Computation*, **6**(2):182–197, April 2002. 45

[47] K. DEJONG. **Learning with genetic algorithms: an overview**. *Mach. Learning*, **3 (3)**:121–138, 1988. 60

[48] T. DEWSON, B. DAY, AND A. D. IRVING. **Least Squares Parameter Estimation of a Reduced Order Thermal Model of an Experimental Building**. *Building and Environment*, **28**:127–137, 1993. 135

[49] A. I. DOUNIS AND D. E. MANOLAKIS. **Design of a fuzzy system for living space thermal-comfort regulation**. *Applied Energy*, **69(2)**:119–144, 2001. 11

[50] B. DRURY, K. LINDA LAWRIEB, C. FREDERICK WINKELMANN, W. F. BUHL, Y. JOE HUANG, CURTIS O. PEDERSEND, RICHARD K. STRANDD, RICHARD J. LIESEND, DANIEL E. FISHERE, MICHAEL J. WITTEF, AND JASON GLAZERF. **EnergyPlus: creating a new-generation building energy simulation program**. *Energy and Buildings*, **33**:319–331, 2001. 58

[51] HD EINHORN. **Discomfort glare: a formula to bridge differences**. *Lighting Research & Technology*, **11**(2):90, 1979. 157

[52] LARRY J. ESHELMAN AND J. DAVID SCHAFFER. **Real-Coded Genetic algorithms and Interval-Schemata**. In *FOGA-92, Foundations of Genetic Algorithms*, Vail, Colorado, 24–29July 1992. Email: lje@philabs.philips.com, ds1@philabs.philips.com. 44

[53] P.O. FANGER. *Thermal Comfort*. McGraw-Hill, New York, 1972. 11, 12, 16, 18, 72, 144

[54] F. FELGNER, S. AGUSTINA, R.C. BOHIGAS, R. MERZ, AND L. LITZ. **Simulation of thermal building behaviour in modelica**. In *Proceedings of the 2nd International Modelica Conference*, **154**. Citeseer, 2002. 24

[55] DIETERT FISCHER. **Optimale Beleuchtungsniveaus in Arbeitsräumen**. *Lichttechnik*, **22(2**, 1970. 159

[56] M. FOSTER AND T. ORESZCYN. **Occupant control of passive systems: the use of venetian blinds**. *Building and Environment*, **36**:149–155, 2001. 31

[57] G. FRAISSE, J. VIRGONE, AND J.J. ROUX. **Thermal control of a discontinuously occupied building using a classical and a fuzzy logic approach**. *Energy and Buildings*, **26**:303–316, 1997. 12

[58] D. FRANCIOLI, J. J. MEYER, AND H. KERKHOVEN. **Méthode rigorously identical in both simulations. PIECLE pour lévaluation du confort visuel dans un local**. In *Proceedings of CISBAT99*, pages 271–276, Lausanne, Switzerland, 1999. 18

[59] M. FRONDEL, P. GRSCHE, H. TAUCHMANN, AND C. VANCE. **Erhebung des Energieverbrauchs der privaten Haushalte fr das Jahr 2005**. *Rheinisch-Westflisches Institut fr Wirtschaftsforschung (RWI Essen)*, 2005. xiii, 6, 7

[60] A. D. GALASIU, M. R. ATIF, AND R. A. MACDONALD. **Impact of window blinds on daylight-linked dimming and automatic on/off lighting controls**. *Energy and Building*, **76(5)**:523–544, 2004. 15, 63

[61] A. D. GALASIU AND J. A. VEITCH. **Occupant preferences and satisfaction with the luminous environment and control systems in daylit offices: a literature review**. *Energy and Buildings*, **38**:728–742, 2006. 14

[62] C. GARCIA, D. PRETT, AND M. MORARI. **Model predictive control: Theory and practice - a survey**. *Automatica*, **25**:335–348, 1989. 122

[63] D. E. GOLDBERG, K. DEB, AND D. THIERENS. **Towards better understanding of mixing in genetic algorithms**. *Journal of the Society of Instrument and Control Engineers*, **32**(1):10–16, jan 1993. 42

[64] DAVID E. GOLDBERG. *Genetic Algorithms in Search, Optimization and Machine Learning*. Addison-Wesley Publishing Company, Reading, Massachusetts, 1989. 12, 41

[65] D. GREENHALGH AND S. MARSHALL. **Convergence criteria for genetic algorithms**. *SIAM Journal for Computation*, **30 (1)**:269–282, 2000. 59

[66] A. GUILLEMIN. *Using genetic algorithms to take into account user wishes in an advanced building control system*. PhD thesis, Lausanne, 2003. 63, 166, 167, 172

[67] A. GUILLEMIN AND S. MOLTENI. **An energy-efficient controller for shading devices self-adapting to the user wishes**. *Building and Environment*, **37**(11):1091–1097, 2002. 17, 75

[68] A. GUILLEMIN AND N. MOREL. **An innovative lighting controller integrated in a self-adaptive building control system**. *Energy and Buildings*, **33**(5):477–487, 2001. 17

[69] A. GUILLEMIN AND N. MOREL. **Experimental results of a self-adaptive integrated control system in buildings: a pilot study**. *Solar Energy*, **72**(5):397–403, 2002. 17

[70] F. HALDI. *Towards a Unified Model of Occupants' Behaviour and Comfort for Building Energy Simulation*. PhD thesis, ÉCOLE POLYTECHNIQUE FÉDÉRALE DE LAUSANNE, 2010. 145

[71] F. HALDI AND D. ROBINSON. **An integrated adaptive model for overheating risk prediction**. *Journal of Building Performance Simulation*, **1**:43–55, 2008. 31

[72] S.R. HASTINGS. *Passive solar commercial and institutional buildings: A sourcebook of examples and design insights*. John Wiley, 1994. 6

[73] S.R. HASTINGS. **Breaking the heating barrier. Learning from the first houses without conventional heating**. *Energy and Buildings*, **36**:373–380, 2004. 6

[74] A.G. HESTNES, R. HASTINGS, AND B. SAXHOF. *Solar energy houses: strategies, technologies, examples, Second Edition*. James & James, London, 2003. 6

[75] H. HJALMARSSON, M. GEVERS, AND F. BRUYNE. **For model-based control design, closed loop identification gives better performance**. *Automatica*, **32**:1659–1673, 1996. 123

REFERENCES

[76] JOHN H. HOLLAND. **Genetic algorithms and the optimal allocation of trials.** *SIAM J. Computing 2, 88-105*, 1973. 12

[77] JOHN H. HOLLAND. *Adaptation in Natural and Artificial Systems*. University of Michigan Press, 1975. 41

[78] W. HUANG AND H.N. LAM. **Using genetic algorithms to optimize controller parameters for HVAC systems**. *Energy and Buildings*, **26**(3):277–282, 1997. 13

[79] M.A. HUMPHREYS AND J.F. NICOL. **The effects of measurement and formulation error on thermal comfort indices in the ASHRAE database of field studies**. *ASHRAE Transactions*, **206 (2)**:493–502, 2000. 145

[80] M.A. HUMPHREYS AND J.F. NICOL. **The validity of ISO-PMV for predicting comfort votes in everyday thermal environments**. *Energy and Buildings*, **34 6**:667–684, 2002. 145

[81] D.R.G. HUNT. **The use of artificial lighting in relation to daylight levels and occupancy**. *Building and Environment*, **14**:21–33, 1979. 28

[82] IEA. **IEA RD&D database. Edition 2006 with 2005 data**. 2006. xiii, 7

[83] IES. **Outline of a Standard Procedure for Computing Visual Comfort Ratings for Interior Lighting lm-42-72**. *Illuminating Engineering Society (IES) of North America*, 1991. 159

[84] T. INOUE, T. KAWASE, T. IBAMOTO, S. TAKAKUSA, AND Y. MATSUO. **The development of an optimal control system for window shading devices based on investigations in office buildings**. *ASHRAE Transactions*, **104**:1034–1049, 1988. 15, 31

[85] B. ISO. **7730. 2005. Ergonomics of the thermal environment. Analytical determination and interpretation of thermal comfort using calculation of the PMV and PPD indices and local thermal comfort criteria**. *International Standardisation Organisation, Geneva*. 147

[86] J.-S.R. JANG, C.-T. SUN, AND E. MIZUTANI. *Neuro-Fuzzy and Soft Computing*. Prentice-Hall, Englewood Cli+s, New York, 1997. 60

[87] W. JIAN AND C. WENJIAN. **Development of an adaptive neuro-fuzzy method for supply air pressure control in HVAC system**. In *Proceedings of the IEEE International Conference on Systems, Man and Cybernetics, vol. 5*, pages 3806–3809, Nashville, Tennessee, USA, 2000. 13

[88] R. JUDKOFF AND J. NEYMARK. **A Procedure for Testing the Ability of Whole Building Energy Simulation Programs to Thermally Model the Building Fabric**. *J. Sol. Energy Eng.*, **117**, 1995. 132

[89] JÉRÔME KAEMPF AND DARREN ROBINSON. **A simplified thermal model to support analysis of urban resource flows**. *Energy and Buildings*, **39(4)**:445–453, 2007. 128, 132

[90] SA. KLEIN, WA. BECKMAN, AND JW. MITCHELL. **TRNSYSa transient system simulation program**. *ASHRAE Transactions*, **82(1)**:623–633, 1976. 58

[91] GEORGE J. KLIR AND BO YUAN. *Fuzzy Sets and Fuzzy Logic: Theory and Applications*. Prentice Hall PTR, May 1995. 11

[92] D. KOLOKOTSA. *Design and Implementation of an Integrated Intelligent Building Indoor Environment Management System using fuzzy logic, advanced decision support techniques, local operating network capabilities and smart card technology*. PhD thesis, Technological Educational Institute of Crete, Chania, 2001. 17

[93] D. KOLOKOTSA. **Comparison of the performance of fuzzy controllers for the management of the indoor environment**. *Buliding and Environment*, **38**:1439–1450, 2003. 15, 17, 63, 81

[94] D. KOLOKOTSA, G. SARIDAKIS, A. POULIEZOS, AND G.S. STAVRAKAKIS. **Design and installation of an advanced EIB fuzzy indoor comfort controller using Matlab**. *Energy and Buildings*, **38**:1084–1092, 2006. 16

[95] D. KOLOKOTSA, D. TSIAVOS, G. S. STAVRAKAKIS, K. KALAITZAKIS, AND E. ANTONIDAKIS. **Advanced fuzzy logic controllers design and evaluation for buildings occupants thermalvisual comfort and indoor air quality satisfaction**. *Energy and Buildings*, **33(6)**:531–543, 2001. 15, 17, 63

[96] C.P. KURIAN, R.S. AITHAL, J. BHAT, AND V.I. GEORGE. **Robust control and optimisation of energy consumption in daylightartificial light integrated schemes**. *Lighting Research & Technology*, **40(1)**:7–24, 2008. 17

[97] C.P. KURIAN, S. KURIACHAN, J. BHAT, AND R.S. AITHAL. **An adaptive neuro-fuzzy model for the prediction and control of light in integrated lighting schemes**. *Lighting Research & Technology*, **37(4)**:343–351, 2005. 17

[98] P. LAGONOTTE, Y. BERTIN, AND J.B. SAULNIER. **Qualitative analysis of reduced nodal models using the two-port (transfer function) method**. *International Journal of Thermal Sciences*, **38**:51–65, 1999. 130

[99] MATEJA TROBEC LAH, BORUT ZUPANCIC, JOZE PETERNELJ, AND ALES KRAINER. **Daylight illuminance control with fuzzy logic**. *Solar Energy*, **80**(3):307–321, 2006. 15, 81

[100] C.C. LEE. **Fuzzy logic in control systems: fuzzy logic controller-Part I and II**. *IEEE Trans. Syst. Man Cybern*, **20 (2)**:404–435, 1990. 55, 60, 82

[101] ES LEE, GD HUGHES, RD CLEAR, LL FERNANDES, S. KILICCOTE, M. PIETTE, FM RUBINSTEIN, AND SE SELKOWITZ. **Daylighting the New York Times Headquarters Building, Final Report: Commissioning Daylighting Systems and Estimation of Demand Response**. *Lawrence Berkeley National Laboratory, Berkeley, CA*. 15

[102] E.S. LEE AND S.E. SELKOWITZ. **The New York Times Headquarters daylighting mockup: Monitored performance of the daylighting control system**. *Energy and Buildings*, **38**:914–929, 2006. 16

[103] J. LEE AND B. COOLEY. **Recent advances in model predictive control and other related areas**. *Chemical Process Control-CPC*, **V**:201–216, 1996. 122

REFERENCES

[104] R.P. Leslie, R. Raghaven, O. Howlett, and C. Eaton. **The potential of simplified concepts for daylight harvesting**. *Lighting Research and Technologies*, **37**:21–40, 2005. 15

[105] David Lindelf. *Bayesian optimization of visual comfort*. PhD thesis, Lausanne, 2007. 157, 160

[106] Friedrich Linhart. *Energetic, Visual and Non-Visual Aspects of Office Lighting*. PhD thesis, Lausanne, 2010. 157

[107] Friedrich Linhart and Jean-Louis Scartezzini. **Minimizing lighting power density in office rooms equipped with Anidolic Daylighting Systems**. *Solar Energy*, page doi:10.1016/j.solener.2009.05.001, 2009. 64, 173

[108] B. Liptak. *Instrument Engineers' Handbook: Process Control*. Radnor, Pennsylvania: Chilton Book Company, 1995. 12

[109] K.J. Lomas, H. Eppel, C.J. Martin, and D. Bloomfield. **Empirical validation of building energy simulation programs**. *Energy and Buildings*, **26**:253–276, 1997. 132

[110] M. Luckiesh and F.K. Moss. *The science of seeing*. Van Nostrand, 1937. 157

[111] G. Zweifel M. Achermann. **RADTEST radiant cooling and heating test cases. A report of Task 22, Subtask C. Building Energy Analysis Tools**. *Comparative Evaluation Tests, IEAInternational Energy Agency, Solar Heating and Cooling Programme*, 2003. 21

[112] A. Mahdavi, A. Mohammadi, E. Kabir, and L. Lambeva. **Occupants' operation of lighting and shading systems in office buildings**. *Journal of Building Performance Simulation*, **1**:57–65, 2008. 31

[113] EH. Mamdani and S. Assilian. **An Experiment in Linguistic Synthesis with a Fuzzy Logic Controller**. *Int. J. Man-Machine Studies*, **7**:1–13, 1974. 52

[114] L. Michel and J.L. Scartezzini. **Méthode expérimentale dévaluation des performances lumineuses de bâtiments**. *PhD Report, Lausanne, EPFL*, 1999. 159

[115] Brad L. Miller and David E. Goldberg. **Genetic Algorithms, Selection Schemes, and the Varying Effects of Noise**. *Evolutionary Computation*, **4**(2):113–131, 1997. 43

[116] M Morari. *Book chapter in Advances in Model-Based Predictive Control Model Predictive Control: Multivariable Control Technique of choice in the 1990s?* Oxford University Press, Oxford, 1994. 122

[117] A. Nabil and J. Mardaljevic. **Useful daylight illuminances: A replacement for daylight factors**. *Energy and Buildings*, **38**(7):905–913, 2006. 160

[118] N. Nakicenovic, J. Alcamo, G. Davis, B. de Vries, J. Fenhann, S. Gaffin, K. Gregory, A. Grubler, T.Y. Jung, T. Kram, et al. *Special report on emissions scenarios: a special report of Working Group III of the Intergovernmental Panel on Climate Change*. Cambridge, 2000. xiii, 2, 5

[119] J.-M. Nataf. **Translator from NMF to SPARK**. *Conference proc. Building Simulation IBPSA*, 1995. 23

[120] D. NAUCK, F. KLAWOON, AND R. KRUSE. *Foundations of Neuro-Fuzzy Systems*. Wiley, New York, 1997. 60

[121] A.A. NAZZAL. **A new daylight glare evaluation method:: Introduction of the monitoring protocol and calculation method**. *Energy and Buildings*, **33**(3):257–265, 2001. 158

[122] A.A. NAZZAL. **A new evaluation method for daylight discomfort glare**. *International Journal of Industrial Ergonomics*, **35**(4):295–306, 2005. 158

[123] G.R. NEWSHAM. **Manual control of window blinds and electric lighting: Implication for comfort and energy consumption**. *Indoor Environment*, **3 (3)**:135–144, 1994. 15

[124] J.F. NICOL AND M.A. HUMPHREYS. **Thermal comfort as part of a self-regulating system**. *Building Research and Practice (Journal of CIB)*, **6 (3)**:191–197, 1973. 145

[125] J.F. NICOL AND M.A. HUMPHREYS. **A stochastic approach to thermal comfort - Occupant behaviour and energy use in buildings**. *ASHRAE Transactions*, **110 (2)**:554–56, 2004. 31

[126] TOKE RAMMER NIELSEN. **Simple tool to evaluate energy demand and indoor environment in the early stages of building design**. *Solar Energy*, **78**:73–83, 2005. 128, 130, 132

[127] UNIVERSITY OF STRATHCLYDE. *Energy Systems Research Unit*. http://www.esru.strath.ac.uk/Programs/ESP-r.htm, 2003. 128

[128] B. W. OLESEN. **International standards for the indoor environment**. *Indoor Air*, **14**:18–26, 2004. 71, 144

[129] RK PACHAURI. *Climate Change 2007: Synthesis Report*. IPCC Secretariat, 7 bis Avenue de la Paix C. P. 2300 Geneva 2 CH- 1211 Switzerland,, 2007. 1, 2

[130] J. PAGE, D. ROBINSON, N. MOREL, AND J.-L. SCARTEZZINI. **A generalised stochastic model for the prediction of occupant presence**. *Energy and Buildings*, **40**:83–98, 2008. xxi, 66

[131] JESSEN PAGE. *Simulating occupant presence and behaviour in buildings*. EPFL, http://library.epfl.ch/theses/?nr=3900, 2007. 24, 26

[132] W. PERDRYCZ. *Computational Intelligence: An introduction*. CRC Press, 1998. 50

[133] L. PEREZ-LOMBARD, J. ORTIZ, AND C. POUT. **A review on buildings energy consumption information**. *Energy and buildings*, **40**(3):394–398, 2008. xiii, 6, 7

[134] E. POLAK AND M. WETTER. **Generalized pattern search algorithms with adaptive precision function evaluations**. *Lawrence Berkeley National Laboratory, Berkeley*, **Technical report LBNL-52629**, 2003. 59

[135] D.A. POWERS AND Y. XIE. *Statistical methods for categorical data analysis*. Emerald Group Publishing, 2008. 147

REFERENCES

[136] L. PRICE, S. DE LA RUE DU CAN, S. SINTON, E. WORRELL, N. ZHOU, J. SATHAYE, AND M. LEVINE. **Sectoral trends in global energy use and greenhouse gas emissions**. *Lawrence Berkeley National Laboratory, Berkeley, CA*, 2006. 2

[137] A. RAHMATI, F. RASHIDI, AND M. RASHIDI. **A hybrid fuzzy logic and PID controller for control of nonlinear HVAC systems**. *Systems, Man and Cybernetics, 2003. IEEE International Conference on*, **3**:2249–2254 vol.3, 2003. 12

[138] G. V. S. RAJU, J. ZHOU, AND R. A. KISNER. **Hierarchical fuzzy control**. *Int. J. Contr.*, **vol. 54, no. 5**:1201–1216, 1991. 54

[139] M. REA. *IESNA 2000 ninth ed. Illuminating Engineering Society of North America The Lighting Handbook*. New York, 2000. 14

[140] MARK S. REA. **The IESNA Lighting Handbook, Ninth Edition**. *Illuminating Engineering Society of North America*, 2000. 158

[141] INGO RECHENBERG. *Evolution strategy: Optimization of technical systems by means of biological evolution*. Fromman-Holzboog, 1973. 12, 41, 45

[142] C. REINHART. **Lightswitch-2002: a model for manual and automated control of electric lighting and blinds**. *Solar Energy*, **77**:15–28, 2004. 16, 27, 29, 66

[143] CF REINHART. **Effects of interior design on the daylight availability in open plan offices**. In *2002 ACEEE Summer Study on Energy Efficiency in Buildings*, pages 309–322, 2002. 159

[144] D. ROBINSON. *Some trends and research needs in energy and comfort prediction*. Windsor, United Kingdom, 2006. 24

[145] L. ROCHE, E. DEWEY, AND P. LITTLEFAIR. **Occupant reactions to daylight in offices**. *Lighting Research & Technology*, **32**(3):119, 2000. 160

[146] B. ROISIN, M. BODART, A. DENEYERC, AND P. D'HERDT. **Lighting energy savings in offices using different control systems and their real consumption**. *Energy and Buildings*, **40**(4):514–523, 2008. 14

[147] P. SAHLIN, L. ERIKSSON, P. GROZMAN, H. JOHNSSON, A. SHAPOVALOV, AND M. VUOLLE. **Whole-building simulation with symbolic DAE equations and general purpose solvers**. *Building and Environment*, **39 (8)**:949–958, 2004. 21, 59

[148] P. SAHLIN, L. ERIKSSON, P. GROZMAN, H. JOHNSSON, A. SHAPOVALOV, AND M. VUOLLE. **Whole-building simulation with symbolic DAE equations and general purpose solvers**. *Building and Environment*, **39**(8):949–958, 2004. 24

[149] E. SANCHEZ, T. SHIBATA, AND L. ZADEH (EDS.). *Genetic Algorithms and Fuzzy Logic Systems. Soft Computing Perspectives*. World Scientifc, Singapore, 1997. 60

[150] NAVRATI SAXENA, ABHISHEK ROY, AND JITAE SHIN. **CHASE: Context-Aware Heterogenous Adaptive Smart Environments Using Optimal Tracking for Resident's Comfort**. In *UIC*, pages 133–142, 2007. 18

[151] M. SCHULER. **Building simulation in application: Developing concepts for low energy buildings through a co-operation between architect and engineer**. In *Proceedings of the Solar World Congress, the International Solar Energy Society (ISES), Harare, Zimbabwe*, 1995. 159

[152] HANS-PAUL SCHWEFEL. *Numerical optimization of Computer models*. John Wiley & Sons, Ltd., Chichester,, 1981. 45

[153] D. SEBORG, T. EDGAR, AND D. MELLICHAMP. *Process Dynamics and Control, 2nd edn*. John Wiley & Sons, Chichester, 2003. 122

[154] S. SOLOMON. *Climate Change 2007: the physical science basis: contribution of Working Group I to the Fourth Assessment Report of the Intergovernmental Panel on Climate Change*. Cambridge Univ Pr, 2007. 2

[155] A. STANDARD. **55, Thermal environmental conditions for human occupancy**. *American Society of Heating, Refrigerating and Air conditioning Engineers*, 1992. 145

[156] H. STEINFELD, P. GERBER, TD WASSENAAR, V. CASTEL, AND C. DE HAAN. *Livestock's long shadow: environmental issues and options*. FAO, 2006. 2

[157] Y. SUTTER, D. DUMORTIER, AND M. FONTOYNONT. **The use of shading systems in VDU task offices: A pilot study**. *Energy and Buildings*, **38(7)**:780–789, 2006. 9, 16

[158] K. TANAKA. *An Introduction to Fuzzy Logic for Practical Applications*. Springer-Verlag, 1996. 11

[159] N. TUAYCHAROEN AND PR TREGENZA. **Discomfort glare from interesting images**. *Lighting Research & Technology*, **37**(4):329, 2005. 158

[160] JA VEITCH. **Lighting for high-quality workplaces. Creating the productive workplace**, 2006. 157

[161] J.A. VEITCH AND S.L. MCCOLL. **Modulation of fluorescent light: Flicker rate and light source effects on visual performance and visual comfort**. *Lighting Research and technology*, **27**:243–254, 1995. 158

[162] E. VINE, E. LEE, R. CLEAR, D. DIBARTOLOMEO, AND S. SELKOWITZ. **Office worker response to an automated venetian blind and electric lighting system: a pilot study**. *Energy and Buildings*, **28**(2):205–218, 1998. 159

[163] L. WANG. **Universal approximation by hierarchical fuzzy systems**. *Fuzzy Sets Syst.*, **93, 2**:223–230, 1998. 56

[164] L. WANG. **Analysis and design of hierarchical fuzzy systems**. *Fuzzy Systems, IEEE Transactions on*, **vol.7, no.5**:617–624, 1999. 57

[165] M. WETTER. **Multizone building model for thermal building simulation in Modelica**. In *Proc. of the 5th International Modelica Conference, Christian Kral and Anton Haumer (ed.)*, pages 517–526, 2006. 24

REFERENCES

[166] M. WETTER AND E. POLAK. **Comparison of a generalized pattern search and a genetic algorithm optimization method**. *In: Augenbroe G, Hensen J, editors. Proceedings of the Eighth IBPSA Conference, NL: Eindhoven*, **III**:1401–1408, 2003. 59

[167] M. WETTER AND E. POLAK. **A convergent optimization method using pattern search algorithms with adaptive precision simulation**. *In: Augenbroe G, Hensen J, editors. Proceedings of the Eighth IBPSA Conference, NL: Eindhoven*, **III**:1393–1400, 2003. 59

[168] M. WETTER AND J. WRIGHT. **A comparison of deterministic and probabilistic optimization algorithms for nonsmooth simulation-based optimization**. *Building and Environment*, **39 (8)**:989–999, 2004. 59

[169] J. WIENOLD AND J. CHRISTOFFERSEN. **Evaluation methods and development of a new glare prediction model for daylight environments with the use of CCD cameras**. *Energy and Buildings*, **38**(7):743–757, 2006. 159

[170] J. WRIGHT AND R. FARMANI. **The simultaneous optimization of building fabric construction, HVAC system size, and the plant control strategy**. *In: Lamberts R, Negro COR, Hensen J, editors. Proceedings of the Seventh IBPSA Conference, Rio de Janeiro, Brazil*, **I**:865–872, 2001. 59

[171] JONATHAN A. WRIGHT, HEATHER A. LOOSEMORE, AND RAZIYEH FARMANI. **Optimization of building thermal design and control by multi-criterion genetic algorithm**. *Energy and Buildings*, **34 (9)**, 959-972. 59

[172] I.H. YANG, M.S. YEO, AND K.W. KIM. **Application of artificial neural network to predict the optimal start time for heating system in building**. *Energy Conversion and Management*, **44**:2791–2809, 2003. 13

[173] H. YING AND G. CHEN. **Necessary conditions for some typical fuzzy systems as universal approximators**. *Automatica*, **vol. 33, no. 7**:1333–133, 1997. 54

[174] L.A. ZADEH. **Fuzzy Sets**. *Information and Control*, **8**:338–353, 1965. 11

[175] L.A. ZADEH. **Soft Computing and Fuzzy Logic**. *IEEE Software*, **11**(6):48–56, 1994. 50

[176] J.M. ZEITZER, D.J. DIJK, R.E. KRONAUER, E.N. BROWN, AND C.A. CZEISLER. **Sensitivity of the human circadian pacemaker to nocturnal light: melatonin phase resetting and suppression**. *The Journal of Physiology*, **526**(3):695, 2000. 157

[177] G. ZHANG, B. E. PATUWO, AND M. Y. HU. **Forecasting with artificial neural networks:: The state of the art**. *International Journal of Forecasting*, **14**(1):35–62, 1998. 13

[178] N. ZHOU. **Energy use in China: Sectoral trends and future outlook**. *LBNL, Energy Analysis Division*, **LBNL-61904**, 2007. xiii, 7

Appendix A

NMF code for the Ligth3 module

CONTINUOUS_MODEL Light3

ABSTRACT "Lightcontroller for daylighting

Made by: David Daum
<david.daum@epfl.ch>

Date: August 12, 2008

Artificial Light is reduced according to the radiation of the daylight and
only if an occupant is in the zone

"

EQUATIONS

```
/* Controller for the artificial lighting */

    E := (limit - MeasureLighting)/limit;

    OutSignalLighting = IF MeasureOcc < 0.5 THEN
              0
              ELSE_IF E > 0 THEN
              E
              ELSE
              0
              END_IF;
```

A. NMF CODE FOR THE LIGTH3 MODULE

LINKS
/* type   name   variables */

   GENERIC   OutLinkLighting   OutSignalLighting; /*NMFZONE.
      CTRLLIGHT (intensity of artificial light (0,1))*/

   GENERIC   MLinkLighting   MeasureLighting; /*NMFZONE.
      EWORKPLANE (daylight illumination on Workplane)*/

   GENERIC   OccLink   MeasureOcc;   /*Input for Occupancy
      */

VARIABLES
/* type   name   role   def   min   max   description   */

   Generic   MeasureOcc   IN   0   −BIG BIG   "Input signal"
   Generic   MeasureLighting   IN   0   −BIG BIG   "Input signal"
   Generic   OutSignalLighting   OUT   0.5   0   1   "Output signal"
   Generic   E   LOC   0   −BIG BIG   "Control
      difference"

MODEL_PARAMETERS

  INT   n   SMP   1   1 BIGINT   "Number of OutSignal
      links"

PARAMETERS
/* type   name   role   def   min   max   description   */

208

Generic   limit   S_P   200   −BIG   BIG   "Low limit for
        OutSignal"

END_MODEL

A. NMF CODE FOR THE LIGTH3 MODULE

Appendix B

Proof of theorem 1

We prove this theorem by constructing a hierarchical fuzzy system $f(x_1, x_2, x_3)$ that satisfies the following

$$\|g - f\|_\infty \leq \sum_{i=1}^{3} \left(\left\| \frac{\delta g}{\delta x_i} \right\|_\infty + \left\| \frac{\delta f}{\delta x_i} \right\|_\infty \right) b_i, \tag{B.1}$$

1. **Step 1:**

   Let the domain of x_i be $[\alpha_i, \beta_i]$ $(i = 1, 2, 3)$ and the domain of y_1 be $[0, 1]$. Define m fuzzy sets $A_i^1, \ldots, A_i^m$ in $[\alpha_i, \beta_i]$ with the following equally spaced triangular membership functions:

$$\begin{aligned} \mu_{A_i^1}(x_i) &= \mu_{A_i^1}(x_i; e_i^1 + \epsilon, e_i^1, e_i^2) \\ \mu_{A_i^j}(x_i) &= \mu_{A_i^j}(x_i; e_i^{j-1}, e_i^j, e_i^{j+1}) \end{aligned} \tag{B.2}$$

   for $j = 2, 3, ..., m - 1$, and

$$\mu_{A_i^m}(x_i) = \mu_{A_i^m}(x_i; e_i^{m-1}, e_i^m, e_i^m + \epsilon), \tag{B.3}$$

   where $i = 1, 2, 3; e_i^j = \alpha_i + (j - 1)b_i$ with $b_i = (\beta_i - \alpha_i)/(m - 1)$, and the triangular membership functions are defined according to

$$\mu_A(x; a, b, c) = \begin{cases} (x - a)/(b - a), & a \leq x \leq b \\ (c - x)/(c - b), & b \leq x \leq c \\ 0, & x < a \vee x > c \end{cases} \tag{B.4}$$

   Similarly, we define m fuzzy sets $C^1, \ldots, C^m$ in $[0, 1]$ with equally-spaced triangular membership functions as in B.3

B. PROOF OF THEOREM 1

2. **Step 2:**

   Define the constants $y_1^{pq} = (p + m(q-1))/m^2$, where $p, q = 1, 2, \ldots, m$. The TSK fuzzy system in the first level is designed as

   $$f_1(x_1, x_2) = \frac{\displaystyle\sum_{p=1}^{m}\sum_{q=1}^{m} \bar{y}_1^{pq} \left[\mu_{A_1^p}(x_1)\mu_{A_2^q}(x_2) \right]}{\displaystyle\sum_{p=1}^{m}\sum_{q=1}^{m} \left[\mu_{A_1^p}(x_1)\mu_{A_2^q}(x_2) \right]}, \tag{B.5}$$

   which is a special case of the TSK fuzzy system in equation 4.21 in section 4.6.2. Since $0 < \bar{y}_1^{pq} < 1$ and $f_1(x_1, x_2)$ is a weighted average of the $\bar{y}_1^{pq}$'s, we have $y_1 \in [0, 1]$.

3. **Step 3:**

   Let the TSK fuzzy system in the second level be

   $$f_2(y_1, x_3) = \frac{\displaystyle\sum_{i=1}^{m}\sum_{j=1}^{m} h_{ij}(y_1) \left[\mu_{C^i}(y_1)\mu_{A_3^j}(x_3) \right]}{\displaystyle\sum_{i=1}^{m}\sum_{j=1}^{m} \left[\mu_{C^i}(y_1)\mu_{A_3^j}(x_3) \right]}, \tag{B.6}$$

   where the function $h_{ij}(y_1$ are chosen as the following $m-1$'s order polynomials of y_1:

   $$h_{ij}(y_1) = d_{0ij} + d_{0ij}y_1 + \cdots + d_{(m-1)ij}y_1^{m-1} \tag{B.7}$$

   and the m^3 parameters $d_{0ij}, \cdots, d_{(m-1)ij}$ $(i, j = 1, 2, \cdots, m)$ are determined as follows. Since $\mu_{A_3^j}(e_3^j) = 1$, $\mu_{A_3^k}(e_3^j) = 0$ for $k \neq j$ and at most two $\mu_{C^i}(y_1)$'s will be nonzero for any $y_1 \in [0, 1]$, we have from B.6 that

   $$f_2(\bar{y}_1^{pq}, e_3^j) = h_{ij}(\bar{y}_1^{pq})\mu_{C^i}(\bar{y}_1^{pq}) + h_{(i+1)j}(\bar{y}_1^{pq})\mu_{C^{i+1}}(\bar{y}_1^{pq}) \tag{B.8}$$

   for some $i \in 1, 2, \cdots, m-1$. Let $f_2(\bar{y}_1^{pq}, e_3^j) = g(e_1^p, e_1^q, e_3^j)$ and substituting B.7 into B.8, we have

   $$\begin{aligned} g(e_1^p, e_1^q, e_3^j) &= \mu_{C^i}(\bar{y}_1^{pq}) \left[d_{0ij} + d_{0ij}\bar{y}_1^{pq} + \cdots + d_{(m-1)ij}(\bar{y}_1^{pq})^{m-1} \right] \\ &\quad + \mu_{C^{i+1}}(\bar{y}_1^{pq}) \left[d_{0(i+1)j} + d_{0(i+1)j}\bar{y}_1^{pq} + \cdots + d_{(m-1)(i+1)j}(\bar{y}_1^{pq})^{m-1} \right] \end{aligned} \tag{B.9}$$

For j fixed and $p, q = 1, 2, \cdots, m$ collect the m^2 equations of (B.9) into the matrix of the form

$$\mathbf{g_j} = \mathbf{W_j d_j} \tag{B.10}$$

where the $m^2 \times 1$ vectors

$$
\begin{aligned}
\mathbf{g_j} &= \left[g(e_1^1, e_2^1, e_3^j), g(e_1^m, e_2^1, e_3^j), \cdots, g(e_1^1, e_2^m, e_3^j), \cdots, g(e_1^m, e_2^m, e_3^j) \right]^T \\
\mathbf{d_j} &= \left[d_{01j}, \cdots, d_{(m-1)1j}, \cdots, d_{0mj}, \cdots, d_{(m-1)mj} \right]^T
\end{aligned}
\tag{B.11}
$$

and the $m^2 \times m^2$ matrix W_j is obtained from (B.9) accordingly. Compute the m^3 parameters $d_{0ij}, \cdots, d_{(m-1)ij}$ $(i, j = 1, 2, \cdots, m)$ from

$$\mathbf{d_j} = \mathbf{W_j^{-1} g_j} \tag{B.12}$$

Substituting the $d_{0ij}, \cdots, d_{(m-1)ij}$ into (B.7) and the resulting $h_{ij}(y_1)$ into (B.6) we obtain the second level TSK fuzzy system.

4. **Step 4:**

   The overall hierarchical fuzzy system is obtained as

   $$f(x_1, x_2, x_3) = f_2(f_1(x_1, x_2), x_3), \tag{B.13}$$

   where f_1 and f_2 are given by (B.5) and (B.6), respectively.

We now show that the hierarchical fuzzy system f designed above satisfies (B.1). First we show that

$$f(e_1^p, e_1^q, e_3^j) = f(e_1^p, e_1^q, e_3^j) \tag{B.14}$$

for $p, q, j = 1, 2, \cdots, m$. According to the membership functions defined in Step 1, we have from (B.5) that

$$f_1(e_1^p, e_1^q) = \bar{y}_1^{pq} \tag{B.15}$$

for $p, q = 1, 2, \cdots, m$. Since the $d_{0ij}, \cdots, d_{(m-1)ij}$ determined from (B.12) guarantee (B.9) which, in return, implies

$$f_2(\bar{y}_1^{pq}, e_3^j) = g(e_1^p, e_1^q, e_3^j), \tag{B.16}$$

we have

$$f(e_1^p, e_1^q, e_3^j) = f_2 \left[f_1(e_1^p, e_1^q), e_3^j \right] = f_2(\bar{y}_1^{pq}, e_3^j) = g(e_1^p, e_1^q, e_3^j) \tag{B.17}$$

B. PROOF OF THEOREM 1

Let $U^{pqj} = [\alpha_1, \beta_1] \times [\alpha_2, \beta_2] \times [\alpha_3, \beta_3]$, where $p, q, j = 1, 2, \cdots, m-1$. Since $[\alpha_1, \beta_1] = [e_i^1, e_i^2] \cup [e_i^2, e_i^3] \cup \cdots \cup [e_i^{m-1}, e_i^m]$ $i = 1, 2, 3$, we have

$$U = [\alpha_1, \beta_1] \times [\alpha_2, \beta_2] \times [\alpha_3, \beta_3] = \bigcup_{p=1}^{m-1} \bigcup_{q=1}^{m-1} \bigcup_{j=1}^{m-1} \tag{B.18}$$

which implies that for any $\mathbf{x} \in \mathbf{U}$, there exists U^{pqj} such that $\mathbf{x} \in \mathbf{U^{pqj}}$. Now let $\mathbf{x}$ be an arbitrary point in U, so there exist fixed numbers $p_x, q_x, j_x \in \{1, 2, \cdots, m-1\}$ (corresponding to the $\mathbf{x}$) such that $\mathbf{x} \in \mathbf{U^{p_x q_x j_x}}$. Let $\mathbf{e^x} = (\mathbf{e_1^{p_x}}, \mathbf{e_1^{q_x}}, \mathbf{e_3^{j_x}})^{\mathbf{T}}$. Using the Mean-Value Theorem and the fact that $f(\mathbf{e^x}) = \mathbf{g}(\mathbf{e^x})$, we have

$$
\begin{aligned}
|g(\mathbf{x}) - \mathbf{f}(\mathbf{x})| &\leq |g(\mathbf{x}) - \mathbf{g}(\mathbf{e^x})| + |f(\mathbf{x}) - \mathbf{f}(\mathbf{e^x})| \\
&\leq \sum_{i=1}^3 \left(\left\| \frac{\partial g}{\partial x_i} \right\|_\infty |x_i - e_i^x| + \left\| \frac{\partial f}{\partial x_i} \right\|_\infty |x_i - e_i^x| \right)
\end{aligned}
\tag{B.19}
$$

where e_i^x is the ith element of $\mathbf{e^x}$. Since $\mathbf{x} \in \mathbf{U^{p_x q_x j_x}}$, we have $|x_i - e_i^x| \leq b_i$, hence

$$|g(\mathbf{x}) - \mathbf{f}(\mathbf{x})| \leq \sum_{i=1}^3 \left(\left\| \frac{\partial g}{\partial x_i} \right\|_\infty + \left\| \frac{\partial f}{\partial x_i} \right\|_\infty \right) \tag{B.20}$$

Since the $\mathbf{x}$ in (B.20) is an arbitrary point in U, we obtain (B.1) from (B.20) $\square$

Appendix C

Structure of EIB implementation

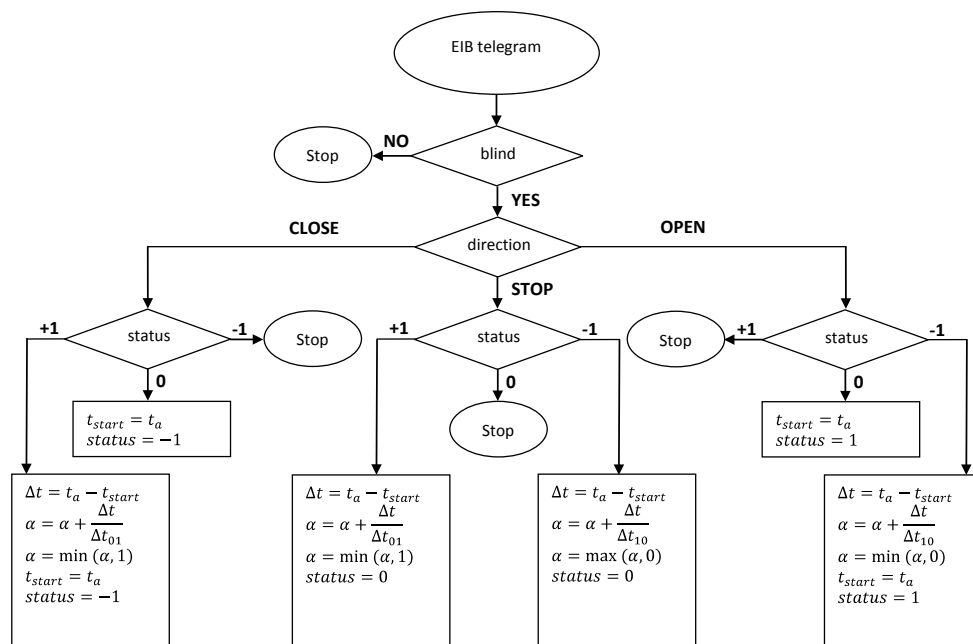Structure of the implementation in the EIB system for the movement of the blinds:

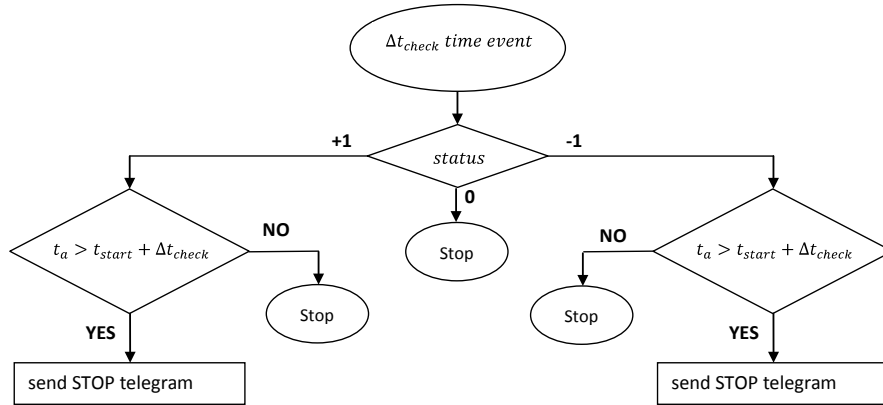**Figure C.1:** Flow Chart for the EIB implementation.

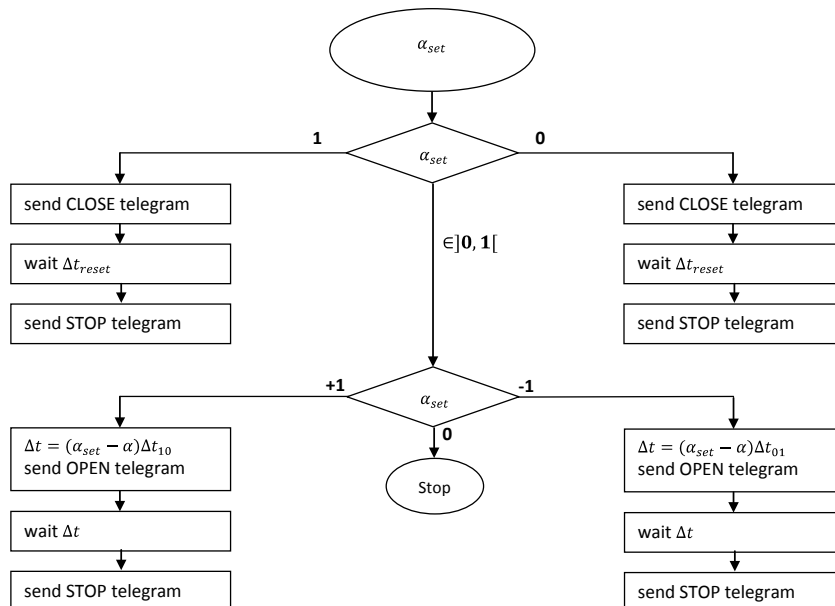**Figure C.2:** Flow Chart for the EIB implementation.

Figure C.3: Flow Chart for the EIB implementation.

David Alexander Daum
Dipl.-Wi.-Ing.
Chemin Du Fau Blanc 12D
1009 Pully · Suisse

David Alexander Daum
Dipl.-Wi.-Ing.

David Alexander Daum
Dipl.-Wi.-Ing.
Chemin Du Fau Blanc 12D
1009 Pully · Suisse

Curriculum Vitae

Work Experience

2008 –2010	**Swiss Federal Institute of Technology (EPFL)**, Lausanne, Switzerland Research assistant at the Solar Energy and Building Physics Laboratory
2007 –2008	**DWS fund manager**, Frankfurt, Germany
2006	**Internship at KPMG**, Munich, Germany
2005	**Internship at Goertz + Schiele**, Auburn Hills, USA
1998	Formation of a company for IT-solutions

Education

2008 –2010	**Swiss Federal Institute of Technology (EPFL)** Preparation of a doctoral thesis in the Doctoral Program "Energy"
2010	Visiting researcher at the **Lawrence Berkeley National Laboratory (LBNL), USA**
2003 –2007	**Universität Karlsruhe (TH), Germany** Graduate studies in Industrial Engineering
2007	**Indian Institute of Technology Kanpur, India** Preparation of master thesis
1992 – 2001	High School in Karlsruhe, Germany
1988 – 1992	Elementary School in Völkersbach, Germany

David Alexander Daum
Dipl.-Wi.-Ing.
Chemin Du Fau Blanc 12D
1009 Pully · Suisse

LANGUAGE SKILLS

German	mother tongue
English	fluent (TOEFL 109/120)
French	fluent
Hindi	notions

SOFTWARE SKILLS

Microsoft Office	profound knowledge
Java, C, C++	profound programming knowledge
R, Matlab	profound knowledge
SAP, HTML	basics

SCHOLARSHIPS

German Academic Exchange Service

PUPLICATIONS

2010   **D. DAUM** AND N. MOREL. Assessing the total energy impact of manual and optimized blind control in combination with different lighting schedules in a building simulation environment. Journal of Building Performance Simulation, 3 (1):1–16, 2010.

D. DAUM AND N. MOREL. Identifying important state variables for a blind controller. Building and Environment, 45 (4):887–900, 2010.

2009   **D. DAUM** AND N. MOREL. Assessing the saving potential of blind controller via multi-objective optimization. Building Simulation, 2 (3):175–185, 2009.

K. DEB, S. GUPTA, **D. DAUM**, J. BRANKE, A.K. MALL, AND D. PADMANABHAN. Reliability-based optimization using evolutionary algorithms. IEEE Transactions on Evolutionary Computation, 13(5):1054–1074, 2009.

2007   **D. DAUM**, K. DEB, AND J. BRANKE. Reliability-based optimization for multiple constraints with evolutionary algorithms. In IEEE Congress on Evolutionary Computation, 2007. CEC 2007, pages 911–918, 2007.